Enhancing the neutrophil-mediated anti-cancer response after oncolytic measles virus therapy in B-cell malignancy:

Dissecting out the mechanism

Aditi Dey

Thesis submitted for degree of Doctor of Philosophy

University College London

2016

Declaration

I, Aditi Dey, confirm that the work presented in this thesis is my own.

Where information has been derived from other sources, I confirm that this has been indicated in the thesis.

Signed:

Date:

Acknowledgements

I would like to thank my supervisor Prof. Adele Kay Fielding, for her guidance, help and support with the work in this thesis. Her patience and encouragement over the years and throughout this work has helped me become a better scientist.

I would also like to thank all my colleagues in Prof Fielding's lab, for their help, assistance, encouragement, friendship and constant support.

My parent's, parent-in-law's and sister's faith in me have encouraged me to choose a path not so easy. And I am forever grateful to them.

Finally, I would like to dedicate this thesis to my husband Debangshu, and my son Diganta, without whose love and support I could have never achieved this. Diganta had once told me "Mummy Never, Never, Never Give Up!!!"

Abstract

Oncolytic measles virus (MV) is being tested in several ongoing clinical trials with encouraging results. There is a demonstrable need to explore the role of the immune system in addition to the direct oncolytic effect of MV. My laboratory has previously shown that neutrophils are involved in MV-mediated tumour regressions, becoming activated, upon MV infection. This thesis further explores the role of neutrophils, one of the key players of the innate immune system in MV oncolysis.

First, I showed that acute lymphoblastic leukaemia (ALL) shows marked sensitivity to MV oncolysis (Patel, Dey et al., 2011). I attempted to enhance neutrophil function at tumour sites by generating a novel strain of MV expressing the human granulocyte colony-stimulating factor (GCSF), a known neutrophil survival factor and enhancer of antibody dependent cellular cytotoxicity (ADCC). Evaluating the effects in two different models of B-cell malignancy, I showed that neutrophil depletion abrogated the MV therapeutic effect in an *in-vivo* Raji - but not Nalm-6 - tumour model. MVhGCSF enhanced the oncolytic capacity of MV in the Raji model *in-vivo*, whereas in the Nalm-6 model, the opposite was unexpectedly the case. MVhGCSF replicated within an MV-infectable CD46 transgenic mouse model with detectable serum levels of hGCSF but no toxicity. My data suggest that a "one-size-fits-all" model of immune response to viral oncolysis is not appropriate, and each tumour target will need full characterisation for the potential of MV to generate benefit (Dey et al., 2016).

Next, I showed that ADCC was NOT a mechanism by which neutrophils kill MV-infected cells.

Finally, I showed that MV infection of target cells can stimulate neutrophils to develop a cytotoxic effector phenotype, all aspects of which are blocked by fusion inhibition. Hence, I suggest a new mechanism for MV-mediated oncolysis; fusion between infected target cells and neutrophils.

Publications and abstracts

Publications and abstracts arising from the work described in this thesis at the time of submission:

- Aditi Dey, Yu Zhang, A. Castleton, K. Bailey, B. Beaton, B. Patel, A. Fielding. *The role of neutrophils in measles virus mediated oncolysis differs between B-cell malignancies and is not always enhanced by GCSF. Mol Ther* advance online publication 22 September 2015; doi: 10.1038/mt.2015.149.

- Aditi Dey, A Castleton, B Rosen, A Fielding. *Fusion between neutrophils (PMN) and target cells mediate cytotoxicity during measles virus (MV) oncolysis - a novel mechanism.* MOLECULAR THERAPY. 23: S247-S247. May 2015 (POSTER PRESENTATION).

- Aditi Dey, A Castleton, B Patel and A Fielding. *MVhGCSF is therapeutic in-vivo B-cell malignancies with neutrophils (PMNs) playing different roles.* MOLECULAR THERAPY. 23: S170-S170. May 2015 (POSTER PRESENTATION).

- Dey, A., Zhang, Y., Castleton, A. Z., & Patel, B. (2014). *Neutrophils (PMNs) in Measles Virus (MV) Mediated Leukaemia Therapy: Good or Bad.* MOLECULAR THERAPY. 22: S250-S250. May 2014 (POSTER PRESENTATION).

- Dey, A., Zhang, Y., Castleton, A. Z., & Patel, B. (2013). *Improving the Oncolytic Activity of Measles Virus by Enhancing the Neutrophil-Mediated Response to Infected Tumour Cells.* MOLECULAR THERAPY. 21: S158-S158. Jun 2013 (POSTER PRESENTATION).

- Dey, A., Zhang, Y., Castleton, A., Patel, B., Ghorani, E., Rai, L., Fielding, A. (2012). *Polymorphonuclear Neutrophils (PMNs) Are Cytotoxic for Measles Virus (MV)-Infected Tumour Cells Ex-Vivo, but their Role in MV-Mediated Oncolysis In-Vivo is Tumour-Type Dependent.* MOLECULAR THERAPY. 20: S271-S271. May 2012 (POSTER PRESENTATION).

- Patel, B., Dey, A., Ghorani, E., Kumar, S., Malam, Y., Rai, L., Fielding, A. K. (2011). *Differential cytopathology and kinetics of measles oncolysis in two primary B-cell malignancies provides mechanistic insights.* Mol Ther 19(6):1034-1040 Jun 2011.

- *American Society of Haematology, 53rd Annual Meeting and Exposition, December 10-13, 2011, San Diego, CA* Patel, B., Aditi, D., Ghorani, E., Malam, Y., Andy, S., Wickremasinghe, R., Fielding, A. (2010). *Vaccine Measles Virus Has Therapeutic Potential In B-cell Malignancy.* BLOOD, 116 (21), 1540. (POSTER PRESENTATION).

Statement of work undertaken

My colleague Dr. Zhang did the neutrophil depletion experiment in Nalm-6 model in Chapter 3 and one experiment in Chapter 5 (Fig 5-13). I have gained her permission to include that part of the work. I carried out rest of the work in this thesis.

Table of Contents

List of figures

List of tables

List of abbreviations

- ADCC Antibody-dependent cellular cytotoxicity
- ALL Acute lymphoblastic leukaemia
- APC Allophycyanin
- ATCC American type culture collection
- BCG Bacille Calmette-Guérin
- BFP Blue fluorescent protein
- BM Bone marrow
- BSA Bovine serum albumin
- CARD Caspase activation and recruitment domain
- CCL C-C motif ligand
- CD Cluster of differentiation
- CDV Canine distemper virus
- CEA Carcino embryonic antigen
- CML Chronic myloid leukaemia
- CNS Central nervous system
- CPA Cyclophosphamide
- cpm Count per minute
- Ct Threshold cycle
- CTL Cytotoxic T lymphocyte
- CTLA4 Cytotoxic T lymphocytes associated antigen 4
- CXCL C-X-C motif ligand
- DC Dendritic cell
- DMEM Dulbecco's modified Eagle medium
- DMSO Dimethyl Sulfoxide
- DNA Deoxy ribonucleic acid
- dNTP 2'-deoxiribonucleoside 5'-triphosphate
- dsRNA Double stranded RNA
- DTT Dithiothreitol
- EGF Epidermal-derived growth factor
- ELISA Enzyme-linked immunosorbent assay

- FACS Fluorescence assisted cell sorting
- FBS Foetal bovine serum
- FDA Food & Drug Administration
- FIP Fusion inhibitory peptide
- FITC Fluorescein isothiocyanate
- GAPDH Glyceraldehyde 3-phosphate dehydrogenase
- GCSF Granulocyte colony stimulating factor
- GFP Green fluorescent protein
- GMCSF Granulocyte monocyte colony stimulating factor
- HIV Human immunodeficiency virus
- HLA Human leukocyte antigen
- hpi Hours post infection
- IFN Interferon
- Ig Immunoglobulin
- IGF-1 Insulin-like growth factor
- IL Interleukin
- IP Intra-peritoneal/Intra-peritoneally
- IPS-1 (VISA virus-induced signalling adapter)
- IRF IFN response factor
- ISGF3 IFN-stimulated gene factor 3
- ISGs IFN-stimulated genes
- IT Intra-tumoural/Intra-tumourally
- IV Intra-venous/Intra-venously
- JAK Janus kinase
- LGP-2 Laboratory of genetics and physiology 2
- mAb monoclonal Antibody
- MAVS Mitochondrial antiviral signalling protein
- MCP1 Monocyte chemotactic protein 1
- MDA5 Melanoma differentiation-associated protein 5
- MFI Mean fluorescent intensity
- MHC Major histo-compatibility
- µl Microliter
- ml Millilitre

- min Minute
- MMP Matrix metalloproteinase
- Mo-DC Monocyte derived dendritic cell
- MOI Multiplicity of infection
- mRNA messenger RNA
- MV Measles Virus
- NIS Sodium iodide symporter
- NK Natural killer cell
- ns Not significant
- OD Optical density
- OV Oncolytic virus
- PAMP Pathogen associated molecular patterns
- PB Peripheral blood
- PBMC Peripheral blood mononuclear cells
- PBS Phosphate buffered saline
- PCR Polymerase chain reaction
- PD Programmed cell death protein
- PD-L Programmed cell death ligand
- PE Phycoerythrin
- PEG Polyethylene glycol
- PFU Plaque forming unit
- PI Propidium iodide
- PRR Pattern recognition receptors
- PVRL4 Poliovirus receptor-related 4
- RBC Red blood cell
- RdRp RNA-dependent RNA polymerase
- RIG-I Retinoic acid-inducible gene 1
- RLRs RIG-I-like receptors
- RNA Ribonucleic acid
- RNP Ribonucleoprotein complex
- ROS Reactive oxygen species
- RPM Rotations per minute
- RQ-PCR Relative quantitative polymerase chain reaction

- SC Subcutaneous/Subcutaneously
- SCCHN Squamous cell carcinoma of the head and neck
- ScFV Single chain fragment variable
- SCID Severe combined immunodeficiency
- SCR Short consensus repeat
- SEM Standard error of the mean
- SLAM Signalling lymphocyte activation molecule
- SSPE Subacute sclerosing pan-encephalitis
- ssRNA Single stranded RNA
- STAT Signal transduction & activator of transcription
- STING Stimulator of IFN genes
- STP Serine-threonine-proline-rich domain
- Th1/Th2 Type 1 T helper cell/ Type 2 T helper cell
- TNF Tumour necrosis factor
- TRAIL TNF-related apoptosis inducing ligand
- T-VEC Talimogene Laherparepvec
- $TCID_{50}$ 50% Tissue culture infectious dose
- TLRs Toll-like receptors
- UV Ultraviolet
- VSV Vesicular stomatitis virus

Chapter 1: Introduction

1.1 CANCER THERAPY OVERVIEW:

1.1.1 Conventional cancer therapy:

Non-specific cytotoxic chemotherapeutic agents[1], which kill rapidly dividing cells and radiation therapy[2], that causes DNA damage in turn killing the cells, still remain the backbone of current cancer treatment and is used on its own or in combination. Though effective, the toxicity of these agents can outweigh the benefits, occasionally by a very large margin and chemo-resistance remains a big hurdle[1].

1.1.2 Small molecules in cancer therapy:

Understanding of the biology of different cancers and knowledge of the defective signalling pathways in cancer has led to an increase in targeted therapies. The first example is the use of small molecules for targeted molecular therapy[3]. Tyrosine kinase inhibitors, which inhibit kinase activity by competing for the ATP binding site[4] of BCR-ABL {the fusion protein product of an aberrant chromosomal translocation (t9;22), which is involved in chronic myeloid leukaemia (CML) and acute lymphoblastic leukaemia (ALL) pathogenesis}, has revolutionised the treatment of CML and ALL[5,6].

Insight into the underlying genetic pathway that helps in maintenance of the tumour has helped uncover growth factor receptors that can be targeted by small molecule agents. For example, deregulated signalling by

the avian erythroblastosis oncogene B (ErbB) family of tyrosine kinase receptors is associated with several cancers[7] making ErbB1/epidermal growth factor receptor (EGFR), ERbB2/human epidermal growth factor receptor 2 (HER2/neu), ErbB3/HER3 and ErbB4/HER4[7,8], excellent targets for small molecule therapy.

1.1.3 Antibody therapy:

Monoclonal antibodies (mAb) have been included as standard of care in cancer therapy. Rituximab, an anti-CD20 antibody, which binds to CD20 on cell surface, has been used in combination with chemotherapies in Non-Hodgkin's lymphoma (NHL) aberrantly overexpressing CD20, with significant improvement in overall survival rates[9]. Another mAb Trastuzumab (Herceptin), that targets the ErbB2, has an excellent anti-tumour activity against breast cancer[10] and prolonged disease free survival and overall survival in patients with HER2 positive breast cancer[11].

1.1.4 Cellular Immunotherapy:

Allogeneic stem cell transplantation, where patients are infused with genetically similar haematological stem cells from HLA-matched sibling or unrelated donors has played a major role in the treatment of haematological malignancies[12,13] and clearly demonstrated the 'graft versus leukaemia effect' mediated by allogeneic T-cells. More recently that concept has been developed further to include modification of patient's T-cells by gene transfer technology, giving rise to engineered T-cells with chimeric antigen receptors (CARS) that can recognise diverse cell surface antigens and signal through

engineered intracellular domains. One of the most commonly targeted antigens to date is CD19, which is expressed on all B-cells[14-16]. CD19 CAR T-cells have proven effective at inducing remissions in patients with CD19 expressing malignancies such as ALL[17] albeit with some considerable adverse reactions such as cytokine storms.

T-cells can also be engineered to express receptors (TCR) against tumour antigens and used as cancer therapy[18]. To generate tumour-specific TCRs different techniques have been used. Once a suitable target sequence is identified it can be isolated from rare tumour reactive T-cells directly from patients[18]; from mice expressing human HLA, immunised with human cancer antigen proteins[19] or by using *in-vitro* technologies to alter the TCR to enhance their anti-tumour properties[20]. Early clinical trials have exhibited feasibility of genetically modified TCRs directed against MART1 antigen in melanoma[21]. Additional clinical trials have demonstrated prolonged tumour regressions in patients with melanoma and sarcoma[22-24].

Approaches to 'vaccinate' patients against cancer are also being studied, for example, Sipuleucel-T for the treatment of prostate cancer is an autologous dendritic cell (DC) vaccine, that stimulates T-cell specific for prostatic acid phosphatase (PAP), a protein overexpressed by prostate carcinoma cells[25].

1.1.5 Immuomodulating agents in checkpoint blockade:

Other novel therapeutic agents termed immune checkpoint inhibitors have gained popularity in the last decade and are being tested in clinical trials. For example Ipilimumab, which is approved by US food and drug administration (FDA) as a first line therapy in patients with advanced melanoma is an antibody that can block the cytotoxic T lymphocytes associated antigen 4 (CTLA4) inhibiting an important signal in the T-cell response pathway, thereby initiating tumour cell destruction[26]. Another agent Pembrolizumab and Nivolumab, that block the interaction between programmed cell death (PD)-1 protein and its ligand PD-L1 has been approved by FDA in patients with Ipilimumab refractory melanoma[27]. PD-1/PD-L1 interaction acts as a co-inhibitory signal to dampen T-cell response. PD-L1 is overexpressed in cancer cells which binds to the PD-1 on activated T-cells thereby deactivating them[28]. One of the limitations of these novel agents is that benefit can be limited by the immunosuppressive nature of the tumour microenvironment[29]. Studies in targeted immunotherapy have suggested that a combinatorial approach of using targeted agents in combination with immunotherapeutic agents is needed to attain a synergistic effect that can achieve more potent cytotoxicity[28,30]. Targeted combinatorial therapy can lead to direct tumour regression, breaking the immunosuppressive tumour microenvironment and sensitise the tumour cells to be targeted by immune therapy[29].

1.1.6 Oncolytic Virotherapy - an overview:

In the last decade, oncolytic viruses have also been increasingly widely been investigated for cancer therapy and numerous viruses are now being tested in early phase clinical trials[31].

Properties of an ideal oncolytic virus[32] include:

- Efficacy: replicates within cancer cells and kills effectively by direct lysis.

- Specificity and selectivity: exclusively infects and preferentially lyses cancer cells.

- Stimulate immune response: can activate an autologous anti-tumour immune response.

- Stable and genetically modifiable: can be engineered to attain additional desirable properties and genetically stable to avoid any possible genetic recombination with other species in the environment.

- Safety: must be safe to the recipient, contacts of the recipient and the environment. The virus should be associated with no or very mild human disease, with no threat to public health. No possibility of spread of the virus in individuals in close contact with the patient or any other living forms in the environment. Ideally availability of means and treatment to control any viral replication is highly desirable.

Many viruses are naturally oncolytic with more than one of the above desirable characters and others can be genetically modified to make them suitable for cancer therapy. Early observations date back to the 19th century[33] where spontaneous tumour regression was observed when

patients acquired natural viral infection[33-36]. In the 1950s and 1960s virotherapy for cancer had gained pace and viruses were tested in clinical trials[37]. However, most of these trials were neither successful nor provided meaningful data, as the types of tumours treated were diverse and lacked consistency with the different viruses used[38]. Moreover, there was clearance of the virus by the immune system and in some cases the uncontrolled viral replication proved fatal, while in other patients, sometimes immunosuppressed, the virus took hold and the tumours regressed[31]. In a particular study, tumour regression was reported in 37 of 90 patients treated with mumps virus, but this work was not continued[39] and the field of cancer virotherapy stalled. The modern era of virus mediated specific and selective killing of cancer cells, with targeted and engineered viruses arguably began during the early 1990s[40]. With the development of molecular virology, viruses once again gained relevance as anti-cancer therapies. An illustrative list of viruses being tested as cancer therapeutics is shown in Table 1.1.

Table 1.1: Illustrative list of oncolytic viruses tested in murine models:

Virus	Structural characteristic	Receptor	Illustrative murine models
Adenovirus	ds DNA, Non-enveloped	CAR	Sarcoma [41], head and neck carcinoma[42], bladder cancer[43]
Reovirus	dsRNA Non-enveloped	Unknown	Melanoma[44], pancreatic[45], NSCL[46], ovarian[47], colorectal[48], head and neck cancers[49]
Measles virus (MV)	ss(-) RNA Enveloped	CD46, SLAM, Nectin 4	Ovarian cancer[50], glioblastoma multiforme[51], multiple myeloma[52]
Vesicular stomatitis virus (VSV)	ss(-) RNA Enveloped	LDLR	Melanoma[53], colorectal carcinoma[54], breast cancer[55]
Newcastle disease virus (NDV)	ss(-) RNA Enveloped	Unknown	Glioblastoma multiforme[56], neuroblastoma[57]
Herpes simplex virus (HSV)	ds DNA Enveloped	HVEM, nectin 1, nectin 2	Glioma[40], metastatic melanoma[58], head and neck cancer[59]
Coxsackie virus	ss(+) RNA Non-enveloped	CAR/ICAM-1/DAF	Multiple myeloma[60], melanoma[61]
Vaccinia virus	dsDNA Enveloped (complex coats)	Unknown	Hepatocellular carcinoma[62], pleural mesothelioma[63], melanoma[64], ovarian[65], breast cancer[66]
Poliovirus	ss(+) RNA, Non-enveloped	CD155	Neuroblastoma[67], glioma[68]

1.1.7 Oncolytic virotherapy and immunotherapy – synergistic roles:

Oncolytic virotherapy can act with both immunotherapy and virotherapy playing synergistic roles to eliminate cancer[69]. Oncolytic viruses can directly kill cancer cells, leading to tumour regression[70]. However, it has become increasingly clear that oncolytic virotherapy has a strong immunotherapeutic component and can activate several aspects of the immune system to attack the tumour. Both the biology of the virus and the cancer environment plays a significant role in the success of oncolytic virotherapy.

Tumours need blood supply to grow and metastasise and angiogenesis plays an important role in tumour development[71]. Vaccinia virus can disrupt the tumour vasculature by attacking the tumour-related endothelial cells in patients with hepatocellular carcinoma, with no evident harmful effect on the normal tissues[72]. In a phase II/III clinical trial of melanoma, intra-tumoural (IT) injection of herpes simplex virus (HSV) expressing granulocyte macrophage colony stimulating factor (GMCSF) led to a potent anti-melanoma immune response[73]. Moreover, viral replication within tumour bed has been shown to attract immune cells, thereby alerting the immune system, leading to tumour associated antigen (TAA) presentation by cross-priming which leads to a more potent anti-tumour response. For example, vaccinia virus infected human melanoma cell line (MelanA TAA positive) were phagocytosed by DCs, which in turn were able to stimulate a MelanA antigen specific T-cell response[74]. Another melanoma

cell line Mel888 infected with reovirus was able to generate a melanoma antigen recognised by T-cells (MART) specific cytotoxic T-cell response[75].

In parallel to the biology of the virus *per se*, the biology of the cancer cells too has a very important role to play in viral selectivity leading to success of oncolytic virotherapy. Among other hallmarks of cancer the cells accumulate genetic defects to become malignant, which helps them in accelerated proliferation[76]. These specific defects that allow the cancer cells to evade detection by the immune system and helps in their proliferation and survival can also provide a thriving environment for the virus to replicate. For example, defective cell signalling pathways, such as the defects in the interferon (IFN) signalling pathways in cancer cells permit better virus replication than in the non-transformed cells, where these pathways are intact[77]. Another hallmark of cancer cells is induction of angiogenesis for survival of the tumour cells. Oncolytic viruses have been used to target this by direct infection of vascular endothelial cells[78], or by arming them using anti-angiogenic transgenes[79].

With oncolytic virotherapy, one single agent can achieve the combinatorial effect of targeted therapy and immunotherapy to produce a robust anti-tumour effect. In the current scenario of cancer therapeutics, an agent that can specifically target and kill the tumour cells, without harming the normal cell, and at the same time generate a long-lasting anti-tumour immune response, looks promising, and an oncolytic virus is a good candidate to fit in that space[69].

1.1.8 Genetic modification of oncolytic virus and their mechanism of action:

While many viruses are able to specifically and selectively kill cancer cells naturally, genetic modification has been widely used to enhance their oncolytic properties. *In-vitro* passaged strains belong to the first generation of oncolytic virotherapeutics, the genetically engineered, selectivity enhanced viruses form the second generation, and the third generation of virotherapeutics are the ones that are genetically engineered, transgene expressing 'armed' oncolytic viruses[80].

Modifications focus on several main areas:

1. Safety - by attenuation of potentially pathogenic properties and targeting of entry or replication:

For example, adenovirus has been modified by deletions of E1B55 and E3B genes, which facilitates replication of the virus only in p53 deleted cells, thereby attenuating it while simultaneously targeting cancer cells lacking p53 function[81]. Another tissue specific, targeted, adenovirus for prostate cancer (CG7060 and CG7870) is regulated by prostate-specific promoter elements (PSE1A and PSE1B), therefore has transcriptional control and replicates only in prostate cells[82,83]. The ICP34.5 neuro-virulence gene deleted herpes simplex virus (HSV) strains (G207, 1716, NV1020, OncoVEX^{GM-CSF})[80] are capable of selective replication in tumour cells[84].

2. Enhancement of anti-tumour immune response:

The Ad5-CD/TKrep strain of adenovirus uses both oncolytic and suicide gene therapy in combination. In addition to the E1B55 gene deletion it expresses the dual pro-drug activating fusion protein cytosine deaminase/ thymidine kinase (CD/TK), which can convert the pro-drug 5-fluorocytosine (5-FC) to more potent 5-fluorouracil (5-FU), and only in cells with p53 mutation (Freytag SO 1998). The HSV strain OncoVEX^{GM-CSF} (Talimogene Laherparepvec/T-VEC) GMCSF, has enhanced immunogenic properties, and has deleted ICP34.5 and ICP47 for reduced pathogenicity and to restore MHC I presentation, respectively[80]. JX-594, a vaccinia virus strain has deletion of a thymidine kinase gene that enhances cancer selectivity and is armed with GMCSF to facilitate immune cells at the site of viral infection[85]. Engineered and non-engineered viruses are being extensively used in clinical trials and shown inTable 1.3.

1.1.9 Virotherapy clinical trials:

Oncolytic viruses that are being tested in different phases of clinical trials are listed in Table 1.3. Some trials have completed whereas others are still ongoing[31]. The first generation oncolytic viruses that were used in clinical trials are the strains passaged in tissue culture to make them attenuated but without any modifications. Examples of first generation non-engineered viruses that have been used in clinical trials are listed in Table 1.2.

Table 1.2: Non-engineered viruses in clinical trials:

Virus	Disease	Publication
Adenovirus	Cervical cancer	Huebner RJ 1956[86]
West Nile virus	Lymphomas and carcinomas	Southam CM 1951[87], Southam CM 1954[88]
Mumps	Carcinomas, lymphomas and different solid tumours	Asada T 1907-1928[39], Shimizu Y 1988[89], Okuno Y1978[90]
Parvovirus	Osteosarcoma	Toolan HW 1965[91]
Vaccinia virus	Metastatic melanoma	Hunter Craig 1970[92], Roenigk 1974[93], Mastrangelo 1995[94]
Newcastle disease virus	Myelogenous leukaemia	Wheelock EF 1964[95]
	Cervical carcinoma	Cassel WA 1965[96]
	Solid tumours	Csatary 1993[97], Csatary 1999[98], Csatary 2004[99]

In recent times, the clinical trials using viruses have become more strict, controlled and rigorous. The second and third generation of oncolytic viruses have become more popular, as they are more targeted, replication-selective and with reduced toxicity[80]. Clinical efficacy was shown in one of the first phase I/II clinical trial that used OncoVex$^{GM\text{-}CSF}$ (T-VEC) directly administered in patients with metastatic melanoma intra-tumourally (IT), which led to complete regression in both injected and non-injected tumours in 8 out of 50 patients[100]. Escalated doses of vaccinia virus, modified to express GMCSF was given to cutaneous melanoma patients IT, and was shown to be safe, effective at expressing functional passenger gene GMCSF and induced significant tumour regression[85]. Additionally, JX594 strain of vaccinia virus was administered IT in patients with hepatocellular carcinoma and led to regression in 3 out of 10 patients[101]. Besides, ONYX-015 (Ad2/5 dl1520) - an oncolytic adenovirus strain used to treat head and neck cancer, where transient anti-tumoural effects were observed[81], showed improved anti-

tumour effect when used in combination with chemotherapy (cisplatin), compared to chemotherapy alone[102]. Recently a phase III randomised controlled study, using T-VEC in metastatic melanoma led to its approval by FDA. Total 436 patients were recruited in this trial with advanced stage (IIIB, IIIC, IVM1a) disease or patients with no prior treatment. T-VEC was well tolerated with significantly improved durable response rates and overall survival in the treated patients compared to the control groups[103]. Furthermore, non-engineered viruses too have revealed some encouraging results. Reolysin®, which is proprietary variant of Reovirus when used in combination with paclitaxel and carboplatin showed efficacy and 26.9% response rate in a dose escalation Phase III clinical trial of head and neck cancer[104]. In another dose escalation Phase I/II trial in recurrent glioblastoma multiforme, unmodified Newcastle disease virus (NDV) used intra-venously (IV), led to minimal toxicity and was well tolerated with some initial response to therapy[105]. All the viruses used so far in the different phases of clinical trials have shown efficacy and most of them were very well tolerated even with very high doses administered[80].

Table 1.3: Oncolytic viruses from different generation in clinical trials:

Virus in clinical trial	Genetic modification	Transgene expression	Name	Proposed cancer target	Tumours	Clinical trials
Adenovirus	E1B-55K(-) (gene bind to and inactivates p53 gene), E3B(-)	Non-armed	*dl*1520 (ONYX-015)	p53 pathway defects; late RNA transport defects	Sarcoma, head and neck cancer, bladder cancer, lung mets, glioma, ovarian cancer, solid tumours, pancreatic cancer, CRC, hepatobiliary, prostate cancer	Phase I, II and III
	E1B-55K(-), E3(-)	Non-armed	H101 (Oncorine)	p53 pathway defects; late RNA transport defects		
	PSE1A, E3B(-)	Non-armed	CG7060	Prostate specific		
	PSE1A, PSE1B	Non-armed	CG7870	Prostate specific		
	E1B-55K(-), E3(-)	CD/TK expression	Ad5-CD/Tkrep	p53 pathway defects; late RNA transport defects		
Coxsackie virus	Non-engineered	Non-armed	CAVATAK	Selective infection of ICAM-1 expressing cells	Melanoma, SCCHN, solid tumours	Phase I and II
Herpes simplex virus	ICP34.5(-)	Non-armed	HSV 1716	Defects in tumour PKR/IFN pathways, attenuated neurotoxicity	Solid tumours, metastatic melanoma, head and neck cancer, glioma, non-CNS solid tumours, mesothelioma, pancreatic cancer, breast cancer,	Phase I, II and III
	ICP34.5(-), ICP6(-)	Non-armed	G207	Tumour cell complementation of ribonucleotide reductase (ICP6-), defects in tumour PKR/IFN pathways, attenuated neurotoxicity		
	ICP34.5(-), UL24(-), UL56(-); replaced with a fragment of	Non-armed	NV1020	Unknown		

	HSV-2 US DNA(US2, US3, gJ and gG)					
	ICP34.5(-), ICP47(-), Us11 upregulation	GMCSF (immunostimulation)	Talimogene Laherparapvec (OncoVEX^{GM-CSF}) (T-VEC)	Defects in tumour PKR/IFN pathways, attenuated neurotoxicity		
Measles virus	Non-engineered (vaccine strain)	CEA – helps in monitoring of virus	MV-CEA	Unknown	Ovarian cancer, glioma, multiple myeloma, mesothelioma, SCCHN	Phase I and II
	Non-engineered (vaccine strain)	NIS (sodium iodide symporter) – facilitates virus tracking	MV-NIS			
Mumps	Non-engineered	Non-armed	-		Carcinoma, lymphoma, solid tumours	
Newcastle disease virus	Non-engineered	Non-armed	-	Unknown	Myelogenous leukaemia, cervical carcinoma, solid tumours	
	Non-engineered	Non-armed	NDV-HUJ		Glioma, solid tumours	Phase I and II
	Non-engineered	Non-armed	PV701			
	Non-engineered	Non-armed	MTH-68/H			
Parvovirus	Non-engineered	Non-armed	H-1PV	Interfering with cell signalling, activation of host immune responses[106]	Glioma	Phase I and II
	Non-engineered	Non-armed			Osteosarcoma	

Reovirus	Non-engineered	Non-armed	Reolysin	Defects in tumour PKR/IFN pathways	Glioma, peritoneal cancer, solid tumours, CRC, sarcoma, melanoma, ovarian, pancreatic cancer, SCCHN, lung cancer	Phase I, II and III
Retrovirus	Cytosine deaminase (CD)	Non-armed	Toca 511	Defects in anti-viral response, expression of CD by cancer cells for later use of Toca FC	Glioma	Phase I and II
Seneca Valley virus	Non-engineered	Non-armed	NTX-010	Unknown (selectivity towards human neuro- endocrine cells)	Small cell lung cancer	Phase II
Vaccinia virus	Non-engineered	Non-armed			Metastatic melanoma	
	Thymidine kinase(-), VGF(-), LacZ, CD somatostatin R	Non-armed	(vvDD-CDSR)	Unknown (EGFR pathway driven)	CRC, solid tumours, HCC, paediatric solid tumours, melanoma,	Phase I and II
Vesicular stomatitis virus	Non-engineered	IFNβ	VSV-hIFNβ	Defects in host anti-viral response	HCC	Phase I
West Nile virus	Non-engineered	Non-armed			Lymphoma, carcinoma	

CD/TK – cytosine deaminase/thymidine kinase, CEA – carcinoembryonic antigen, CRC – colorectal cancer, EGFR – epidermal growth factor receptor, GMCSF – granulocyte macrophage colony stimulating factor, HCC – hepatocellular carcinoma, ICP - infected cell protein, ICAM1 – intercellular adhesion molecule 1, IFN – interferon, IRES - internal ribosomal entry site, MV – measles virus, NDV – Newcastle disease virus, PKR – double stranded RNA activated inhibitor of translation – known as PKR, PSE1A – prostate-specific promoter-driven E1A, PSE1B – prostate-specific promoter-driven E1B, SCCHN – squamous cell carcinoma of the head and neck, VSV – vesicular stomatitis virus

1.2 MEASLES VIRUS OVERVIEW:

1.2.1 Measles virus structure:

Measles virus (MV) is a negative stranded RNA virus of the *Morbilivirus* genus from the *Paramyxoviridae* family. The schematic representation of MV structure is shown in Fig 1-1a. The genome of the virus consists of 15,894 bases that encodes for 6 structural and 2 non-structural proteins. The terminator region of each gene is followed by a three nucleotide-long conserved region (GAA) called intergenic (IG) region. The Nucleocapsid (N) protein encapsidates the viral RNA and is closely associated with the viral Large protein (L) and Phosphoprotein (P). The N, P and L proteins together form the ribonucleoprotein (RNP) complex, which is the core virus structure. The L protein is the RNA dependent RNA polymerase (RdRp) and the P acts as a chaperone during nucleocapsid assembly[107]. The Matrix (M) protein is on the inside surface of the envelope, it helps in anchoring Fusion (F) and Haemaglutinin (H) proteins and aids viral assembly and budding[108,109]. Other than the 6 structural proteins, the P gene of the MV also encodes for 2 non-structural proteins C and V. The C protein is translated from the P gene by an alternative reading frame at the second start codon. The C protein has been implicated in mediating efficient viral replication in peripheral blood cells[110], RNA synthesis[111], virulence dependence[112] and RdRp activity by blocking type I IFN response[113]. The V protein is produced from the P gene by a frame shift due to incorporation of a G residue at the conserved RNA editing site. It is known to bind both to the N and L proteins and therefore believed to regulate RNA synthesis[114].

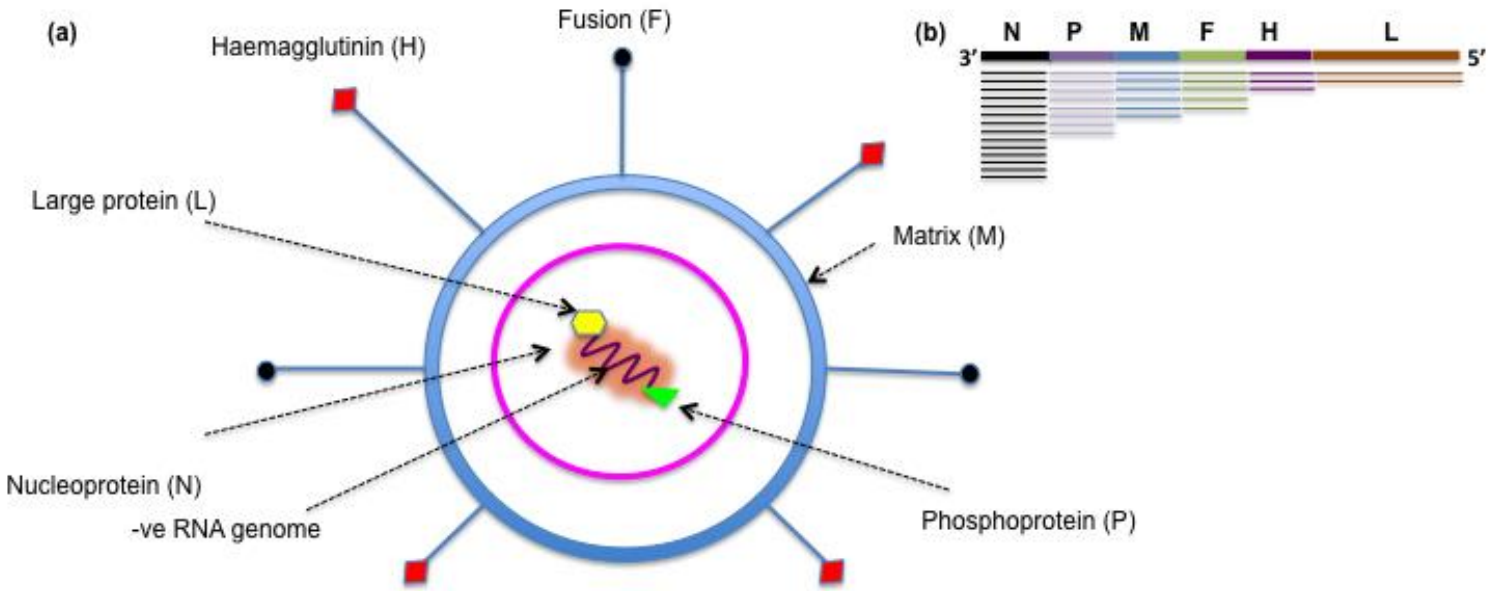

Figure 1-1: MV Structure: (a) Schematic diagram of virion structure showing MV -veRNA genome and viral proteins H, F, M, P, L and N. (b) Organisation of MV genome and MV transcription gradient showing mRNA of the genes at the 3' end are produced more abundantly compared to the 5' end.

1.2.2 MV replication:

MV infection and replication can be broadly seen as 7 steps[115] as shown in Fig 1-2:

Step 1 - Attachment: The H and the F are the membrane glycoproteins. The H binds to its receptor on the target cell, and this leads to conformational change in H and the adjacent F. The hydrophobic fusion peptide within the F protein becomes exposed and is inserted into membrane of the target cell.

Step 2 - Cell entry: Further conformational change leads to fusion of virus and target cell membranes and the genomic material enters the cell.

Step 3 - Viral mRNA transcription: During MV replication, the polymerase (L) associates with the MV RNA inside the RNP core structure at the 3' end and the mRNA of the first gene is made and polyadenylated. The polymerase dissociates or 'falls off' at the junction of the genes, known as the IG region and re-starts transcription at the beginning, ultimately producing polyadenylated mRNAs.

Step 4 - Protein synthesis: The polyadenylated mRNAs act as a template for protein synthesis. The amount of each protein synthesised depends on the position of the gene on the genome, leading to a transcription gradient wherein proteins at the 3' end are synthesised more abundantly than at the 5' end. The viral genome and the transcription

gradient are shown in Fig 1-1b. Therefore, the N is the most abundant protein synthesised, followed by P, M, F, H and L proteins.

Step 5 - Viral genome replication: Once sufficient N protein is produced, it blocks the IG regions on the MV genome, and prevents the polymerase from ‘falling off’. This enables the replication of the entire viral genome, which is transcribed to obtain the sense, genomic viral RNA.

Step 6 - Viral assembly: Once the viral genome is synthesised, it initiates the virus assembly. The viral genome, the N, P and L, forms the RNP complex to form the core structure.

Step 7 - Release: The core structure travels towards the cell membrane, and along with the M, F and H proteins gets released from the cells as virus particles.

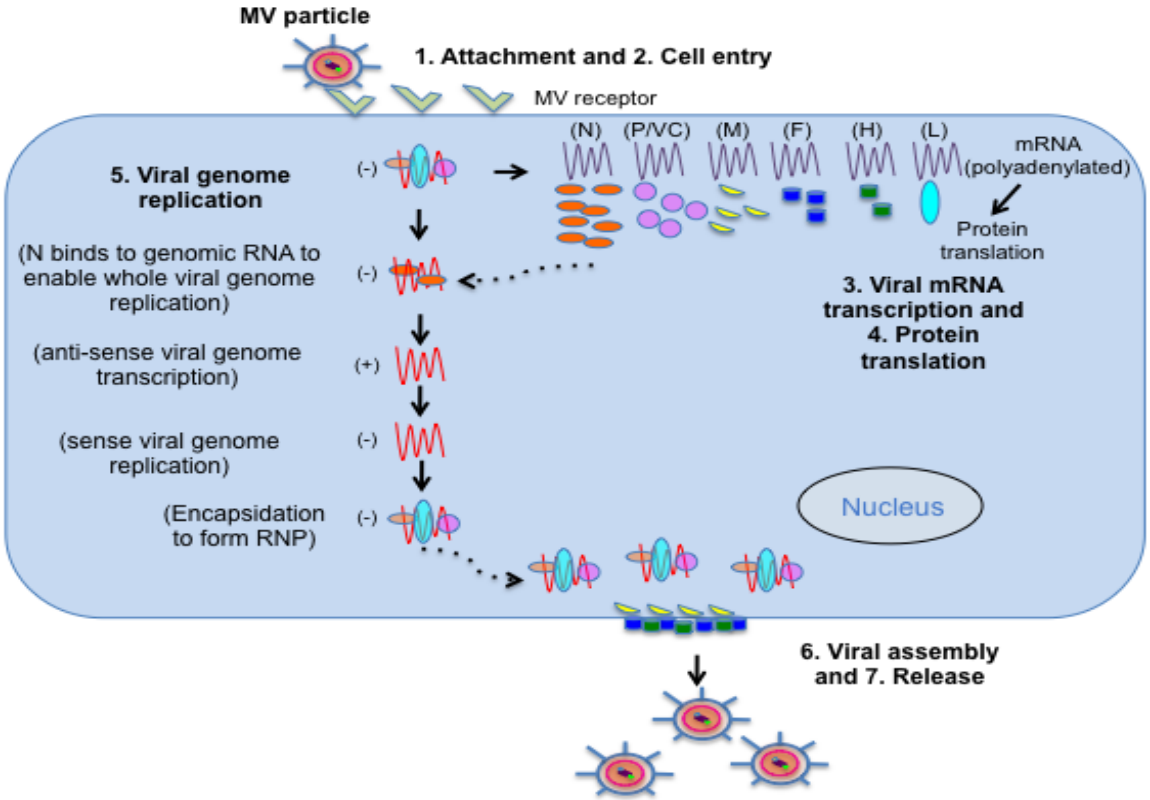

Figure 1-2: The MV replication cycle: Schematic representation of MV replication cycle and the steps involved. Adapted from Griffin et al. 2007[107].

1.2.3 MV receptors:

There are three known MV receptors CD46, signalling lymphocyte activation molecule (SLAM) also called CD150, and Nectin-4 (also called polio-virus-receptor-like 4 or PVRL4). Fig 1-3 shows a cartoon of all the three receptors.

1.2.3.1 CD46:

CD46 is a type I transmembrane glycoprotein and is ubiquitously expressed on all nucleated human cells. CD46 helps to protect cells from complement mediated lysis and is often upregulated by tumour cells[116]. The extracellular region of the CD46 receptor comprises of four short consensus repeats (SCR1-SCR4)[117]. The four SCR domains are followed by one or two O-glycosylated serine/threonine/proline (STP) rich domain, a transmembrane region and have two alternative cytoplasmic tails that result from alternative splicing[118]. The SCR1 and SCR2, present at the N-terminal are known to interact with the MV-H glycoprotein[117] (Fig 1-3). A system based on inhibition of cell fusion by MV glycoproteins was used to screen a library of 3000 different monoclonal antibodies raised against the cell surface proteins in cell lines permissive to MV infection[119]. This system helped identify one single monoclonal antibody (MCI20.6), that blocked MV binding and infection and recognised a membrane glycoprotein (57 to 67 kDa) which was sequenced and identified to be the human membrane cofactor protein CD46[119].

CD46 is a cellular receptor for many other human pathogens. For example human herpes virus 6, pestivirus, different adenovirus serotypes

Ad3, Ad11, Ad35 and Ad37 and also two types of bacteria Streptococcus pyogenes and Neisseria, all use CD46 for cellular entry[120]. Different viruses interact with different domains of the CD46 to gain cellular entry, and the cellular mechanisms that facilitates CD46 dependent cell entry also varies between different pathogens and therefore, what makes CD46 a common receptor for different pathogens is still not very clear[120]. It is suggested that the two cytoplasmic domains of the CD46 receptor can “fine-tune” T-cell mediated response, as it can drive T-cell differentiation[121] and T-cell induced inflammation[118], thereby connecting the innate and adaptive immune response[120]. The pathogens targeting the CD46 receptor can possibly interfere with the cytoplasmic tail mediated intracellular signalling pathways thereby creating an immune response imbalance[120]. Engagement of the CD46 receptor affects the host immune response and might explain to certain extent why viruses use complement receptors for cellular entry[116].

CD46 has been shown to play an important role in MV pathogenesis. One proposed mechanism is down regulation of CD46 upon MV infection due to interaction between the MV-H and the CD46 receptor, rendering the cells more susceptible to complement mediated lysis[122]. Only laboratory adapted MV vaccine strains are able to use this receptor to enter cells.

1.2.3.2 CD150:

SLAM or CD150 is a cellular receptor for the wild-type (WT) strain of MV[123]. Nevertheless the vaccine strain can also use this receptor to enter cells[124]. SLAM is a member of the immunoglobulin superfamily of receptor

molecules, which is a subset of the CD2 family of receptors. The structure is shown in Fig 1-3. It consists of two immunoglobulin (Ig)-like domains, and MV binds to the N terminal domain[125]. The extracellular domain consists of a variable region (V) and a constant (C2) region and the cytoplasmic tail is made of three repeats of tyrosine-based motifs[126]. B95a is a marmoset lymphoblastoid cell line and was first used to identify SLAM as a receptor for WT MV. This cell line is commonly used to isolate WT MV strains and therefore was considered a good source of mRNA encoding for the WT MV receptor and consequently used to create a cDNA library with the eukaryotic expression vector pCAGGS[127]. 293T cells that are not infectable by WT MV strain was transfected with different clones of the cDNA expressing pCAGGS. At the same time, the 293T cells were infected with VSVΔG* complemented with H glycoprotein of KA WT strain of MV isolated on the B95a cells and F protein from Edmonston vaccine strain (VSVΔG*-KAHF)[123]. Extensive screening of more than 400 clones of cDNA, helped in isolating the cDNA clone that showed highest level of infection in the 293T cells. DNA sequencing revealed that the clone was 91% identical to the human SLAM gene in the coding region and hence SLAM was identified to be the cellular receptor for the WT strain of MV[124].

SLAM proteins function as co-receptors for lymphocyte activation and/or adhesion and mediate tyrosine phosphorylation signals[128]. SLAM receptor expression is mainly restricted to immune cells. It is upregulated on immature thymocyte and activated B-cells and T-cells[129], mature DCs[130,131] and activated monocytes[132], but down regulated on Th2 polarised cells.

SLAM ligation promotes the activation of Th0/Th1 cells, B-cells, eosinophils, mast cell, and macrophages[133].

1.2.3.3 Nectin-4:

Nectin-4 is the most recently identified receptor for MV and is expressed at the epithelial adherens junction[134,135]. This is the putative epithelial receptor (EpR), which was long proposed[136,137] to be the receptor used by MV during natural infection, as MV can infect epithelial, endothelial and neuronal cells, which are SLAM negative[138,139]. Nectin-4 shares homology with the poliovirus and is involved in the formation of adherens junction. MV interacts with the membrane distal domain of the Nectin-4 protein (Fig 1-3). Two different groups identified this receptor independently[134,135] using similar approach of comparing upregulated membrane-associated genes in WT MV susceptible and non-susceptible cell lines using genome wide microarray expression analysis. It has been identified as a receptor for other viruses and is involved in differentiation, polarisation, movement and other cellular activities. It is expressed on cancer cell lines[140] and therefore might be relevant to MV oncolytic activity.

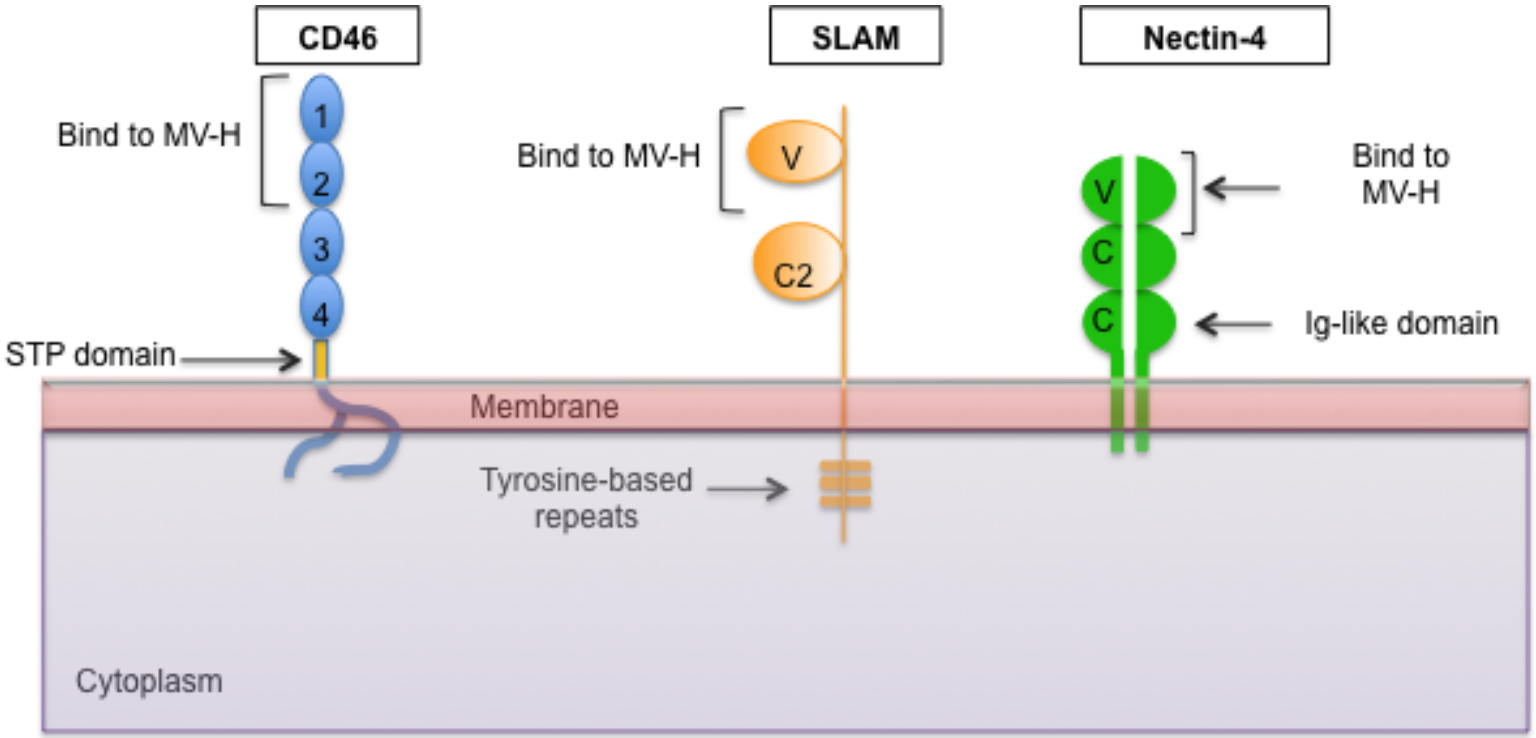

Figure 1-3: MV receptors: Schematic representation of CD46, SLAM and Nectin 4. STP domain - serine-threonine-proline rich domain; V: variable domain; C: constant domain; Ig: Immunoglobulin. Numbers 1-4 represent CD46 short consensus repeat (SCR). Adapted from Dhiman et al. 2004[116].

1.2.4 MV Strains:

WT MV is highly pathogenic and responsible for numerous deaths worldwide among unvaccinated children[141]. Enders and Peebles first isolated MV from a patient David Edmonston in the year 1954[142]. After serial passage in human kidney and human amnion tissue cultures, a strain was adapted to growth in the amniotic sac of developing chick embryos. The resultant vaccine strains underwent numerous passages in chick embryo-cell cultures, at 37°C and then at 32°C which was first used in clinical trials in USA, England and Nigeria[143,144]. The resultant Edmonston strain (Edm) had lost its pathogenicity but could still generate an immune response. Vaccination against MV infection was introduced in 1960s with both attenuated and killed vaccines[145], although the killed vaccine strain was soon withdrawn due to complications. Safe and efficacious vaccine strains have been now developed mostly from the Edm strain as shown in Fig 1-4. AIK-C, Schwarz, Moraten, Rubeovax and Zagreb are vaccine strains derived from the Edm lineage. Other vaccine strains that were obtained from different WT MV strains independently are also available in different parts of the world, for example, CAM-70 (Japan), Changchun-47 (China), Leningrad-4 (Russia) and Shanghai-191 (China)[146]. In 1963, the first live attenuated vaccine was licensed in the USA under the trade name Rubeovax[147]. Later, the more attenuated Moraten strain replaced it[148]. The AIK-C strain is used in Japan[149] and the Zagreb, is produced by serum institute of India and is most commonly used in the Expanded Programme on immunisation of the World Health Organisation (WHO)[150]. The vaccine strains had good sero-

conversion rates but still induced fever in 46% of vaccinees and therefore were replaced by more attenuated strains[147]. The Schwarz strain, generated in 1962 is more attenuated and is produced in Europe and Brazil[151] while Moraten strain (Attenuvax, Merck and Co. in the Unites States), generated by further passage in chick embryo fibroblasts[147] is used in the United Kingdom. MV vaccine is given either as a single agent or combined with other vaccine viruses such as mumps and rubella (MMR)[152,153]. In the developed countries MV vaccine is usually given in the form of MMR at 12-15 months of age, but in countries where MV is endemic, vaccines are typically administered at the age of 9 months[153].

Based on the MV-H and MV-N gene sequences, MV is assigned to 1 of 23 genotypes and one provisional genotype[154]. All vaccine strains are grouped under genotype A[155]. However, there is only one serotype, and serum samples collected from vaccinated individuals can neutralise viruses from different genotypes with variable neutralising titres[156,157]. Reported sub-optimal sero-conversion after vaccination is possibly due to lack of coverage, improper administration, age of the vaccine recipient and transport and storage of vaccine[158-160]. The vaccine strain of MV is not pathogenic in healthy individuals, and there is no evidence of the MV vaccine strain reverting to a pathogenic phenotype[161]. Humans are the only known hosts for MV, and no other animal or environmental reservoir is known to exist[145]. Some non-human primates are susceptible to MV infection[162], but to be assigned as a natural reservoir of MV that can sustain and transmit MV

infection, the size of the worldwide wild population of primates required, is not sufficient[145].

The vaccine strain derived from the Edm strain has an excellent safety record of more than 50 years as it is being used in the vaccination programmes worldwide, and has been administered to millions of people[107,163] with rare occurrence of adverse events, the most common one being fever and rash at 8-12 days post vaccination[151]. Rubeovax caused fever in 46% and rash in 16% of the recipients[147]. More attenuated strains Zagreb and Schwarz had reduced side effects such as fever in 2% and 21% recipients respectively[146]. Three percent of MV Moraten and 20% of AIK-C vaccine recipients presented with rash[146]. However, there are reports of severe adverse effects in vaccine recipients who are severely immunocompromised and are incapable of clearing the virus[164-166]. The vaccine is therefore not recommended for immunosuppressed patients, while people with HIV infection should have >200 cell/microL count of $CD4^+$ T-cell for safe administration of the virus[32]. WT MV can spread transiently to the central nervous system (CNS) in up to 50% of infected patients[167], and lead to CNS complications soon after infection as in acute encephalomyelitis (AME), or years after infection, as in subacute sclerosing panencephalitis (SSPE)[168], which is a rare, fatal consequence of CNS infection[169,170]. The third MV-induced CNS disease, progressive infectious encephalitis or measles inclusion body encephalitis (MIBE), occurs in immunosuppressed patients several months post MV infection[167]. However, there is no evidence of the vaccine strain of the virus causing any of the CNS related

complications[168,169], and immunisation by the vaccine strain has been suggested to prevent SSPE[168].

1.2.5 MVs used as oncolytic virus and relation to vaccine strains:

The different genetically modified strains derived from the MV EdmB strains are shown in the red boxes in Fig 1-4. Most MV vaccine strains used today comprise of very closely inter-related laboratory strains, derived from the 1954 clinical isolate[142,171,172]. Initially, the commercially available strains, such as the Moraten[50] and Edm-Zagreb[173] were tested as oncolytic viruses due to their excellent safety profile and commercial availability[174]. MV Moraten had shown similar anti-tumour potency in an *in-vivo* model of ovarian cancer when compared to the MV-tag-Edm modified strain used at $1x10^6$ infectious units[50]. Although the MV Moraten was packaged and available commercially at $1x10^3$ infectious doses, it was impractical to use it in clinical trials where an effective dose in excess of $1x10^8$ was required. The phase I clinical trial using the Edm-Zagreb strain in cutaneous T-cell lymphoma had shown some promising results[173] but awaits further studies. The MV-tag-Edm and its derivatives showed extensive anti-tumour properties in mouse models of different human malignancies[51,52,175-179]. The MVNSe was derived from the MV-tag-Edm and has unique NarI and SpeI cleavage sites[180] to facilitate easier genetic manipulation. MVs has been genetically modified to express different gene of interest, for e.g. MV expressing green fluorescent protein (MV-GFP), carcinoembryonic antigen (MV-CEA), sodium iodide symporter (MV-NIS), all developed from the EdmB vaccine strain and are discussed in detail in section 1.3.1. The MVhGCSF strain was derived

from the MVNSeGFP strain. The vaccine strains used as a part of this thesis are shown in blue in Fig 1-4.

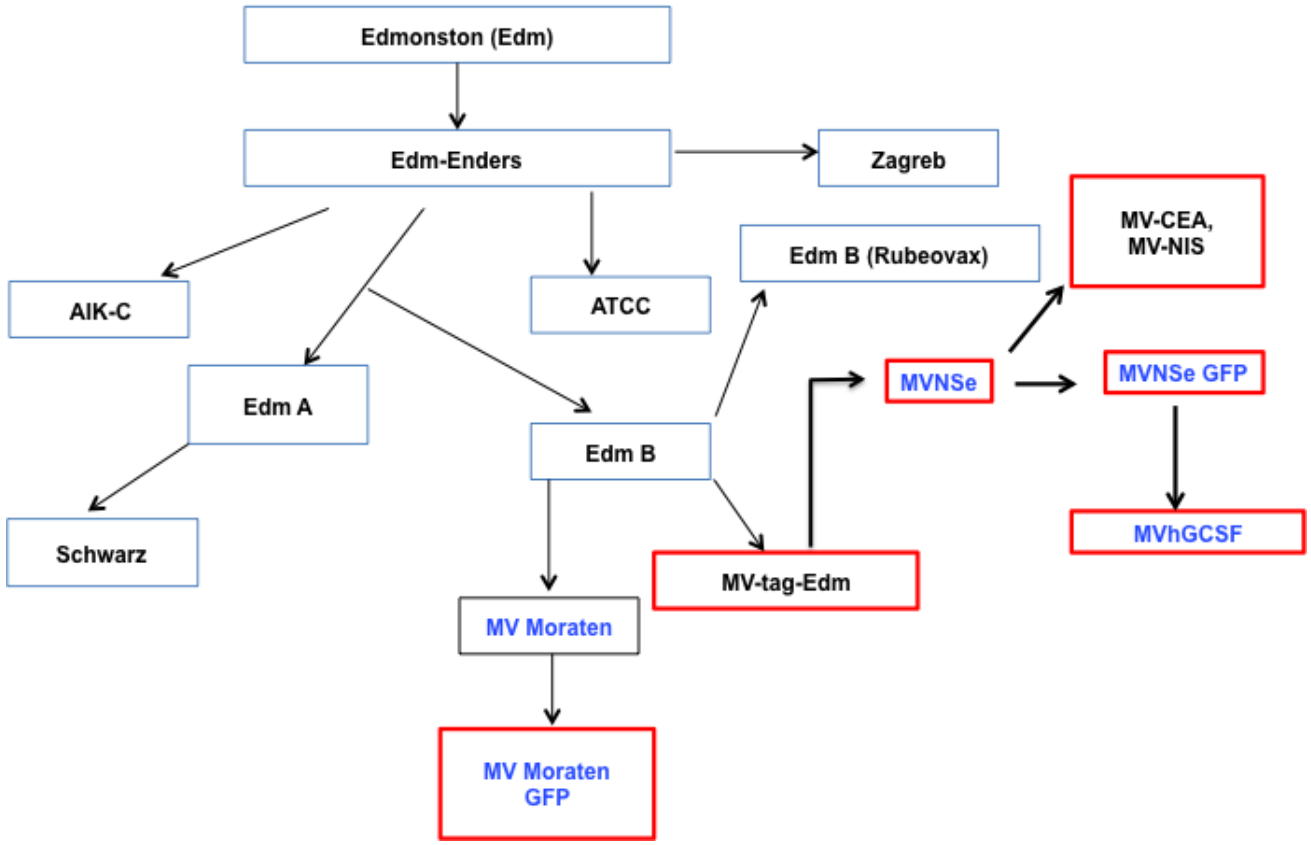

Figure 1-4: Edmonston vaccine lineage: MV strains in the red boxes are genetically modified strains derived from EdmB strain. Highlighted in blue are the MV strains used in this thesis. Adapted from Rota et al. 1994[171].

1.2.6 Rescue of MV by reverse genetics:

MV can be rescued from cloned cDNA by reverse genetics[181]. Fig 1-5 shows the schema for this procedure. The full length MV cDNA plasmid is under the control of T7 promoter. Vero (African green monkey kidney epithelial cells) is first infected with the recombinant modified vaccinia virus (Ankara) (MVA). This virus allows expression of the T7 RNA polymerase {DNA dependent RNA polymerase (DdRp)} without vaccinia virus replication. Next, the cells are transfected with individual plasmids coding MV proteins N, P and L under the CMV promoter, and the full length MV, which is under the T7 promoter. T7 RNA polymerase help synthesise the anti-genomic RNA template from the full-length MV plasmid in the cytoplasm of the Vero cells, while the N, P and L proteins are synthesised in the nucleus of Vero cells, which encapsidates the RNA template formed from the cloned MV cDNA, to form the RNP core structure. Encapsidation initiates MV-N, P and L dependent replication of MV genomic RNA. When all the individual components of the virus are present in optimum quantities, they are assembled and released as viral particles, as during natural infection. In the laboratory, successful rescue is recognised by the occurrence of multinucleated syncytia, which can be ‘picked’ to further propagate the novel clone.

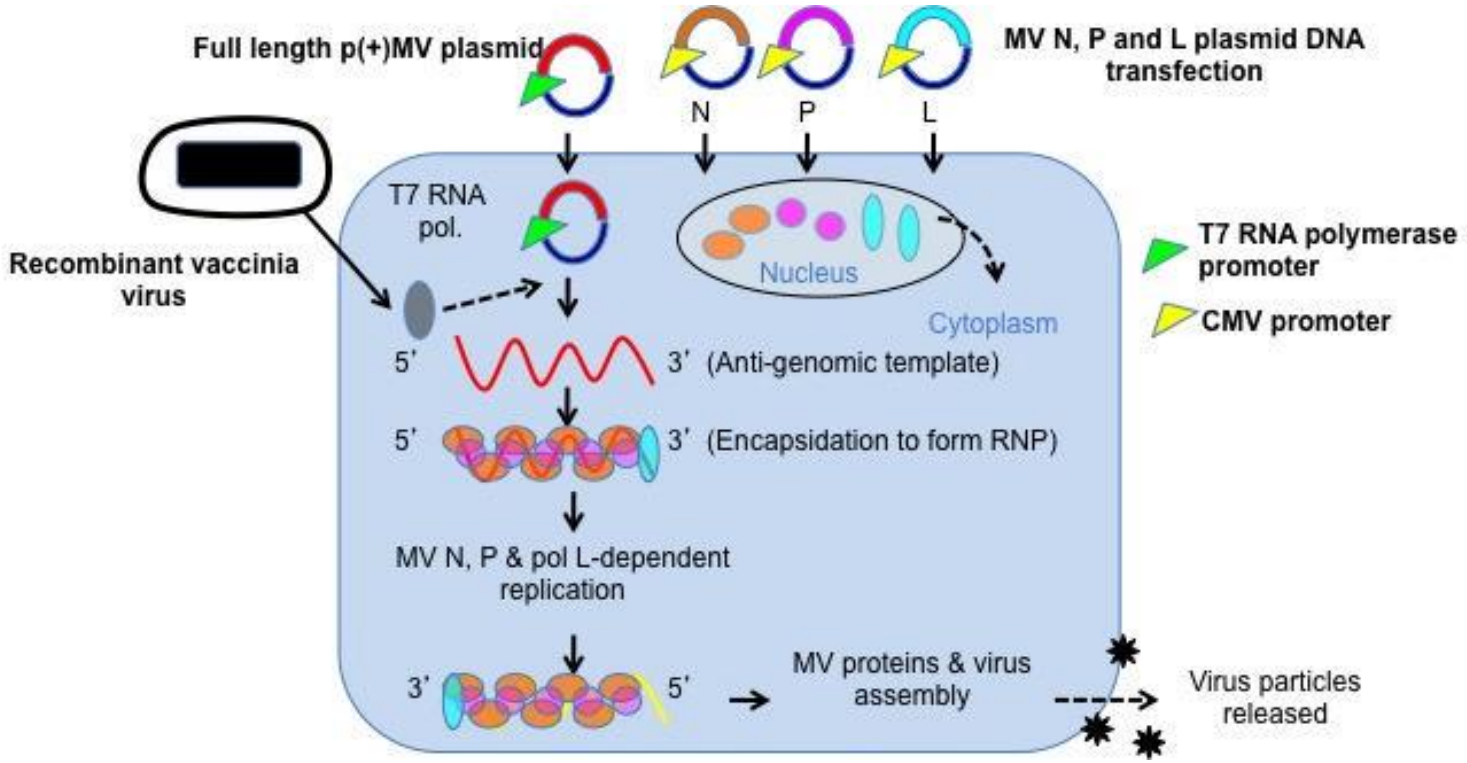

Figure 1-5: Rescue of MV from cloned cDNA: Schematic representation of reverse genetics methodology using multiple plasmid transfection approach and recombinant Vaccinia Ankara virus to obtain MV particles. Adapted from Radecke F. et al. 1995[181].

An alternative to the use of MVA is the rescue of MV using a cell line (293-3-46 – derived from a human embryonic kidney cell line 293, transformed by adenovirus type 5 DNA)[182], stably expressing the MV-N, MV-P and the T7 RNA polymerase[181]. This cell line is then transfected with the full-length MV plasmid and the MV-L plasmids, subsequently forming the MV particles as described above.

1.2.7 Models for studying MV pathogenesis and vaccination:

Naturally infected humans, naturally and experimentally infected macaques, experimentally infected cotton rats and murine models and numerous *in-vitro* systems have contributed to our understanding of MV infection and pathogenesis[107].

1.2.7.1 Primates:

Old world primates were the first animal models used to study MV pathogenesis and for vaccine development, as they were highly susceptible to MV infection. They are among the non-human primates closely similar in their clinical, virological, immunological and pathological parameters associated with measles infection in humans[115]. Two different species, Rhesus macaque (*Macaca mullata*) and Cynomolgus macaques (*Macaca fascicularis*) has been widely used in MV pathogenesis studies and vaccine development[139,183-187]. The macaques develop a measles-like illness when challenged with WT MV but not with the attenuated vaccine strain (EdmB)[183,185,188]. However, a drawback of using the macaques as a model to study the MVEdmB strain of measles is the abundant expression of MV

receptor CD46 in their red blood cells (erythrocytes) as opposed to their absence in humans. Therefore, MVEdmB can agglutinate the macaque erythrocytes thereby slowing virus dissemination, which potentially abates the relevance of virulence study of the vaccine strain of virus in this model[189]. Although they still remain an important model of choice for studying WT strains.

The new world monkeys are even more susceptible to MV infection when compared to the old world monkeys, but develop a different pathogenesis than in humans, associated with very high rates of mortality[190,191]. Squirrel monkey was chosen to be an ideal model to test attenuated MV-NIS in pre-clinical toxicology and bio-distribution study, as they express a truncated version of the CD46 that does not bind vaccine strain of MV[192], and therefore upon infection (via SLAM interaction) can cause measles like illness comparable to humans.

1.2.7.2 Rodent:

Mice are popular models for scientific research because they are small, cost effective, and easy to house and have shorter gestation compared to non-human primates. Unfortunately mice are not susceptible to MV infection and therefore, several CD46 transgenic mice have been generated to study MV pathogenesis[193]. Among them CD46 transgenic mice, which are also lacking the IFN-α/β receptor ($Ifnr^{KO}$ CD46 Ge) have been used for most toxicology studies. These mice express human CD46 with tissue distribution similar to CD46 expression in humans, including low to

absent expression on erythrocytes[194]. Upon intranasal route of infection the virus shows enhanced spread into the lungs and a potent inflammatory response due to lack of type I IFN signalling[195,196]. Though the lack of IFN response limits their application in immune response related studies, this remains a choice for most toxicology pre-clinical studies.

Another model for studying WT clinical isolates of MV is transgenic mice expressing the CD150 or SLAM receptor as CD46 transgenic mice are not susceptible to WT strains. Several transgenic lines expressing CD150 has been described[197-202], which differs in the promoter used to drive CD150 expression. These mice have proven very successful in studying WT MV, and some of them follow the natural routes of MV infection making them very desirable[115].

Cotton rats have shown to support MV replication and are more practical and less expensive models compared to the macaque. It has been evaluated as a pre-clinical model of MV vaccine strains[203]. Though the vaccine strain of MV doesn't cause overt disease in these animals, they have been shown to replicate in the lung tissue, immunosuppress the animal and disseminate from the lungs[204]. Although clinical isolates fail to infect cotton rats limiting their utility in replacing non-human primates, they remain one of the closest models for studying MV[203].

1.2.7.3 Ferret:

Ferrets' susceptibility to a range of respiratory viruses and their relatively small size makes them an attractive animal model to study viral pathogenesis. They are not susceptible to MV infection but develop sub-acute encephalitis upon infection with sub-acute sclerosing panencephalitis (SSPE) isolates[205]. Additionally they are natural host for canine distemper virus (CDV), which is closely related to MV and causes measles like characteristic rashes in ferrets with all signs of disease seen in MV-infected humans[206]. This model has been used to study the C and V proteins of MV and how they contribute in immunosuppression and overall pathogenesis upon binding to SLAM[115].

1.2.7.4 Humans:

Being the only natural host of MV infection, data from humans are unparalleled. The peak of viral replication in humans is generally reached before the onset of observable symptoms and viral clearance coincide with clinical symptoms, which makes it challenging to study MV pathogenesis in human cases[207]. Therefore, current understanding of measles comes from studies in macaques[208] (see 1.2.7.1).

1.2.8 Natural MV infection:

Natural MV infection leads to a complicated cascade of innate, cellular and humoral immune response, which helps in clearing the infection. Use of the models described above (section 1.2.7) has helped elucidate the immune

response to MV. These models are vital in understanding both pathogenesis of natural measles infection and the immune response to the use of oncolytic, vaccine strains.

MV infection is initiated at the respiratory tract, from where it spreads to local secondary lymphoid tissue most probably after uptake by lung DCs or alveolar macrophages[209,210]. MV replicates in lymphatic tissue efficiently and infected cells enter the blood circulation and can be detected by 7-9 days post infection in peripheral blood mononuclear cells (PBMCs), including B-cells, T-cells and monocytes[183,185]. Infection spreads from the blood to the distal lymphoid tissues and to epithelial and endothelial cells in multiple organs including liver, brain and skin[211,212].

1.2.8.1 Host immune response to MV infection:

1.2.8.1.1 Innate immune response:

MV is transmitted by aerosols and thought to first infect the cells located in the respiratory epithelial tissues, including mucosal DCs[115]. Macrophages, DCs and NK cells have all been implicated in the innate immune response at the site of primary infection. The macrophages can engulf the entire virus and destroy them into pieces[115]. Furthermore, the viral components can be recognised by cellular sensors, which can induce an inflammatory response, via type I IFNs. The type I IFNs released by the infected cells can activate NK cells to produce type II IFN, IFNγ, which can directly kill the infected cells[213].

1.2.8.1.2 Viral RNA recognition:

Signature molecules from microorganisms - glycoproteins, lipopolysaccharides, proteoglycans, nucleic acids including ssRNA are the pathogen associated molecular patterns (PAMPs) that are detected by the host innate immune cell receptors - pattern recognition receptors or PRRs. PRRs implicated in MV detection are toll-like receptors (TLRs) and retinoic acid inducible gene I (RIG-I)-like receptor (RLR)[214-216]. Recognition of PAMPs by the PRRs leads to a type I inflammatory response and plays a central role in eradication of the viral infection[217]. Upon binding to these cellular sensors, the viral components induce the JAK/STAT signalling pathway leading to the formation of the IFN stimulated gene factor 3 (ISGF3) complex, comprising of the STAT1, STAT2 and IFN regulatory factor 9 (IRF9)[218,219]. The ISGF3 complex then translocate to the nucleus, where it activates the IFN-stimulated response element (ISRE) gene mediated transcription leading to IFN production and establishment of the anti-viral state[220].

1.2.8.1.3 TLR mediated viral recognition:

TLR family members play a very important role in initiating an anti-viral response. Of the 10 human TLRs, TLR2, 3, 4 7 and 8 are known to be involved in RNA virus recognition[216]. WT MV-H glycoprotein interacts with TLR2 on macrophages and activates signalling via a pro-inflammatory pathway and stimulates induction of interleukin 6 (IL6) and increases surface expression of CD150. The vaccine strain is unable to do this, but a single mutation at the H protein at position 481, can turn the vaccine strain back as

a TLR2 agonist[221]. In the plasmacytoid DCs (pDCs), the TLR receptors TLR7 and TLR8 are present at the endosomal compartment and detect ssRNA via internalisation and digestion of the virus[222,223]. MV infects cells by direct membrane fusion, and therefore are less likely to be detected by TLR7 and TLR8 in the endosome of pDCs[216], and consequently the IFN response to *paramyxoviruses* have been shown to be independent of the TLR7 and endosome acidification[224]. Nevertheless, the MV Schwarz vaccine strain has been shown to interact with TLR7 and TLR9 on pDCs and inhibit IFNα and IFNβ production by pDCs, which may contribute towards the characteristic immune suppression, super infection and Th2 biased immunopathology of MV[225].

1.2.8.1.4 RLR mediated viral RNA recognition:

The RLR family are a group of cytosolic PRRs that can detect PAMPs to distinguish between self host RNA from non-self genetic material from the RNA viruses thereby leading to activation of downstream effector molecules such as type I IFNs and other pro-inflammatory cytokines involved in an innate anti-viral and inflammatory gene expression[226]. The RLR family consists of the RIG-I, MDA5 (melanoma differentiation gene 5) and LGP2 (laboratory of genetics and physiology-2). RIG-I and MDA5 possesses caspase activation and recruitment domains (CARDs) on their N-terminal that upon activation interacts with the MAVS (mitochondrial antiviral signalling) protein present on the mitochondria, and lead to the activation of the downstream IFN signalling pathway[226].

Both RIG-I and MDA5 RNA helicases contribute to the induction of IFNα/β in MV-infected human cells[227]. MV can interact via the RIG-I/MDA5 signalling pathway with MDA5 preferentially binding to (+) sense RNA of MV, while RIG-I binding to the (-) sense RNA within the trailer region and the adjacent L, which leads to downstream signalling[228]. WT MV has been reported to inhibit the JAK/STAT mediated type I IFN signalling pathway largely than the attenuated vaccine strain[229]. The MV-C protein of the WT MV has been shown to inhibit the production of type I IFNs[230] while the P and V proteins block the phosphorylation of STAT1 and eventually translocation of STAT1/STAT2 complex into the nucleus[231-233]. Mutant MV deficient in V or C genes produce very high levels of IFNβ compared to their parental counterpart, and require protein kinase PKR and mitochondrial adapter MAVS for maximum IFNβ induction[234]. Both V and C proteins are important in controlling the inflammatory response to the virus and the innate immunity[235].

1.2.8.1.5 Adaptive immune response:

Humoral and cellular immunity play a very important role in MV clearance and long-term protection from subsequent infection. MV infection leads to a very robust cellular response with activated $CD4^+$ and $CD8^+$ cells that can be isolated from the MV-infected epithelial cells. The activated T-cells play a major role in clearance of the virus in macaques, where depletion of $CD8^+$ T-cells leads to prolonged viremia[236]. This Th1 type response, which is associated with, increased level of IFNγ and IL2 is designed to promote

clearance of virus infected cells. This switch to a Th type 2 (Th2) response later, that leads to the production of type 2 cytokines - IL4, IL10, and IL13 and helps in generation of anti-MV antibodies and immunological memories. The $CD8^+$ cells are rapidly cleared upon clearance of the infection and no infectious virus is detected. However, MV RNA can be isolated from the patients for weeks after recovery, which is responsible for the presence of activated $CD4^+$ T-cells and helps in maintaining long-term protection[237].

Post MV infection, anti-MV antibody is detected within 72 hours of the onset of rash, which is mostly IgM. The IgM response lasts for up to 28 days, after which an IgG response begins and provides lifelong immunity[115,238]. The antibody response is against the main structural proteins, with anti-N antibody at the highest, followed by H, F and very little to the M protein[239]. Anti-MV antibody can be both neutralising and non-neutralising and though anti-F neutralising antibody is present, the majority of the neutralising antibody is against MV-H[240,241]. World Health Organisation (WHO) has assigned presence of 200mIU/ml of neutralising antibody as a necessary level to confer protection to MV[242,243]. The MV-specific neutralising antibody plays a key role in preventing MV infection, and contributes to MV clearance with the help of the cellular immune response from the start of MV infection[244-246].

1.2.8.1.6 MV-mediated immune suppression:

MV infection is associated with increase in susceptibility to other infections and this is due to the immunosuppressive effects of MV infection

and measles related deaths are often caused by secondary infections, most commonly diarrhoea or pneumonia[247]. Evidence of immune suppression is first detected with the onset of measles rash and generation of the immune response to MV, which eventually results in clearing of the virus and lifelong immunity[237]. A number of MV-induced mechanisms of direct and indirect immunosuppression have been proposed which includes lymphopenia, type 2 skewing of cytokine responses and suppression of lymphocyte multiplication[237]. MV infection is associated with lymphopenia, which is caused by susceptibility of the lymphocytes to increased cell death[212,248]. Engagement of the CD150 receptor causes CD95 mediated apoptosis[249,250], and MV infection per se can induce bystander lymphocyte apoptosis[251,252], which possibly contributes to lymphopenia. MV infection *in-vitro* can cause inhibition in lymphocyte proliferation by halting lymphocyte cell cycle progression associated with G1 arrest[253,254].

1.3 MEASLES VIRUS AS AN ONCOLYTIC AGENT:

One of the first observation of MV as a potential oncolytic agent was spontaneous regression of lymphomas in a 8-year-old boy, after contracting natural MV infection[255]. Almost three decades later, some of the initial work was done in B-cell malignancies with MV as an oncolytic virus. In 2001, Grote et al[175] from my group showed that MVEdm vaccine strain is capable of causing regression of large established lymphoma tumours. In this model, the effect of the presence of anti-MV antibody was also tested and it did not abrogate the anti-tumour effect. In 2004, Dingli et al[256] showed the oncolytic

effect of MV in myeloma xenografts. Both IV and IT routes of MV administration were successful in tumour regression in this model. The potential of MV as an oncolytic virus was extrapolated to solid tumours and it has been shown to be oncolytic in numerous other tumour models like medulloblastoma[257] that used the MV expressing green fluorescence protein (GFP), in an intra-cerebral murine xenograft model and mesothelioma[258] that used MV encoding for IFNβ and the sodium iodide symporter (NIS). Different routes of MV administration, IV, IT and IP were investigated in several studies and various modifications were introduced into MV genome to enable tracking of the virus *in-vivo* conveniently (MV-GFP, MV-CEA, MV-NIS) or increase its therapeutic effect (MV-IFNβ). A non-exhaustive list of different tumour models, routes of MV administration and several MV modifications are shown in Table 1.4. All these models described in Table 1.4, where MV was shown to be oncolytic were human xenografts established in immunocompromised mice. The limitations to these models are obvious, as immune responses cannot be studied. Some efforts have been made to address this within immunocompetent syngeneic mouse tumour models using MV, with entry re-targeted to murine cells.

Table 1.4: MV as an oncolytic agent in different mouse tumour models:

Tumour model	MV modification	Routes of MV administration	Publications
Medulloblastoma	MV-GFP	IT	Studebaker et al., 2012[257]
Mesothelioma	MV-IFNβ; MV-NIS	IT	Li et al., 2010[258]
Breast cancer	MV-GFP	IV; TT (intrapleural)	Iankov et al., 2009[259]
Prostate cancer	MV-luc, MV-GFP, MV-CEA	IT	Msaouel et al., 2009[260]
Glioma	MV-GFP-H (AA)-IL-13, MV-GFP,	IT	Allen et al., 2008[261]
Ovarian cancer	MV-CEA	IP	Galanis E et al., 2008[262]
Myeloma	MVEdm	IV, IT	Peng et al., 2001[52]
Lymphoma	MVEdm, MV-LacZ	IV, IT	Grote et al., 2001[175]

In a murine colon adenocarcinoma model developed from MC38cea cell line (that express the CEA protein) in a C57BL/6 mice, a re-targeted MV expressing scFvCEA was used to treat the tumour. The MV-CEA was armed with a pro-drug convertase, purine nucleoside phosphorylase (PNP) to enhance the oncolytic activity of MV. When pro-drug MeP-dR (9-2-deoxy-beta-D-ribofuranosyl-6-methylpurine) was used with the MV-CEA-PNP, very significant tumour regression was observed when compared to MV-CEA or the MeP-dR pro-drug alone. This correlated with pro-longed survival[263]. Another way in which MV has been studied in immunocompetent models has provided assistance with the toxicology and bio-distribution studies, which are crucial before clinical trials. There are by now several lines of mice transgenic for MV receptors including SLAM[193,200,202,264-266]. Most toxicology studies in MV to date[267] have been done in CD46 transgenic mice, which are also lacking the IFNα/β receptor ($Ifnr^{KO}$ CD46 Ge). These mice express

human CD46 in a tissue distribution that mimics the pattern of CD46 expression in humans, including low to absent expression on erythrocytes[194].

The different modification strategies of MV to enhance its oncolytic properties are discussed in detail in the next section (see 1.3.1).

1.3.1 Modifications to MV for more effective cancer therapy:

1.3.1.1 MV targeting:

MV is one of the few viruses where full re-targeting by modification of the envelope glycoprotein has been achieved. Targeting strategies have relied upon display of growth factors or single chain fragment variable (scFv) antibodies. MV entry targeted via the epidermal growth factor receptor (EGFR) and insulin-like growth factor-1 (IGF-1) receptor were the first to be reported[268]. The genes coding for EGF and IGF-1 were cloned into MV-H in frame linked by a serine and glycine rich linker sequence and then cloned into the MV backbone sequence replacing the H. The new virus was able to enter and infect CD46-negative rodent cells - Chinese hamster ovary (CHO) stably expressing the hEGFR and mouse NIH-3T3 cells stably expressing the hIGF1 receptor. scFv-CD20[269], scFv-anti-hCEA[270] and scFv-anti-CD38[271] have all been displayed on the MV-H to facilitate targeted entry to CD20, CEA and CD38 expressing cancer cells, respectively.

This targeting strategy, whilst permitting entry to non-permissive target cells still allowed MV to enter and infect permissive cells via CD46 and SLAM. Therefore, attempts at fully re-targeting MV were carried out by

introducing mutations in the receptor-binding domain of MV-H to render the H, CD46 and SLAM “blind”. Introducing mutations at amino acids which were carefully chosen as being putatively involved in receptor binding within the MV-H protein prevented the viral cell entry via CD46 or SLAM, making the virus effectively CD46 or SLAM “blind”[272]. Nakamura et al. employed a related set of mutations in the development of a method to rescue fully re-targeted CD46 and SLAM blind MV. An anti-CD38 scFv was fused to the C terminus of the MV-H protein wherein residues involved in binding to CD46 (451,481) and SLAM (529, 533) were mutated. Paired mutations were introduced at positions 451 and 529, or 481 and 533 on the MV-H to make the virus blind to both CD46 and SLAM[273]. These mutations supported fusion via the targeted CD38 receptor but not via CD46 or SLAM. The viruses were rescued on CHO-CD38 cells. Later, a system was developed to rescue this virus by introduction of a His-Tag, a peptide containing 6 histidine residues at the C terminus of the mutated H protein[273]. The virus could now be rescued and propagated on Vero cells expressing a receptor for α-His peptide. Other MVs, which are fully re-targeted have since been generated which can enter the target cells via EGF[273], EGFvIII[274], and IL-13-Rα2[261] receptors. MV selectively activated by human tumour cells overexpressing matrix metalloproteinases has also shown to have enhanced specificity of replication within tumours[275,276].

1.3.1.2 Tracking:

MV has also been modified to add genes to facilitate tracking of the virus *in-vivo*. Marker genes such as GFP, CEA, luciferase (luc), have been

used for tracking, monitoring and imaging purposes both *in-vitro* and *in-vivo*. CEA antigen is a non-immunogenic soluble glycoprotein, which is present in normal mucosal cells and can be over expressed by adenocarcinoma cells. It has the advantage of being quantitated by a standardised routine laboratory assay. MV expressing human CEA has been used in the ovarian cancer clinical trial for non-invasive monitoring of patients after therapy by monitoring the CEA level in the serum[277]. Due to characteristic elevation of CEA in certain tumour types, MV expressing NIS was developed as a clinical reporter gene.

1.3.1.3 Therapeutic enhancements:

NIS has the advantage of potentially facilitating the therapeutic effect of oncolytic MV. NIS is normally expressed in the thyroid tissue on thyroid follicular cells and facilitates the accumulation of iodine by thyroid follicular cells[278]. When MV-NIS infected cells express NIS, uptake of exogenously administered radioiodine can occur and this provides a basis for *in-vivo* radioiodine imaging studies that can reveal the profile of MV-NIS gene expression and the location of MV-NIS infected cells. Isotypes like ^{123}I and ^{124}I were used in a medulloblastoma tumour model[279]. MV-NIS treatment, both on its own and in combination with ^{131}I, enhanced tumour stabilisation and regression in treated mice and significantly extended their survival times. Radioiodine was concentrated at the tumour sites in mice given ^{131}I. In addition, mice with localised tumours that were given ^{131}I after MV-NIS treatment exhibited a significant survival advantage over mice given MV-NIS alone[279].

In another approach of enhancing therapeutic activity of MV in our laboratory, in an *in-vivo* model of lymphoma, MV expressing murine GMCSF (mGMCSF) led to significant infiltration of neutrophils in the injected tumour resection when compared to the unmodified MV. This led to much superior tumour regression[280]. Furthermore, MV expressing neutrophil-activating protein (NAP) of helicobacter pylori - a powerful enhancer of inflammatory reaction showed Th1-polarised immune response that improved survival in breast cancer and aggressive lung metastatic breast cancer models. High level of NAP was secreted by the infected tumour cells, which led to high levels of TNFα, IL6 and IL12/23 cytokine concentrations in the pleural effusion[281].

Arming the MV with pro-drug convertase and cytokines is an alternative approach of adding a therapeutic layer to MV-mediated oncolysis. Pro-drug convertase are enzymes that can convert a non-toxic substrate to a toxic drug. For example, Escherichia coli purine nucleoside phosphorylase (PNP) can convert non-toxic fludarabine and purine analogue 6-methylpurine 2'-deoxyriboside (MeP-dR) to toxic 2-fluoroadenine and 6-methylpurine respectively[263,282]. These are highly diffusible and can inhibit DNA, RNA and protein synthesis[283]. MV have been armed with PNP and has shown enhanced oncolytic activity in lymphoma[282,284], pancreatic cancer[285] and a murine colon carcinoma model[263]. However, fludarabine is considerably cytotoxic when administered systemically[286]. Another example is cytosine deaminase (CD), which converts pro-drug 5-fluorocytosine (5-FC) to 5-fluorouracil (5-FU) and subsequently to 5-fluorouridine-monophosphate. MV

armed with CD was shown to improve oncolytic effect of MV in cholangiocarcinoma[287] and head and neck squamous cell carcinoma[288].

1.3.2 MV Clinical Trials:

MV is being evaluated in several phase I and II clinical trials (see Table 1.5 - modified from Russell 2012[31], Guillerme 2013[289], clinicaltrials.gov - NCT02192775). Some trials are completed while others are still recruiting. Different routes of administration are being evaluated in these studies. The first phase I clinical trial was carried out in Cutaneous T-cell Lymphoma (CTCL) and used IFNα to prevent infection in IFNα sensitive healthy cells in combination with MVEdm-Zagreb therapy. In this trial, MV induced cytopathic effect locally, after IT injections even in the presence of anti-measles antibodies. Additionally, tumour regression was observed in three patients with notable regression of distant lesions that were not injected[173]. The data from the ovarian cancer trial, which used MV-CEA, showed no dose related toxicity in all 21 patients recruited with clinical response observed in 14 out of 21 patients[262,290,291]. A recent preliminary report from a phase I clinical trial have shown very good response rate in 2 patients with multiple myeloma. Both the patients were treated with MV-NIS at $1x10^{11}$ dose IV, and one of the two patients showed a durable complete remission of 9 months[292]. There are currently 5 Phase I/II clinical trials that are open and recruiting and two that are active but not recruiting yet, and one more in the pipeline to start this year (clinicaltrials.gov).

Table 1.5: MV in Clinical Trials:

Virus Strain	Phase	Cancer Type	Route	Combination	Status	Centre
MV-CEA	I	Glioblastoma multiforme	CNS	-	Recruiting	Mayo Clinic
MVEdm-Zagreb	I	CTCL	IT	IFNα	Completed	Zurich University
MV-NIS and MV-CEA	I	Ovarian cancer or primary peritoneal cancer	IP	-	Completed	Mayo Clinic
MV-NIS	I	Head and neck cancer	IT	-	Recruiting	Mayo Clinic
MV-NIS	I	Pleural mesothelioma	IP	-	Active	Mayo Clinic
MV-NIS	I	Peripheral nerve sheath tumour	IT	-	Starting June 2016	Mayo Clinic
MV-NIS	I/II	Ovarian cancer	IPMSc	-	Active	Mayo Clinic
MV-NIS	II	Multiple myeloma	IV	CTX	Recruiting	University of Arkansas
MV-NIS	II	Ovarian, fallopian, peritoneal cancer	IP	-	Recruiting	Mayo Clinic

1.4 MECHANISMS OF MEASLES VIRUS MEDIATED ONCOLYSIS:

The mechanism by which MV selectively kills tumour cells is not completely understood. Different mechanisms, both direct and indirect, have been proposed and are summarised in Fig 1-6, and is discussed below.

1.4.1 MV receptor overexpression by tumour cells:

One of the proposed mechanisms of direct oncolysis is selective entry of MV into tumour cells. MV vaccine strains preferentially enter the cells via CD46 receptor, which mediates attachment of the virus, cell entry and cell-cell fusion, and is known to present on all nucleated cells, and is often overexpressed on transformed cells[119,293]. The ability of the attenuated MV to enter a cell via CD46 have been shown to help the virus preferentially enter and infect transformed cells making it a potential mechanism of oncolysis by MV. Anderson et al. showed that cells engineered to express different densities of CD46 on their surface, led to progressively increased rate of cell infection and cell-cell fusion with higher densities of CD46[294]. Also, the recently identified receptor of MV, Nectin 4, which is considered a tumour marker for breast, lung and ovarian cancers, is overexpressed on these cells, suggesting the possible MV selectivity in these cells[295-297]. Other than the viral receptors, cancer cells overexpress specific proteases like matrix metalloproteinases and MV and other *paramyxoviruses* require protein cleavage of the fusion F protein to facilitate cell entry, suggesting a possible mechanism[298-300].

In addition to CD46, all MV strains including vaccine strains retain the ability to enter cells via SLAM[301] and certain SLAM positive haematological malignancies have regressed following natural MV infection[255,302]. In an *in-vitro* study, SLAM was shown to be a dominant oncolytic MV receptor in mantle cell lymphoma and blocking SLAM with antibodies reduced MV entry by 70%. MV modified to enter via SLAM alone elicited a tumour regression

equivalent to unmodified MV, whereas MV modified to enter via CD46 alone was comparable to vehicle control. This study showed that MV infection and spread in mantle cell lymphoma is entirely SLAM dependent[301].

1.4.2 Enhancement of apoptosis:

MV infection can also induce direct cytotoxicity by enhancing the apoptotic signalling pathway in the infected cells. For instance, MV infection of glioblastoma multiforme cells in combination with radiation therapy led to higher apoptosis inducing cleavage of the poly ADP-ribose polymerase (PARP), mediated mainly by the extrinsic caspase pathway[303]. In another model of mesothelioma, MV infection led to apoptotic cell death of the infected mesothelioma cells, which were readily phagocytosed by DCs[304].

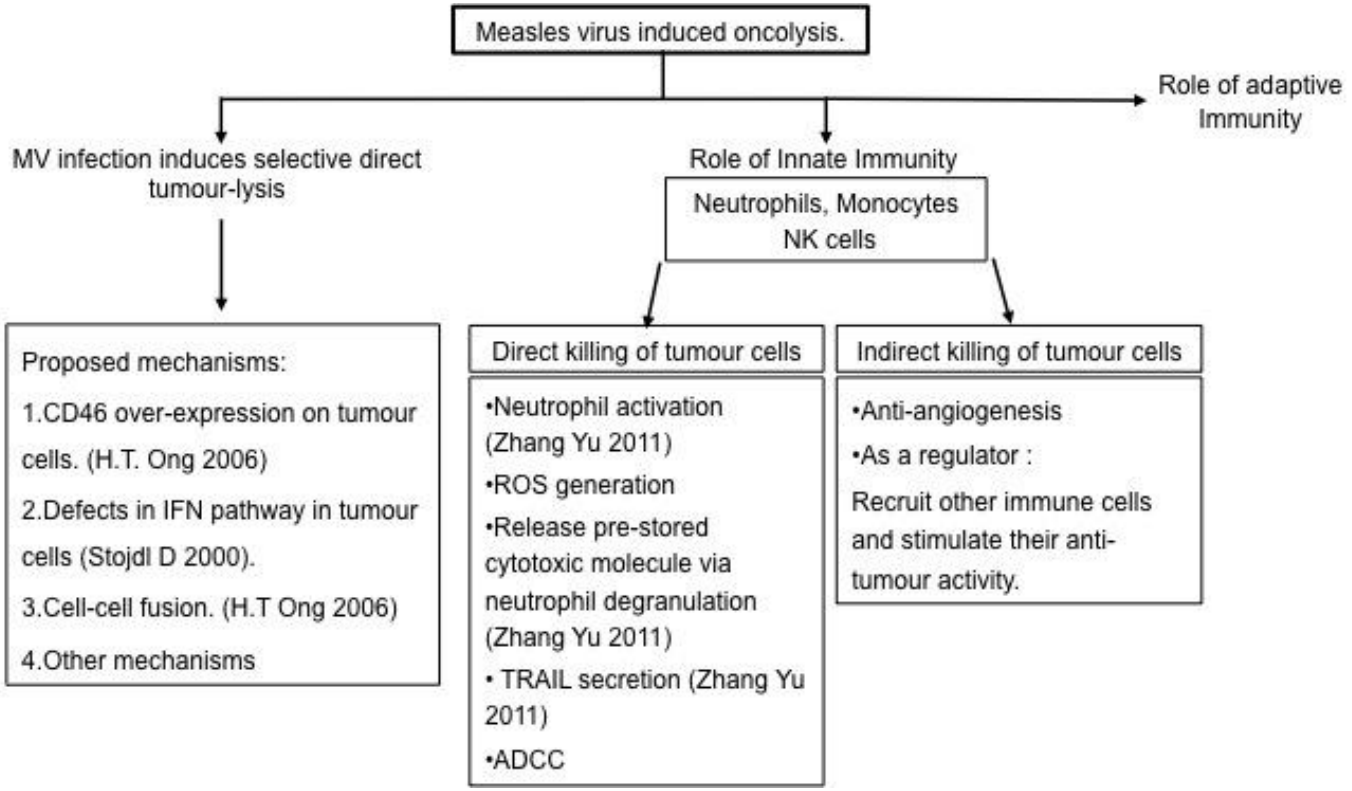

Figure 1-6: Proposed mechanisms of MV-mediated oncolysis: Diagram showing the different mechanisms of MV-mediated oncolysis proposed in the literature.

1.4.3 Cellular responses:

Oncolytic MV can elicit a systemic anti-viral/anti-tumour response, which can greatly contribute to viral oncolysis. The relatively low infection efficiency *in-vivo* suggests that for complete eradication of any tumour, the virus should be able to activate the immune system. In a SCID model of Burkitt's lymphoma, the virus regressed tumours efficiently, but the MV distribution in the sections of resected tumours was found to be patchy, suggesting some role of the immune system[175]. Moreover, tumour regression was associated with a significant neutrophil infiltration that was enhanced by MV expressing murine GMCSF, and correlated with superior tumour regression. The role of one of the key players in the innate immune system – neutrophils, was very clear in this model[280]. Both innate and adaptive immune system may play a very important role in virus mediated oncolysis[70] but has been difficult to study in MV-mediated oncolysis for the lack of an ideal *in-vivo* model, as MV does not infect murine cells. Although others have shown in human *in-vitro* studies that MV could induce monocyte-derived DC (Mo-DC), another important player of the innate immunity, to mature *in-vitro*[304],[305]. The Mo-DCs were shown to cross prime $CD8^+$ T-cells specific for a tissue-associated antigen (TAA) of mesothelioma tumour cells. This showed a possible connection between MV infection and the innate immune cells being able to cross talk to the adaptive immune cells to initiate a more tumour specific immune response initiated by an oncolytic virus[304]. In another *in-vitro* study with melanoma cell line, PBMCs treated with MV was shown to enhance innate anti-tumour immunity within the PBMC effectors. Besides,

Mo-DCs and NK cells were both activated by MV infected melanoma cells, and in a killing assay, CTL primed by DCs co-cultured with MV infected melanoma cells were shown to be more potent killer of tumour cells compared to DCs co-cultured with uninfected melanoma cells alone[305]. In a similar study, plasmacytoid DCs (pDCs), another class of DC, that play an important role in an anti-viral immune response, were shown to upregulate the pDC maturation marker CD83, and produced high levels of IFNα when exposed to MV-infected tumour cells. The pDCs exposed to the MV-infected melanoma were also able to cross present another TAA, NY-ESO-1 positive melanoma cells to $CD8^+$ T-cells specific for the same TAA, and activated them to produce IFNγ. All this was not true for pDCs exposed to UV treated tumour cells and showed a potential role of MV-infected tumour cells in generating an immune response[289].

1.5 NEUTROPHILS - OVERVIEW:

The focus of this thesis is the neutrophil response to MV-infected cancer cells. An overview of the biology of neutrophils in response to viral infection and cancer is given below.

1.5.1 Neutrophil biology:

Neutrophils comprise approximately 60% of the white blood cells in humans[306]. They provide first line of defence against infection and are potent effectors of inflammation. Neutrophils release soluble factors that act as chemo attractants and guide recruitment of both specific and non-specific

effector cells[307]. They are produced in the bone marrow from myeloid precursors, controlled in part by granulocyte colony stimulating factor (GCSF)[308].

Neutrophils are recruited to sites of tissue injury in a multistep process. Cytokines produced by macrophages result in upregulation of the transmembrane adhesion molecules, selectins on endothelial cells, which tether to the neutrophils' p-selectin glycoprotein ligand-1 (PSGL-1) (step 1). Next, 'rolling' occurs, mediated by E selectin. An adhesion step mediated by adhesion molecule 1 and 2 (ICAM1 and ICAM2) on the endothelial cells binding to neutrophil lymphocyte function-associated antigen 1 (LFA1). Finally integrins, ICAM1, ICAM2, vascular cell adhesion protein 1 (VCAM1), other junctional adhesion molecules (JAMs), and platelet/endothelial cell adhesion molecule (PECAM1) facilitate transmigration of the neutrophil into the tissue by a process called diapedesis[309].

1.5.2 Neutrophils' mechanism of action to combat viral infection:

Neutrophils are crucial players in defence against bacterial, fungal and viral infections. They can respond to both non-self PAMPs and self, danger associated molecular patterns (DAMPs). Once triggered, neutrophils activate PRRs like, TLRs[310], RLRs[311] and nucleotide-binding oligomerisation domain (NOD)-like receptors (NLRs)[312] and mediate downstream inflammatory signalling.

Activated neutrophils release reactive oxygen species (ROS), which are highly damaging to the invading microorganism. ROS production can induce degranulation with release of cytotoxic contents to kill microorganisms. Neutrophil extracellular traps (NETs) are another way neutrophils effectively contain infection. NETs are made of chromatin and protein and are released from granules. They have been shown to be quite effective in binding with both gram-positive and gram-negative bacteria, and against fungal infections. NETs have been mainly studied in relation to bacterial and fungal infection[313]. However, one report documents the role of NETs in HIV-1 infection, wherein engagement of HIV-1 with TLR7 and 8, induced ROS-triggered release of NETs[314]. Neutrophils are also part of a link with the adaptive immune system and has been shown to act as an antigen-presenting cell in influenza A infected mouse lungs, where infected neutrophils expressing viral antigen, cross-presented to anti-viral $CD8^+$ T effector cells[315]. Neutrophil granule proteins can also activate TLR-9 in DCs, which can trigger IFN release[313]. The role of neutrophil degranulation and ROS generation in the anti-viral response is highly relevant to this thesis and merits a more detailed discussion.

1.5.2.1 Neutrophil granules:

The four neutrophil granules are:-

1. Primary (Azurophilic granules): store the most potent hydrolytic enzymes, for example elastase, myeloperoxidase (MPO), cathepsins and defensins.

2. Secondary (Specific granules): enriched in metalloproteinases such as lactoferrin, and metalloproteinase 9. Contain some overlapping components to tertiary granules but can be separated by gradient centrifugation, due to their difference in distinct buoyant densities.

3. Tertiary (gelatinase granules): contains matrix metalloproteinases and microbial lectin ficolin-1.

4. Secretory vesicles: contain human serum albumin, indicating that they are formed via endocytosis. They contain pre-formed cytokines such as transforming growth factor alpha (TGFα), TNFα, IL6, IL12 and CXCL2[316] formed during immune activation. They are able to form small golgi structure in mature neutrophils[317].

1.5.2.2 Neutrophil degranulation mechanism:

The process of neutrophil degranulation is highly regulated, and is mediated by a receptor-coupled mechanism[318]. Firstly, the neutrophil granules are recruited onto the cell surface by translocation of the granules, which is triggered by signalling of cell surface receptors, in response to a potential infection. Once recruited the next step is tethering and docking of the granule onto the cell surface, which exposes the granule's outer surface of the lipid bilayer to the neutrophil's inner surface of lipid bilayer. This is followed by granule priming, which helps the granules to rapidly fuse by making them fusion-competent. A reverse pore structure is formed that helps in complete fusion of the granule membrane to the neutrophil membrane, to release its granular content[318]. Increase in the intercellular Ca^{2+}, hydrolysis of ATP and GTP is essential for the translocation and exocytosis of the granules. The granules are released in an orderly manner - secretory

vesicles first followed by tertiary, secondary and finally the primary granules - dependent on the concentrations of Ca^{2+}[318]. Upon degranulation, contents are released into the extracellular or phagolysosomal spaces and fusion of membranes[319], which aids the killing of engulfed microorganisms[320]. Phagolysosome biogenesis, essential for killing the pathogens, occurs through fusion of newly formed phagosomes with other granules and/or endosomes[321].

1.5.2.3 Respiratory Burst:

Respiratory burst by which neutrophils produce ROS is deleterious for invading microorganisms. Receptors like formyl peptide receptors (FPRs) and G protein coupled receptors (GPCRs) present on neutrophils can recognise peptides like N-formyl-Met-Leu-Phe (fMLP) and inflammatory proteins like C5a and IL-8, triggering a rapid downstream signalling response. This leads to assembly of a multi-protein oxidase complex called nicotinamide adenine dinucleotide phosphate (NADPH) oxidase. The individual components of this NADPH oxidase complex are present separately in the non-activated cells. Upon activation they assemble on the membrane of the cell, which helps catalyse NADPH-dependent reduction of O_2 to superoxide anions (O_2^-) and ROS including hydrogen peroxide (H_2O_2), hydroxyl radical (OH.) and hypochlorous acid (HOCl)[322]. A fraction of the NADPH oxidase (approx. 5%) is located in the plasma membrane and phagosomal membrane, the secretory vesicle harbors approximately 10% of the NADPH oxidase complex, and the specific and gelatinase granules comprises of almost 85% of the NADPH oxidase. The MPO or

myeloperoxidase is located in the azurophilic granules, which is essential to generate HOCl, from O_2^-, and plays an important role in killing phagocytosed microorganism. It has been proposed that to generate HOCl, the primary, secondary, tertiary granules and the secretory vesicle must fuse, along with the phagosome[323,324], which is an important step of ROS generation or respiratory burst.

1.5.2.4 Neutrophils and phagocytosis:

Phagocytosis is another mechanism by which phagocytes (neutrophils and macrophages) can eliminate microorganisms, primarily bacteria[325]. In contrast, some microbes including viruses are not directly phagocytosed, instead they are eliminated when the infected cells are engulfed by phagocytes, and is referred to as indirect phagocytosis. It is initiated by recognition of viral components expressed on the host cells bound to antibodies. These antibodies are in turn recognised by the Fcγ receptors on the phagocytes[326]. Another example of indirect phagocytosis is when phagocytes engulf apoptotic cells, by inherent defence mechanism of cells to maintain homeostasis[327]. Apoptosis induced in virus-infected cells can also trigger phagocytosis in a similar way[327,328]. For instance, in C57BL/6 mice, infected with influenza virus, both neutrophils and macrophages were shown to phagocytose infected cells, which were apoptotic[329]. There are several reports of neutrophils phagocytosing viruses such as hepatitis C[330], hepatitis B[331,332], HIV-1[333] and CMV[334]. Avian influenza virus H5N1 has been suggested to enter neutrophils by phagocytosis as H5N1 cellular receptor is

expressed on neutrophils and this might help in viral replication within the neutrophils[335].

1.5.3 Neutrophils in cancer:

Neutrophils plays a crucial role in mediating anti-cancer activity and this has been documented both *in-vitro* and *in-vivo*[336]. Neutrophils may migrate towards the site of tumour by a regulated multistep interaction between neutrophils and endothelial cells in much the same way as occurs for pathogens[337]. They are able to produce the same sort of cytotoxic mediators as discussed earlier, like ROS, proteases, membrane perforating agents and soluble mediators of cell killing, such as TNFα, IL-1β and IFNs[338-340] which can kill the tumour cells. This is a delicate balance as the pro-inflammatory activities of neutrophils can also facilitate tumour growth.

1.5.3.1 Anti-tumour:

In a murine bladder cancer model, where mycobacterium BCG (Bacillus Calmette-Guérin) was used as a treatment, neutrophils were shown to play a key role in therapeutic success. The activated neutrophils from BCG treated mice attracted monocytes, which in turn resulted in $CD4^+$ T-cell migration. Depletion of neutrophils in the same model eliminated the anti-tumour effect of the BCG treatment[341]. Neutrophils stimulated with both viable and heat killed BCG were shown to release TRAIL/Apo-2L, suggesting a direct anti-tumour effect[342,343]. In relation to virotherapy, in which a model of murine colon cancer was treated with vesicular stomatitis virus (VSV)[344], shut down of blood flow to the tumours was observed, which was proposed to be

mediated by neutrophils as shown by the increase in the transcripts encoding the neutrophil chemo attractants CXCL1 and CXCL5. This suggested the possible role of neutrophils in the recruitment of inflammatory cells that led to the shutdown of IT blood flow. Moreover, the shutdown of the blood flow to the tumours led to apoptosis in even those tumour cells that were not infected by the VSV. Additionally, neutrophil depletion in this model failed to stop the blood flow to the uninfected tumour cells, thereby enhanced spread of the tumour [344]. The same group[345] showed that VSV attacks the tumour vasculature and induces clot formation in the tumour vasculature that correlates with decrease in tumour cell proliferation. This was tested in mice after neutrophil depletion and correlated with decrease in clot formation and hence proliferation in tumour cells, implying the role of neutrophils in intra-tumoural coagulation[345].

1.5.3.2 Pro-tumour:

In spite of the well-documented anti-cancer properties of neutrophils, there is a growing body of literature suggesting a dual role of neutrophils in cancer where it can be either pro-tumour or anti-tumour depending on the microenvironment and cytokine profile of the neutrophils. Several studies, primarily in murine models have shown that neutrophils can promote tumours by promoting angiogenesis[346] and can augment tumour cell dissemination and metastatic seeding of tumour cells in distant organs[347-349]. In contrast, other studies have emphasised the role of neutrophils as anti-tumour. They have shown that neutrophils can limit progression of disease through direct cytotoxicity of tumour cells[350,351], by enhancing anti-tumour mediators[338], and

can limit metastatic seeding by acquiring a cytotoxic phenotype[348,349]. Although reports regarding the role of neutrophils in cancer are conflicting, it is getting increasingly clear from different studies that the pro and anti-tumour characteristic of neutrophils can be attributed to their functional plasticity[352] and the cancer microenvironment has been suggested to play an important role. For example, presence of TGFβ, often available in high concentrations in the tumour sites have been shown to switch neutrophils from a pro-inflammatory anti-tumour N1 phenotype to anti-inflammatory pro-tumour N2 phenotype[353]. More recently Mishalian et al.[354] have found that the distribution of neutrophils on discontinuous density gradient (Ficoll-Hypaque) is different from what was believed earlier. Although the neutrophils are generally found in the high-density (HD) gradient, there is an additional population, which is present in the low-density (LD) gradient and co-separates with the PBMCs. They found that this LD fraction increases with tumour growth, and in mice when compared to the HD neutrophils that has anti-tumour properties, LD neutrophils show reduced chemotaxis toward tumour cells, reduced phagocytic ability, augmented oxidative burst and no cytotoxicity towards the tumour cells[355]. In humans, neutrophilia has been associated with poor prognosis[76,356]. Although distinct population of neutrophils have been shown to be present in mice and suggested to be present in human[355], careful and detailed investigation is needed to support the notion that the existence of multiple sub-types of neutrophils, and its activity in the tumour microenvironment has any role to play in determining neutrophil function.

1.5.4 Neutrophils in MV-mediated oncolysis:

Data from my laboratory has previously implicated neutrophils as potential effector cells of MV-mediated oncolysis. In an *in-vivo* Raji (Burkitt's lymphoma) tumour model, MV infection augmented the host $CD45^+$ leukocyte response, which was further elicited in the group where MV modified to express murine GMCSF (MVmGMCSF) was used. Further analysis showed massive neutrophil infiltration in sections of Raji (Burkitt's Lymphoma) tumours treated with MVmGMCSF when compared to MV alone[280]. However, there was no difference observed in the number of NK cells and macrophages in these groups. Additionally, higher neutrophils also correlated with a superior anti-tumour response in MVmGMCSF treated tumours when compared to the MV alone group.

In another study from my laboratory[357], human neutrophils were shown to get infected by the vaccine strain of MV and could replicate within them over 24 hours. When compared to a WT strain of MV, the vaccine strain was able to activate the neutrophils within 4 hours of infection. Besides, the neutrophils infected with the vaccine strain of MV survived longer *ex-vivo*. Upon MV infection, pro-inflammatory cytokines like TNFα, which is known to destruct tumour vasculature; IL-8, a potent chemo attractant and activator of neutrophils; MCP-1, a monocyte and T lymphocyte attractant and IFNα gene expression and protein secretion were upregulated. Furthermore, TRAIL, which has a tumour specific cytotoxic activity, was secreted in response to MV infection from neutrophil granules because of neutrophil degranulation initiated by vaccine MV infection. MFI of three

different neutrophil degranulation markers CD35, CD63 and CD66b were significantly higher than the uninfected control or the WT MV[357]. All these data from our previous publication suggested that the effect of MV infection of neutrophils, specifically the oncolytic vaccine strain of MV might have a potential role in MV oncolysis.

1.6 GRANULOCYTE COLONY STIMULATING FACTOR (GCSF):

1.6.1 GCSF:

GCSF was one of the first cytokines to enter clinical trials. The murine GCSF was first isolated in 1983 from lung tissue of endotoxin treated mice[358], which was followed by the human form in 1985 from the bladder carcinoma cell line 5637[359]. In pre-clinical mouse models, GCSF was shown to mobilise haematopoietic cells from all lineages in large numbers[360]. In subsequent clinical trials, GCSF treatment was demonstrated to mobilise large number of haematopoietic cells into circulation in patients and normal donors from where it could be collected for autologous and allogeneic haematopoietic cell transplantation respectively[361-363].

Infectious complications due to prolonged chemotherapy treatment in leukaemia patients have been one of the main reasons of morbidity and mortality. Several trials have looked into the use of GCSF in treatment of ALL patients with or after intensive chemotherapy regimens and have shown significant improvement in the rates of morbidity and mortality in both children and adults[364]. In some studies, use of GCSF has been shown to

accelerate neutrophil recovery, which allows the use of higher chemotherapy doses, and may improve survival[364].

1.6.2 GCSF and neutrophils:

GCSF has been used for more than two decades to manage neutropenia in patients after chemotherapy. The mechanism by which GCSF helps in neutrophil mobilisation is well studied and shows that GCSF can directly stimulate the production of neutrophils from myeloid cells and enhance production of mature neutrophils from metamyelocytes[358]. GCSF acts via the GCSF receptor (GCSFr), which is expressed on neutrophils, all precursors of neutrophils and on primitive haematopoietic stem cells[365]. GCSF has helped reduce neutropenia after chemotherapy by accelerating neutrophil recovery, and is now routinely used in patients with malignancies like breast cancer, lymphoma, and leukaemia. Along with neutrophils, GCSF treatment could lead to mobilisation of a large number of other progenitor and stem cells, and a number of multiple lineage progenitor cells (myeloid, erythroid, megakaryocytic) including platelets[366]. This was proved beneficial for patients undergoing chemotherapy, as they receive stem cells from normal human donors, and the increased number of the haematopoietic stem cell (HSC) in the blood after GCSF administration facilitated the collection of these cells from the blood of donors, and since has been routinely used in stem cell donors[362].

GCSF has been long thought to be effective in granulopoiesis, but studies suggest GCSF to have a much wider role as an immune regulator[367].

Resting T-cells usually do not express GCSF receptor (GCSFr), though some activated T-cells have been shown to express GCSFr[368]. Exposure of GCSF tend to change T-cell function from an Th1 type (IFNγ and TNFα) to Th2 type (Secreting IL4 and IL10) thereby reducing their response to allo-antigens[369,370], and this has been shown to inhibit a T-cell mediated graft versus host disease (GVHD) in GCSF mobilised stem cell allogeneic transplant when compared to standard BM transplants. GCSF was also shown to induce production of regulatory DC[371,372] and DC like myeloid cells, which in turn have an effect on T-cell development and function. With such a vast range of functions, GCSF is now recognised as a poly functional cytokine, and although it is a key regulator of neutrophil function, elucidating the complete signalling mechanism between GCSFr gene expression and responses will help in specifically tailoring GCSF treatment in clinical settting[367].

1.7 Current Project Hypotheses and Aims:

In this thesis, I have focussed on the innate immune system, specifically looking at the role of neutrophils, and their involvement in MV-mediated oncolysis of B-cell malignancies – acute lymphoblastic leukaemia (Nalm-6) and Burkitt's lymphoma (Raji). The heterogeneity of the two different malignancies has led me to compare the two different B-cell malignancies and their susceptibility to neutrophil mediated MV oncolysis both *in-vitro* and *in-vivo*.

1.7.1 Hypotheses and Aims:

The central hypothesis of the thesis is that neutrophils play an anti-tumour role in MV-mediated oncolysis in B-cell malignancies.

Stemming from this hypothesis, we would expect that it would be possible to improve the oncolytic effect of MV by enhancing the neutrophil-mediated immune response towards the MV-infected target cells; first part of the thesis addresses that. Understanding the mechanisms of how neutrophils may contribute to MV oncolysis is clearly vital; this overall aim has been addressed in the second part.

Chapter 3: The role of neutrophils in measles virus mediated oncolysis differs between B-cell malignancies in-vivo and is not always enhanced by GCSF

Aims:

1. To determine the therapeutic effect of MV in an *in-vivo* model of ALL.

2. To establish the role of neutrophils and determine the therapeutic role of the novel MV expressing hGCSF (MVhGCSF) in two different *in-vivo* models of B-cell malignancies - Raji (Burkitt's lymphoma) and Nalm-6 (acute lymphoblastic leukaemia) *in-vivo*.

Chapter 4: Mechanism of neutrophil mediated cytotoxicity in MV-infected target cell, differ between tumour types and the MV strain used

Aims:

1. To investigate if neutrophils from healthy human donors can mediate killing of MV-infected targets *in-vitro*.

2. To determine whether ADCC is a mechanism by which neutrophils may mediate MV oncolysis.

Chapter 5: Fusion between neutrophils and target cells mediate cytotoxicity during measles virus oncolysis - a novel mechanism of oncolysis

Aims:

1. To determine the effect of fusion on degranulation and reactive oxygen species (ROS) generation in neutrophils when co-cultured with MV-infected targets.

2. To determine the effect of fusion on type I IFN production and RLR signalling pathway in neutrophils when co-cultured with MV-infected targets.

3. To visualise fusion between neutrophil and MV-infected targets.

Chapter 2: Materials and Methods

2.1 GENERAL CELL AND TISSUE CULTURE:

2.1.1 Cell lines:

- Vero - African green monkey kidney cell line, adherent (CCL-81; ATCC).
- 293T - human embryonic kidney cell line, adherent (CRL-11268; ATCC).
- Phoenix AMPHO - human embryonic kidney cell line, adherent (CRL-3213; ATCC).
- Raji - human Burkitt's lymphoma cell line, suspension (CCL-86; ATCC).
- Nalm-6 - human pre-B acute lymphoblastic leukaemia cell line, suspension (ACC128; DSMZ).
- Jurkat - human T-cell acute lymphoblastic leukaemia cell line, suspension (TIB-152; ATCC).
- DND41 – human T-cell acute lymphoblastic leukaemia cell line, suspension (ACC 525; DSMZ).

Adherent cell lines were grown and maintained in Dulbecco's Modified Eagle's Medium (DMEM) high glucose (Gibco® by life Technologies™) with 5% heat inactivated Foetal Bovine Serum (FBS) (Gibco® by life Technologies™), 100µg/ml streptomycin, 100 units/ml penicillin G (Penicillin-Streptomycin 10,000U/ml) (Gibco® by life Technologies™) and 2mM L-glutamine (Gibco® by life Technologies™). 293T and Phoenix AMPHO required 10% FBS.

Suspension cell lines were all grown and maintained in RPMI (Roswell Park Memorial Institute) 1641 medium with L-glutamine (Gibco® by life Technologies™), with 10% FBS, 100µg/ml streptomycin, 100 units/ml penicillin G and 2mM L- glutamine (R10 complete media).

Cell lines were grown in a humidified incubator (HERA cell, Thermo Scientific, Surrey, UK) at 37°C with 5% CO_2. The cell lines were passaged twice a week, upon reaching 80-90% confluency.

All the cell lines were grown in tissue culture flasks (T-75, Corning, NY, US). The suspension cells were passaged twice a week, when 90% of the cells were removed and replaced with fresh medium. The adherent cell lines were passaged at 90% confluency. The old media was removed and the cells were washed with 5ml of 1X phosphate buffer saline (PBS) (Gibco® by life Technologies™) and incubated with 2ml TrypLE™ Express Enzyme (Gibco®) for 2-4 minutes (mins) at 37°C. Once the cells were detached, they were cultured at a dilution of 1:10 in a new T-75 tissue culture flask with new medium.

2.1.2 Cell culture reagents:

- Dimethyl Sulfoxide (DMSO) (Sigma Aldrich, Poole, UK).
- Dulbecco's Modified Eagle Medium (DMEM) – high glucose 4.5g/l (Invitrogen, Paisley, UK).
- Foetal Bovine Serum (FBS), heat inactivated (Invitrogen, Paisley, UK).
- L-glutamine 200mM, final concentration in media 2mM (Invitrogen, Paisley, UK).

- OptiMEM® medium (Invitrogen, Pailsey, UK).
- Penicillin-Streptomycin containing 10,000units/ml penicillin and 10,000µg/ml streptomycin, final concentration 100units/ml and 100µg/ml respectively (Invitrogen, Paisley, UK).
- Phosphate Buffered Saline (PBS) (Invitrogen, Paisley, UK).
- RPMI-1640 medium (Invitrogen, Paisley, UK).
- TrypLE^{TM} Express Enzyme (Invitrogen, Paisley, UK).

2.1.3 Active compounds used in cell culture:

- Z-D-Phe-Phe-Gly-OH – fusion inhibitory peptide (FIP), used at 40µg/ml (Bachem, Switzerland).
- IFNα 2b human (Sigma-Aldrich®, UK).
- lFNβ 1a human (Sigma-Aldrich®, UK).
- Recombinant human GCSF (Peprotech, UK).

2.1.4 Cryopreservation and cell recovery:

Cells were cryopreserved by resuspending in freezing mix consisting of 10% DMSO and 90% FBS. The cells were aliquoted at a concentration between $1x10^6$/ml-$5x10^6$/ml in polypropylene cryovials (Nunc, ThermoScientific), and frozen in a freezing container (Nalgene, Rochester, US) filled with 100% isopropyl alcohol, at -80°C overnight to achieve a -1°C/min freezing rate. The cryovials were transferred to a liquid nitrogen cylinder the following day for long-term storage.

For recovery, cells were rapidly thawed in a 37°C water bath and 10ml of FBS was added drop wise, with gentle mixing to remove the DMSO. The cells were then centrifuged at 1200 RPM for 5mins without brake. The cell

pellet obtained was washed again with the respective culture medium supplemented with 50% FBS to remove any traces of DMSO. The pellet was transferred into 10ml medium and cultured in a T-25 (Corning, NY, USA) tissue culture flask until 80-90% confluency. Cells were then transferred to a T-75 flask and maintained and passaged as described previously.

2.1.5 Cell counting and viability assay:

Cells were counted by trypan blue (Sigma Aldrich Poole, UK) exclusion method on a haemocytometer or a Cellometer Auto T4 Cell Viability Counter (Nexcelom Bioscience).

2.2 MEASLES VIRUS:

2.2.1 Measles virus propagation:

MV was propagated on Vero cells, plated in 14cm diameter plates (Corning), and grown to 90-95% confluency. Cells were infected in OptiMEM® at a multiplicity of infection (MOI) of 0.01 and incubated at 37°C for 2 hours. At the end of the incubation, the virus was removed and DMEM media (supplemented with 5% FBS, 2mM L-glutamine and 100units/ml penicillin G + 100µg/ml streptomycin) was added to the plates. The plates were incubated until maximum cytopathic effect was observed and then scraped and collected into 1-2ml OptiMEM®. The cells were subjected to two rounds of freeze thaw cycle to release the virus. The cell debris was removed by centrifugation at 14000 RPM for 10mins and the supernatant containing the virus was aliquoted into small volumes.

2.2.2 MV titration:

MV was titrated on Vero cells. $5x10^3$ Vero cells were plated into each well of a 96-well plate. Fifty microliters of 10 fold dilutions was dispensed into each well. The plate was incubated at 37°C for 4 days and syncytia were counted. The 50% tissue culture infectious dose ($TCID_{50}$) was calculated using the modified Kärber[373] formula:

$Log10\ TCID_{50} = -[Log10x – d\ (p-0.5)] + Log10\ (1/v)$.

x = highest dilution that gives 100% of wells positive for infection.

d = Log10 of dilution interval (e.g. for 10-fold dilution, d=1).

p = sum of values of the proportion of wells positive for infection at all dilutions.

v = volume of viral inoculum for each well in milliliters.

The plaque forming units (PFU/ml) was estimated by multiplying the $TCID_{50}$ value with 0.7 (a factor derived from Poisson distribution).

The viral stocks were stored at -80°C in small aliquots to avoid multiple freeze thaw.

2.2.3 Measles virus rescue:

Vero cells were infected with T7 RNA polymerase expressing Vaccinia Ankara Virus. After an hour of incubation the virus was taken off and the Vero cells were transfected with the full length cloned MV cDNA and the plasmids encoding the MV polymerase complex (pCG-N, pCG-P, pCG-L), using Lipofectamine® 2000 transfection reagent (ThermoFisher Scientific,

UK) in OptiMEM® reduced serum medium, GlutaMAX™ supplement (Gibco® by life Technologies™). Twenty-four hours later, the lipofectamine plasmid mix was replaced with fresh media. Four to five days later syncytia were obtained which are hallmark of MV infection. Individual syncytium were picked and propagated for further experiments.

2.2.4 Measles virus infection:

Cells were washed with PBS. The viral stock was thawed and diluted in OptiMEM® at desired PFU/ml to obtain the required MOI. The required number of cells were then resuspended in the virus OptiMEM® mix and incubated at 37°C with 5% CO_2 for 2 hours. For adherent cell infection, the media was removed from the cells, washed with 1xPBS and then the virus-OptiMEM® mix was added onto it before incubation. After the incubation, the virus-OptiMEM® mix was removed from the cells and they were resuspended in fresh media.

2.2.5 UV irradiation of MV:

Aliquots of MV were incubated in a UV-cross-linker (CL-1000 Ultraviolet Crosslinker; UVP, UK) for 3-4 hours to inactivate the virus.

2.3 PRODUCTION OF RETROVIRAL VECTOR EXPRESSING LUCIFERASE GENE:

The Phoenix AMPHO packaging cell line (CRL-3213; ATCC) was used for preparation of retroviral particles by co-transfecting with the

retroviral vector plasmid containing the luciferase gene using a high-density transfection reagent Fugene® (Roche, Sussex, UK). On Day 1, Phoenix AMPHO cells were harvested by trypsinisation, washed and then resuspended in fresh medium ($2x10^6$ cells resuspended in 8mls of fresh media) and plated into 10cm diameter petri dishes. They were then incubated at 37°C and 5% CO_2 overnight. On Day 2 the following transfection mix was prepared:

Solution A: 10µl Fugene® and 150µl OptiMEM®.

Solution B: 1.5µg pCL-ampho retrovirus packaging vector (Imgenex, CA, USA), 2.6µg vector construct (SFG.Fluc_opt_2A_eBFP2; gifted by Dr. Martin Pule, UCL, UK), volume up to 50µl with H_2O.

The Solution B was then added to the Fugene® solution A, and then gently mixed by pipetting. The mix was incubated at room temperature for 15-20mins, after which it was directly added to the Phoenix AMPHO cells and returned to the incubator. On day 3, the media was removed from the cells and replaced with 5mls of fresh R10 media. The virus supernatant was harvested on day 4.

2.4 RETROVIRAL VECTOR TRANSDUCTION OF NALM-6 AND RAJI LUCIFERASE EXPRESSING CELL LINES:

Six well tissue culture plates were coated with 2.5ml/well of Retronectin (Clontech, France) at a concentration of 30ng/ml and incubated at room temperature for 2-3 hours. The Retronectin was then removed and the wells blocked with 2ml of filter sterilised 2% BSA (Sigma Aldrich; Poole;

UK) for 30mins and wells were washed with 3ml/well PBS twice. Pre-cultured Raji cells were taken at a concentration of $1x10^6$ cells/ml and 2.5ml of cell suspension was added to each well of the Retronectin coated 6-well plate. The plate was then incubated at 37°C for 30mins to allow attachment of the Raji cells to the plates. Retroviral supernatant prepared in section 2.3 was then added to each well of Raji cells and incubated at 37°C overnight. The following day, the viral supernatant was removed and fresh R10 media added at 5mls/well. The cells were then incubated for 3 days at 37°C, harvested, washed and analysed by flow cytometry for eBFP transgene expression. The cells were sorted to >95% purity before use.

2.5 NEUTROPHIL ISOLATION:

Twenty to 50ml of peripheral blood (PB) was obtained from healthy donors in preservative free heparin (100µl per 10ml) {obtained from Royal Free Hospital (RFH) pharmacy} after informed consent. It was then incubated with 10-25ml (half the PB volume) of 3% dextran (Amersham Biosciences, UK) to sediment the red blood cells (RBCs) for 45-60mins. The supernatant was collected in a 50ml tube and centrifuged at 290g for 12mins to obtain a pellet. The pellet was subjected to hypotonic lysis in 12ml of ice-cold, sterile ddH_2O and 4ml of 0.6M KCl to eliminate any contaminating RBCs and then made up to 50ml with PBS. It was then centrifuged at 393g for 5mins. After centrifugation the pellet was resuspended in 1xPBS and overlaid onto LymphoPrep™ (Axis-shield, Oslo, Norway). After centrifugation, the supernatant was discarded and the pellet containing the neutrophils was

washed in RPMI1640 without serum, twice. The neutrophils obtained were resuspended in desired volume of RPMI and used for further experiments. The purity of neutrophils was determined by light microscopy of Giemsa-stained cytospin slides.

2.6 CYTOTOXICITY ASSAY (^{51}CR RELEASE):

To assess the neutrophil mediated MV cytotoxicity, ^{51}Cr Release Assay was used. Cell lines were infected with MV at an MOI of 1.0 or mock infected. At 24 hours or 48 hours post infection (hpi), the cells were labelled with Chromium-51 radionuclide (sodium chromate) (PerkinElmer) at a concentration of 1.85MBq/10^6 cells. After 1-2 hours incubation at 37°C they were washed thrice and resuspended in R10 media. ^{51}Cr labelled cells ($5x10^3$ cells/well) were aliquoted in 96-well round bottom plates and incubated with neutrophils extracted from healthy donors (see section 2.5) at different Effector:Target (E:T) ratios (2:1; 8:1; 20:1; 40:1) in triplicates. The plates were then incubated at 37°C for another 24 hours. The following day, the 96-well plates were centrifuged and 50ul of the supernatant was transferred into clear 96-well round bottom (Flexible PET Microplate; PerkinElmer) plates containing 150ul of OptiPhase Supermix scintillation cocktail (PerkinElmer). The plates were then sealed with TopSeal-ATM (PerkinElmer) and placed on a plate shaker for 5mins to ensure complete mixing of the supernatant with the scintillation cocktail. The amount of ^{51}Cr released was measured in 1450 Microbeta Liquid Scintillation Counter

(PerkinElmer). The percent specific lysis was calculated using the following formula:

Percentage (%) of neutrophil-specific lysis = (experimental cpm – spontaneous cpm) / (maximal cpm – spontaneous cpm) x 100.

The spontaneous cpm was the negative control with infected or uninfected cells in the absence of neutrophils, and the maximal cpm was the positive control where all the cells were lysed using an acid. The minimum threshold for % specific lysis was set at 5%.

To assess the effect of presence of anti-MV antibody, pooled serum from individuals with high anti-MV Ab {(titrated using VIDAS® enzyme linked fluorescent immunoassay (FIA); Biomérieux, France} was obtained from the Virology department at the RFH. The serum was then heat inactivated in the lab at 56°C for 30mins to eliminate the complements. The serum was added at 1:100 dilution in the experiments.

Where fusion inhibition was required, the chromium release assay was performed in the presence or absence of fusion inhibitory peptide (FIP) at 40µg/ml dissolved in 100ul of DMSO before adding to the media, or media containing only 100ul DMSO.

2.7 *IN-VITRO* RECOMBINANT HUMAN GCSF (rhGCSF) ASSAY:

Raji and Nalm-6 cells were plated at $2x10^4$/ml in T25 tissue culture flasks in R10 media supplemented with 0, 5 and 10ng/ml rhGCSF (Peprotech, UK). The cells were incubated at 37°C. They were counted using

the trypan blue dye exclusion method to determine the number of viable cells/ml at 24 hourly intervals.

2.8 MOLECULAR BIOLOGY TECHNIQUES:

2.8.1 Molecular biology reagents:

- Agar (Sigma-Aldrich®, UK).
- Agarose (Sigma-Aldrich®).
- Chloroform (VWE International, UK).
- DNase/RNase free water (Invitrogen, UK).
- Ethanol 100% (VWR International, UK).
- Glycerol (VWR International, UK).
- HiSpeed Plasmid Midi Kit (Qiagen, UK).
- Isopropanol (VWR International, UK).
- LB broth (Invitrogen, UK).
- One Shot® TOP10 competent cells (Invitrogen, UK) (New England Biolabs, UK).
- pCRII-TOPO TA cloning kit (Invitrogen, UK).
- pORF9-hGCSFb (Invivogen, USA).
- QiaexII gel purification kit (Qiagen, UK).
- QIAprep Spin Miniprep Kit (Qiagen, UK).
- QuikChange II XL Site-Directed Mutagenesis Kit (Agilent Technologies, UK).
- Random hexamer (Promega, UK).
- Restriction enzymes (New England Biolabs, UK).
- RNasin® Plus RNase Inhibitor (Promega, UK).

- SuperScript™ III reverse transcriptase (Invitrogen, UK).
- SYBR® safe DNA gel stain (ThermoFisher Scientific, UK).
- T4 DNA Ligase (New England Biolabs, UK).
- TRIzol® (Invitrogen, UK).
- 0.1M DTT (Invitrogen, UK).
- 2xYT microbial growth medium (Sigma-Aldrich®, UK).
- 5x first strand buffer (Invitrogen, UK).
- 10mM dNTPs (Promega, UK).

2.8.2 Cloning:

Specific details for cloning MVhGCSF are given in chapter 3, section 3.2.1.

2.8.3 Plasmid Preparation:

Bacteria were propagated on 2xYT agar plates overnight, and then propagated in 2xYT broth. Plasmid DNA was extracted from 5ml or 50ml 12-16 hours bacterial culture using QIAprep Spin Miniprep Kit and HiSpeed Plasmid Midi Kit. DNA extracted was checked for its concentration and purity at 260nm (A260) and 280nm (A280) on a NanoDrop™1000 spectrophotometer (Thermo Scientific, Essex, UK). DNA preparations with a ratio of 1.75-2.0 only were used further for the experiments. All plasmid DNA was stored at -20°C.

Glycerol Stock: Glycerol stocks of the bacterial cultures were prepared using 200µl of bacterial culture and 800µl of 99% glycerol and stored at -80°C.

2.8.4 RNA extraction:

Total RNA was extracted from cells at appropriate time-points by using TRIzol®. Cell pellets were resuspended in 1ml of TRIzol® and mixed vigorously using a pastette. It was incubated at room temperature (RT) for 5mins and the 200µl of chloroform was added to it and mixed well till it turned cloudy and then incubated at RT for a further 2mins. The tube was then centrifuged at 12,000 RPM for 10mins at 4°C. The aqueous layer was carefully transferred into a clean tube without disturbing the white middle layer. 500µl of isopropanol was added to it and left at -80°C overnight. The next day the vial was thawed and centrifuged at 13000 RPM for 10mins. The supernatant was removed and the RNA pellet was washed with 70% ethanol and centrifuged at 13000 RPM. The pellet was then air dried while still on ice for 20mins. Once dried, the pellet was resuspended in 30µl of DNase/RNase free water and quantified at 260nm (A260) and 280nm (A280) on a NanoDrop^{TM}1000 spectrophotometer (Thermo Scientific, Essex, UK). RNA with a ratio of 1.75-2.0 were considered good and used further for the experiments. All RNA stocks were stored at -80°C.

2.8.5 First strand cDNA synthesis:

Total RNA (0.4-1µg) per sample was used for cDNA synthesis. To each sample the following was added: Random hexamer - 2µl (334ng), 0.1M DTT - 1µl, 10mM dNTPs - 2µl.

Samples were then incubated at 65°C for 5mins and then incubated on ice for a further 5-10mins. Next, to each sample the following was added:

5x first strand buffer - 1µl, RNasin® Plus RNase inhibitor - 1µl (40 units), SuperScript™ III reverse transcriptase - 1µl (200 units). The samples were transferred onto a PCR machine DYAD (MJ Research; BioRad) and run on the following programme:

25°C for 10 mins

50°C for 50 mins

70°C for 15 mins

The cDNA was stored at -80°C till further use.

2.8.6 Relative quantification by RQPCR:

2.8.6.1 RIG-I/MAVS/MDA5 quantification:

QuantiTect® Primer assay (Qiagen, UK) was used for relative quantification of RIG-I, MDA5 and MAVS mRNA. 0.3µM forward and reverse primers, 12.5µl of 2x QuantiTect® SYBR Green PCR Master Mix (Qiagen) was mixed with the cDNA in 25µl reactions. They were run on an ABI7500 (Applied Biosystems) according to the following conditions:

50°C for 2 mins

95°C for 10 mins

40 cycles of:

94°C for 15 seconds; 55°C for 30 seconds; 72°C for 35 seconds

The primer sequences are as below:

RIG-I s 5’-ACCAGAGCACTTGTGGACGCT-3’

RIG-I a 5’-TGCCGGGAGGGTCATTCCTGT-3’

MDA5 s 5’-GGCACCATGGGAAGTGATT -3’

MDA5 a 5’-ATTTGGTAAGGCCTGAGCTG -3’

MAVS s 5’-GAGACCAGGATCGACTGCGGGC- 3’

MAVS a 5’-AGAGGCCACTTCGTCCGCGA -3’

GAPDH was used as a housekeeping gene for all assays. The PCR was run in triplicates and non-template control was included for each primer sets. Relative expression was determined using the following ΔΔCt formula[374]:

$$\Delta Ct = Ct_{(experiment)} - Ct_{(GAPDH)}$$

$$\Delta\Delta Ct = \Delta Ct_{(sample)} - Ct_{(calibrator)}$$

$$RQ = 2^{\wedge}(-\Delta\Delta Ct)$$

2.9 FLOW CYTOMETRY:

2.9.1 General flow cytometry method:

Cells were pelleted and resuspended in 200µl of PBS and aliquoted into FACS tubes (BD Biosciences, UK). Two to three microliter of the desired antibody/antibodies conjugated to fluorescein isothiocyanate (FITC), phycoerithrin (PE), allophycocyanin (APC) was added to the tube and incubated at 4°C for 30-45mins in the dark. For non-conjugated primary antibody, goat anti-mouse secondary antibody conjugated to PE (BD

Pharmingen) was used. After incubation the tubes were centrifuged at 2000 RPM for 2mins and then run on a BDTM LSR II or BD LSR Fortessa analyser (Beckton Dickinson, Oxford, UK) with 5000-10000 events being recorded. In some assays, 2µl of propidium iodide (PI) (BD Pharmingen^{TM}), which is a DNA binding dye, was used to select out the viable cells by gating on PI negative cells. The data was analysed using FLOWJO (Tree Star) single cell analysis software (version 7.4.1). Name of antibodies used are listed in Table 2.1.

Table 2.1: List of antibodies used for flow cytometry:

Target	Company	Clone	Conjugate
CD35	BD Pharmingen	E11	FITC
CD66b	BD Pharmingen	G10F5	FITC
CD63	BD Pharmingen	H5C6	FITC
CD11b	BD Pharmingen	M1/70	APC
CD10	BD Biosciences	HI10a	APC
CD19	BD Biosciences	4G7	FITC
CD20	BD Biosciences	L27	APC
Ly6G6C	BD Pharmingen	RB6-8C5	FITC
MV-H	Millipore	CV1, CV4	None
Pan NK/CD49b	BD Pharmingen	DX5	PE
Mac 3	BD Pharmingen	M3/84	PE

2.9.2 Fluorescent activated cell sorting:

Cell sorting was performed on either a MoFLo XDP (Beckman Coulter, Fullerton, CA, USA) or on BD FACS Aria (Beckton Dickinson, Oxford, UK). The enhanced blue fluorescent protein (eBFP) marker was excited by the 350 UV laser (100mW) and the emission was collected by 653/40 filter.

2.10 ENZYME LINKED IMMUNOSORBENT ASSAY (ELISA):

Cell culture supernatants were collected at appropriate time-points and ELISA performed according to the manufacturer's guidelines. Optical density (OD) was measured at appropriate wavelength using Tecan Sunrise absorbance reader (Jencon-PLS, UK). The OD of the standards was plotted against their concentration to obtain a standard curve and the sample concentrations were extrapolated directly from the standard curves.

- Human GCSF standard ABTS ELISA Development Kit (Peprotech, UK).
- Verikine^{TM} Human IFNα Multi-Subtype ELISA (PBL Assay Science, NJ).
- Verikine^{TM} Human IFNβ ELISA (PBL Assay Science, NJ).
- TRAIL/ APO2L/ CD253 ELISA Kit (2BScientific, UK).
- Measles virus IgG ELISA (IBL International, Hamburg, Germany).

2.11 ANTI-MV ANTIBODY SERUM HEAT INACTIVATION:

Anti-MV antibody containing serum, pooled from different donors was obtained from the Virology Department at RFH. The serum was then heat inactivated at 56°C for 30mins and then titrated by ELISA. The high titre antibody containing serum was then aliquoted into small volumes and stored at -80°C for future experiments.

2.12 ANIMAL METHODS:

2.12.1 Animal Strains:

- Six to eight week old CD17 severe combined immunodeficient (SCID) mice (Charles River Laboratories, UK).

- $Ifnar^{KO}$ CD46 Ge mice (provided by Roberto Cattaneo, Mayo Clinic).

All the mice were housed, bred and cared for in barrier facility in accordance with UK home office approved protocol. The establishment of the xenograft models and the bioluminescent imaging protocols are described in more details in the chapter method (see 3.2.2).

2.13 STATISTICAL ANALYSIS:

Prism 5.0 (GraphPad Software) and Microsoft Excel were used to plot all graphs. The data are presented as mean±SEM where appropriate. The statistical analysis was performed either by paired/unpaired student's t test or Mann Whitney U test as appropriate. In the animal experiments, Kaplan-Meier curves were used to analyse survival and the different groups were compared using the log-rank test. All the P-values quoted are one/two-tailed.

Chapter 3: The role of neutrophils in measles virus mediated oncolysis differs between B-cell malignancies *in-vivo* and is not always enhanced by GCSF

3.1 BACKGROUND:

3.1.1 MV in B-cell malignancy:

The Edmonston-B derived vaccine strain of measles virus (MV) is oncolytic in various tumour models *in-vivo* and is currently being tested in several phase 1 clinical trials (chapter 1, section 1.3.2). MV is naturally lymphotropic and B-cell malignancies appear particularly sensitive. *In-vivo* models of B-cell malignancies like Burkitt's lymphoma[175] and multiple myeloma[176] have been shown to be an excellent target for MV therapy. Our laboratory is particularly interested in acute lymphoblastic leukaemia (ALL), an immature B-cell malignancy that is largely curable in children but often has a poor outcome in adults[375]. The treatment is long and toxic, and novel, non-chemotherapy-based therapies have a clear role. Previous work from the Fielding lab[376] suggested that ALL might be exquisitely sensitive to MV.

3.1.2 Oncolytic MV and neutrophils:

In addition to the direct oncolytic effect of MV, work from the Fielding lab has shown that neutrophils are involved in MV-mediated tumour regressions in a Burkitt's lymphoma model. MV treatment led to significant neutrophil infiltration in the tumours injected with MV. When a modified MV

expressing mGMCSF, which is a known neutrophil survival factor was used there was significantly higher neutrophil infiltration, which correlated with superior tumour regression[280]. In further work, Fielding laboratory showed that neutrophils from healthy human donors became activated upon oncolytic (but not wild-type) MV infection and survived significantly longer in culture. Upon oncolytic MV infection, neutrophils produced various anti-tumour cytokines like MCP-1, TNFα, IL-8 and IFNα and upregulated neutrophil degranulation markers in response to MV infection, resulting in the release of TRAIL directly from pre-formed granules[357].

As discussed in chapter 1 section 1.5.3, neutrophils have also been implicated by other groups in additional, microorganism-mediated tumour regressions[338,340]. Briefly, in a bladder cancer model, where mycobacterium BCG (Bacillus Calmette-Guérin) was used as a treatment, neutrophils were shown to play a key role in therapy[342]. In relation to virotherapy in which a model of murine colon adenocarcinoma was treated with vesicular stomatitis virus (VSV), shut down of blood flow to the tumours was observed, which was proposed to be mediated by neutrophils[344]. The shut down of the blood flow to the tumours led to apoptosis in even those tumour cells that were not infected by the VSV. It was also shown that VSV attacks the tumour vasculature and induces clot formation, which correlates with decrease in tumour cell proliferation[345].

3.1.3 Granulocyte colony stimulating factor (GCSF):

Murine GCSF was first isolated in 1983 from lung tissue of endotoxin treated mice[358]. In 1985, the human form was first isolated from the bladder carcinoma cell line 5637[359]. In pre-clinical mouse models, GCSF was shown to mobilise haematopoietic cells from all lineages in large numbers[360]. In subsequent clinical trials, GCSF treatment was demonstrated to mobilise large number of haematopoietic cells into circulation in patients and normal donors from where it could be collected for autologous and allogeneic haematopoietic cell transplantation respectively[361-363].

Infectious complications due to prolonged chemotherapy treatment in leukaemia patients have been one of the main reasons of morbidity and mortality. Several trials have confirmed the role of GCSF in treatment of ALL, showing significant improvement in morbidity and mortality in both children and adults[364].

3.1.4 Effect of GCSF on neutrophils and immune function:

GCSF can directly stimulate the production of neutrophils from immature myeloid cells and enhance production of mature neutrophils from metamyelocytes[358], via its action on the GCSF receptor (GCSFr), which is expressed on neutrophils, their precursors, and on early haematopoietic stem cells[365]. GCSF binds to GCSFr, which is a single homodimer transmembrane protein that upon stimulation signals via multiple signalling pathways including Janus kinase/Stat[377-379] (JAK/STAT), mitogen-activated protein kinases (MAPK) and extracellular signal-regulated kinase (Erk1/2,

Erk 5)[380,381]. GCSF also has a much wider role as an immune regulator[367]. Resting T-cells typically do not express GCSFr, although some activated T-cells have been shown to express GCSFr[368]. Exposure of GCSF converts Th1 (IFNγ and TNFα secreting) T-cells to Th2 (IL4 and IL10 secreting) thereby reducing their response to alloantigens[369,370]. This can inhibit a T-cell mediated graft versus host disease in GCSF mobilised stem cell allogeneic transplant when compared to standard BM transplants. GCSF also induce production of regulatory DC[371,372] and DC-like myeloid cells, which in turn can affect T-cell development and function.

3.1.5 Hypothesis:

Expressing the human GCSF as an additional transcription unit of MV can enhance the therapeutic efficacy of MV.

3.1.5.1 Aims:

1. To determine the therapeutic effect of MV in an *in-vivo* model of ALL.

2. To establish the role of neutrophils and determine the therapeutic role of the novel MV expressing hGCSF (MVhGCSF) in two different *in-vivo* models of B-cell malignancies - Raji (Burkitt's lymphoma) and Nalm-6 (acute lymphoblastic leukaemia) *in-vivo*.

3.2 METHODS:

3.2.1 Cloning:

3.2.1.1 Plasmid Construction:

Prior to PCR amplification, site directed mutagenesis was performed on the hGCSF gene using QuikChange II XL Site-Directed Mutagenesis Kit (Stratagene, Agilent Technologies, UK) to remove an AatII site that was present on the gene in order to enable the use of AatII restriction enzyme for cloning it into MV genome. The primer sequences used for site directed mutagenesis are shown below:

Forward:

5'-CACACTGCAGCTGGAtGTaGCCGACTTTGCC-3'

Reverse:

5'GGCAAAGTCGGCtACaTCCAGCTGCAGTGTG-3'

hGCSF was PCR amplified using the following primers:

Forward: FP_MluI+hGCSF (new):

5'-agtattacACGCGTATGGCTGGACCTGCCACCCAGAGC-3'

Reverse: RP_AatII_hGCSF (correct):

5'-TACAGTCGgacgtcATtcagggctgggcaaggtggcg-3'

Replicating MV was rescued from cloned cDNA, as described in chapter 2, section 2.2.3.

3.2.2 *In-vivo* experiments:

All animal experiments were performed according to the UK Home Office approved protocols and institutional guidelines.

3.2.2.1 Nalm-6 disseminated model:

Disseminated ALL xenografts were established by tail vein injection of $1x10^6$ Nalm-6 cells. Three days after tumour cell transfer $1x10^6$ PFU of MV was administered IV by tail vein injection and repeated at weekly intervals for total six doses. Control mice were injected with UV inactivated MV (MVUV). Mice were monitored daily and euthanised when pre-defined humane end-point (hind limb paralysis) was reached.

3.2.2.2 Raji and Nalm-6 subcutaneous (SC) models:

Raji (Burkitt's lymphoma) and/or Nalm-6 (ALL) SC xenografts were established in 6-8 weeks old CB17-Prkdc^{SCID} (SCID) mice (Charles River, Margate, UK). To establish Nalm-6 xenografts, $5x10^6$ or $10x10^6$ viable Nalm-6 cells (ATCC, LGC, UK) were mixed with 2µg pre-thawed Matrigel™ (BD Biosciences) in a total volume of 200µl and injected into the right flank of each mouse. For the Raji xenografts, $10x10^6$ viable Raji cells (ATCC, LGC, UK) was injected in 200µl of RPMI 1640 medium. The tumours were administered with MV (MVNSe, MVUV, MVhGCSF) IT for 10 doses at an MOI of 1.0.

3.2.2.3 Neutrophil depletion in-vivo:

The schematic design of the neutrophil depletion experiment is shown in Fig 3-4a and 3-4b. Neutrophils were depleted *in-vivo* using a rat anti-mouse Gr-1 monoclonal antibody (anti-Ly6G6C, clone RB6-8C5; BD biosciences, UK) via IV, intra-peritoneal (IP) and/ or IT routes, with first injection via the IV route on Day 0. The control mice received equivalent amount of a rat immunoglobulin isotype antibody ($IgG2_b$, BD Biosciences, UK) via the same routes. 35-50µg of antibody was used for IV or IT routes whereas 150µg of antibody was used for IP routes per dose.

Neutrophil depletion was confirmed and monitored by flow cytometry regularly. Approximately 50µl of peripheral blood was collected by tail vein bleed and red blood cells were removed by hypotonic lysis. The white blood cells were then stained with rat anti-mouse CD11b-APC (clone M1/70; BD Bioscience, UK) and rat anti-mouse Ly6G6C-FITC (anti-GR1) (clone RB6-8C5; BD Biosciences, UK). Flow cytometry analysis was performed on the stained cells. The neutrophil depletion was repeated every 3-5 days and maintained throughout the MV therapeutic window.

Mice were injected with MV from Day 1 after neutrophil depletion at an MOI of 1.0 daily in a total volume of 100µl. A total of 8 and 10 MV injections were administered IT to Nalm-6 and Raji tumours respectively. Tumour volume was calculated using the formula:

$V=a^2b/2$ cm^3, where a = the shortest diameter and b = the longest diameter.

Mice were euthanised by Schedule 1 procedure when they reached their pre-determined humane end-points (tumour volume ≥2.5cm^3 or systemic spread of disease = onset of hind limb paralysis).

The *in-vivo* work on the Nalm-6 neutrophil depletion model was partly carried out by my colleague Dr. Zhang, and I have received her permission to include data obtained from Nalm-6 experiment alongside my own data from Raji neutrophil depletion experiment.

3.2.2.4 Raji and Nalm-6 luciferase disseminated models:

Disseminated xenografts were established by tail vein injection of 1x10^6 Nalm-6/Raji luciferase cells. Three days after tumour cell transfer 1x10^6 PFU of MV (MVNSe, MVUV, MVhGCSF) or 120 µg/kg of Pegylated hGCSF (Peg hGCSF) (Neulasta - Amgen) was administered at weekly intervals for total six doses for Nalm-6 and 3 doses for Raji. The dosage of Peg hGCSF was based on the literature[382-385]. MV was administered via the IV route by tail-vein injection while Peg hGCSF was administered SC. Mice were monitored daily and euthanised when pre-defined humane end-points were reached (on set of hind limb paralysis). At the humane end-point, spleens from the mice were analysed for the number of total cells recovered and percentage of neutrophil, macrophage and NK cells by flow cytometry. Serum from all these mice was collected by exsanguination and hGCSF level determined by ELISA.

3.2.2.5 In-vivo imaging:

Nalm-6/Raji luciferase-injected mice were imaged once a week by bioluminescent imaging. Mice were shaved and injected IP with 200µL of D-luciferin (Caliper Life Sciences, Cheshire UK). They were then imaged under anaesthetic (Isofluorane) under IVIS® 100 Lumina (Caliper Life Sciences, Cheshire, UK). The results were analysed using Living Image® 3.2 software.

3.2.2.6 Toxicity studies in Ifnar^{KO} CD46 Ge mice:

Ifnar^{KO} CD46 Ge mice were kindly provided by Roberto Cattaneo (Mayo Clinic), and then bred and housed in caged barrier. They were injected with 1x10^{6} PFU of MVNSe or MVhGCSF IV, via tail vein. The mice were then monitored twice a week for 35 days for any sign of ill health. On day 35, all the mice from both the cohorts were sacrificed and their spleen analysed for size and percentage of neutrophils, macrophages and NK cells by flow cytometry. Serum from all these mice was collected by exsanguination and hGCSF level determined by ELISA (Peprotech, UK).

3.2.3 Flow Cytometry:

3.2.3.1 Confirmation of neutrophil depletion:

Neutrophil depletion was confirmed by flow cytometry. Approximately 50µl of peripheral blood (PB) was collected by tail vein bleed and RBCs were removed by hypotonic lysis. The white blood cells were then stained with rat anti-mouse CD11b-APC (clone M1/70; BD Bioscience) and rat anti-mouse Ly6G6C-FITC (clone RB6-8C5; BD Biosciences) at 4°C for 30mins. The cells

were then washed and resuspended in PBS. The flow cytometry was performed on LSRII (BD Biosciences). The data was analysed using Flow Jo (version 7.6).

3.2.3.2 Detection of tumour cells:

Cells from the BM and spleen of the mice were isolated and stained with CD10-APC (BD) and CD19-PE (BD) for Nalm-6 cells and CD19-FITC (BD) and CD20-APC (BD) for Raji cells at 4°C for 30mins. The cells were then washed and resuspended in PBS. The flow cytometry was performed on LSRII and analysed using Flow Jo (version 7.6).

3.2.3.3 Detection of Neutrophils, NK and Macrophages in mouse spleen:

The spleen from mice was dissected and crushed and then treated with ACK lysis buffer (Lonza, UK). The cells were then isolated and stained with Pan NK (CD49b; clone DX5; BD biosciences) or rat anti-mouse CD11b-APC (clone M1/70; BD Bioscience), rat anti-mouse Ly6G6C-FITC (clone RB6-8C5; BD Biosciences) and Mac3-PE (BD) or isotype controls. The stained cells were washed and resuspended in PBS and then run on LSRII and analysed with Flow Jo (version 7.6).

3.3 RESULTS:

3.3.1 MV is therapeutic in an acute lymphoblastic leukaemia (ALL) model *in-vivo*:

First the therapeutic effect of MV was established in an ALL model *in-vivo.* To determine whether MVNSe is oncolytic in an *in-vivo* model of ALL, SC Nalm-6 tumours were established using $10x10^6$ Nalm-6 cells in SCID mice. On detection of first palpable tumour, they were treated with 10 IT injections of $1x10^6$ PFU of MVNSe or UV inactivated MV (MVUV) (Fig 3-1a). Median tumour volumes in both the groups were not significantly different at the start of the injections with MV group at $0.22cm^3$ and in MVUV group at $0.27cm^3$. MV treatment had a significant anti-tumour effect as shown in Fig 3-2a. Eleven of 12 established SC tumours regressed completely in MVNSe treated group by day 44 with the single remaining tumour fully disappearing by day 62. In contrast, all MVUV treated tumours progressed. The difference in tumour growth between the MVNSe treated and MVUV control groups was highly statistically significant ($p < 0.0001$).

To assess the oncolytic activity of MV in a disseminated model of ALL, SCID xenograft was established to evaluate IV MV administration, using $1x10^6$ Nalm-6 cells IV via the tail vein on Day 0, with MV treatment starting from Day 3 post tumour inoculation for total 6 injections (Fig 3-1b). Five of 10 mice receiving MVNSe survived beyond 100 days whereas all mice receiving the non-replicating MVUV succumbed by day 67. The BM of every mouse was analysed by flow cytometry for human $CD19^+/CD10^+$ cells, which

confirmed the presence of leukaemia in all mice (Fig 3-2b, bottom panel). A Kaplan-Meier analysis (Fig 3-2b) showed that the median survival was 54 days in MVUV controls compared to 114 days in the MVNSe group ($p<0.0001$). At the termination of the experiment at 123 days, no evidence of leukaemia was observed in the 5 surviving mice, indicating a complete remission rate of 42%.

.

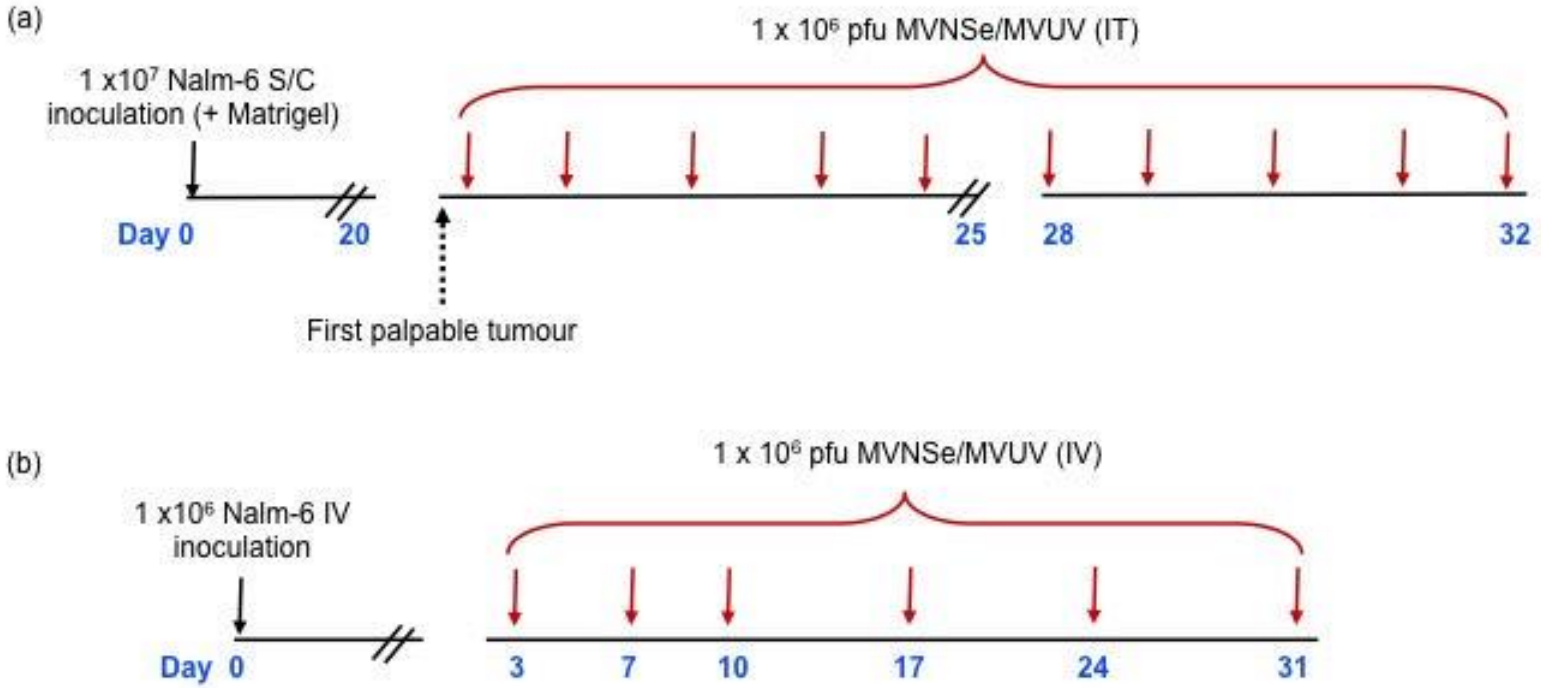

Figure 3-1: Experimental design of Nalm-6 SC and disseminated SCID xenografts: (a) SC Nalm-6 tumours were established with $10x10^6$ Nalm-6 cells mixed with Matrigel™. The tumours were treated with 10 IT injections of MVNSe/MVUV after the first palpable tumour was observed. (b) The disseminated tumours were established by IV injections of $1x10^6$ Nalm-6 cells. The mice received a total of 6 MV injections IV from day 3 after inoculation of the tumour. (Adapted from Patel, Dey et al. 2011)[386].

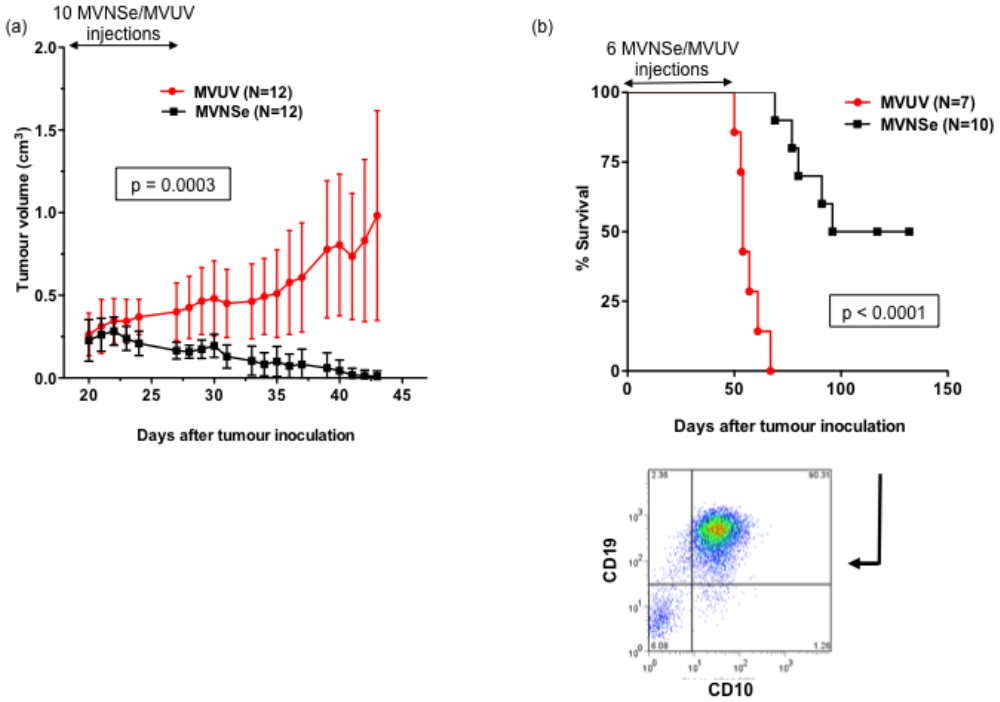

Figure 3-2: Nalm-6 SCID treated with MVNSe: (a) Tumour volumes in cm^3 after IT injection of MV (black closed squares) or MVUV (red closed circles) into Nalm-6 ALL xenografts, developed from $1x10^6$ Nalm-6 cells. (b) Kaplan–Meier survival curves of mice bearing disseminated Nalm-6 xenografts treated IV with a total dose of $6x10^6$ plaque forming unit (PFU) of MV (black line) or MVUV control (red line). Data represent the results from three independent experiments (N=3-6 per group). Representative FACS plot of CD10/CD19 positive cells from BM of mice confirming leukaemia is shown in the bottom panel. Arrows indicate the period of MV/MVUV administration. Log Rank test and Wilcoxon signed rank test was performed to obtain the P-values. (Adapted from Patel, Dey et al. 2011)[386].

3.3.2 Neutrophil depletion *in-vivo* abrogates MV therapeutic effect in Raji but not Nalm-6:

Based on the data from others and our own lab suggesting neutrophils as a potential effector in different microorganism mediated oncolysis, it was hypothesised that, if neutrophils are playing a role in MV oncolysis *in-vivo*, then depleting them should abrogate the MV-mediated oncolytic effect *in-vivo*. To investigate this in the Nalm-6 and Raji models, SC tumours were established by injecting respective tumour cells on the right flank of the SCID mice. When the tumours reached a certain comparable volume (mean tumour volume 0.4cm^3 in Nalm-6 and 0.8cm^3 in Raji) (Fig 3-3a and 3-3b), they were divided into the depleted/experimental group and the non-depleted/control group. A detailed schematic of the experimental design is shown in Fig 3-4a (Nalm-6) and Fig 3-4b (Raji). The experimental group received the anti-GR1 antibody (RB6-8C5 clone) and the control received the isotype antibody by IP, IV or IT routes, on the days shown by the blue, black and green arrows respectively. Depletion of neutrophils in the PB was monitored on the days shown in red arrows by flow cytometry (Fig 3-4a and b) in different representative mouse from each group on each day. As per the project license, a mouse can be bled only once a week, and therefore, different representative mouse was selected from each group for analysis of neutrophil depletion on each day. The flow cytometry plots showing neutrophil depletion in both Nalm-6 (Fig 3-5a-f) and Raji (Fig 3-6a-f) models on different days, compared to their non-depleted controls are shown in Fig 3-5 and Fig 3-6. A gate was drawn around the GR1^{high}CD11b$^+$ cell population

(mostly neutrophils in this model), in the non-depleted group compared to which the %GR1^{high}CD11b^{+} cells in the depleted group were calculated on each day.

In the Nalm-6 xenografts (Fig 3-5), RB68C5/isotype control antibody was administered on Day 0 IV. On day 1 (Fig 3-5a), analysis of PB by flow cytometry showed only 0.779% of GR1^{high}CD11b^{+} cells (red box) (also referred to as neutrophils) compared to the controls with 69.7% cells, showing effective depletion. Based on the literature[387,388], the PB was again checked 72 hours after first antibody injection on day 4 (Fig 3-5 b), and the percentage neutrophils was 11.7% in the depleted group, which was significantly lower than the control group (65.2%), and showed that one IV injection (50µg) can maintain neutrophil depletion for 3 days in this model. On Day 5, second dose of RB68C5/isotype antibody was administered IV, and checked on Day 6 (Fig 3-5c) and Day 7 (Fig 3-5d). On Day 8 and Day 13 another two doses of RB6/8C5 antibody was administered IT, to maintain local neutrophil depletion. The PB was further monitored on Day 8 (Fig3-5e) and Day 11 (Fig-3-5f). Throughout the period of antibody administration, the GR1^{high}CD11b^{+} cells were intact in the control population. We noticed a GR1^{low}CD11b^{+} population in both the control and depleted group, which was much higher in the depleted group compared to the control group, but the GR1^{high}CD11b^{+} (neutrophils) was appropriately depleted in the experimental group when compared to the control group.

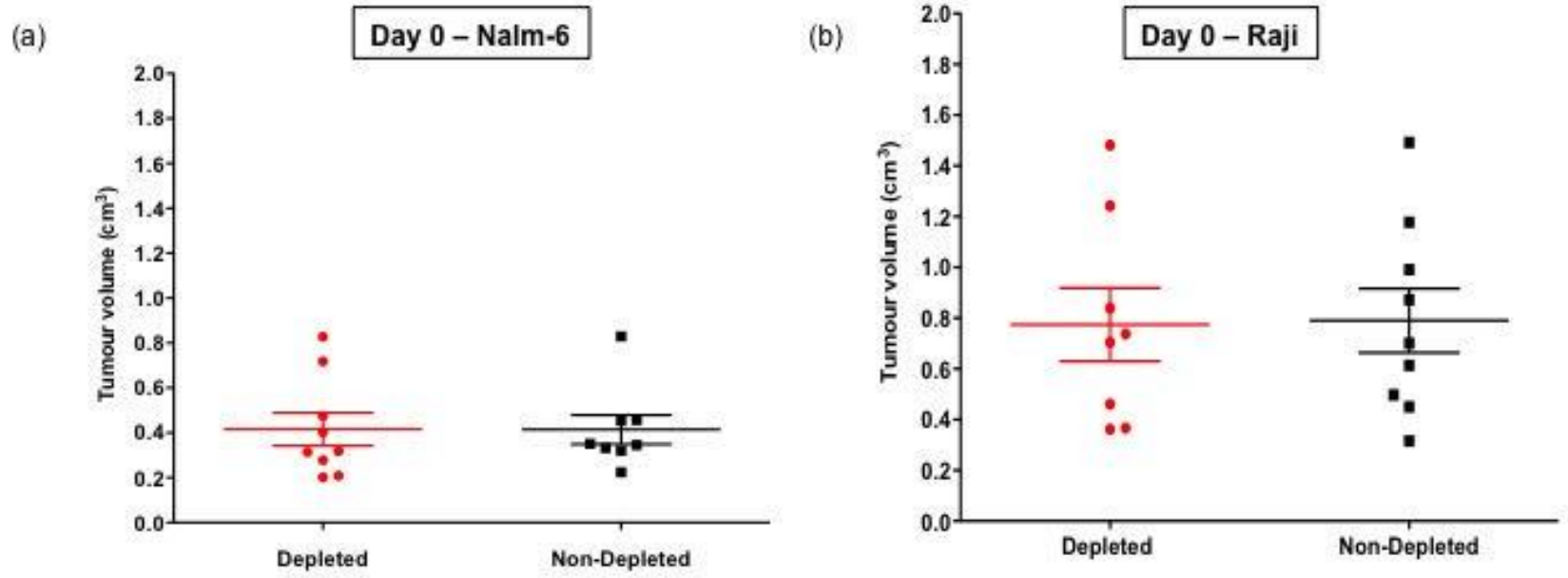

Figure 3-3: Tumour volume comparison on Day 0: Graphs showing tumour volumes of Nalm-6 (a) and Raji (b) before start of MV treatment. In the Nalm-6 and the Raji models, the mean tumour volumes in the neutrophil depleted (red solid circles) and non-depleted (black solid squares) groups were 0.4cm^3 and 0.8cm^3 respectively.

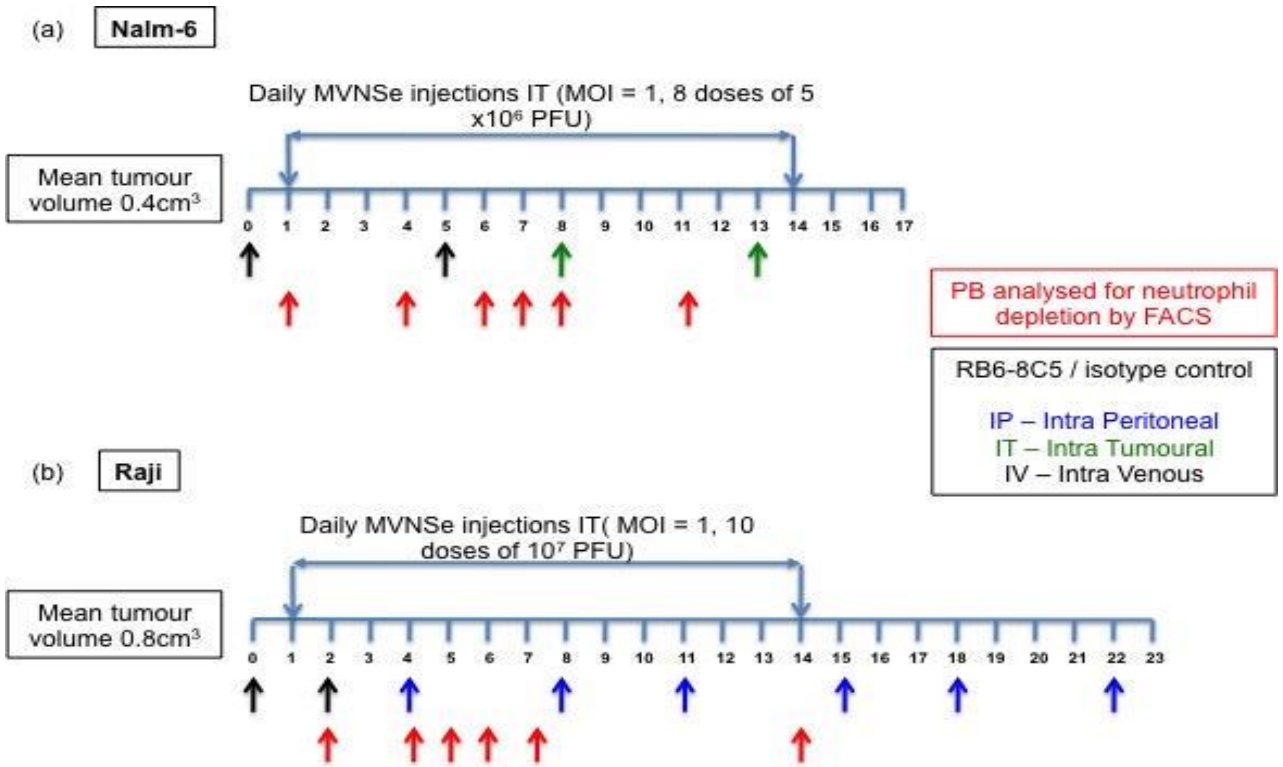

Figure 3-4: Experimental design of neutrophil depletion: (a) Nalm-6 (b) Raji: At 0.4cm^3(Nalm-6) and 0.8cm^3(Raji) mean tumour volume, the mice received IP, IT or IV injections of RB6-8C5/isotype control antibody on days shown by blue, green or black arrows respectively. PB

samples were analysed by FACS on days shown by red arrows. Tumours in both the group received 8 (Nalm-6) and 10 (Raji) doses of MV injections IT at an MOI of 1.0, between days 1 and 14 after first day of neutrophil depletion.

Figure 3-5:

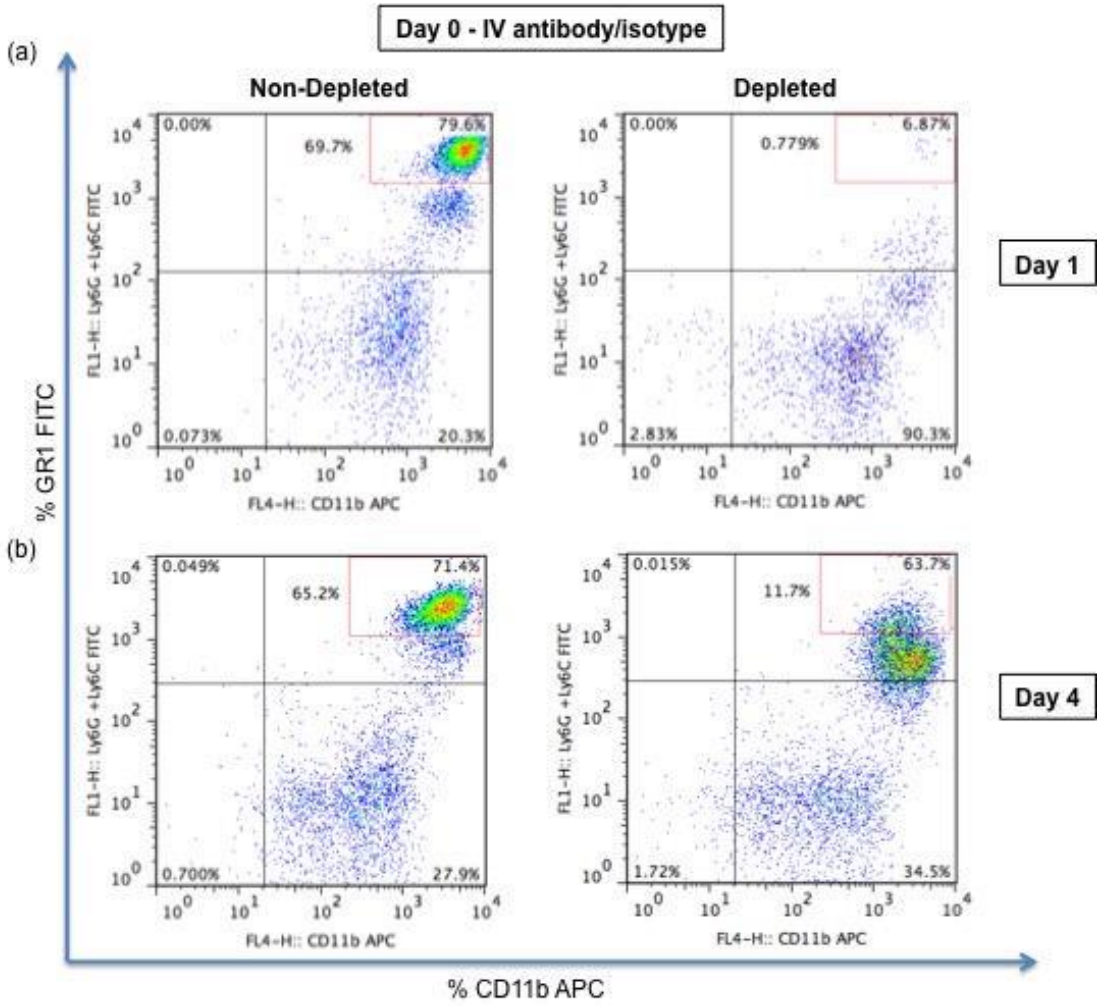

figure continued on the following page

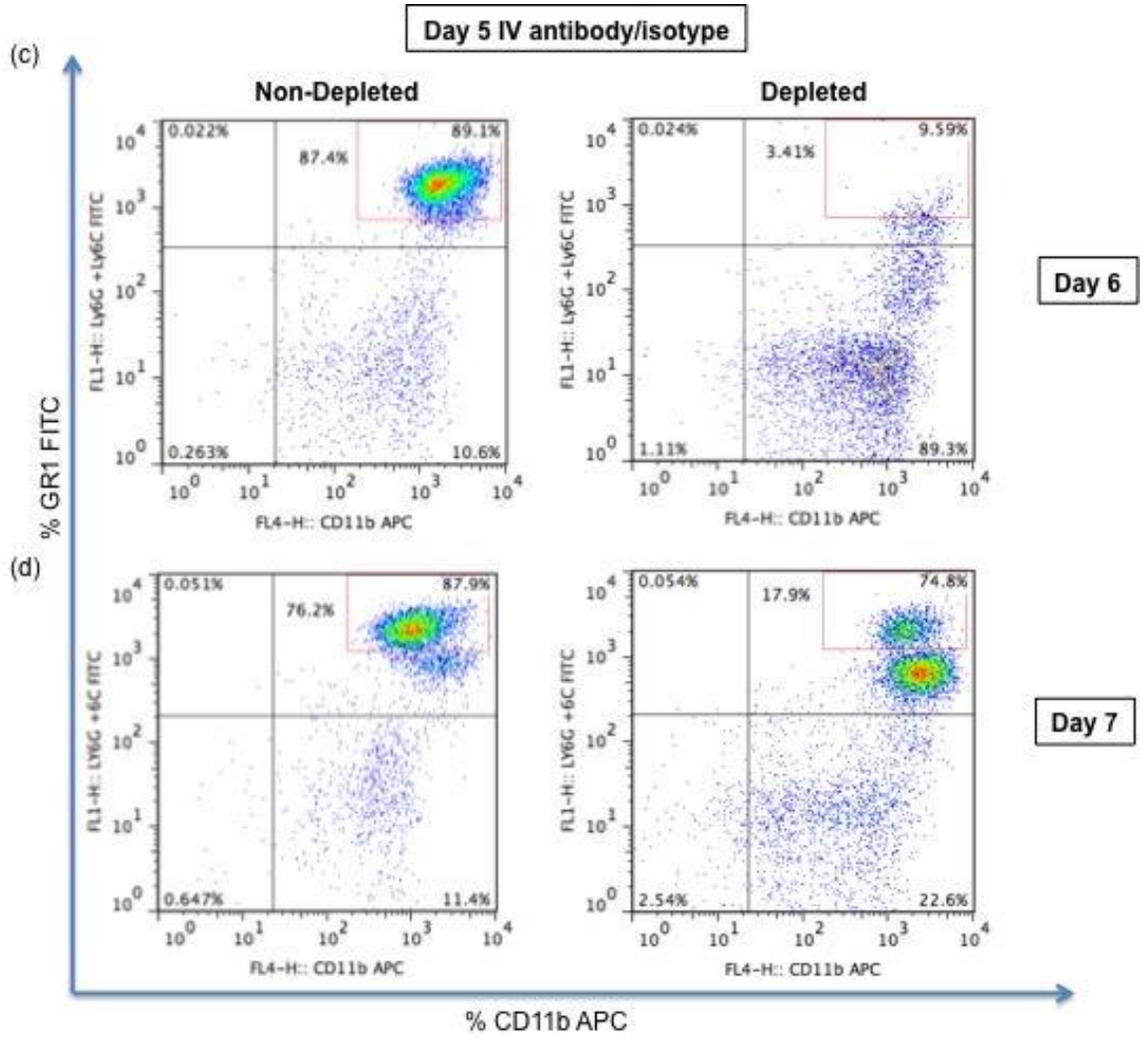

figure continued on the following page

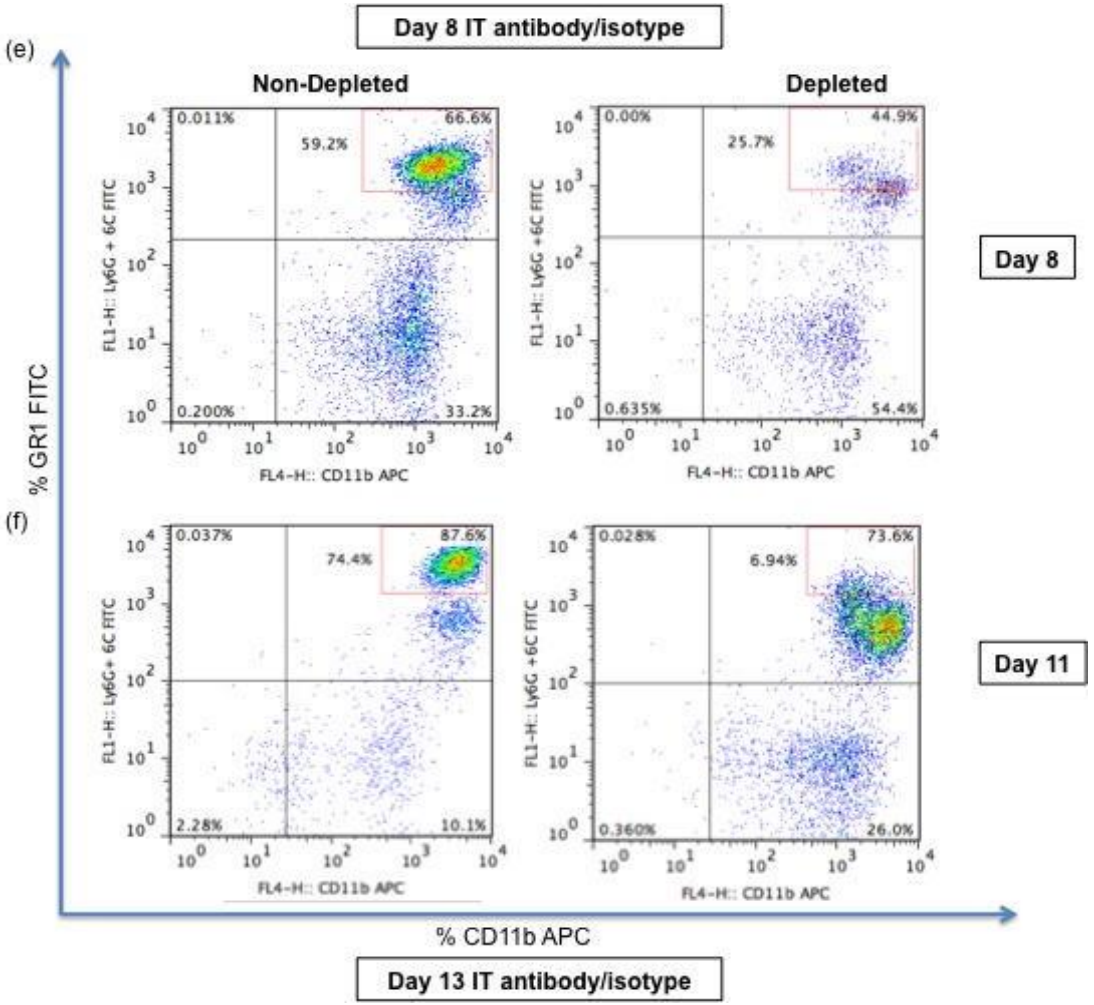
Day 8 IT antibody/isotype
(e)
Non-Depleted
Depleted
0.011%
66.6%
59.2%
0.200%
33.2%
0.00%
44.9%
25.7%
0.635%
54.4%
Day 8
(f)
0.037%
87.6%
74.4%
2.28%
10.1%
0.028%
73.6%
6.94%
0.360%
26.0%
Day 11
FL1-H:: Ly6G + 6C FITC
FL4-H:: CD11b APC
% GR1 FITC
% CD11b APC
Day 13 IT antibody/isotype

Figure 3-5: FACS plots confirming neutrophil depletion in Nalm-6 SCID xenografts: PB from different mice were analysed for neutrophil depletion on day 1 (a), day 4 (b), day 6 (c), day 7 (d), day 8 (e) and day 11 (f) by flow cytometry using anti-Ly6G6C (GR1) FITC (y-axis) and anti-CD11b APC (x-axis) antibodies. The percentage of cells in neutrophil gates of the control/non-depleted mice ranged between 59.2% - 87.4% compared to the depleted mice which showed 0.779 – 25.7% cells in the neutrophil gates (red rectangles) on the specified days during the experiment. Anti-GR1/isotype antibody was administered on day 0 and day 5 IV and on day 8 and day 13 IT (shown in the black boxes).

In the Raji xenografts (Fig 3-6), the RB68C5/isotype was administered IV on Day 0. As we had observed in the Nalm-6 model that IV injection of antibody could maintain the depletion for 3 days, the PB was checked on Day 2 (Fig 3-6a). The depleted group still showed presence of 45.1% of the neutrophils in the PB and therefore, a second dose of RB68C5/isotype antibody was administered on Day 2, IV. On Day 4 (Fig 3-6b), the flow cytometry analysis of the PB revealed 38.3% of neutrophils remaining. Hence a higher dose of the RB68C5/isotype antibody was administered (150µg) on the same Day 4, IP[389], and the PB was checked on Day 5 (Fig 3-6c), which showed complete and more effective neutrophil depletion (0.317%). After IP administration of the antibody, the percentage neutrophil on Day 6 (Fig 3-6d) and Day 7 (Fig 3-6e) remained very low at 0.059% and 0.788% respectively. The neutrophils remained depleted for 4 days after IP administration of the antibody and therefore were administered every 3-4 days on Day 8, Day 11, Day 15, Day 18 and Day 22. On day 14 (Fig3-6f), the percentage neutrophil started rising back and in the depleted group 16.6% neutrophils were present, but this was still significantly lower than the control group (80.5%). Even in the Raji model, we constantly observed a $GR1^{low}CD11b^{+}$ population, especially in the depleted group but the neutrophils remained depleted when compared to the control group.

Figure 3-6:

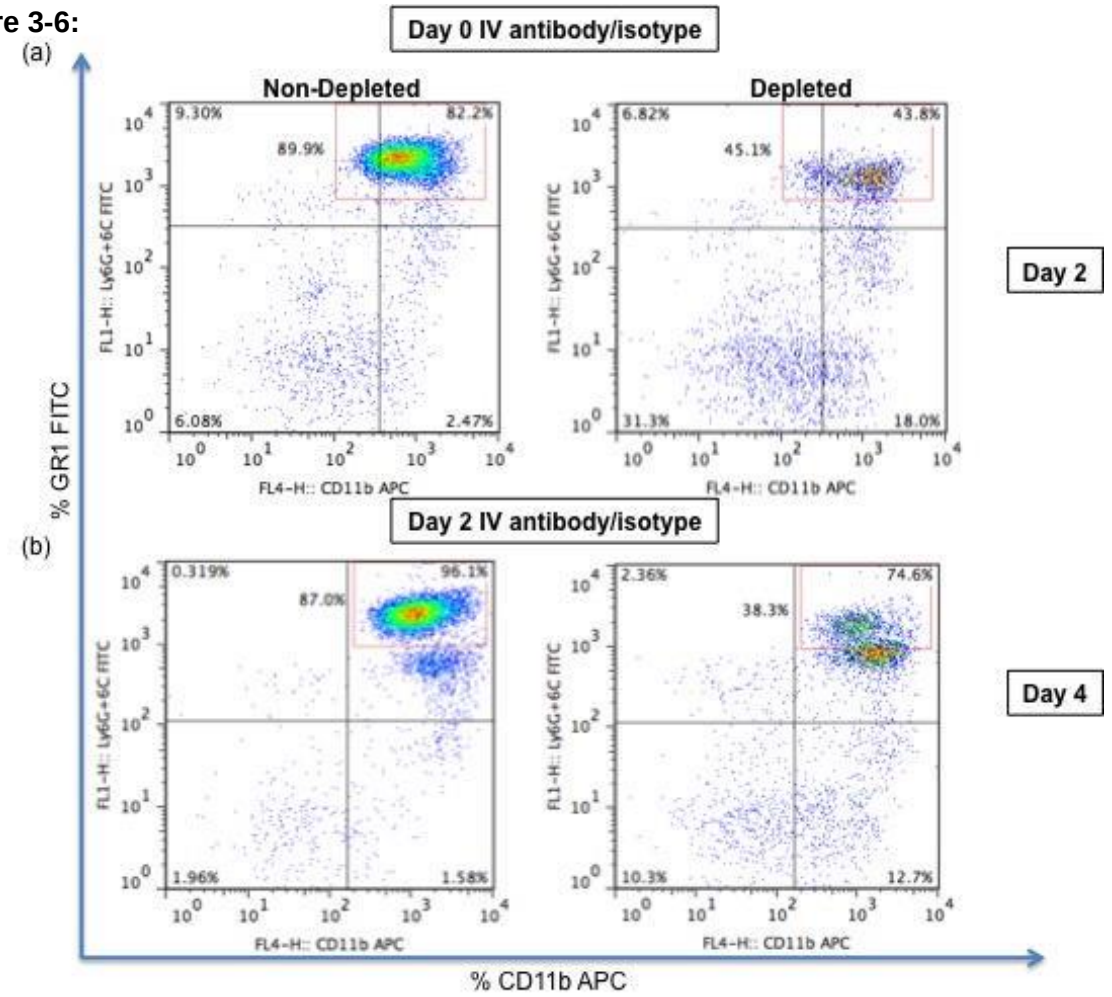

figure continued on the following page

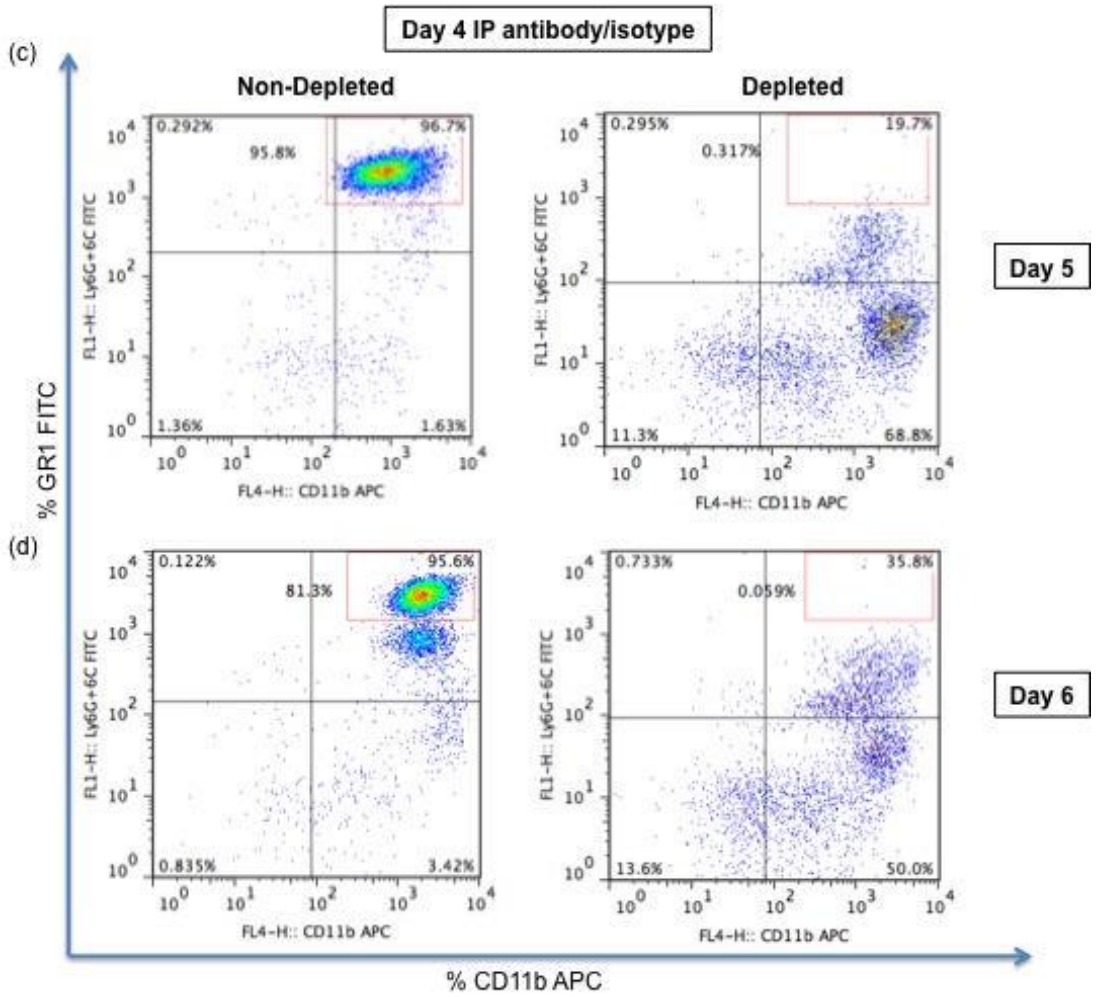

figure continued on the following page

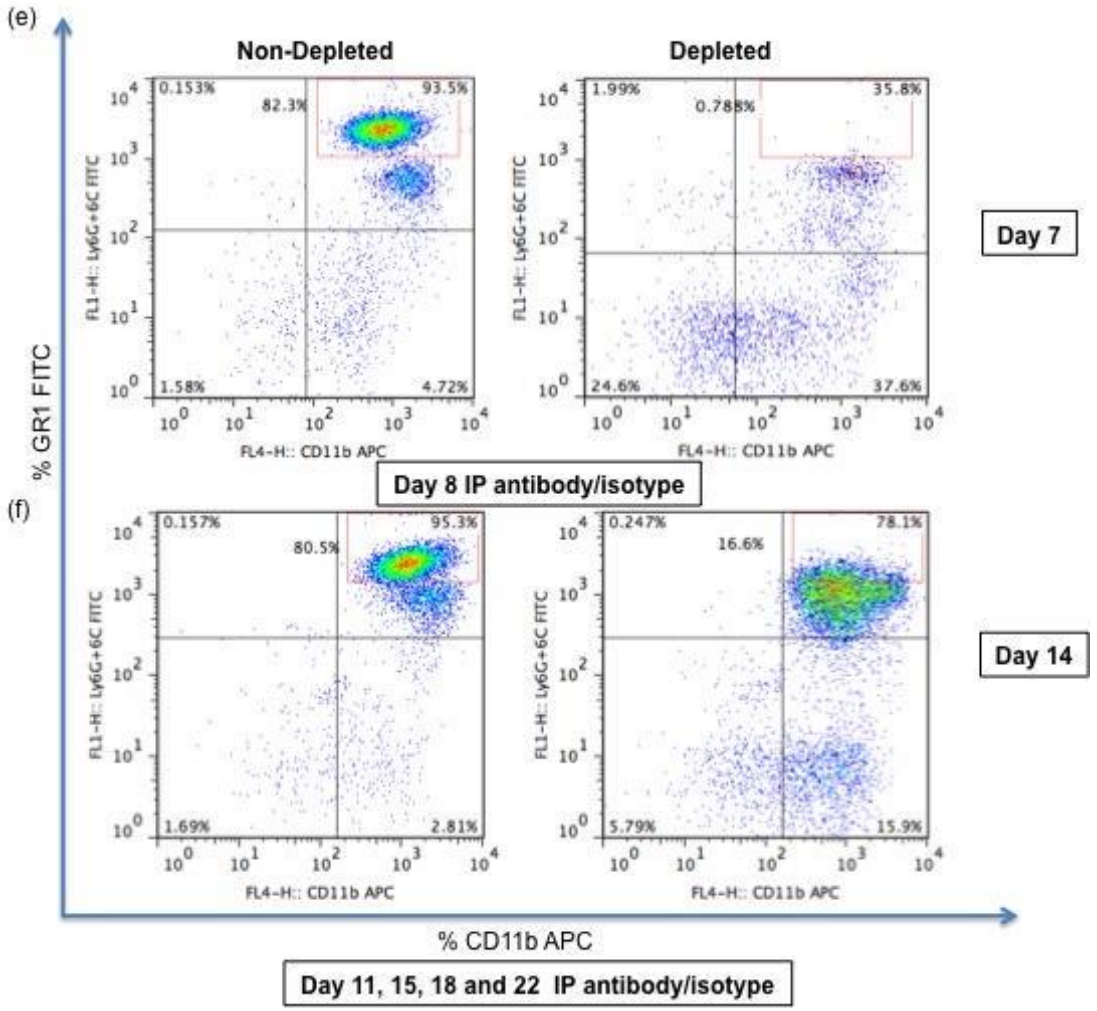
(e)
Non-Depleted
Depleted
0.153%
82.3%
93.5%
1.58%
4.72%
1.99%
0.788%
35.8%
24.6%
37.6%
FL1-H:: Ly6G+6C FITC
FL4-H:: CD11b APC
Day 7
Day 8 IP antibody/isotype
(f)
0.157%
80.5%
95.3%
1.69%
2.81%
0.247%
16.6%
78.1%
5.79%
15.9%
Day 14
% GR1 FITC
% CD11b APC
Day 11, 15, 18 and 22 IP antibody/isotype

Figure 3-6: FACS plots confirming neutrophil depletion in Raji SCID xenografts: PB from different mice were analysed for neutrophil depletion on day 2 (a), day 4 (b), day 5 (c), day 6 (d), day 7 (e) and day 14 (f) by flow cytometry using anti-Ly6G6C (GR1) FITC (y-axis) and anti-CD11b APC (x-axis) antibodies. The percentage of cells in neutrophil gates of the control/non-depleted mice ranged between 80.5% - 95.8% compared to the depleted mice which showed 0.059 – 45.1% cells in the neutrophil gates (red rectangles) on the specified days during the experiment. Anti-GR1/isotype antibody was administered on day 0 and day 2 IV and on day 4, day 8, day 11, day 15, day 18 and day 22 IP (shown in the black boxes).

The overall percentage of $GR1^{high}CD11b^{+}$ double positive cells, collated from all the different mice tested in Nalm-6 and Raji xenografts are shown in Fig 3-7a and Fig 3-7b respectively during the period of therapeutic MV administration. The representative flow cytometry histogram plots are shown in the top panels of Fig 3-7. Though variable, compared to the control mice receiving an irrelevant isotype control antibody the neutrophils were appropriately depleted in the experimental group (Fig 3-7a) Nalm-6 (43.92 median in depleted and 75.25 median in non-depleted) and Raji (Fig 3-7b) (35.93 median in depleted and 93.05 median in non-depleted) models. The Raji and Nalm-6 tumours were treated with MV at an MOI of 1.0 by IT injection starting from Day 1 after neutrophil depletion was confirmed. The MV was administered between days 1 and 14 starting from the first day of neutrophil depletion.

The Nalm-6 tumours regressed rapidly and completely after MVNSe injection in both depleted (N=9) and non-depleted group (N=8) and there was no difference in tumour size between non-depleted and neutrophil depleted (Fig 3-8a) cohorts. By contrast, in the Raji model the tumours responded less well in the neutrophil depleted group (N=8) than the non-depleted group (N=9) - all mice in the depleted group had reached the humane endpoint (tumour size 2.5cm^3 and/or hind limb paralysis) by day 27, whereas only half in the non-depleted group (Fig 3-8b). There was a significant difference (p= 0.0001) in the survival between the two groups in the Raji model (Fig 3-9a) but not in the Nalm-6 model (Fig 3-9b). Taken together, the depletion experiments suggested that the neutrophil-mediated enhancement of MV's

oncolytic activity is likely to play a more prominent role where the direct anti-tumour effect is less pronounced as observed in the Raji model.

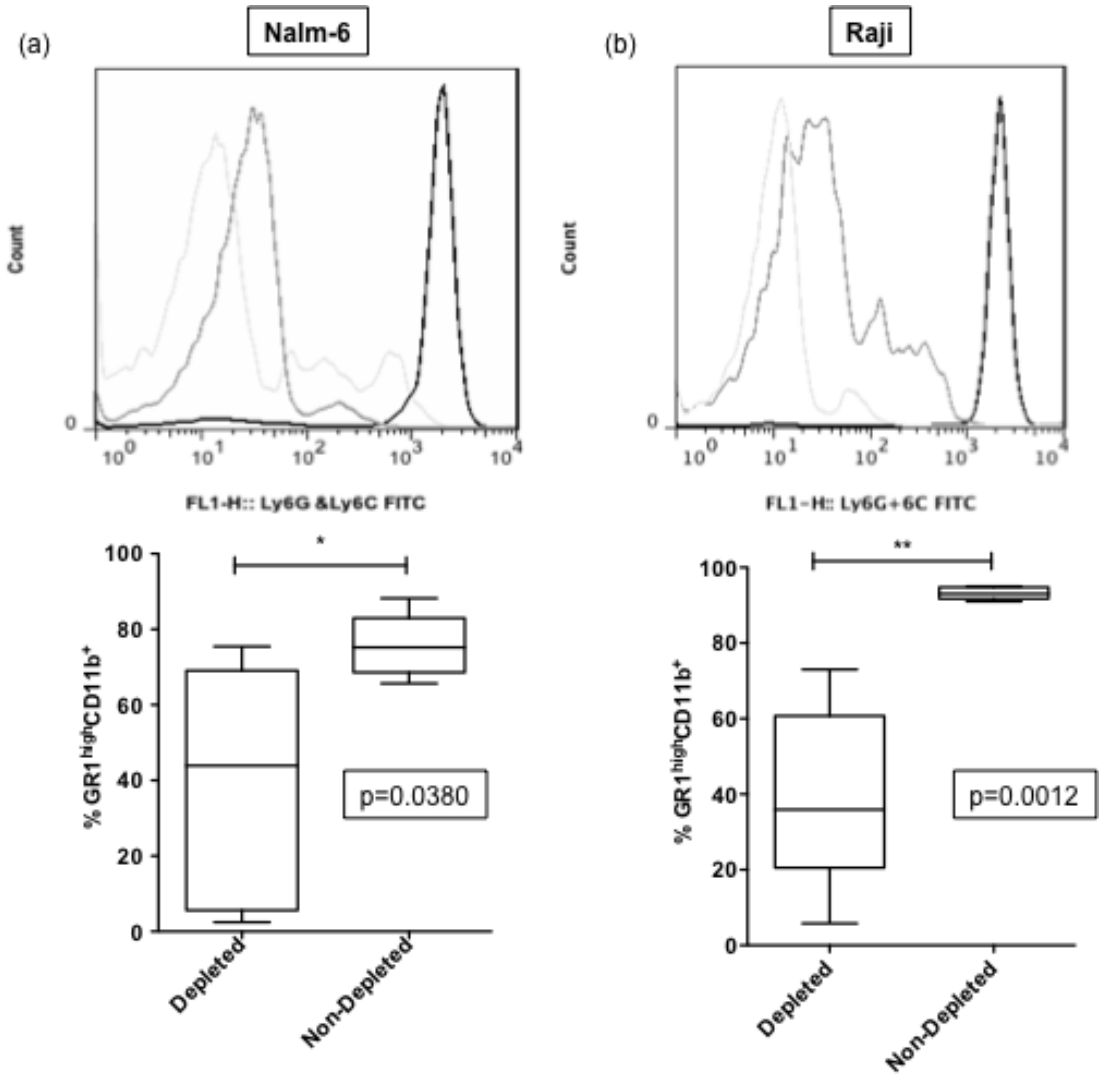

Figure 3-7: Cumulative neutrophil depletion data: Flow cytometry data for neutrophil depletion from all the different mice bearing (a) Nalm-6 and (b) Raji tumours tested are shown. For each tumour type, representative histograms plots are shown in the upper panels (light grey line = isotype control, dark grey line = depleted group, black line = non-depleted group) and in the lower panel box plots showing aggregate data of percentage $CD11b^{+}GR1^{+}$ double positive cells in Nalm-6 (a) and Raji (b) models. Unpaired t test was performed to obtain the P-values

Figure 3-8:

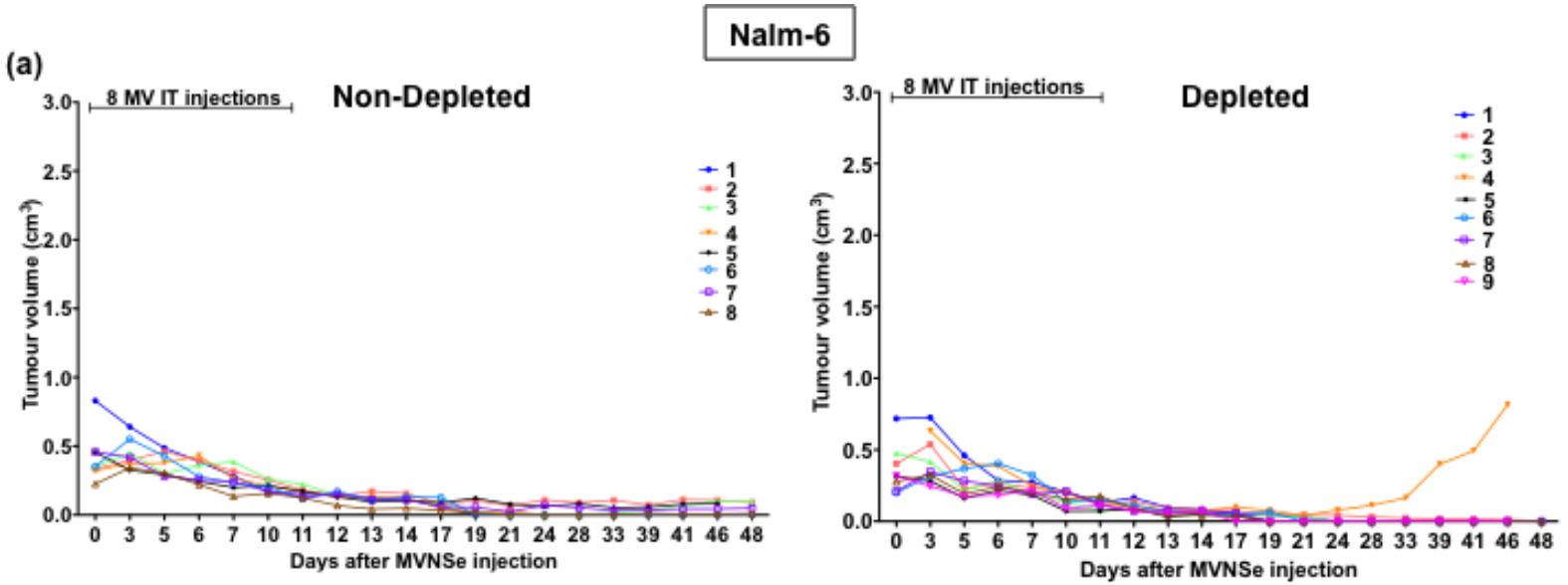

figure continued on the following page

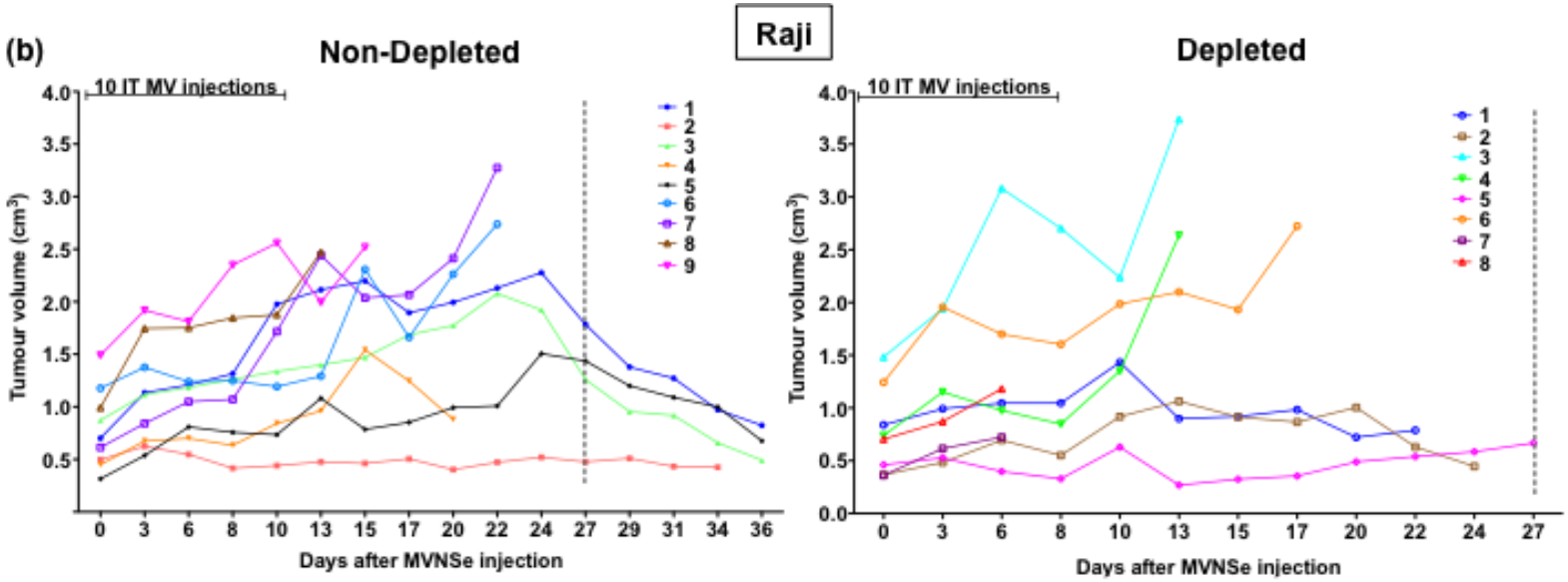

Figure 3-8: Tumour volumes in Nalm-6 and Raji models: Graphs showing tumour volumes in individual mice (each coloured line represent a mouse) in Nalm-6 (a) {non-depleted (N=8); depleted (N=9)} and Raji (b) {non-depleted (N=9); depleted (N=8)} after MV treatment. The vertical dashed lines in (b) shows Day 27.

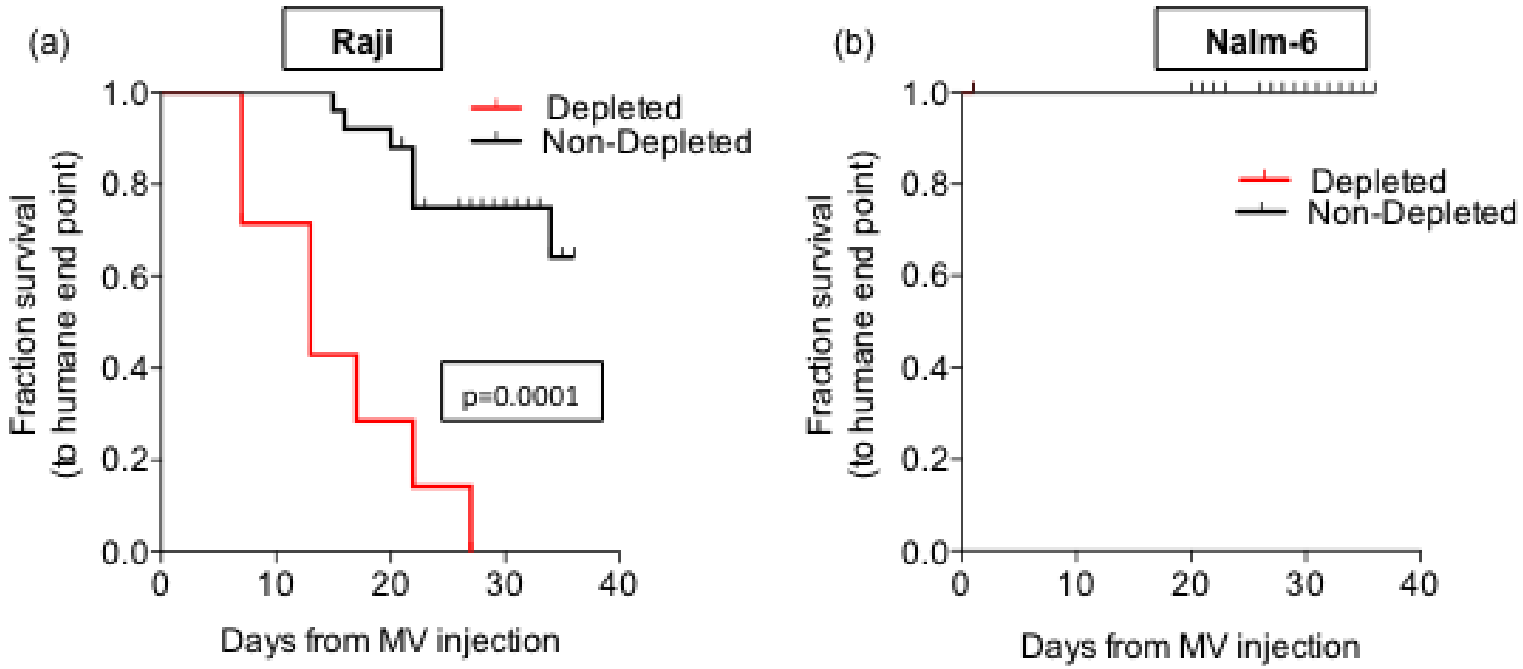

Figure 3-9: Kaplan Meier survival curve in Raji and Nalm-6: Kaplan Meier survival curves from start of MV injection in the Raji (a) and Nalm-6 (b) neutrophil depletion models are shown with black line representing the non-depleted group and red line representing the depleted group. Log Rank test was performed to obtain the P-value.

3.3.3 Generating novel MV expressing hGCSF:

To disentangle the intriguing and different roles of neutrophil in the two models and to enhance neutrophil survival and function at the tumour site, a novel strain of MV was generated expressing the cytokine gene human GCSF (hGCSF). Figure 3-10 shows the strategy for cloning hGCSF into the MVNSe backbone by replacing the GFP using MluI and AatII restriction enzymes downstream of the MV-P gene. As the hGCSF gene had an AatII site within the gene, site directed mutagenesis was performed first to replace the restriction enzyme site AatII - GACGTC with GATGTA, leaving no amino acid change (Fig 3-10b). The cloned MV plasmid was then rescued using reverse genetics technique described in materials and methods (chapter 2, section 2.2.3). Fig 3-11a shows syncytium formed by the MVhGCSF on Vero cells from which they were picked and then further propagated and characterised.

3.3.4 Characterisation of the novel virus:

3.3.4.1 Growth curves:

One step growth curves were performed to assess the growth pattern of the new virus. Vero cells infected with the virus at an MOI of 1.0 were collected at different time-point post infection and the virus was titrated using $TCID_{50}$ in a 96-well plate. The virus grew to similar titres (10^6-10^7 PFU) as the backbone MVNSe virus with the viral production peaking at a later time-point compared to the MVNSe (48 hour for MVNSe; 62 hour for MVhGCSF) (Fig 3-11b).

3.3.4.2 Cytokine production:

hGCSF production was quantified in all the cell lines over 5 days and neutrophils over 24 hours post infection (hpi) (Fig3-11c and d respectively). Supernatants from both infected and uninfected Raji and Nalm-6 cell lines and infected and uninfected neutrophils (from healthy human donors) were collected and quantified by ELISA for the cytokine production. The three cell lines produced hGCSF in the range of 200 – 700ng/ml at different time-points (Fig 3-11c). Neutrophils from 3 different donors showed hGCSF (Fig 3-11d) production in the range of 2-3ng/ml. No hGCSF was detected in the cell lines or neutrophils infected with the control virus MVNSe.

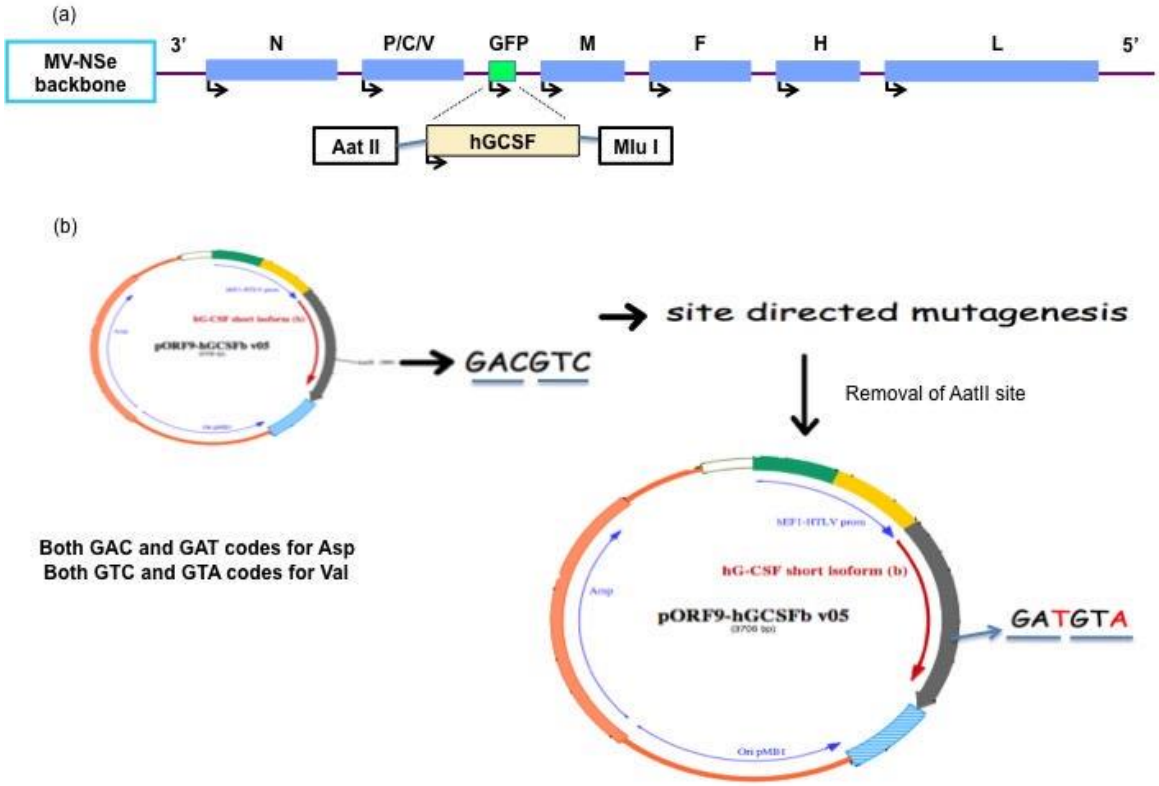

Figure 3-10: Construction of MV expressing hGCSF: (a) Schematic showing cloning of DNA encoding human cytokine, hGCSF into p (+) MVNSe, upstream of M, using AatII and MluI restriction enzymes. (b) Site directed mutagenesis strategy used to introduce mutations to change GAC to GAT and GTC to GTA in the hGCSF gene to remove AatII site within the gene, facilitating easy cloning into MV genome.

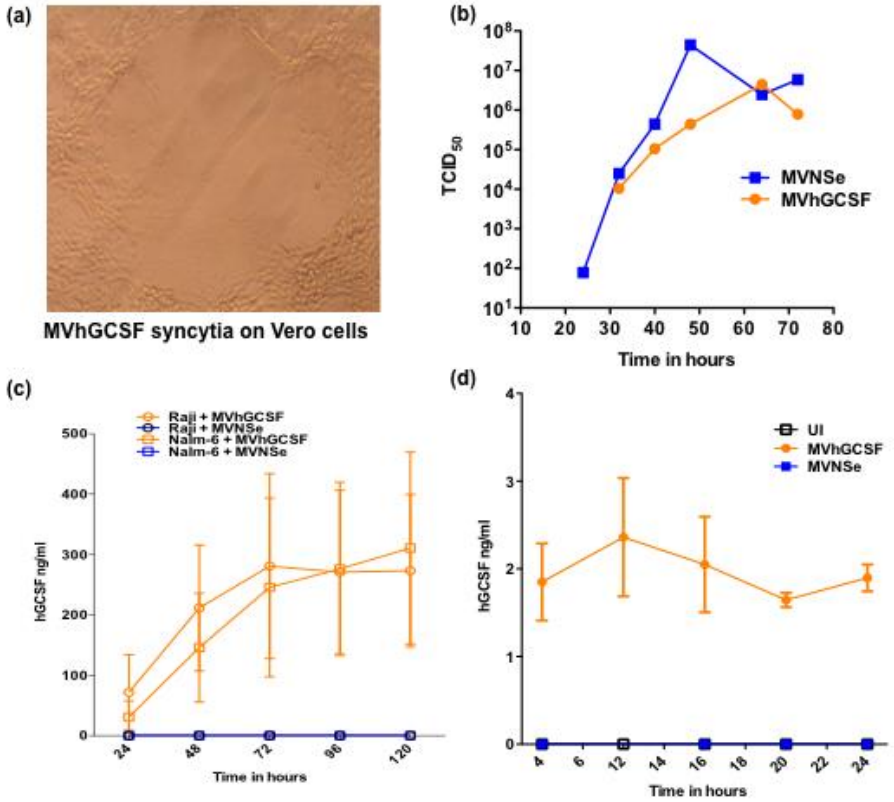

Figure 3-11: Characterisation of MV expressing hGCSF: (a) MVhGCSF syncytia on Vero cells. (b) One step growth curve of MVhGCSF performed on Vero cells {MVhGCSF (orange); MVNSe (blue)}. (c) hGCSF quantitation in supernatant of Nalm-6 (□) infected with MVhGCSF (orange) or MVNSe (blue) (N=3) and supernatant of Raji (○) infected with MVhGCSF (orange) or MVNSe (blue) (N=3). (d) hGCSF quantitation in supernatant of neutrophils from healthy donors infected with MVhGCSF (orange), MVNSe (blue) or mock infected (black) (N=3).

3.3.5 MVhGCSF is therapeutic in Raji and Nalm-6 SC *in-vivo* xenografts:

After characterisation of the virus, the therapeutic effect of expressing hGCSF by MV was determined *in-vivo.* The therapeutic efficacy of MVNSe was compared with that of MVhGCSF in SC models of both Nalm-6 and Raji tumours. In these mice, the tumours were allowed to reach 0.2 to 0.4cm^3 in size (Fig 3-12a and 3-12b), after which they were treated with 10 IT injections of MVNSe (N=5), MVhGCSF (N=6) or UV-irradiated non-replicating MV control (MVUV) (N=7). In the Raji model, MVhGCSF treated tumours regressed very efficiently and completely and generated a highly significantly superior (p=0.0020) anti-tumour effect by comparison to MVNSe (Fig 3-13a) treated tumours. The Kaplan Meier analysis showed that the MVhGCSF treated mice survived significantly longer than MVNSe treated mice (p=0.0098) (Fig 3-13b). In the Nalm-6 model, both the MVhGCSF and MVNSe treated tumours resulted in complete regression of the tumours in both cohorts (Fig 3-13c), and all mice survived tumour free in both the groups, hence there was no survival advantage to MVhGCSF therapy (Fig 3-13d).

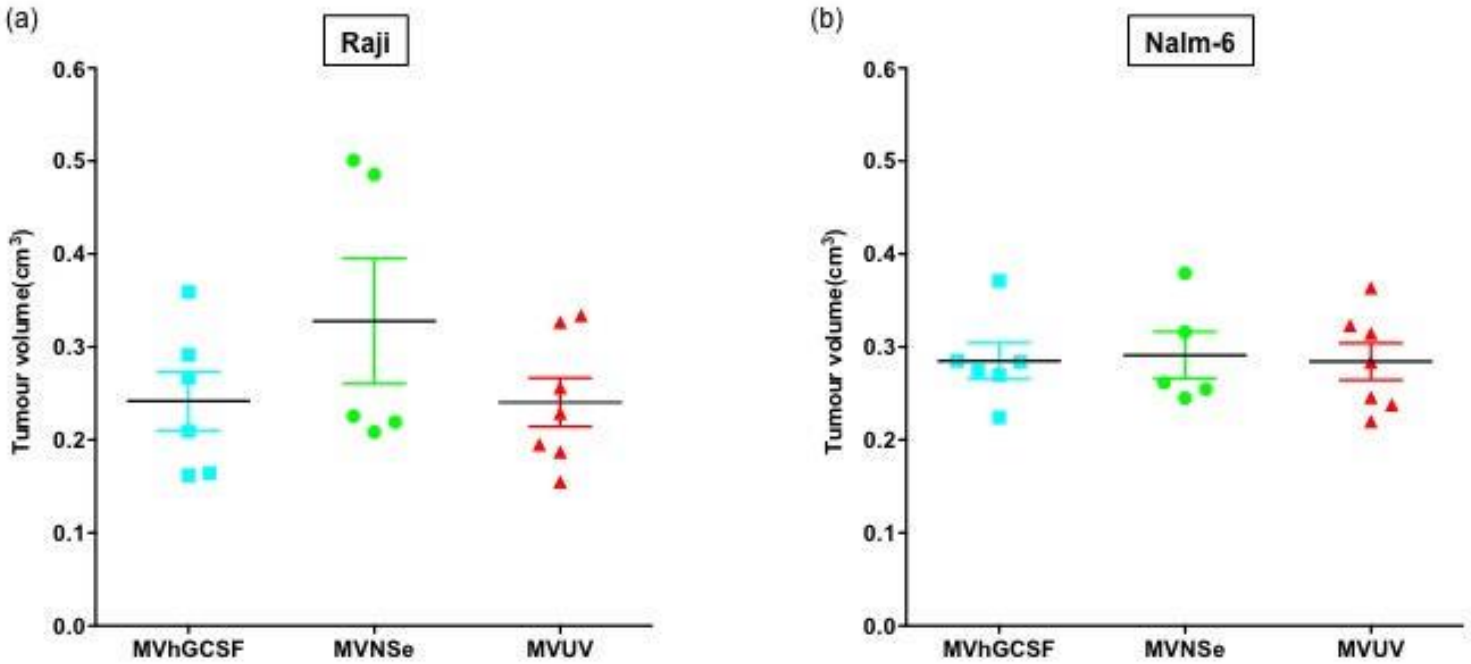

Figure 3-12: Tumour volume before start of MV therapy in two different SC B-cell malignancies: Raji (a) and Nalm-6 (b) xenografts were established SC in SCID mice. Tumour volumes before commencing the MV injections in the three treatment groups MVhGCSF (cyan), MVNSe (green) and MVUV (red) are shown in both (a) and (b).

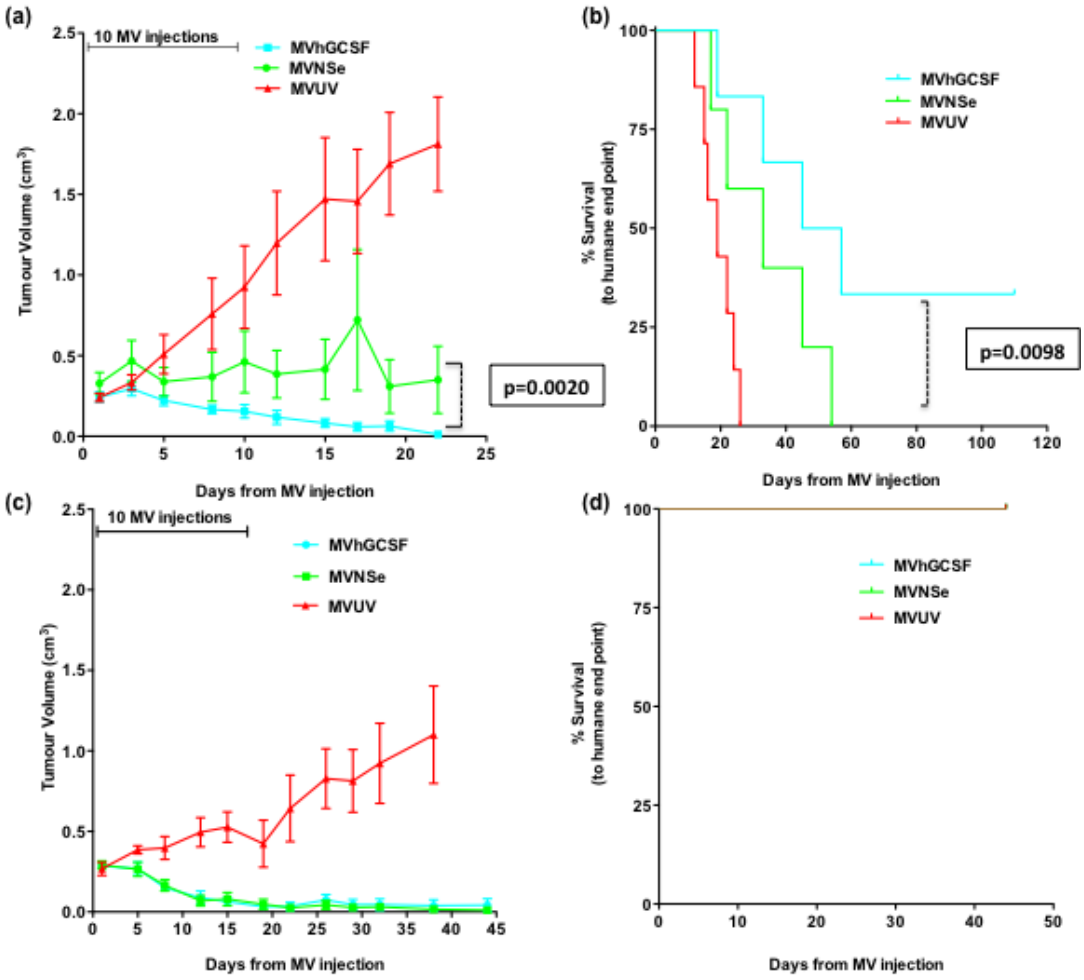

Figure 3-13: Tumour volumes and Kaplan Meier survival curves in two different SC B-cell malignancies: Raji (a and b) and Nalm-6 (c and d) xenografts were established SC in SCID mice. Tumour volume measurement was documented after MVhGCSF (cyan), MVNSe (green) and MVUV (red) injections in both the model (a - Raji and c – Nalm-6). Kaplan Meier survival plots in MVhGCSF (cyan line), MV-NSe (green line) and MVUV (red line) treated cohorts in Raji (b) and Nalm-6 (d). MVhGCSF N=6; MVNSe N=5; MVUV N=7. Wilcoxon signed rank test and Log rank statistical tests were performed to obtain the P-values in (a) and (b) respectively.

3.3.6 MVhGCSF play different roles in disseminated model of B-cell malignancies:

MVhGCSF was shown to be therapeutic in both Raji and Nalm-6 SC models, but B-cell malignancies are disseminated diseases, therefore, the therapeutic efficacy of MVhGCSF was tested in systemic therapeutic models.

In this experiment, Nalm-6 and Raji tumour cells expressing luciferase (luc) were used, in order to enable *in-vivo* monitoring of disease progression by live imaging. In the Nalm-6 luc model, mice were treated with 6 injections of $1x10^6$ PFU of MVNSe (N=7), MVhGCSF (N=6), or MVUV control (N=3) and an additional control of hGCSF alone, using pegylated hGCSF (Peg hGCSF) (N=5) at 120µg/kg once a week, for total 6 injections was also included. In the Raji luc model, only 3 of the 6 planned weekly injections of $1x10^6$ PFU of MVNSe (N=10), MVhGCSF (N=10), MVUV (N=8) and Peg hGCSF (N=9) were possible before the mice succumbed.

Fig 3-14a shows weekly *in-vivo* images in the Nalm-6 luc experiment. In this Nalm-6 luc model (Fig 3-14a), the two non-therapeutic/control groups MVUV and Peg hGCSF (Fig 3-14(a)(i)), and the two therapeutic/experimental groups MVNSe and MVhGCSF (Fig 3-14(a)(ii)) were carried out at slightly different times, so the luciferase signal can only be appropriately compared between those groups imaged at the same time, due to threshold setting. In the Nalm-6 luc model, signal was detected as early as week 2 in Peg hGCSF treated group when compared to the MVUV treated group, and by week 6 in the Peg hGCSF treated group, 2 of 5 mice had to be taken down (Fig 3-14(a)(i)). Similarly, in the MV therapeutic groups, the signal was detected at week 5 in the MVhGCSF treated group when compared to the MVNSe treated group and by week 10, 2 of 6 mice had to be taken down in the MVhGCSF group (Fig 3-14(a)(ii)). Total signal was quantified by plotting individual values for luminescence (photons/second) performed on each surviving animal in the non-therapeutic groups at week 6 (Fig 3-14b) and the

therapeutic groups at week 10 (Fig 3-14c). These data show a significant difference between the groups with a higher tumour signal in the mice, which had received any therapy including GCSF (either the Peg hGCSF control or MVhGCSF). In the Raji luc model (Fig 3-15), tumour signal was detected at week 2 (Fig3-15a). Quantification of total signal (Fig 3-15b) at week 2 showed that, by contrast to the Nalm-6 luc model, the MVhGCSF treated mice had significantly lower tumour burden compared to the MVNSe treated group ($p=0.0457$).

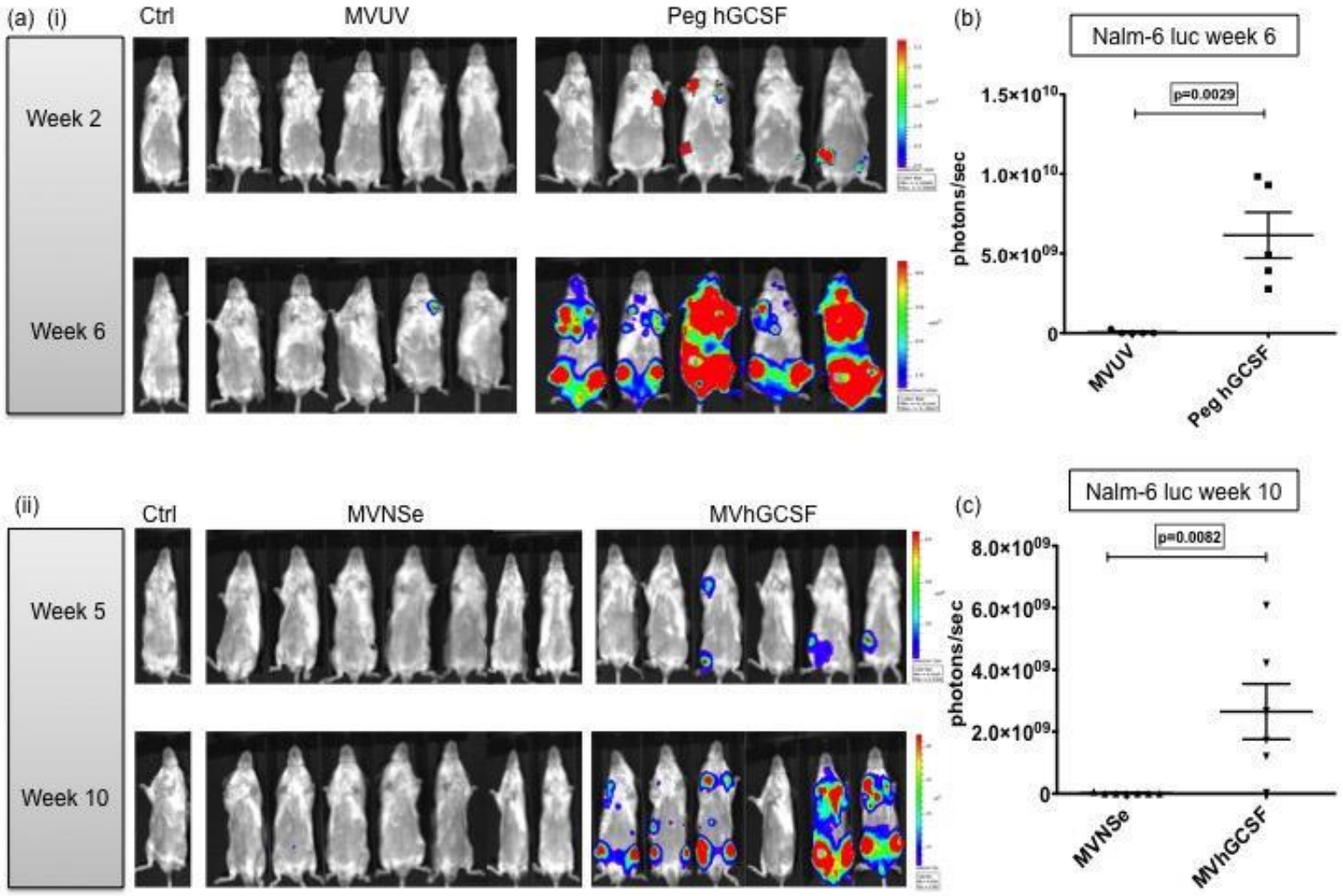
(a) (i)
Ctrl
MVUV
Peg hGCSF
Week 2
Week 6
(b)
Nalm-6 luc week 6
p=0.0029
1.5×10^10
1.0×10^10
5.0×10^09
0
photons/sec
MVUV
Peg hGCSF
(ii)
Ctrl
MVNSe
MVhGCSF
Week 5
Week 10
(c)
Nalm-6 luc week 10
p=0.0082
8.0×10^09
6.0×10^09
4.0×10^09
2.0×10^09
0
photons/sec
MVNSe
MVhGCSF

Figure 3-14: *In-vivo* imaging of Nalm-6 luciferase disseminated SCID model: Bioluminescent images showing comparison of leukaemia signal in Nalm-6 model; (a)(i) non-therapeutic MVUV (middle panel) and Peg hGCSF (right panel) groups at week 2 and week 6 post tumour inoculation and (a)(ii) therapeutic MVNSe (middle panel) and MVhGCSF (right panel) groups at week 5 and week 10 post tumour inoculation. Both (a) (i) and (a) (ii) images were taken with PBS injected controls (Ctrl) to account for background luminescence. The scales are on the right, next to the set of images compared at each week. (b) and (c) Quantification of tumour burden using bioluminescence; Scatter dot plot showing individual values for luminescence (photons/second) performed on each surviving animal in each treatment group at week 6 (Nalm-6 luc non-therapeutic groups) (b), week 10 (Nalm-6 luc therapeutic group) (c). Values are represented minus background activity. Unpaired t test was performed to obtain the P-values.

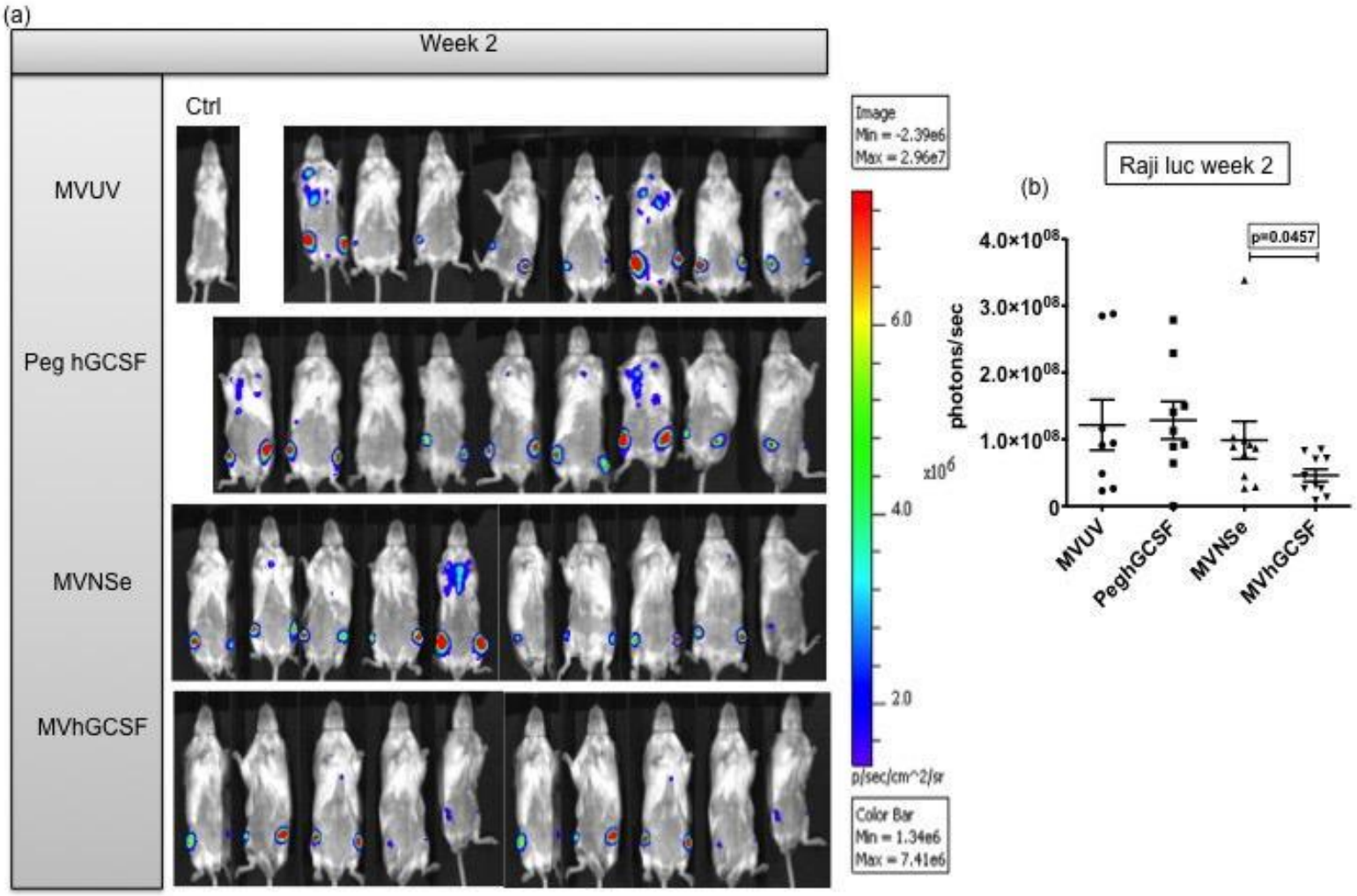
(a)
Week 2
Ctrl
MVUV
Peg hGCSF
MVNSe
MVhGCSF
Image
Min = -2.39e6
Max = 2.96e7
6.0
4.0
2.0
x10^6
p/sec/cm^2/sr
Color Bar
Min = 1.34e6
Max = 7.41e6
(b)
Raji luc week 2
p=0.0457
photons/sec
4.0×10^08
3.0×10^08
2.0×10^08
1.0×10^08
0
MVUV
PeghGCSF
MVNSe
MVhGCSF

Figure 3-15: *In-vivo* imaging of Raji luciferase disseminated SCID model: Bioluminescent images comparing all the groups in the Raji luciferase model at week 2, post tumour inoculation (a). Images were taken with PBS injected control (Ctrl) to account for background luminescence. The scale is on the right side of the image. (b) Quantification of tumour burden using bioluminescence - scatter dot plot showing individual values for luminescence (photons/second) performed on each surviving animal in each treatment group at week 2 (Raji luc). Values are represented minus background activity. Unpaired t test was performed to obtain the P-value.

The survival and post mortem analysis of the mice in the two different B-cell malignancy models Nalm-6 luc (Fig 3-16; 3-17) and Raji luc (Fig 3-18; 3-19) were compared. The Kaplan Meier curves, shown in Fig 3-16a illustrate that, in the Nalm-6 luc model, mice treated with the controls alone succumbed to leukaemia the most quickly; the survival was least good in the group treated with GCSF alone, where the median survival was 50 days compared to 75 days in the MVUV treated group (p=0.0120). Seventy five percent of the mice treated with MVNSe responded well and were alive at the end of the experiment. Surprisingly, mice receiving treatment with MVhGCSF had a significantly inferior outcome with a median survival of 78.5 days compared to the MVNSe treated cohort where the median was not reached by the end of the experiment (p=0.0149) (Fig 3-16a). At humane end-point, $CD10^{+}CD19^{+}$ cells were detected in the BM of the mice confirming presence of leukaemia (Fig 3-16b). hGCSF was detected at comparable levels in the serum of the Peg hGCSF and MVhGCSF treated cohorts confirming the appropriate dosing of the exogenously administered Peg hGCSF (Fig 3-17a). There was no significant difference in total cell numbers recovered from the spleens (MVNSe - mean = 2.338, range 2.0-2.675 million; MVhGCSF - mean = 5.922, range 0.625-25.0 million; MVUV - mean = 2.275; range 0.5-2.275 million; Peg hGCSF – mean = 4.450, range 1.75-8.5 million) indicating that hyperleucocytosis was not the cause of increased death in the MVhGCSF treated ALL mice. Flow cytometric analysis of $GR1^{+}$ neutrophils (Fig 3-17b) and percentage NK and Mac3 (Fig 3-20a) did not show any difference in the neutrophil, macrophage and NK cell percentages between the different groups. Taken together these data indicate that expression of hGCSF by MV

results in a much poorer survival of Nalm-6 ALL leukaemic mice compared to MVNSe and that this is due to enhanced tumour progression.

In the Raji luc model (Fig 3-18; 3-19), the disease progressed very quickly in all the groups. The Kaplan Meier survival curve (Fig 3-18a) shows that by Day 32 all the mice had reached their humane end-point (hind limb paralysis). BM analysis showed the presence of $CD19^{+}CD20^{+}$ cells in all these mice confirming presence of disease (Fig 3-18b) at the time of death. Very high levels of hGCSF in the serum of the mice treated with MVhGCSF and Peg hGCSF (Fig 3-19a) was detected, which correlated with significantly higher levels of $GR1^{+}$ neutrophils in the spleen of these mice, MVhGCSF (median 59.88), MVNSe (median 37.41), MVUV (median 39.64) and Peg hGCSF (median 59.48) (MVhGCSF vs. MVNSe; p=0.0016) (MVhGCSF vs. MVUV; p=0.0217) (MVNSe vs. Peg hGCSF; p=0.0049) (Fig 3-19b). There were also significantly higher levels of macrophages infiltration in the spleens of MVhGCSF treated mice when compared to the MVNSe treated groups (Fig 3-20b), consistent with the higher levels of circulating hGCSF.

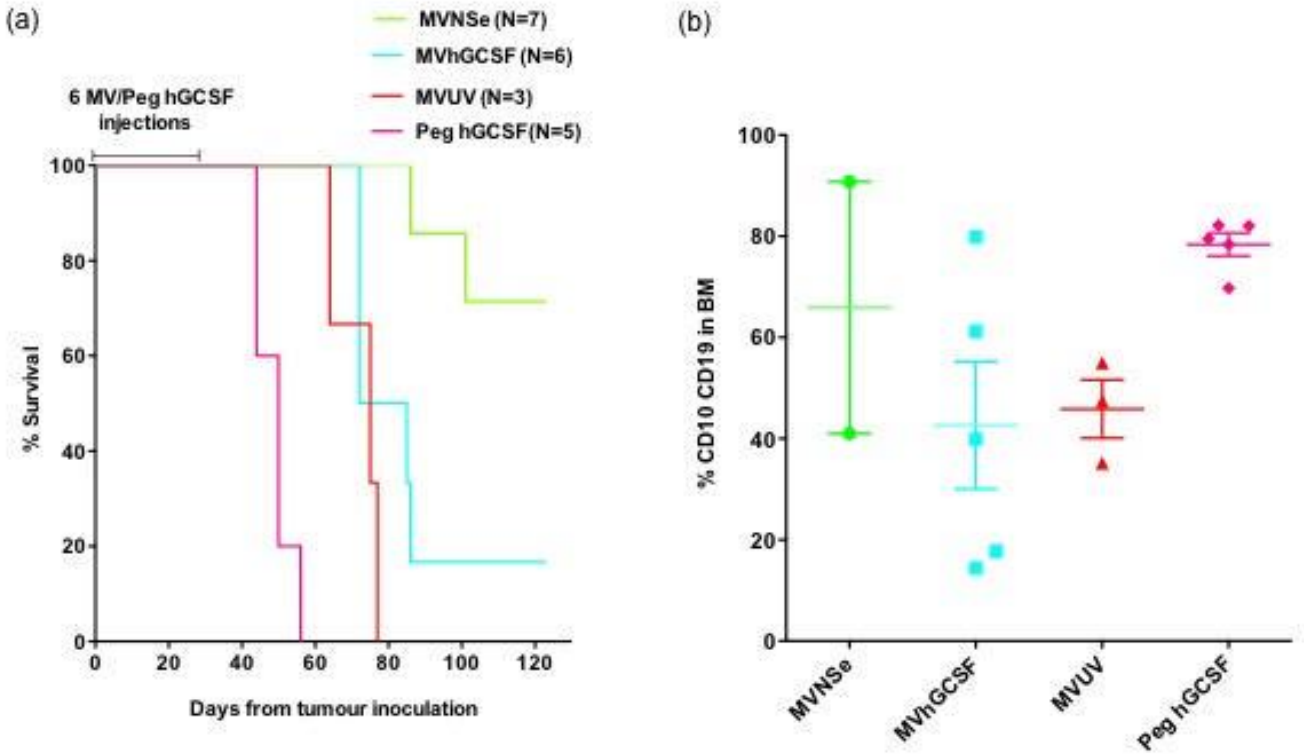

Figure 3-16: Survival and %CD10CD19 positive cells in disseminated Nalm-6 model: (a) Kaplan Meier survival curve showing MVhGCSF (cyan), MVNSe (green), MVUV (red) and Peg hGCSF (pink) treated mice. (b) At humane end-point (hind limb paralysis), the presence of disease was confirmed by flow cytometry by %CD10CD19 in the BM compartment.

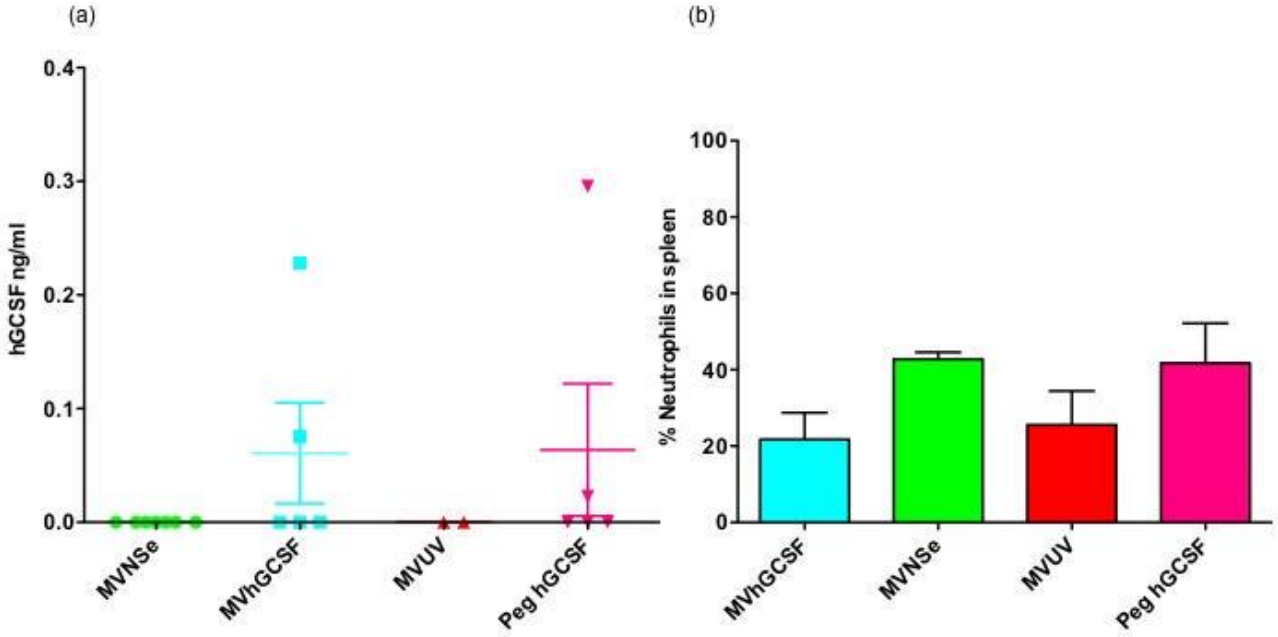

Figure 3-17: hGCSF levels in serum and %neutrophils in spleen of Nalm-6 disseminated model: (a) hGCSF levels (ng/ml) in the serum of the mice quantified by ELISA. (b) %Neutrophils in the spleens determined by flow cytometry.

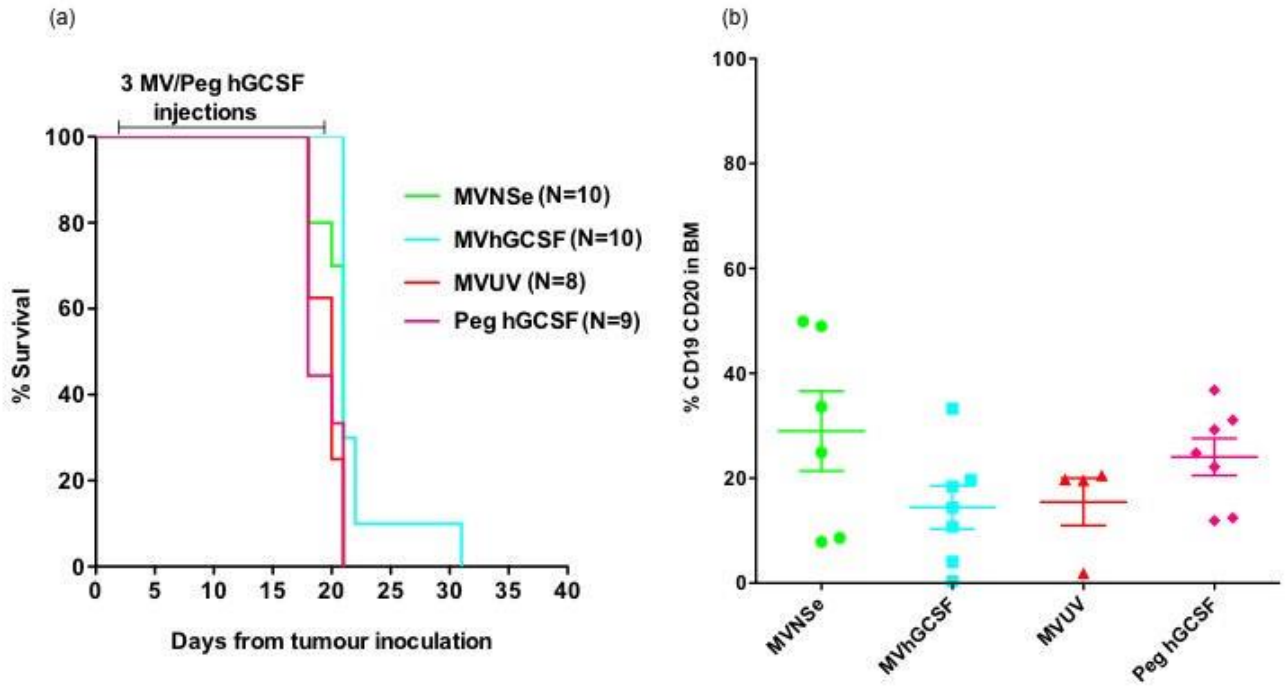

Figure 3-18: Survival and %CD19CD20 cells in disseminated Raji model: (a) Kaplan Meier survival curve showing MVhGCSF (cyan), MVNSe (green), MVUV (red) and Peg hGCSF (pink) treated mice. (b) At humane end-point (hind limb paralysis), the presence of disease was confirmed by flow cytometry by %CD19CD20 in the BM compartment.

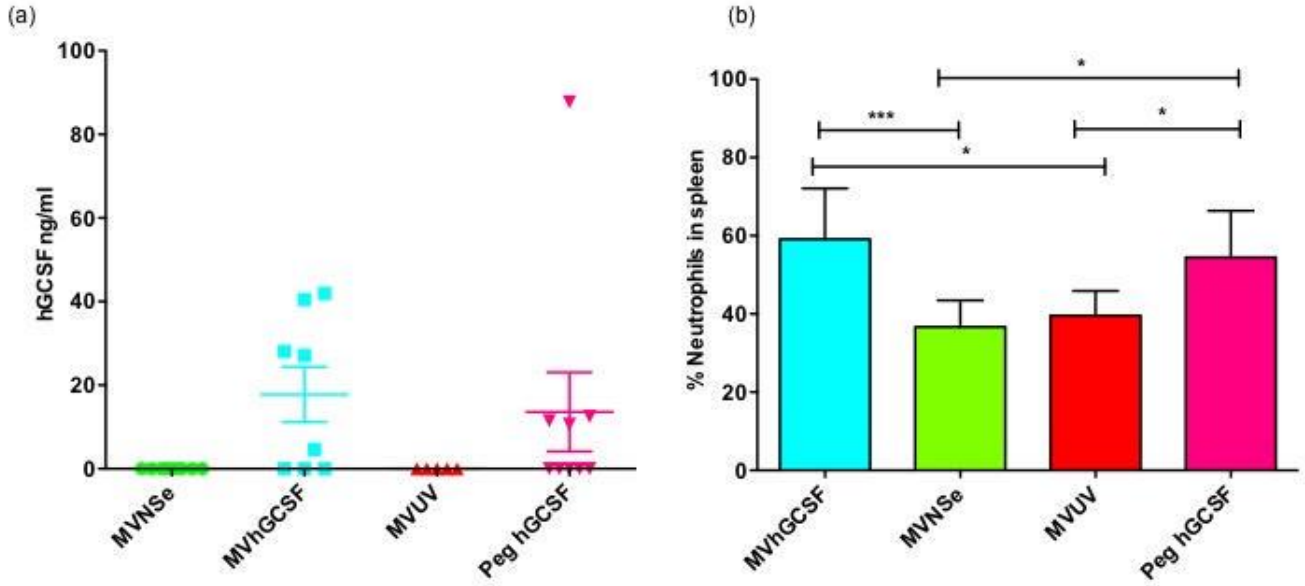

Figure 3-19: hGCSF levels in serum and percentage neutrophils in spleen of Raji disseminated model: (a) The level of hGCSF in the serum of the mice was quantified by ELISA. (b) Percentage of neutrophils in the spleens was determined by flow cytometry. ***p<0.002; *≤p0.04. Unpaired t test was performed to obtain the P-values.

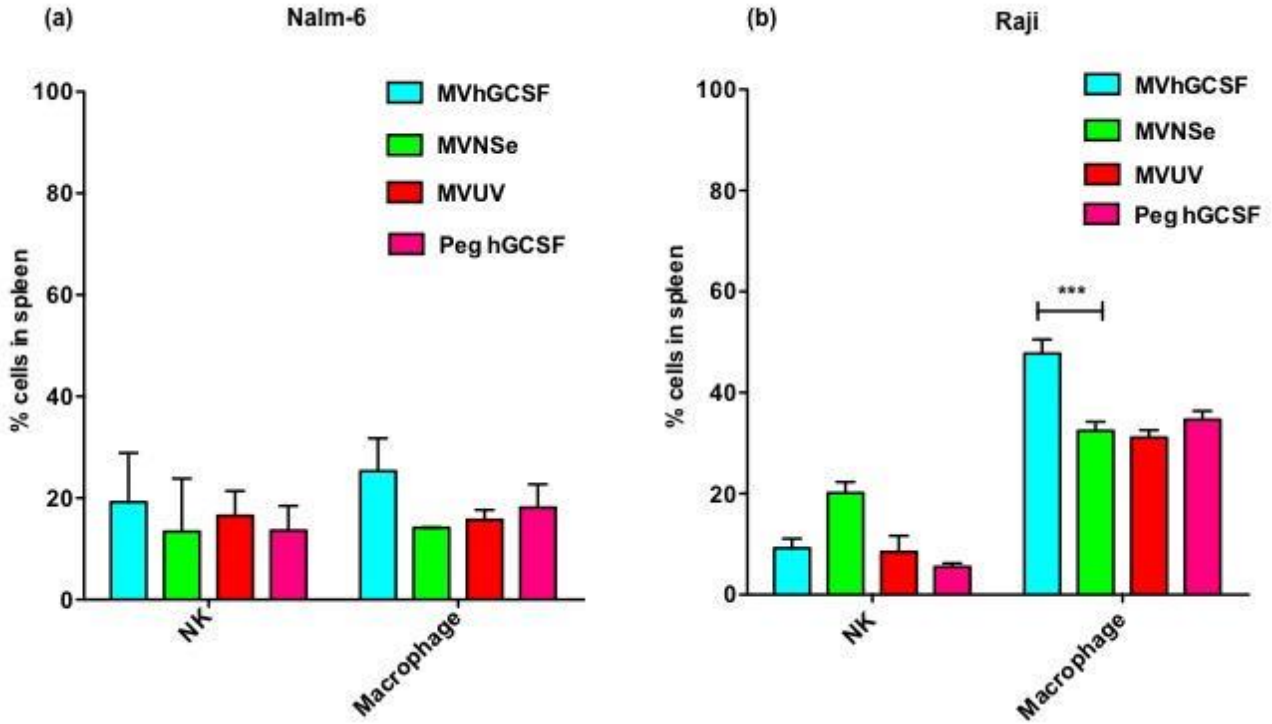

Figure 3-20: Spleen analysis in disseminated models of Nalm-6 and Raji: At humane end point, the percentage of NK cells and macrophages were determined in the spleen of mice treated with MVhGCSF (cyan), MVUV (red), MVNSe (green) and Peg hGCSF (pink) in the disseminated models of Nalm-6 luciferase (a) and Raji luciferase (b) models. ***p=0.0006. Unpaired t test was performed to obtain the P-value.

3.3.7 MVhGCSF does not enhance cell proliferation *in-vitro*:

To ensure that the *in-vivo* data did not simply result from a direct effect of GCSF on cell proliferation, the cell lines were treated with increasing concentrations of recombinant hGCSF *in-vitro* and the cell numbers were enumerated over 4 days (Fig 3-21). No significant difference between GCSF treated and control cell lines *in-vitro* was observed in either Raji (Fig 3-21a) or Nalm-6 (Fig 3-21b) cells.

3.3.8 MVhGCSF in MV-infectable, CD46 transgenic mice is not toxic:

Finally, MVhGCSF was evaluated in CD46 transgenic mice, in which all cells, not just tumour cells, are infectable by MV. To assess this, $Ifnar^{KO}$ CD46 Ge mice[194] were injected IV with either MVNSe or MVhGCSF. They were monitored carefully for signs of ill health for 35 days after which spleen size, and differential cell count in spleen cells (NK, macrophage, neutrophil percentages) as well as serum hGCSF level were determined. There was no difference in spleen size (Fig 3-22a) or cellular contents in the spleen between the groups (Fig 3-22b). None of the mice became unwell. The mice treated with MVhGCSF showed significant levels of hGCSF in the serum at Day 35 (Fig 3-22c), but there was no toxicity seen. Taken together these data in the disseminated Nalm-6 model, suggests that any adverse effect of expressing hGCSF as an additional transcription unit in tumour bearing mice relates solely to promotion of tumour growth and not to toxicity of GCSF production.

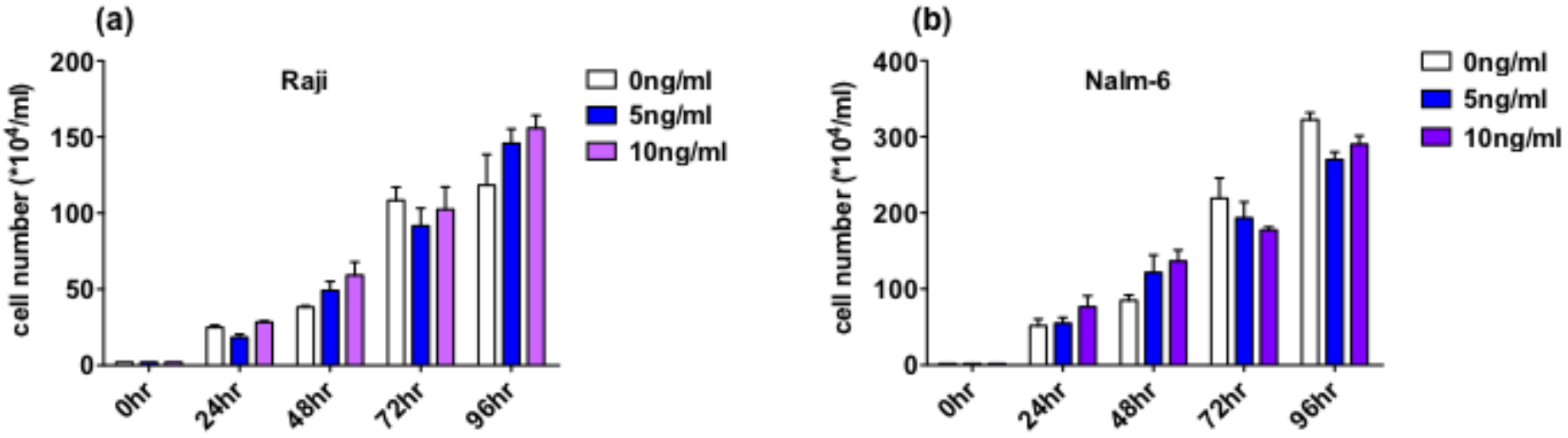

Figure 3-21: Effect of human GCSF on Raji and Nalm-6 cells *in-vitro*: Raji (a) and Nalm-6 (b) cells were treated with increasing amounts of rhGCSF and counted every 24 hours by trypan blue exclusion method *in-vitro*. The number of cells/ml is plotted against the time.

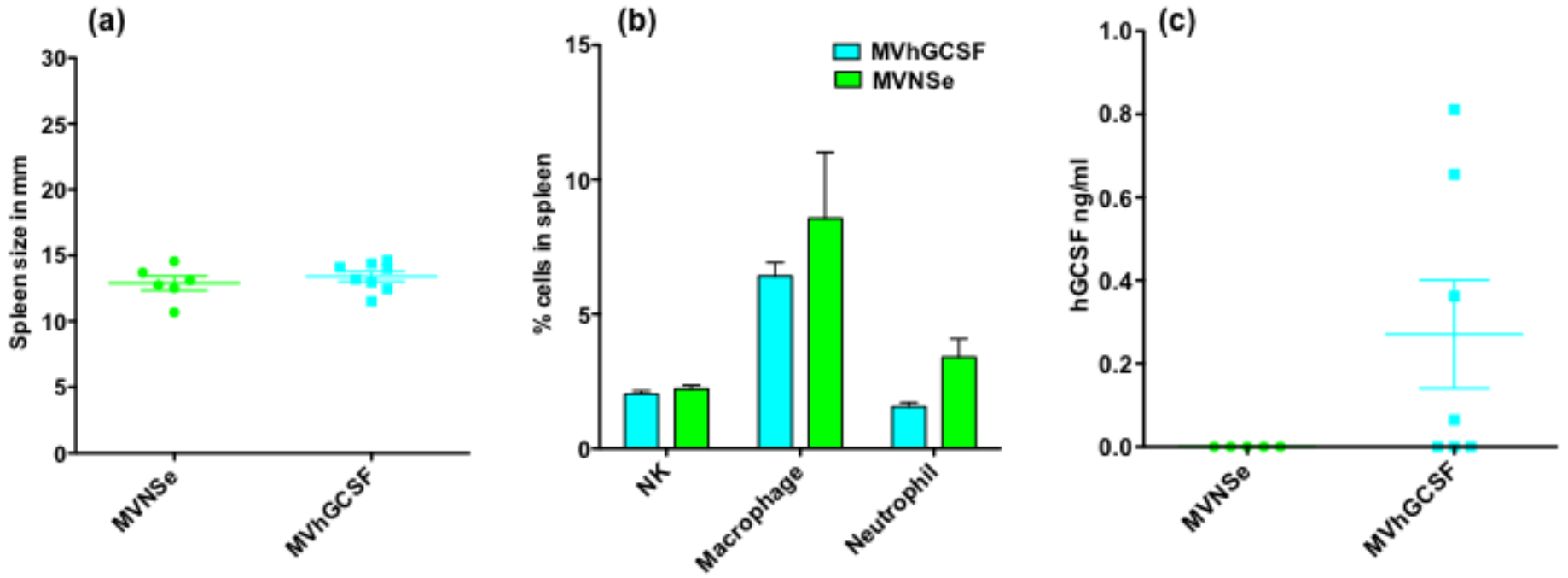

Figure 3-22: MVhGCSF treatment in Ifnar^{ko} CD46 Ge mice: CD46 transgenic mice were injected IV with MVNSe (N=5) or MVhGCSF (N=7). Evaluation was carried out at day 35 after injection for (a) spleen size in mm, (b) percentage of NK cells, macrophages and neutrophils in the spleens, and (c) serum hGCSF levels (ng/ml).

3.4 DISCUSSION:

The interest of the lab in developing MV as a therapy in B-cell malignancies specifically ALL, led to the investigation of the Nalm-6 model to get an insight into the therapeutic efficacy of MV in this model. It was shown that like other B-cell malignancies, ALL too is sensitive to MV therapy *in-vivo* in both SC and disseminated xenograft models.

We know that lymphoid malignancies are disseminated diseases. A key component of success of oncolytic virotherapy lies in engendering an overall “positive” interaction with the immune system. The ability to deliver a replicating virus to individuals with pre-existing adaptive immunity, although not the focus of the present work is crucial. However, the stimulation and exploitation of positive immune responses to target cells infected by oncolytic viruses is a key counterbalance. Just as it was seen in the phase 1 trial of MV in multiple myeloma an initial ‘free pass’ for measles viruses, but only in patients with highly compromised antibody response[292], a balance between anti-tumour immune response by the T-cells[390] and anti-viral activity of T-cells may be expected.

Hence, innate immunity, which may be less compromised and quicker to recover after anti-cancer chemotherapy - may play a pivotal role in viral oncolysis. On this basis, and taking into account previous work from the lab, in which it was clearly demonstrated that oncolytic MV is able to beneficially affect their anti-tumour properties, an attempt to augment these properties by cloning human GCSF as an additional transcription unit to MV was made, as

GCSF is known to stimulate the survival, proliferation and cytotoxic function of neutrophils both *in-vitro* and *in-vivo*[391].

Two tumour models of relatively similar aggressive B-cell malignancies were chosen, both of which are known to respond to MV-oncolysis. Raji - Burkitt's lymphoma-derived cells - respond to MV therapy, but less quickly and completely than does the Nalm-6 model derived from ALL.

In the initial neutrophil depletion experiments, the therapeutic effect of MV in the Raji model was significantly abrogated, whereas in the Nalm-6 SC model, depletion of neutrophils did not abrogate the 100% response rate. The animal project license at the time of the Nalm-6 experiment allowed only 2 IV injections of antibody and therefore to maintain the neutrophil depletion, 2 IT antibody injections were introduced, which was successful in maintaining the depletion throughout the course of the MV treatment. By the time the Raji experiment was performed the project license had been amended allowing IP route of antibody administration along with IV route to deplete neutrophils. This facilitated the experiment, as the IP route of administration was more straightforward technically. Both the IV and IP routes of neutrophil depletion were effective, but the IP administration of the antibody could maintain the depletion for 3-4 days and therefore the antibody was given every 4 days in the Raji model. In both the Raji and Nalm-6 models, the neutrophils did start coming back at a later time-point in the experiment, but the depletion was stringently maintained throughout the course of MV treatment in both the

models. The observations confirmed that MV was oncolytic in both the tumour models as expected, but the role of neutrophils seemed to be different between the models. A possible explanation could be the kinetics of tumour sensitivity to virus, as the Nalm-6 tumours simply regressed so rapidly compared to the Raji tumours, that the direct oncolytic effect of MV in the Nalm-6 tumours superseded any involvement of neutrophils *in-vivo*. It may also relate to the initial size of the tumour, as the threshold tumour volume of Raji tumours was higher than that of the Nalm-6 tumours at the start of therapy. However, it is also possible that the individual targets are differentially responsive to neutrophil effects.

Murine and human GCSF share 73% amino acid sequence homology and full cross reactivity[392] and hence can be tested in both human and murine experimental systems, and therefore was cloned into MV. In the *in-vivo* SC tumour models, the MV expressing hGCSF had a significantly superior therapeutic effect to MVNSe in the Raji model, but was equivalently good at tumour eradication to MVNSe in the Nalm-6 model, both in the proportion of responding tumours and time to response, consistent with the expectations from the neutrophil depletion experiments.

As B-cell malignancies are disseminated diseases, systemic tumour models of Nalm-6 and Raji were established and the therapeutic efficacy of the MV expressing human GCSF was tested in a systemic therapeutic approach by delivering the treatment IV. In disseminated Nalm-6 xenografts, previous data showed that approximately 42% of mice have complete

regression of the tumours with IV delivered MV[386], offering a greater probability to observe any potential therapeutic benefit to MVhGCSF. In the Raji model the previous data showed that neutrophils could play a beneficial role in improving therapeutic efficacy of MV[280]. Surprisingly, in the Nalm-6 disseminated model, not only was there no benefit to MVhGCSF treatment, there was an increased rate of death in those mice, which also occurred with the Peg hGCSF alone control conditions. The level of GCSF detected in the mouse sera was confirmed to be almost identical between exogenously administered and GCSF produced by administration of MVhGCSF suggesting an active, productive infection of tumour targets. The disease progression rather than GCSF toxicity was suggestive to be responsible for these observations and further analysis showed that the immune cell composition of the spleens from MVNSe and MVhGCSF did not differ, especially, there was no excess of neutrophils, ruling out direct toxicity of GCSF. Furthermore, lack of toxicity in the CD46 transgenic model confirmed this. In the Raji disseminated model, the disease progressed very rapidly in all the groups. By third week all of them had succumbed to hind limb paralysis, and had to be sacrificed. In contrast to the Nalm-6 model, the Raji disseminated model showed significantly higher level of infiltrating neutrophils in the spleen of the mice treated with MVhGCSF or Peg hGCSF when compared to the MVNSe and MVUV treated groups. Human GCSF levels in the serum of these mice were also very high. At week 2, some therapeutic benefit of using MVhGCSF over MVNSe was observed by the live *in-vivo* imaging quantification (Fig 3-15b), but this was short lived. The percentage of tumour cells in the BM of the mice at the time of death was

similar all across the groups (Fig 3-18b), whereas in the Nalm-6 model, the peg hGCSF treated group had significantly high level of tumour cells in their BM in comparison to the other groups at the time of death (Fig 3-16b), which again showed a proliferating effect of GCSF on Nalm-6 cells *in-vivo*. But this effect was not demonstrated for Raji cells *in-vivo.*

It can be concluded that the Raji model can benefit from use of MVhGCSF, as neutrophils have consistently shown to play a role in MV-mediated oncolysis in this model. It is possible that the short-term benefit observed in this model was due to the tumour cell inoculation dose (1 million cells) and the schedule of weekly injections of MV therapy, which was kept similar to that of the Nalm-6 model, to be able to directly compare the two models. As Raji is more aggressive than the Nalm-6 model, with lowering of tumour inoculation dose and increasing the therapeutic dose and frequency of MV, it is possible to see a more robust therapeutic benefit.

GCSF is widely used in the clinical treatment of patients with aggressive B-cell malignancies and has been shown to improve outcome[393], although it is long known that GCSF when used to mobilise normal haematopoietic stem cells can also facilitate mobilisation of leukaemia from the bone marrow niche[360]. However, pre-clinical studies of the CXCR4 antagonist plerixafor, typically used in conjunction with GCSF, have shown promising results in *in-vivo* models of primary ALL, suggesting that bone marrow microenvironment disruption may be therapeutically beneficial[394,395] by increasing chemo sensitivity of resistant, possibly quiescent, leukaemia,

clones after removal from their niche. A clinical trial NCT01331590 is being conducted, evaluating the role of GCSF in priming the bone marrow of ALL patients for subsequent chemotherapy targeting[396]. By contrast, GCSF accelerated disease progression in a sub set of primary ALL patient xenografts in NSG mice[397]. Additionally, microarray analysis in samples where disease progression was promoted by GCSF, revealed significantly higher expression of cell cycle regulators like cyclin A1 and ALCAM than in mice without disease progression. In the same article, no evidence for a direct mitogenic effect of GCSF could be demonstrated in any of the xenografts using exogenous GCSF in *in-vitro* cultures in the presence or absence of human or murine stromal support. It has also been shown that quiescent leukaemia cells can be induced to enter the cell cycle by treatment with GCSF[398] and then targeted by chemotherapy.

This chapter echoes the multiple roles of GCSF when used in the treatment of B-cell malignancies. It was confirmed that MVhGCSF could be used as a potent oncolytic agent in the Raji model. Serum GCSF level was comparable to those seen when GCSF is administered to patients[399]. In this model, MVhGCSF potentially carry an advantage, especially in combination with non-myelosuppressive chemotherapies. However, based on these data that showed an unexpectedly aggressive progression of Nalm-6 leukaemia *in-vivo* by MV expressing hGCSF, future studies would need to proceed very cautiously as any benefit from hGCSF as expressed by oncolytic viruses could be difficult to predict and may even vary from patient to patient.

Chapter 4: Mechanism of neutrophil mediated cytotoxicity in MV-infected target cell, differ between tumour types and the MV strain used

4.1 BACKGROUND:

4.1.1 Antibody Dependent Cellular Cytotoxicity – ADCC:

In this chapter, my work aims to decipher, whether MV-induced, neutrophil mediated killing that was observed in the previous chapter, may result from neutrophil-mediated antibody dependent cellular cytotoxicity (ADCC). ADCC, is a mechanism by which, antibody coated target cells are killed by a cytotoxic effector cell in a non-phagocytic process, by releasing cytotoxic cellular contents or by expression of cell-death inducing molecules[400-402]. ADCC is activated when the Fc components of the antibodies (IgG, IgA and IgE classes) bind to their respective Fc receptors (FcγR, FcαR and FcεR) present on the effector cells. Although typically framed as a function of monocytes and NK cells, ADCC has been clearly identified as a mechanism by which neutrophils can eliminate cancer cells[403,404]. Neutrophils from healthy donors constitutively express FcγRII (CD32) and FcγRIII (CD16), but not FcγRI (CD64), but do not lyse tumour cells without activation[405]. Upon stimulation with GMCSF[405], IFNγ[406] or GCSF[407], neutrophils are activated to lyse cells via the different Fc receptors (FcRs). Neutrophils can also mediate cytotoxicity via FcαRI (CD89), which binds to IgA[404]. An anti-FcγRI bi-specific antibody directed against the proto-

oncogene product Her2/neu have shown enhanced lysis of Her2/neu expressing tumour cells by GCSF primed neutrophils[403]. Furthermore, a bi-specific antibody directed against CD20 and FcαRI was shown to effectively kill a broad range of malignant B-cell lines[404].

Challacombe et al. showed that topical PEP005 (ingenol-3-angelate) treatment induces primary necrosis of tumour cells and an inflammatory response, characterised by a pronounced neutrophil infiltrate. Tumours treated with PEP005, led to elevation in anti-cancer antibodies, which could induce neutrophil mediated ADCC. Furthermore, in Foxn1 (nu) mice, depleted of neutrophils and in CD18-deficient mice (in which neutrophil extravasation is severely impaired), PEP005 treatment was associated with a >70% increase in tumour relapse rates[408]. Additionally neutrophils play a critical effector role in mAb treatment of cancer. In a SCID xenograft model of Burkitt's lymphoma, when neutrophils were depleted, the therapeutic effect of rituximab (chimeric antibody targeted to CD20) was partially lost[389]. In a recent study, reovirus was shown to enhance killing of CLL cells by NK cell mediated ADCC when used in combination with anti-CD20 antibodies[409].

Previous published work from my lab has shown that MV Moraten (MVMor) (a vaccine, oncolytic strain – see Fig 1-4) infected neutrophils from healthy donors were activated and survived longer in culture compared to infection with a WT MV strain. Besides, infection with MVMor promoted a more cytotoxic effector phenotype, whereby the neutrophils produced pro-inflammatory cytokines - TNFα, MCP-1, IL8 and IFNα[357]. Direct MVMor

infection of neutrophils also led to the secretion of pre-formed soluble TRAIL from granules (i.e. did not require protein synthesis) and induction of neutrophil degranulation[357]. Furthermore, three lines of evidence from the lab (Dr. Zhang, unpublished data) suggested that ADCC might be a mechanism. First, Dr. Zhang showed that MV-infection of neutrophils lead to FcαRI upregulation. Second, while investigating TRAIL mediated killing of MV-infected Jurkat T-cells in the presence of neutrophils, Dr. Zhang made an interesting observation. Upon addition of an antibody (RIK2), which was used to block TRAIL-mediated apoptosis[410], there was enhancement rather than blocking of neutrophil mediated killing. This was completely unexpected, and generated the hypothesis that the RIK2 antibody was binding to cell surface TRAIL on the Jurkat cells, and to the Fc receptor on the neutrophils, thereby mediating ADCC. To test this, Jurkats were infected with MV and co-cultured with neutrophils in the presence of anti-MV antibody containing serum (anti-MV serum), which augmented the neutrophil mediated killing, further suggesting ADCC as a possible mechanism (Dr. Zhang, unpublished data).

In chapter 3, MV expressing human GCSF enhanced the neutrophil mediated killing *in-vivo* resulting in improved therapeutic effect in the Raji SCID model and showed increased infiltration of neutrophils in the spleen compared to the unmodified MVNSe treatment, and stimulated neutrophil-mediated oncolysis in B-cell malignancy. GCSF greatly enhances the cytotoxic activity of neutrophils; in particular, it can enhance ADCC. In an *in-vivo* study of B-cell malignancy, GCSF primed neutrophils were shown to efficiently lyse antibody coated malignant B-cells, compared to non-primed

neutrophils[411] by ADCC. In a different study, neutrophils isolated from patients undergoing rhGCSF therapy showed higher cytotoxicity against Daudi cells (B lymphoma cell line) *in-vitro* when compared to the neutrophils isolated from non-treated control patients or healthy donors. The neutrophils from these rhGCSF treated patients were also shown to express the FcγRI in significantly higher proportion than the untreated or healthy controls, which correlated with higher cytotoxicity[407].

Hence, based on the literature, preliminary data from my laboratory and my own findings in chapter 3, I chose to investigate ADCC as a mechanism of neutrophil mediated MV oncolysis in more detail. Two different vaccine strains of MV were used; MVNSe and MVMor. MVNSe has been the parental virus in most of the *in-vivo* studies of oncolysis to date and has been administered to humans in the completed and ongoing MV clinical trials[50]. The MVMor strain was included in this chapter as a comparator, as this strain helped generate some of the preliminary data (Dr. Zhang, 2012[357] and unpublished data).

A schematic representation of the hypothesis, that ADCC might be involved in MV-mediated tumour cell killing is shown in Fig 4-1. MV-infected target tumour cells (dark blue) express MV-H (yellow) and MV-F (red) proteins on their cell surface. Anti-MV antibody in the serum, which is primarily directed against the MV-H (light blue) and to a lesser extent to MV-F (brown)[241,412] can bind to the MV-H (yellow) and MV-F (red) on the target cells whilst also binding by their Fc portions to Fc receptors (green) on

neutrophils (orange). Once bound by Fc receptor, the neutrophils can bring about target cell lysis by ADCC (grey).

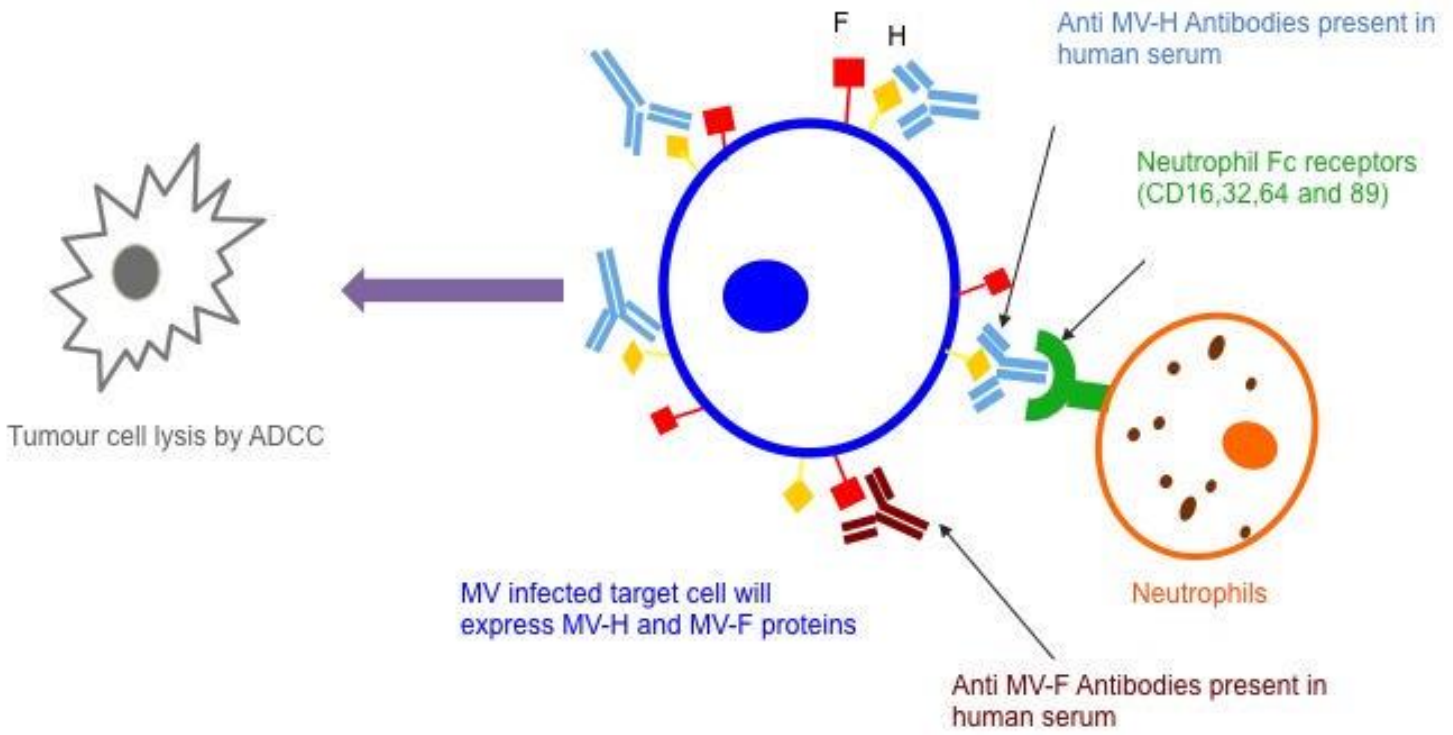

Figure 4-1: Schematic representation of neutrophils' antibody dependent cellular cytotoxicity (ADCC) as a mechanism of MV-infected tumour cell lysis:

4.1.2 Hypothesis:

ADCC is a possible mechanism by which neutrophils can eliminate MV-infected tumour cells.

4.1.2.1 Aims:

1. To investigate if neutrophils from healthy human donors can mediate killing of MV-infected targets *in-vitro*.

2. To determine whether ADCC is a mechanism by which neutrophils may mediate MV oncolysis.

4.2 RESULTS:

4.2.1 Comparison of MVNSe with MVMor at induction of neutrophil-specific lysis:

To specifically look at the role of neutrophils and mechanisms involved in MV oncolysis, *in-vitro* assays were designed with the B-cell lines of interest - Raji and Nalm-6. In the previous chapter, in Raji SCID xenografts, neutrophils were shown to play a role and using a MV expressing hGCSF (MVhGCSF) significantly improved the oncolytic effect, reiterating the role of neutrophils. Nalm-6 on the other hand was not susceptible to neutrophil mediated effect. However, data in both Raji and Nalm-6 models were obtained *in-vivo* and the effect observed was with murine neutrophils and therefore, to study the effect of human neutrophils in both these model was of interest. The human T-cell line Jurkat was also included, as previous work in the lab had suggested possible susceptibility to neutrophil mediated ADCC in this cell line.

First, the percentage neutrophil mediated specific cell death (called neutrophil-specific lysis from here on) in all the three cell lines was determined by chromium release assay. Briefly, cells were infected with MVNSeGFP or MVMorGFP and imaged to confirm MV infection (Fig 4-2). Twenty-four or forty-eight hours post infection they were labelled with ^{52}Cr. Neutrophils were extracted from the blood of 10 different individual healthy donors, and added to the MV-infected target cells at different E:T ratio. Twenty-four hours later, the supernatant was collected and read in a beta emission counter. The cells infected with MV alone in the absence of neutrophils were used as negative control (spontaneous cpm) to account for MV-mediated cell death, and cells treated with 1% tri fluoro acetic acid (TFA), which ensured complete lysis was used as positive control (maximal cpm). The neutrophil-specific lysis was calculated taking into account both positive and negative controls using the formula: % of neutrophil-specific lysis = (experimental cpm – spontaneous cpm)/(maximal cpm – spontaneous cpm) x100; (cpm – count per min).

Fig 4-3 shows the neutrophil-specific lysis of the MV-infected cells. The cell lines infected with MVMor were not susceptible to neutrophil-specific lysis at any E:T ratio, except for Nalm-6 (Fig 4-3a, dark red line). In Nalm-6, a maximum of 20% neutrophil-specific lysis was observed, more pronounced at the lower E:T ratios. In contrast, MVNSe infection (Fig 4-3b) led to high percentage of neutrophil-specific lysis in Jurkat cells (25-45%) (black line) and Nalm-6 (10-20%) (dark red line) across all different E:T ratio, and around 10% in Raji at higher E:T ratio of 20:1 and 40:1 (blue line).

These experiments in different cell lines showed that neutrophils were playing a role in MV oncolysis *in-vitro* but similar to the observation in chapter 3, the neutrophils seemed to play very different roles in different malignancies, with some of them less dependent on neutrophil mediated MV oncolysis than others. Interestingly and somewhat unexpectedly, MVNSe and MVMor had very different effects in the different cell lines and though there are not many differences known between the two strains of viruses used, difference in fusogenicity might have a role to play[50], as it is known that MVMor is less fusogenic than the MVNSe strain. Overall in all the cell lines, neutrophil-specific lysis in MVNSe infected cells was higher than MVMor infected cells.

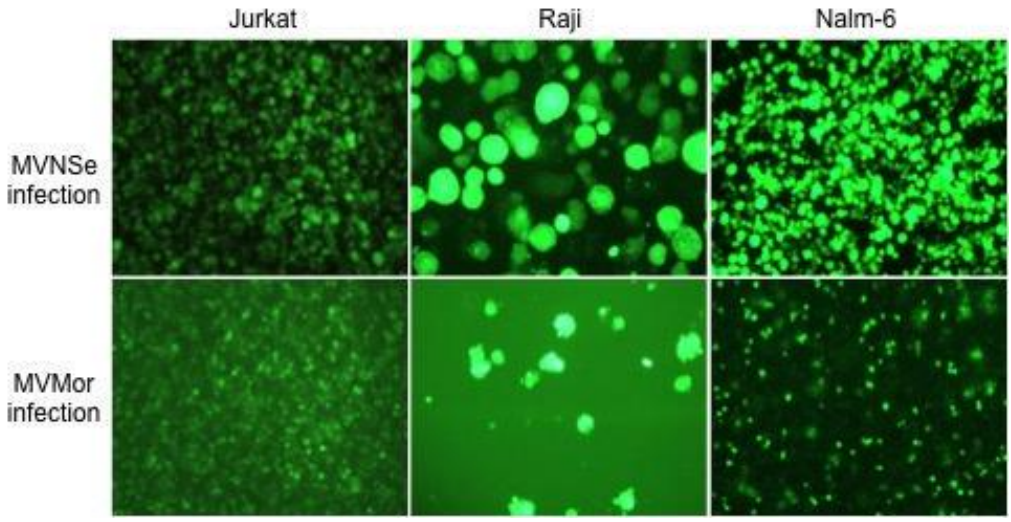

Figure 4-2: Images confirming MV infection of cell lines: Jurkat cells (left panel), Raji cells (middle panel) and Nalm-6 cells (right panel) infected with MVNSeGFP (top row) or MVMorGFP (bottom row) and imaged at 24 or 48 hours at 10X zoom.

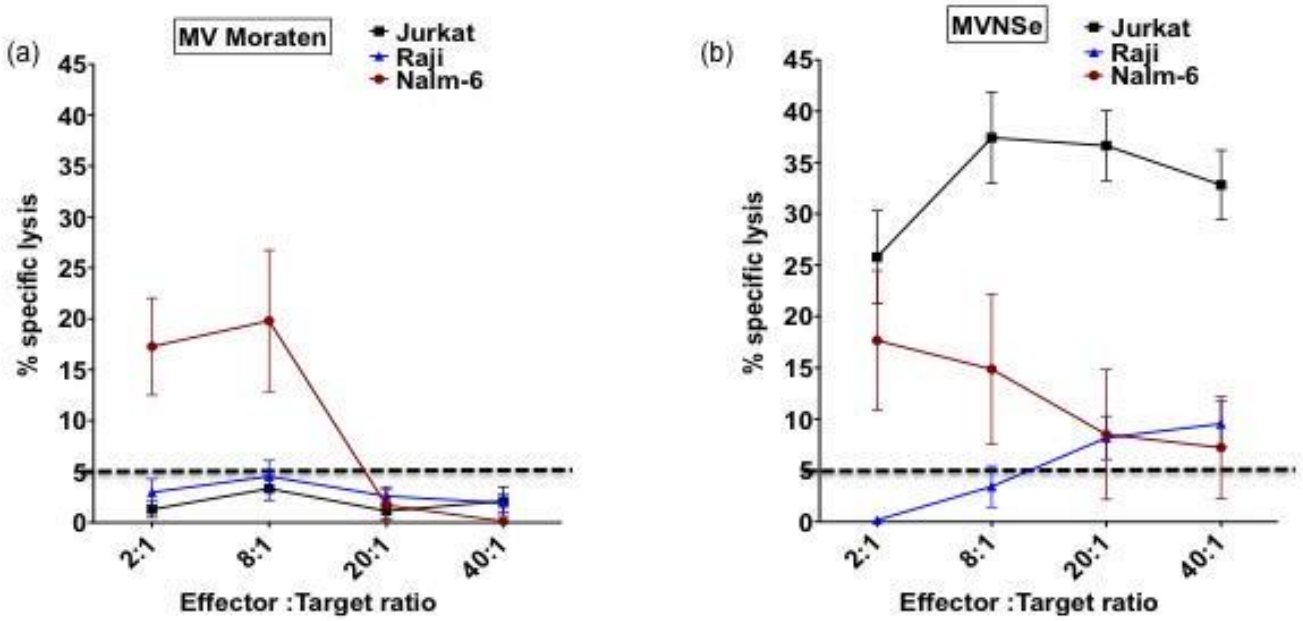

Figure 4-3: Neutrophil-specific lysis in MV-infected cell lines: Percentage neutrophil-specific lysis calculated at different E:T ratio in Jurkat cells (black), Raji cells (blue) and Nalm-6 cells (dark red), infected with MVMor (a) or MVNSe (b). The black dashed line shows the minimum threshold percentage (5%) of neutrophil-specific lysis used for the experiment.

4.2.2 Investigating ADCC as a mechanism:

Next, ADCC was investigated as a mechanism of neutrophil-specific lysis of MV-infected target cells. Neutrophil-specific lysis was determined by chromium release assay in the presence or absence of anti-MV anti-serum. Pooled serum from individuals with high anti-MV antibody titres {titrated using VIDAS® enzyme linked fluorescent immunoassay (EIA) (Biomérieux, France)}, was obtained from the virology department at the Royal Free Hospital. The serum was heat inactivated in the lab at 56°C for 30mins to inactivate complement. The concentration of serum added at 1:100 dilution was based on previous experiments in the lab where highest percentage of neutrophil-specific lysis was observed in MV-infected Jurkat cells at this dilution (Dr. Zhang, unpublished data).

In the Nalm-6 cell line, infected with MVNSe, there was no change in the neutrophil-specific lysis upon addition of serum (Fig 4-4a green line) in comparison to the absence of serum (Fig 4-4a black line). When the same cell line was infected with MVMor, the neutrophil-specific lysis was abrogated upon addition of serum (Fig 4-4c, red line) when compared to no serum control (Fig 4-4c black line).

In the Raji cell line, infected with MVNSe, neutrophil-specific lysis was abrogated upon addition of serum (Fig 4-4b, green line) in comparison to no serum control (Fig 4-4b black line). However, MVMor infection of Raji cells did not show any neutrophil–specific lysis in the presence or absence of

serum (Fig 4-4d, red line and black line respectively). Both Nalm-6 and Raji cell lines infected with either of the viruses did not show any ADCC.

The experiments with Jurkat cells demonstrated significant abrogation ($p \leq 0.0001$) of neutrophil-specific lysis upon addition of serum (Fig 4-5a green line), when they were infected with MVNSe in comparison to absence of serum (Fig 4-5a black line). By contrast, after infection with MVMor (Fig 4-5b), the neutrophil-specific lysis was lower than the threshold of 5% in the absence of serum (Fig 4-5b black line) but addition of anti-MV serum (Fig 4-5b red line), significantly enhanced the neutrophil-specific lysis ($p \leq 0.0347$) at 8:1 and 20:1 E:T ratio, showing ADCC as a possible mechanism, and in keeping with the previous observation from the lab.

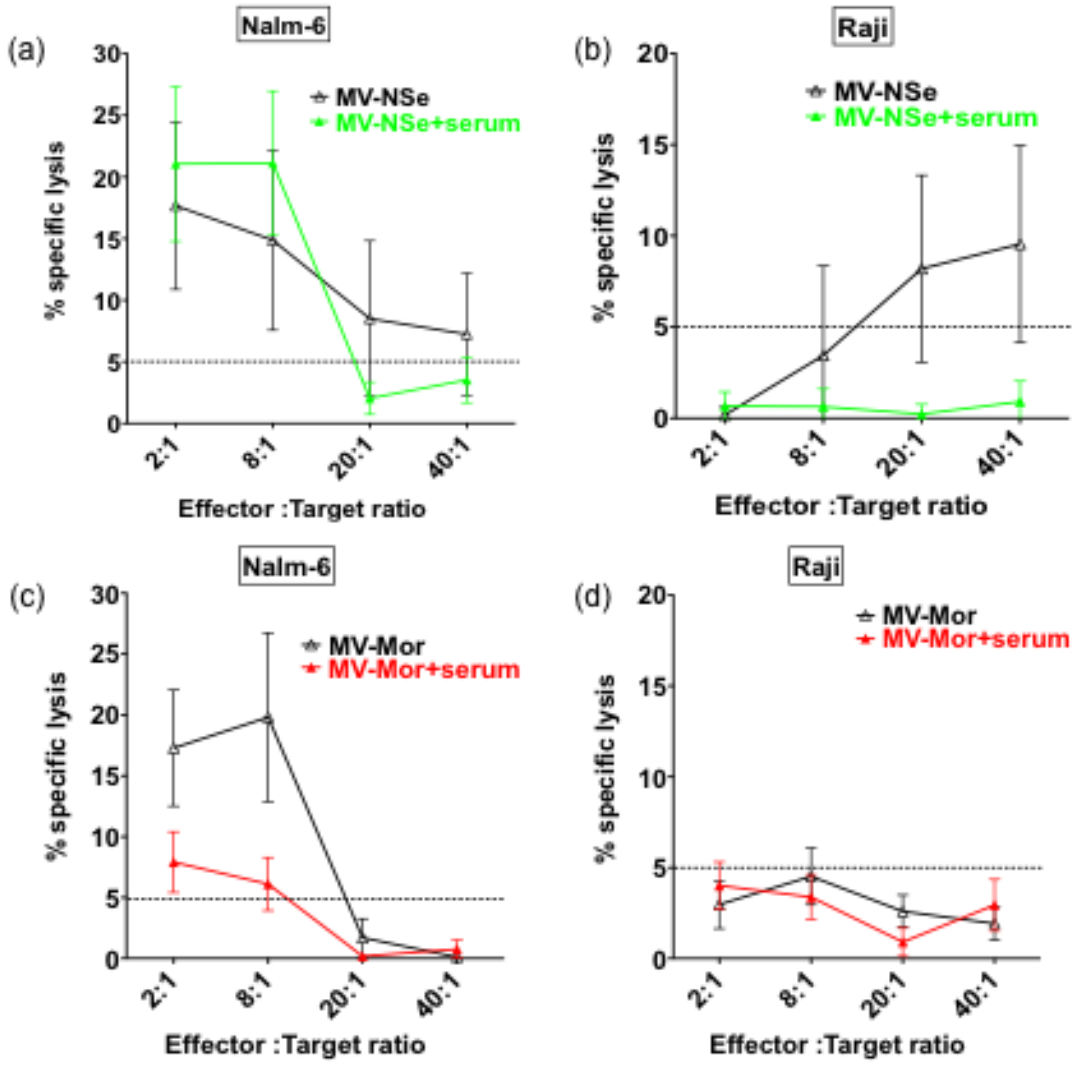

Figure 4-4: ADCC as a mechanism of neutrophil-specific lysis in MV-infected cell lines: Nalm-6 (a and c) and Raji (b and d) cell lines were infected with MVNSe (a and b) or MVMor (c and d) in the presence (black lines) or absence (green or red lines) of anti-MV serum. Percentage neutrophil-specific lysis was calculated for all with 5% (black dashed line) as minimum threshold of neutrophil-specific lysis.

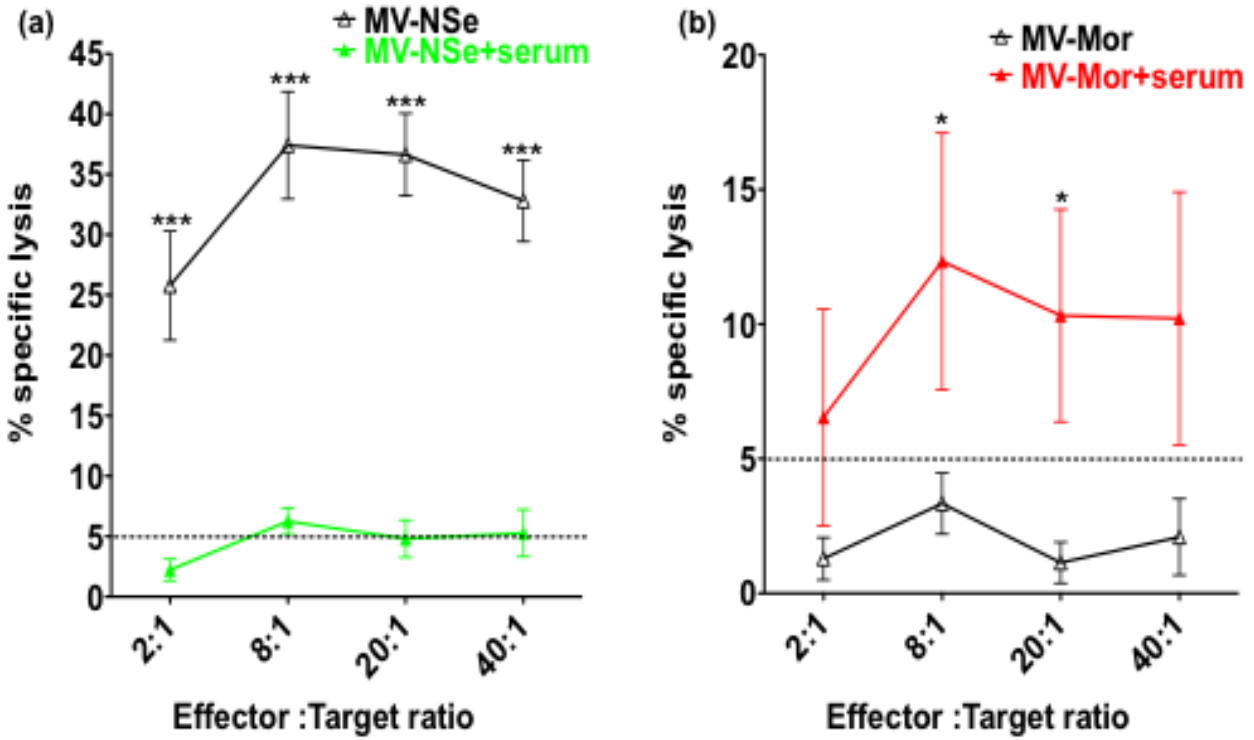

Figure 4-5: ADCC as a mechanism of neutrophil-specific lysis in MV-infected Jurkat cell line: Jurkat cell line was infected with MVNSe (a) or MVMor (b) and percentage neutrophil-specific lysis determined in the presence (black lines) or absence (green and red lines) of anti-MV serum. 5% was used as the minimum threshold of neutrophil-specific lysis (black dashed line). Paired t test was performed to obtain the P-values. *** p≤0.0001, *p≤0.0347.

4.2.3 Neutrophil-specific lysis and ADCC is not a T-cell specific phenomena:

Substantial neutrophil-specific lysis after MV infection was observed only in Jurkat cells after infection with MVNSe. Enhancement upon the addition of anti-MV antibody containing serum was observed only when Jurkat cells were infected with MVMor. In order to rule out whether this observation is related to the fact that Jurkat cells were of T-cell origin, another T acute lymphoblastic leukaemia cell line, DND41 was chosen and examined for neutrophil-specific lysis and ADCC.

The chromium release assay was carried out for DND41 as described earlier, in the presence and absence of anti-MV serum. No neutrophil-specific lysis was observed with either strain of MV in the absence of serum, as shown in Fig 4-6a and b; black lines, showing that DND41 was not susceptible to neutrophil-specific lysis *in-vitro*. Addition of anti-MV serum too did not have any effect - the neutrophil-specific lysis remained below the 5% set threshold level (Fig 4-6a and b; green and red lines respectively). Taken together these data suggested that the results obtained from Jurkat cells was likely to be a non-generalisable finding.

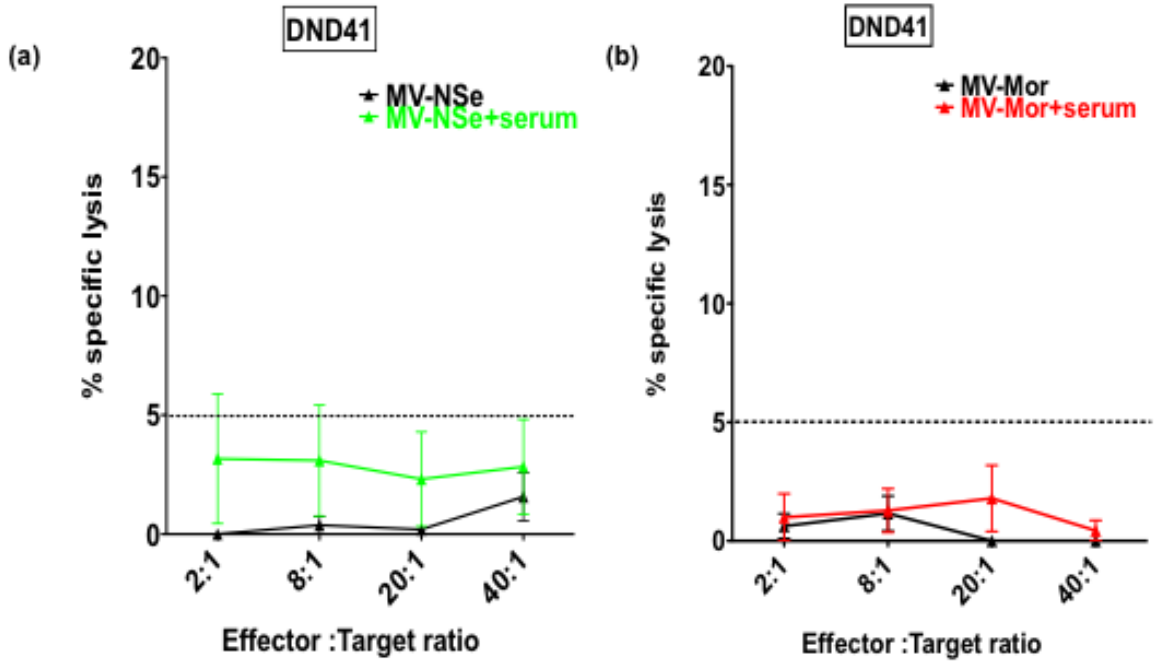

Figure 4-6: Neutrophil-specific lysis and ADCC in MV-infected DND41 cell line: DND41 cell line was infected with MVNSe (a) or MVMor (b) and percentage of neutrophil-specific lysis calculated in the presence (green and red lines) and absence (black line) of anti-MV serum. 5% was used as the minimum threshold of neutrophil-specific lysis (black dashed line).

4.2.4 MVhGCSF infected Jurkat does not enhance the neutrophil mediated ADCC:

MV expressing hGCSF has the potential to enhance neutrophil-mediated ADCC. Since Jurkat cells were the only cells in which possible ADCC was observed, they were the only cell line selected for evaluation with MVhGCSF. Cytotoxicity assays were performed after addition of neutrophils from individual healthy donors (N=10) at different E:T ratios. The neutrophil-specific lysis was 15-35% at different E:T ratios. This was completely and significantly abrogated in the presence of anti-MV serum at all E:T ratios { 2:1 ($p=0.0343$), 8:1 ($p=0.0045$), 20:1 and 40:1 ($p\leq0.0008$)} (Fig 4-7). Hence, MVhGCSF showed exactly the same pattern of neutrophil-specific lysis as the parental MVNSe (Fig 4-5a). The expression of GCSF by MV did not have any additional effect on the neutrophil-specific lysis in the presence or absence of serum *in-vitro*. For this reason, MVhGCSF was not tested on any of the other cell lines.

Taken together, the data make ADCC very unlikely as a possible mechanism by which neutrophils may enhance target cell killing by MV.

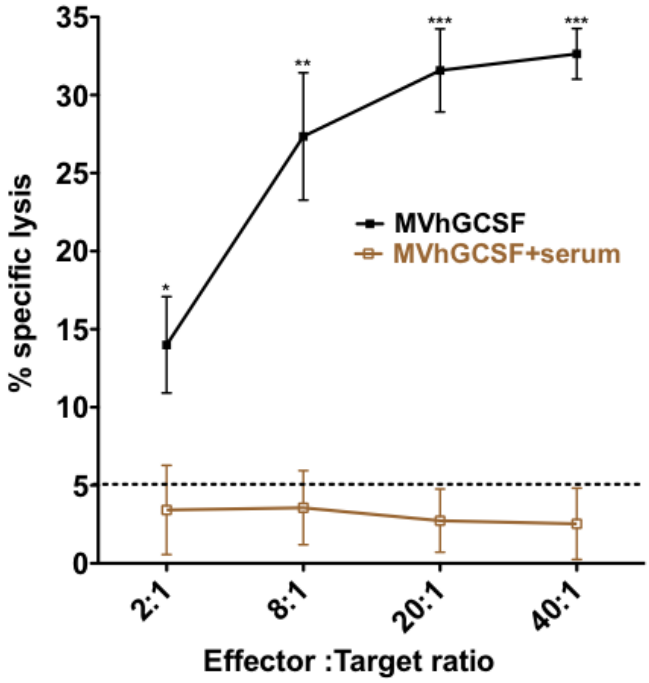

Figure 4-7: Neutrophil-specific lysis and ADCC in MVhGCSF infected Jurkat cell line: Jurkat cells were infected with MVhGCSF and percentage neutrophil-specific lysis determined in the presence (black lines) or absence (brown line) of anti-MV serum. 5% was used as the minimum threshold of neutrophil-specific lysis (black dashed line). Paired t test was performed to obtain the P-values. *p=0.0343, **p=0.0045, ***p≤0.0008.

4.2.5 Dissecting the difference between MVNSe and MVMor in provoking neutrophil-specific lysis:

One interesting finding from these experiments so far was the difference in neutrophil-specific lysis observed in Jurkat cells between the two different strains of MV which was unexpected and not readily explained. It was also unclear why this response was enhanced by serum only with MVMor but not MVNSe. Both of these attenuated vaccine strains of MV are derived from the MVEdmB strain, and there are very few known differences.

MVMor has been sequenced in both their coding and non-coding regions[413,414] and differs with the MVNSe only in few amino acids, isolated in the H and L part of the genome[232]. There are also phenotypic differences in the cytopathic effects between the two strains, which cannot at present be directly related to their modest genetic differences. One key difference is that MVMor is less fusogenic than MVNSe strain[50] and infection results in fewer and smaller multinucleated syncytia. At the functional level too, some differences in the expression of MV proteins has been reported between different vaccine strains[415]. Whether some of these functional differences in fusogenicity are responsible for the difference in the cytotoxicity observed between the two strains, were tested further.

4.2.5.1 Is MV-H expression after MVMor and MVNSe infection responsible for the differential stimulation of neutrophil-specific lysis?

It was hypothesised (Fig 4-8) that the surface area of the cell membrane expressing the viral envelope protein MV-H, may be higher overall in the individually infected cells after infection with the less fusogenic MVMor (Fig 4-8a) compared to in the large syncytia formed by the highly fusogenic MVNSe (Fig 4-8b). This could be highly relevant to ADCC, as it would allow more antibody binding and facilitate greater Fc receptor interaction.

First, the MV-H expression on Jurkat cells after infection with the two different viruses was investigated. The Jurkat cells were infected with

MVNSe or MVMor at an MOI of 1.0. Twenty-four hours later, the percentage of MV-H cell surface expression (Fig 4-9a) and MFI of MV-H expression (Fig 4-9b) was determined by flow cytometry. There was significant difference in both the percentage MV-H expression ($p=0.0025$) (Fig 4-9a) and MFI MV-H expression ($p<0.0001$) (Fig 4-9b) with higher MV-H in MVMor in comparison to MVNSe infected cells.

The relevance of fusion to H expression was further determined by the use of fusion inhibitory peptide (FIP), which blocks cell-cell fusion. After addition of FIP, MV-H expression would be expected to result in an increase in H expression in MVNSe infected cells. When the percentage MV-H expression was determined in the presence of FIP, there was a very small, but non-significant ($p=0.0652$) augmentation observed in the MVNSe infected cells (Fig 4-10, dark grey bar), whereas in the MVMor infected cells there was significant abrogation ($p=0.0071$) in MV-H expression (Fig 4-10 dark pink bar); this was opposite of the hypothesis, and the reason is not clear. The increase in MV-H expression due to blocking of fusion was evident in MVNSe infected cells albeit not significant. It was expected that, MVMor would either show increase in MV-H expression or no change after FIP treatment, but there was decrease in MV-H expression and this was unexpected.

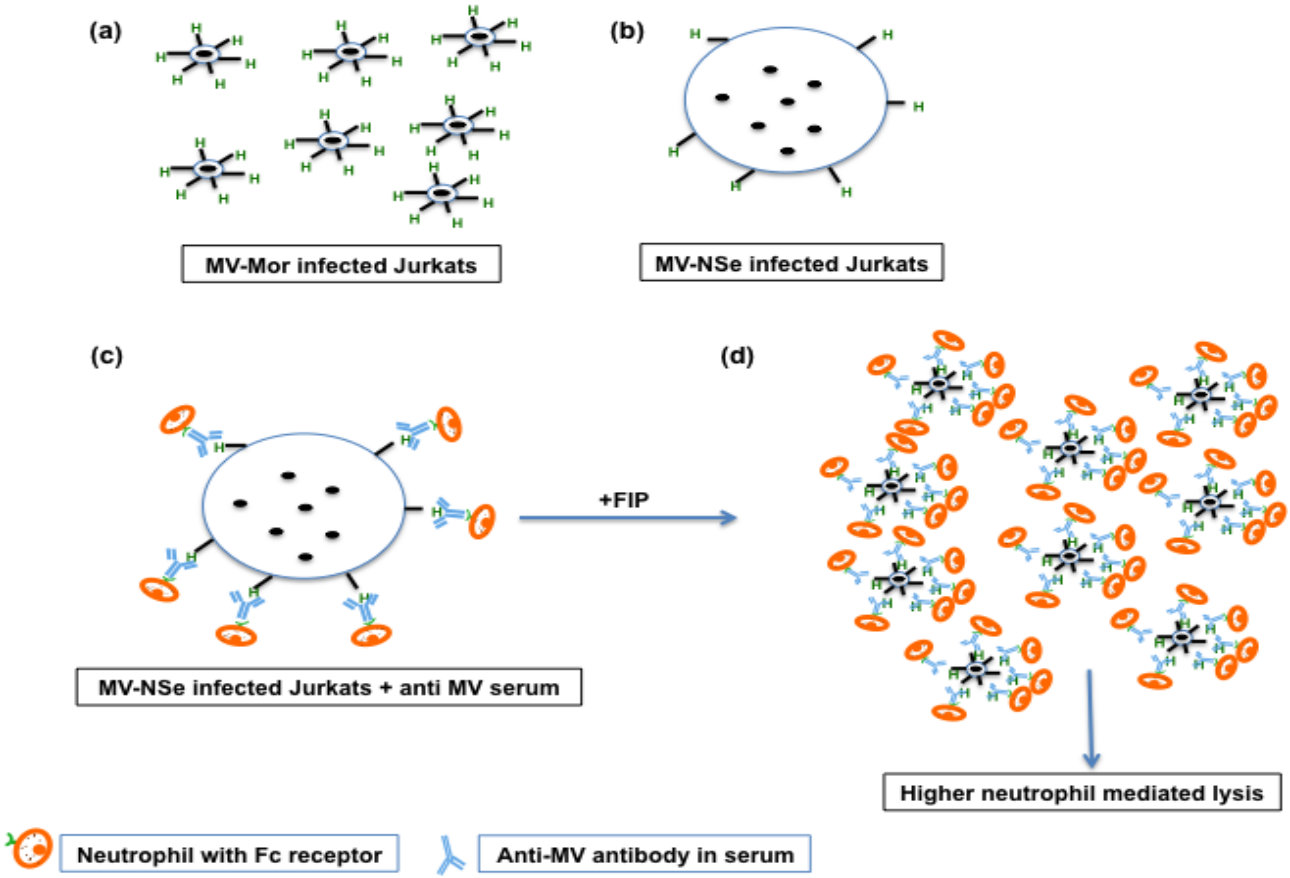

Figure 4-8: Schematic representation of MV-H expression hypothesis after MVNSe and MVMor infection of Jurkat cells in the presence and absence of FIP:

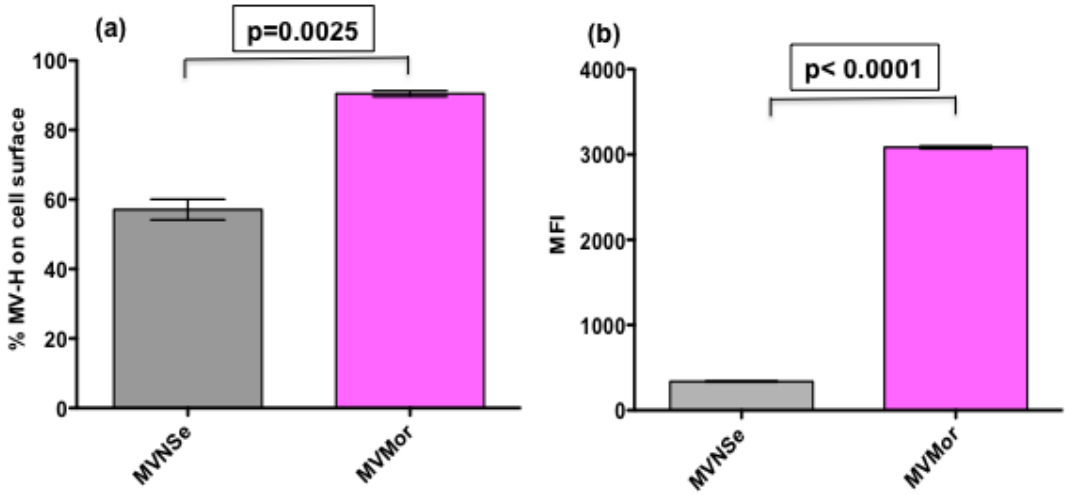

Figure 4-9: MV-H expression on Jurkat cells: Jurkat cells infected with MVNSe (grey) or MVMor (pink) were quantified for percentage MV-H expression (a) and MFI (b) on Jurkat cell surface by flow cytometry. Paired t test was performed to obtain the P-values.

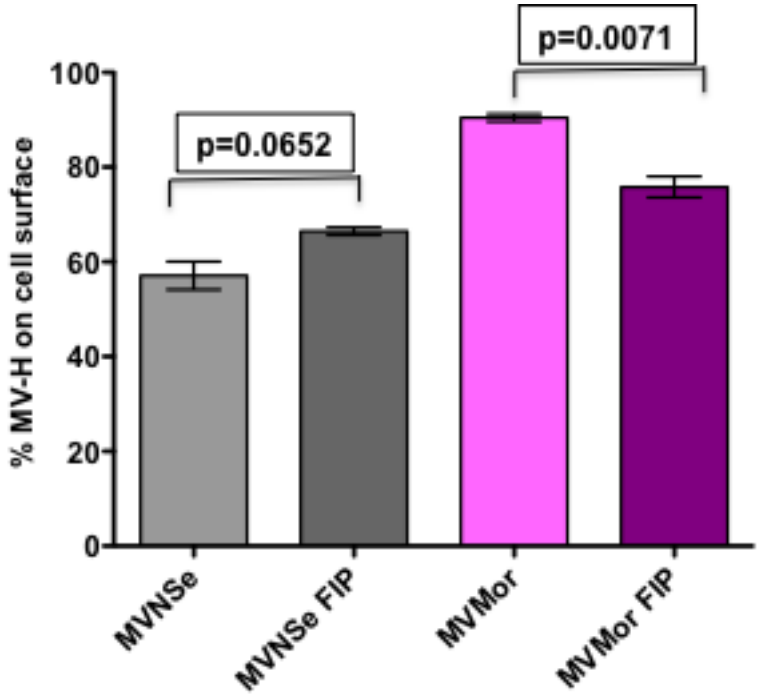

Figure 4-10: MV-H expression on Jurkat cells in the presence and absence of FIP: Jurkat cells infected with MVNSe (grey) or MVMor (pink) were quantified for percentage MV-H expression on Jurkat cell surface by flow cytometry in the presence (dark colours) or absence (light colours) of FIP. Paired t test was performed to obtain the P-values.

4.2.5.2 Effect of fusion inhibition on neutrophil ADCC in MV-infected Jurkat:

It was concluded that ADCC is not a possible mechanism of neutrophil-mediated MV oncolysis, but the difference observed in MV-H expression in Jurkat cells infected with MVNSe with and without FIP above (Fig 4-10) and ADCC observed with MVMor infection earlier (Fig 4-5b) was very intriguing and led to the second hypothesis illustrated in Fig 4-8 c and d; upon blocking fusion in MVNSe infected Jurkat cells, the higher MV-H expression may enable the binding of more anti-MV-H antibody, enhancing neutrophil Fc receptors interaction, in turn enhancing the neutrophil mediated killing (Fig 4-8c and d).

To determine whether the difference in the MV-H expression on MV-infected Jurkat cells between the two viruses was responsible for the difference in the ADCC observed earlier in section 4.2.2, FIP was used to block fusion. The chromium release cytotoxicity assay was performed in the Jurkat infected with MVNSe or MVMor in the presence or absence of FIP. These results are shown in Fig 4-11. Upon MVNSe infection (Fig 4-11a), in the presence of FIP (black empty triangle) the neutrophil-specific lysis disappeared completely and significantly ($p \leq 0.0003$) across all the E:T ratios, compared to the absence of FIP (black filled triangle) showing abrogation of neutrophil mediated killing on inhibition of fusion. Addition of anti-MV serum (Fig 4-11a - red empty and filled circle), when the fusion was blocked did not show any enhancement in killing by ADCC. After MVMor infection (Fig 4-11b) too, there was a significant decrease in the neutrophil-mediated killing in the

presence of FIP (black empty triangle) but only in 20:1 (p=0.0421) and 40:1 (p=0.0017) E:T ratios, compared to the no FIP control (black filled triangle). However, there was no enhancement in ADCC by addition of FIP (red empty circle) compared to the no FIP control (red filled circle). Overall, though a difference in the percentage of MV-H expression was seen on Jurkat after infection with the viruses, this did not facilitate ADCC. The main significant observation from the work in this chapter was that, upon addition of FIP, the neutrophil-specific killing after MVNSe infection of Jurkat was completely and significantly abrogated. This suggested a potential role for MV-induced cell-cell fusion as a mechanism of neutrophil-mediated MV oncolysis. This question is investigated in detail in chapter 5.

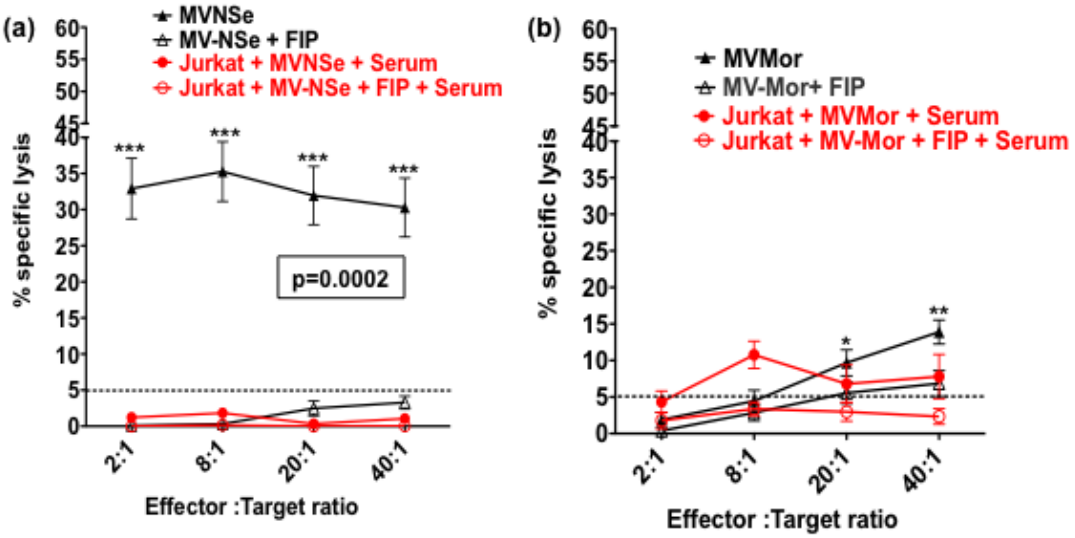

Figure 4-11: Neutrophil-specific lysis and ADCC in Jurkat cells in the presence and absence of FIP: Percentage neutrophil-specific lysis in Jurkat cell line infected with MVNSe (a) or MVMor (b) with (red lines) or without (black lines) anti-MV serum in the presence (empty symbols) or absence (solid symbols) of FIP using chromium release assay. 5% was used as the minimum threshold of neutrophil-specific lysis (black dashed line). Paired t test was performed (between MVNSe (a) or MVMor (b) treated conditions to their FIP treated counterparts) to obtain the P-values. ***p≤0.0003, **p=0.0017, *p=0.0421.

4.3 DISCUSSION:

In this chapter, I investigated ADCC as a possible mechanism of neutrophil mediated MV oncolysis (neutrophil-specific lysis). Except in Jurkat cells infected with MVMor, ADCC was not shown to be a mechanism. Neutrophil-specific lysis also varied among the different cell lines used and most interestingly, the two vaccine strains of MV used showed unexpected and highly significant difference in their ability to mediate a neutrophil effector response, specifically in the Jurkat cells.

ADCC has been established as a mechanism by which effector cells can kill target cells infected by different viruses like HSV[416,417], VZV[418] and MV[419] after natural infection. The presence of ADCC was shown to correlate with reduction in viral load after WT MV infection[244,420]. Previous data from my lab have shown enhanced killing of target tumours in SCID xenografts when MV using a murine GMCSF was used, which also correlated with higher neutrophil infiltration[280]. From data in chapter 3, *in-vivo* observation of neutrophil mediated enhancement of MV killing was very clear in the two B-cell malignancy models, but different susceptibility to neutrophils in the two models suggested more than one mechanism of neutrophil mediated MV oncolysis in play. SCID mice lack any adaptive immune cells and therefore are unable to produce antibodies, also, as murine cells are not susceptible to MV infection, the enhancement of MV oncolysis by MVhGCSF in the Raji SCID xenografts with increased neutrophil infiltration in the spleen, that was observed is unlikely by ADCC in the models described *in-vivo*. However,

there is a report suggesting that certain IgGs can enhance MV entry and infection in murine monocytes and macrophages, via a Fc receptor mediated mechanism[421], and also in older SCID mice presence of mature lymphocytes has been reported as they are known to be “leaky”[422], and therefore some direct infection of the effector cells and presence of ADCC like effect cannot be completely ruled out even in the *in-vivo* models.

Choosing an appropriate model to test the role of the immune system and the mechanisms involved in oncolysis can be tricky due to difference in the effector functions between different species[423]. Though mice are frequent experimental tools of choice, and have helped us understand the working of the human immune system, there are significant differences and known discrepancies in both innate and adaptive immunity[424]. The overall structure of the immune system in mice and humans are similar, but among other differences, the balance of lymphocytes and neutrophils is striking, with mouse blood more rich in lymphocyte (75-90% lymphocytes, 10-25% neutrophils), while human blood more rich in neutrophils (50-70% neutrophils, 30-50% lymphocytes)[425]. Mouse and human neutrophils also differ in their Fc receptor expression. In mice a single gene encodes for each class of Fc receptors whereas in human eight genes have been identified[426]. Additionally, mice don't express FcαRI, FcγRIIa, FcγRIIIB and FcγRIIC, which are important Fc receptors present on human neutrophils, and there is also difference in the IgG sub classes that are present in mice and humans[425]. Moreover, mouse FcγRI is mainly expressed on macrophages. Further, human FcγRI, which is a high affinity receptor does not bind mouse

IgG1[423]. How these differences can affect their functions in studying the effector mechanism is still not very clear. Besides, MV does not readily infect and replicate within murine cells, therefore the *in-vivo* observations in mice will not always reciprocate the same mechanisms that may be expected in human *in-vivo*. Human donors were used as the source of neutrophils in this chapter due to the wider clinical relevance, in the hope of providing better insight into the potential mechanisms in trial scenarios.

The neutrophil-specific lysis was variable between the three cell lines *in-vitro*. Jurkat cells were particularly susceptible to neutrophil-specific lysis with MVNSe infection. However, it was only Jurkat cells infected with MVMor that were lysed via an apparent ADCC. The two B-ALL cell lines and the other T-ALL cell line DND41 did not show any susceptibility to neutrophil-mediated ADCC.

By contrast to the apparent ADCC finding with MVMor infected Jurkat cells, there was significant decrease in the neutrophil-specific lysis of MVNSe infected Jurkat cells upon addition of serum. One possible explanation is neutralisation of the virus by the anti-MV neutralising antibody present in the serum[174]. Pooled serum from donors with high anti-MV antibody was used for the ADCC experiments in this chapter. Anti-MV serum contains both neutralising and non-neutralising (ADCC and complement-mediated lysis) antibodies. Neutralising antibodies against both MV-F and MV-H are present in the serum, with majority of neutralising antibody against MV-H[240,241]. After natural MV infection, most robust antibody response is observed against N

protein followed by MV-H, MV-F and to a very small extent against MV-M[239]. Though MV-N is an intracellular protein, it has been shown to associate with the FcγRIIB in the late endocytic compartment and transported to the cell surface, where it interacts with other non-infected cells[427] and therefore might be important in ADCC. Since antibodies against different MV proteins could be capable of mediating ADCC, the purpose and possible advantage of using pooled serum from patients in the ADCC experiment was to cover the whole repertoire of anti-MV antibodies that might be relevant in ADCC. However, a high level of anti-MV IgG would not necessarily reflect a high level of antibody with capacity to mediate ADCC[419].

Jurkat cells were the only cell line where neutrophil-mediated lysis observed was highest after MV infection. They were first chosen in the lab as they belong to the lymphoid lineage and are a cell line of choice for cytotoxicity assay studies. They are also sensitive to TRAIL mediated killing and MV has been shown to upregulate TRAIL via degranulation of neutrophils[357]. Jurkat cells are often used to study acute leukaemia, cell signalling, expression of different surface receptors or studying mechanisms of action of anti-cancer drugs and radiation[428]. They are known to produce high levels of IL-2 upon stimulation with phorbol esters, lectins or monoclonal antibodies[429]. After screening several leukaemic T and B-cell lines, Jurkat cells were shown to produce 100-300 times more IL2 upon stimulation with lectin like phytohaemagglutinin (PHA) and concanavalin A (con A)[430]. Moreover, Jurkat cells have also been shown to produce IL-2, when persistently infected with vaccinia virus[431]. The IL2 receptor is present on

neutrophils[432], and the binding of the IL2 to the IL2 receptor has been shown to have important regulatory effect on neutrophil functions[433]. It is possible that MV infection stimulates Jurkat cells to produce IL2, which can modulate the function of neutrophils via the IL2 receptor to induce higher neutrophil toxicity in this cell line and not the others, as observed in the experiments in this chapter. T-cells do not normally express Fc receptors, however some T-cell lines like the $CD4^+$ T lymphoblastoid cell line C8166 have been shown to express various Fc receptors[434]. Jurkat cells have also been shown to express the FcγRIII receptor in our lab (Dr. Zhang, unpublished data), and others have shown that FcγRIII receptor can activate and mediate both proximal and distal signalling in Jurkat cells and it is cell type restricted[435]. This allows another possible alternative explanation to ADCC in my findings, which are very specific to Jurkat cells. Fc receptors on the Jurkat may be able to bind to the Fc portion of the anti-MV-H antibody in the serum, which can bind to MV-H proteins expressed on the neutrophils and bring about lysis by "reverse ADCC"[436]. This can lead to induction of signalling through both FcγRIII on Jurkat cells and Fc receptors on neutrophils leading to enhanced killing of Jurkat cells.

The two different vaccine strains acting very differently on neutrophils to cause different cytotoxic effects in the Jurkat cells, was also unexpected. There are few differences between the two vaccine strains of virus. Firstly, there are some known differences in the coding and non-coding sequences between the MV strains[414]. MVMor and MVNSe are both derived from the Edmonston seed B (see 1.2.4). To obtain MVNSe MV-tag-Edmonston B was

slightly modified, to exhibit unique NarI and SpeI sites (MVNSe stands for "Nar-Spe eliminiated")[180] to enable easier cloning. MVNSe is derived from p(+)MV15894[181] which contains the Edmonston molecular clone Genebank Z66517 with 13 point mutations including the "tag" AC>GA at positions 1818-9 of the genome and a point mutation in P gene resulting in 272Cys>272Arg mutation in the V coding region, that disables this protein. MVNSe contains an additional sequence CGTACGATGACGTCCTAG inserted just after nucleotide 3368 to introduce unique restriction sites while maintaining the genome length in compliance with the rule of six (www.addgene.org/58799/). MVMor also has been sequenced[413,414] and differs from the MVNSe only in few amino acids, isolated to the H and L genes[232]. Whether and how these minor genetic differences may play a role in my findings is not clear. Secondly, the difference could be at the functional level with dissimilarity in expression of the MV glycoproteins on the cell surface after infection with different strains. Functional differences have been reported between polymerase L protein of different vaccine and WT MV strains and might depend on the passage history of each attenuated strain[437]. And thirdly, the known difference between the fusogenicity of the two strains could be responsible for the differences observed[50].

I was able to explore one of the potential functional differences by assessing the MV-H expression on Jurkat cells after infection with either of the viruses. MV-H expression was much higher after infection with MVMor than with MVNSe. This was in keeping with the hypothesis that the surface area of cell membrane expressing the viral envelope protein MV-H may be

higher overall in the individually infected cells after infection with the less fusogenic MVMor (Fig 4-8a) compared to in the large syncytia formed by the highly fusogenic MVNSe (Fig 4-8b). Therefore, blocking of fusion with FIP showed slight increased in the %MV-H expression on Jurkat cells infected with MVNSe, possibly due to the increase in surface area of cell membrane expressing MV-H as hypothesised (Fig 4-8). Interestingly, the MVMor infected Jurkat cells showed slight abrogation of %MV-H expression upon blocking of fusion, which was unexpected and opposite of the hypothesis. One probable explanation could be decrease in the level of infection in the cells (and therefore MV-H expression) due to inhibition in viral spread resulting from blocking of fusion, as cell-cell fusion is one known way by which the virus can spread[438]. Additionally, as the MV-H expression was determined by flow cytometry, there is a possibility of an experimental bias in this observation, whereby large syncytia might 'break' while passing through the flow cytometer, artificially reducing the level of cell surface MV-H expression by concentrating the observations to cells which are less well infected. Furthermore, determination of syncytia formation by flow cytometry requires the capacity to distinguish between simple cell aggregates and genuine doublets due to actual syncytium formation. When syncytia are observed on a flow cytometer, their FSC/SSC profile should be very similar to that of doublets, i.e. they are large (high FSC-A) and have unusual shapes (high FSC-W) and granularity (high SSC). These characteristics would typically be gated out of the analysis[439]. So, I have tried to interpret any data where cell-cell fusion is estimated by flow cytometry cautiously.

In this chapter I began to observe the effects of fusion inhibition and its relation to tumour cell cytotoxicity. It has been reported that blocking virus mediated cell-cell fusion can lead to abrogation of tumour cell cytotoxicity[440], where addition of FIP to tumour cells infected with a modified fusogenic strain of adenovirus, led to inhibition of syncytium formation, which in turn decreased the cytotoxicity. In the experiments in this chapter too, upon addition of FIP to the MVNSe infected Jurkat cells, there was significant abrogation of neutrophil-specific lysis of the Jurkat cells.

All the data from this chapter taken together have showed that ADCC is not a likely mechanism of neutrophil-mediated MV oncolysis. The results in Jurkat cells appear as an exception and have potential alternative explanations. Based on the data in this chapter, I have proposed that possible cell-cell fusion between the neutrophils and MV-infected target cells might have a role to play in MV oncolysis. This will be investigated further in chapter 5.

Chapter 5: Fusion between neutrophils and target cells mediate cytotoxicity during measles virus oncolysis - a novel mechanism of oncolysis

5.1 BACKGROUND:

5.1.1 Virus mediated fusion:

Numerous viruses and fusogenic viral envelope glycoproteins - termed "fusion membrane glycoproteins" (FMG) are reported in the literature to cause cell-cell fusion and multi-nucleated syncytium formation, a cytopathic effect (CPE) which may eventually lead to cell death, at least *in-vitro*. Virus mediated cell-cell fusion is a multistage process and is used by enveloped viruses primarily to gain host cell entry. For example, during MV infection, the interaction of the MV-H protein with its receptors (CD46/ CD150) initiates a conformational change in the MV-F glycoprotein, which in turn mediates fusion of the viral envelope and the host cell membrane, facilitating cell entry[441]. Although not characteristic of non-enveloped viruses, the oncolytic virus Reovirus expresses non-structural, fusion associated small transmembrane (FAST) proteins. FAST proteins are not necessary for Reovirus entry or replication in host cells; they appear to have evolved to mediate cell-cell fusion rather than virus-cell fusion, thereby contributing to the rapid dissemination of the infection[442-445].

Virus-mediated cell-cell fusion has been shown to induce apoptosis. For instance, HIV infected $CD4^+$ cells show extensive CPE *in-vitro*. Co-

culturing $CD4^+$ cells with HIV glycoprotein or MV glycoprotein-expressing cells led to apoptosis, which was exclusively induced by cell-cell fusion[446]. In another study, Sendai virus infection of primary paediatric bronchial epithelial cells induced enhanced CPE with evidence of syncytia that led to apoptosis. The observed syncytia were associated with secretion of several pro-inflammatory cytokines - RANTES, TRAIL, IP-10, IL-6, IL-8, etc.[447].

5.1.2 Measles Virus-mediated fusion:

MV-induced syncytia have been implicated in stimulating anti-viral immune responses. In a normal human fibroblast cell line (IMR-90) and in A549 cancer cells MV-induced syncytia led to the down regulation of different cell cycle regulators of the retinoblastoma protein (pRB) pathway and the fused cells showed a senescent phenotype with a halt in cell cycle progression[448]. Furthermore, MV-induced syncytia in human epithelial cells and in mature DCs, led to IFNβ amplification in epithelial cells and both IFNα/β amplification in mature DCs. Interestingly, IFNβ amplification was inhibited in a dose dependent manner by FIP in the epithelial cells. Moreover, MV-induced syncytia in epithelial cells showed highly dynamic behavior with an unexpectedly long lifespan[449]. This finding was later echoed by findings from our lab, where neutrophils from healthy donors infected with oncolytic MV became activated and survived longer *ex-vivo* than uninfected cells, although in this study, syncytia formation between neutrophils was not investigated[357].

Cell-cell fusion within different cells and tissues after MV infection can be variable. Our own published data show substantial differences in the levels of syncytia formation - as an example there was minimal cell-cell fusion in MV-infected primary patient chronic lymphocytic leukaemia (low grade B-cell malignancy) cells for which the reasons were not clear; since the virus demonstrably replicated within the cells and the MV-H and MV-F expression was confirmed in all cases indicating that lack of cell-cell fusion in these cells was not due to a failure of viral envelope protein expression[386]. In spite of this, published data on MV therapy in a variety of tumours consistently report substantial induction of fusion in tumour targets, at least *in-vitro*[51,52,175,176,260,450], and thus regarded as a potential mechanism of MV-induced oncolysis.

5.1.3 Other FMG-mediated fusion:

Virally derived FMGs reported in the literature as having potential relevance to cancer therapy include not only F and H glycoproteins of MV, but also the rhabdoviral VSV-G envelope[451] and retroviral Gibbon Ape Leukaemia Virus (GALV) envelope protein[452]. F/H and GALV delivered by adenoviral and lentiviral vectors have shown therapeutic activity in xenograft models[453]. When compared to herpes simplex virus thymidine kinase or cytosine deaminase suicide genes, one log more potent cytotoxicity was observed by using FMGs in an *in-vivo* model of human xenograft, with a significant bystander effect[454]. Cell death observed was due to sequestration of cell nuclei and nuclear fusion. In this model, syncytia formation was accompanied by the induction of immune-stimulatory heat shock proteins,

which can act as non-specific stimulants of innate immune system[454]. FMG mediated cell death occurs predominantly by non-apoptotic pathways with mitochondrial failure and ATP depletion. With progression of syncytium formation, the nuclei fuse; this is associated with premature chromosome condensation and autophagic degeneration and the subsequent release of the cellular vesicles termed 'syncytiosomes' (vesicles reminiscent of exosomes)[455,456].

5.1.4 Fusion mediated immunogenicity:

The immune-stimulatory mechanisms of FMG mediated cell death have been exploited therapeutically to enhance anti-tumour immune responses[457]. Loading DCs with fusing tumour cells has been used as a strategy to cross present tumour antigens to T-cells[457]. In a human *in-vitro* model, syncytiosomes from dying syncytia more effectively loaded DCs for cross presentation of a melanoma tumour-associated antigen for T-cell priming than normal cells or cells killed by irradiation[455]. Additionally, GALV-mediated cell fusion reversed the suppressive effect of human melanoma Mel888 cells on DC maturation and potentiated IL-12 production by activated DCs. These DCs when loaded with fusing Mel888 cells were able to present the melanoma specific cytotoxic response against Mel888 *in-vitro*[453]. In a different mouse melanoma model, tumour cells that were fused *ex-vivo* acted as a potent vaccine against a live tumour challenge and against a pre-established disease[457].

5.1.5 Replicating fusogenic viruses as oncolytic agents:

The concept of fusogenicity as a therapeutic component of replicating virus therapy has also been explored using viruses other than MV. Several studies have reported the implication of direct cell-cell fusion to enhance oncolytic virotherapy. Bioknife™, a modified Sendai virus (SeV) with enhanced fusogenic ability is oncolytic in different tumour types *in-vitro* where cell-cell fusion and cell death were observed[458]. A single Gly-to-Ala substitution in the SeV F protein generates a hyperfusogenic mutant, which is more cytopathic in prostate cancer cell lines *in-vitro* than the non-fusogenic counterpart. Additionally, prostate cancer xenografts responded better to therapy with the hyperfusogenic mutant SeV compared to the non-fusogenic counterpart[459]. Moreover, oncolytic adenovirus expressing the GALV envelope glycoprotein under the control of the adenovirus major late promoter (ICOVIR16), induced extensive syncytia formation and enhanced tumour cell killing in various tumour types including melanoma and pancreatic cancer both *in-vitro* and *in-vivo* compared to the non-fusogenic virus (ICOVIR15). *In-vivo* injection of ICOVIR16 led to tumour cell fusion *in-vivo* with extensive and enhanced viral spread within the tumour[460]. Another fusogenic adenovirus created by expressing the MV-H and MV-F proteins replacing the E1 gene of the adenovirus showed enhanced cytotoxicity in HER911 cells (human embryonic retinoblast 911) compared to the non-fusogenic control[440].

5.1.6 Fusion inhibitory peptide:

Fusion inhibitory peptide or FIP (Z-D-Phe-Phe-Gly-OH) is a polypeptide originally designed to resemble the N-terminal regions of the *paramyxovirus* F_1 polypeptide or the myxovirus HA_2 polypeptide[461,462]. The mechanism of cell-cell fusion relies on a conformational change in the lipid bilayer membrane structure, which is temperature sensitive. FIP can raise the temperature of the lipid bilayer by 10 degrees thereby disrupting the conformational change, which inhibits the cell membranes from fusing[461]. FIP may also compete for the binding sites on the cell plasma membranes and inhibit fusion and has been shown to work by stabilising the H-F complex[463]. FIP has mainly been used *in-vitro* to block cell-cell fusion. The MV-induced syncytia are formed by co-ordinated action of MV-H and MV-F glycoproteins. MV-H engages with its receptor, which leads to structural transition in MV-F that facilitates fusion of MV with target cell membrane. FIP can interfere with this structural transition of MV-F thereby inhibiting cell infection at the entry stage[464]. Exploiting this characteristic, FIP has been recently used to prevent MV infection *in-vivo* in animal models, where intra-nasal administration results in accumulation of the peptide in the airway epithelium that efficiently blocks MV infection[464].

5.1.7 The current study:

In this chapter, the question of whether fusion between MV-infected tumour cells and neutrophils can activate neutrophils and engage their cytotoxic mechanisms will be investigated. The hypothesis was derived from

findings in chapter 4 in which the neutrophil-specific lysis of MV-infected Jurkat cells was higher after target cells were infected with a fusogenic MVNSe strain than after infection with the less fusogenic MVMor strain. The complete abrogation of neutrophil-specific lysis in the presence of FIP was also striking.

5.1.8 Hypothesis:

The cytotoxic effector function(s) of MV-infected neutrophils relates, at least in part, to fusion between neutrophils and target cells.

5.1.8.1 Aims:

1. To determine the effect of fusion on degranulation and reactive oxygen species (ROS) generation in neutrophils when co-cultured with MV-infected targets.

2. To determine the effect of fusion on type I IFN production and RLR signalling pathway in neutrophils when co-cultured with MV-infected targets.

3. To visualise fusion between neutrophil and MV-infected targets.

5.2 METHODS:

5.2.1 Neutrophil degranulation:

Neutrophils were added to MVNSe infected Jurkat cells (24hpi) at an E:T ratio of 8:1, and co-cultured in the presence or absence of FIP. Twenty-four hours later, the cells were collected, washed and resuspended in

1xPBS. To determine neutrophil degranulation, the cells were stained with CD35 FITC, CD63 FITC, CD66b FITC or IgG isotype antibodies before performing the flow cytometric analysis as described in chapter 2, section 2.9. The neutrophil population was gated on the forward scatter (FSC)/side scatter (SSC) in the co-cultures and the percentage degranulation calculated based on the isotype control. The results were compared to the uninfected co-culture controls. This experiment was repeated in neutrophils from 3 donors.

5.2.2 ROS production:

Neutrophils were added to MVNSe infected Jurkat cells (24hpi) at an E:T ratio of 8:1, and co-cultured in the presence or absence of FIP. Twenty-four hours later, the cells were collected, washed and resuspended in 1xPBS. To determine ROS generation, the cells were stained with 5mM CellROX® Green reagent (Life Technologies^{TM}) according to manufacturer's instructions and then washed 3 times with 1xPBS before performing the flow cytometric analysis as described in chapter 2, section 2.9. The neutrophil population was gated on the FSC/SSC in the co-cultures and the %ROS generation was calculated only in the neutrophil population compared to the uninfected controls. This experiment was performed in 3 different neutrophil donors.

5.2.3 RIG-I/MDA5/MAVS gene expression:

Neutrophils were added to MVNSe infected Jurkat cells (24hpi) at an E:T ratio of 8:1, and co-cultured in the presence or absence of FIP. Twenty-

four hours, later the cells were collected, and total RNA was extracted using TRIzol® extraction (chapter 2, section 2.8.4). First strand cDNA was synthesised from the total RNA (chapter 2, section 2.8.5) and then the relative expression of RIG-I, MDA5 and MAVS was determined by Quanti Tect® Primer assay (Qiagen, UK) as described in chapter 2, section 2.8.6.

5.2.4 Live cell imaging:

5.2.4.1 Jurkat cells:

Jurkat cells were infected with MVNSeGFP at an MOI of 1.0. To immobilise the cells, they were aliquoted into 24-well plates coated with 20µg/ml of Fibronectin (R&D Systems, USA). At 24hpi, either neutrophils, extracted from a healthy donor or uninfected Jurkat cell controls were stained with 3µM concentration of CellTracker^{TM} Red CMTPX Dye (Molecular Probes, Life technologies) for 30-45mins in serum free medium (RPMI1640, pre-warmed at 37°C) according to manufacturer's guidelines. The cells were then washed 5-6 times and added onto the infected Jurkat cells at a ratio of 1:1. The cells in co-culture were then imaged on a Nikon ECLIPSE Ti-S inverted microscope system for 2-3 hours every 5mins using the 40X ELWD (extra length working distance) objective, to facilitate imaging through plastic. The sequence of images was stitched together and analysed using FIJI (ImageJ) software.

5.2.4.2 Vero cells:

Vero cells were plated at $0.5x10^6$ per well in a 12-well tissue culture plate and infected with MVNSeGFP at an MOI of 1.0. Twenty-four hpi the neutrophils were extracted and stained as described before (5.2.4.1) and added to the infected Jurkat cells. They were then imaged on a Nikon ECLIPSE Ti-S inverted microscope system for the first 3 hours every 5mins, and the next 2 hours every 10mins using the 40X ELWD objective and analysed using FIJI (ImageJ) software.

5.3 RESULTS:

5.3.1 Neutrophil degranulation when co-cultured with MVNSe infected Jurkat cells in the presence and absence of FIP:

Direct MVMor infection of neutrophils has already been shown to lead to neutrophil degranulation[357]. Neutrophil degranulation is a multi-stage process, which leads to release of the granule contents into the extracellular or phagolysosomal spaces and fusion of membranes[319]. The granules translocate to the neutrophil cell surface, where they interact with the lipid bilayer, leading to priming of the granules. This facilitates rapid fusion of the granule membrane to the neutrophil membrane, thereby releasing the granule contents[318], showing fusion as an inherent mechanism during neutrophil degranulation. To determine whether co-culture of MVNSe infected Jurkat target cells with neutrophils could enhance neutrophil degranulation, MVNSe infected Jurkat cells were incubated with neutrophils (N=3) from healthy donors in the presence or absence of FIP for 24 hours.

The cells were then analysed by flow cytometry for the presence of granule markers on the cell surface. The gating strategy is shown in Fig 5-1. FSC/SSC was used to gate on the neutrophil population (Fig 5-1a). Based on the isotype control (Fig 5-1b), the percentage degranulation (Fig 5-1c) and MFI of degranulation were calculated on the neutrophils for degranulation markers CD66b (specific granules), CD35 (secretory vesicles) and CD63 (azurophilic granules). The representative FACS histogram plots for each of the degranulation markers are shown in Fig 5-2. FIP did not have any direct effect on neutrophil degranulation *per se*, as is evident from the uninfected controls treated with FIP (Fig 5-3, 5-4, 5-5). No significant change in the percentage of neutrophils expressing CD66b (Fig 5-3a) and CD35 (Fig 5-4a) or in the MFI (Fig 5-3b; Fig 5-4b) of these two markers was observed on co-culture with MVNSe infected Jurkat targets and FIP did not have any effect on those processes.

By contrast, the percentage of neutrophils expressing azurophilic granule markers CD63 on their cell surface (Fig 5-5a) and MFI of CD63 (Fig 5-5b) significantly increased upon co-culture with MV-infected targets ($p=0.0073$ and $p=0.0494$ respectively) compared to the uninfected targets. Moreover, the percentage of CD63 was significantly abrogated upon blocking of fusion with FIP ($p=0.0417$). However, the MFI reduction upon addition of FIP though evident, was not statistically significant.

Overall, the data showed that neutrophil degranulation was variably affected when in contact with MVNSe infected Jurkat target cells compared

to the uninfected Jurkat cell controls; more affected was azurophilic granules (CD63). When fusion was blocked, there was abrogation in degranulation, which was most significant in the percentage of azurophilic granules, suggesting that MVNSe infection of Jurkat target cells plays a role in neutrophil degranulation upon co-culture.

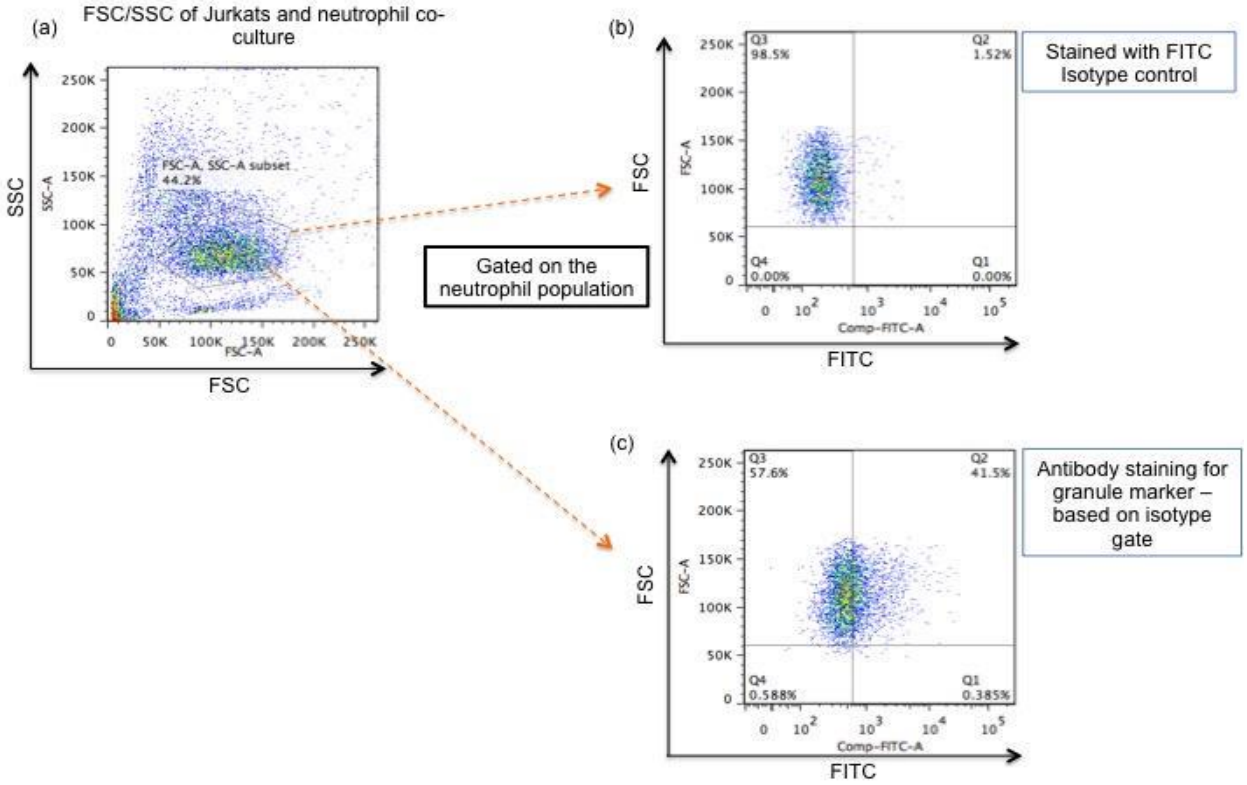

Figure 5-1: Gating strategy to assess degranulation markers on neutrophils in co-culture: Representative FACS plots (from MVNSe infected Jurkat cells showing %CD63 expression on the FITC channel) showing the gating strategy used to assess neutrophil degranulation. Based on the FSC/SSC in Jurkat cells and neutrophil co-culture, neutrophil subset was gated (a). The degranulation percentage was determined on the neutrophil population alone by FITC conjugated antibodies. The quadrant gates for FITC isotype antibody control were set (b), based on which the percentage degranulation on neutrophils was determined (c).

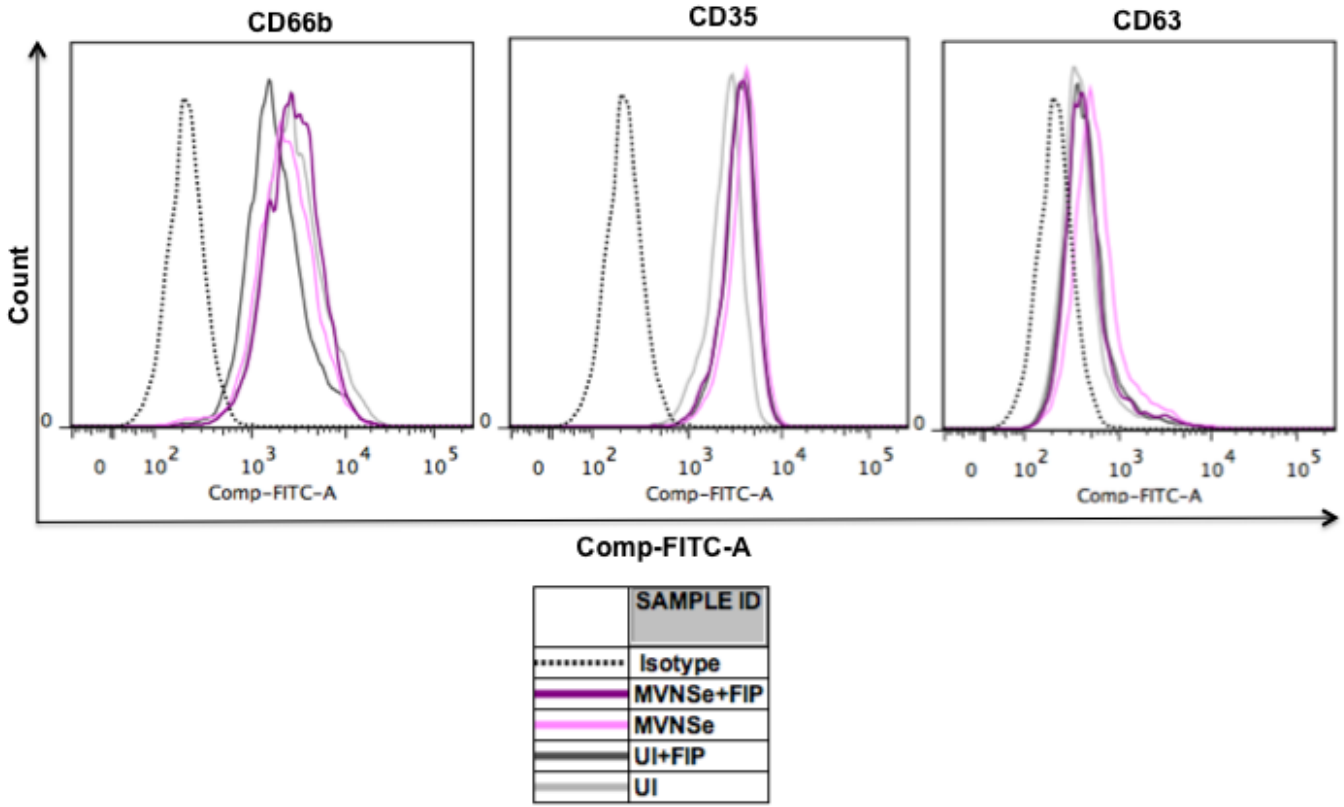

Figure 5-2: Representative histogram FACS plots for neutrophil granules marker expression on neutrophils in co-culture: Representative histogram FACS plots are shown for CD66b, CD35 and CD63 on neutrophils co-cultured with uninfected (light grey and dark grey lines) or MVNSe infected (light pink and dark pink lines) Jurkat cells in the presence (darker shades) or absence (lighter shades) of FIP.

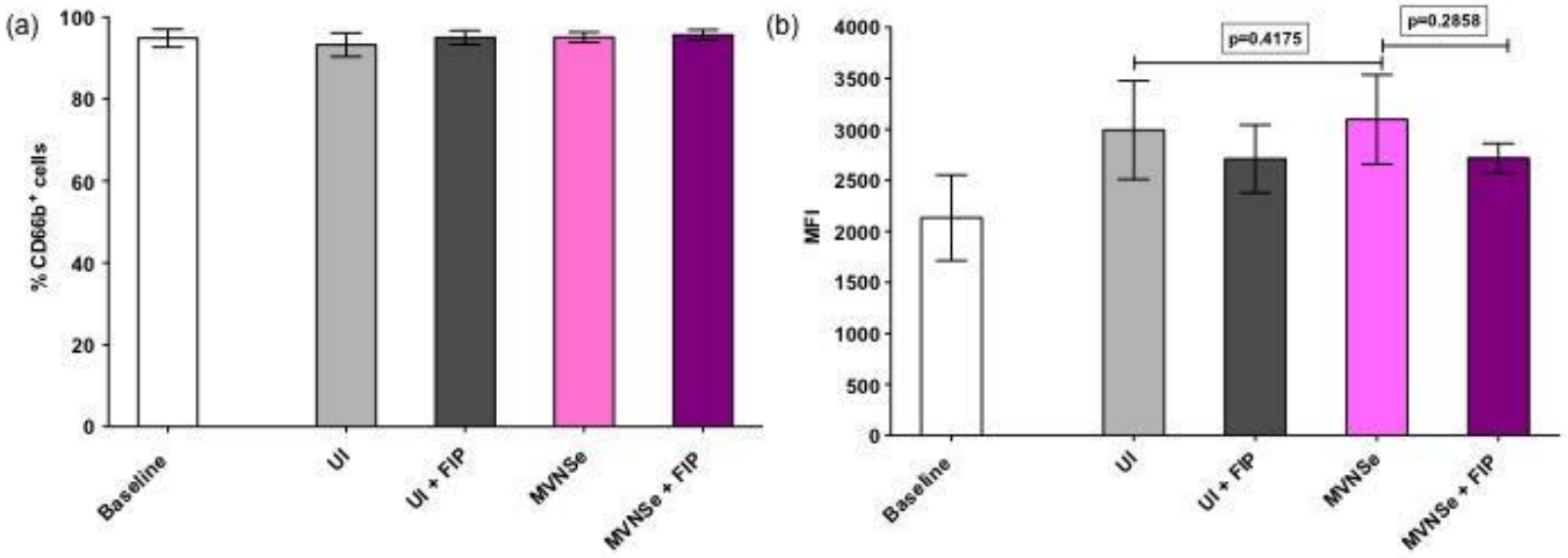

Figure 5-3: Specific granules marker expression on neutrophils in co-culture: The percentage of cells expressing (% positive cells) (a) MFI (b) of CD66b on neutrophils at baseline (white) (n=3), after MVNSe infection (n=3) in the presence (dark pink) or absence (light pink) of FIP and uninfected control (n=3) in the presence (dark grey) or absence (light grey) of FIP. MFI of the degranulation marker was normalised against the respective isotype controls. 'Baseline' represents the expression on freshly isolated neutrophils. The bars show the mean±SEM. Paired t test was performed to obtain the P-values.

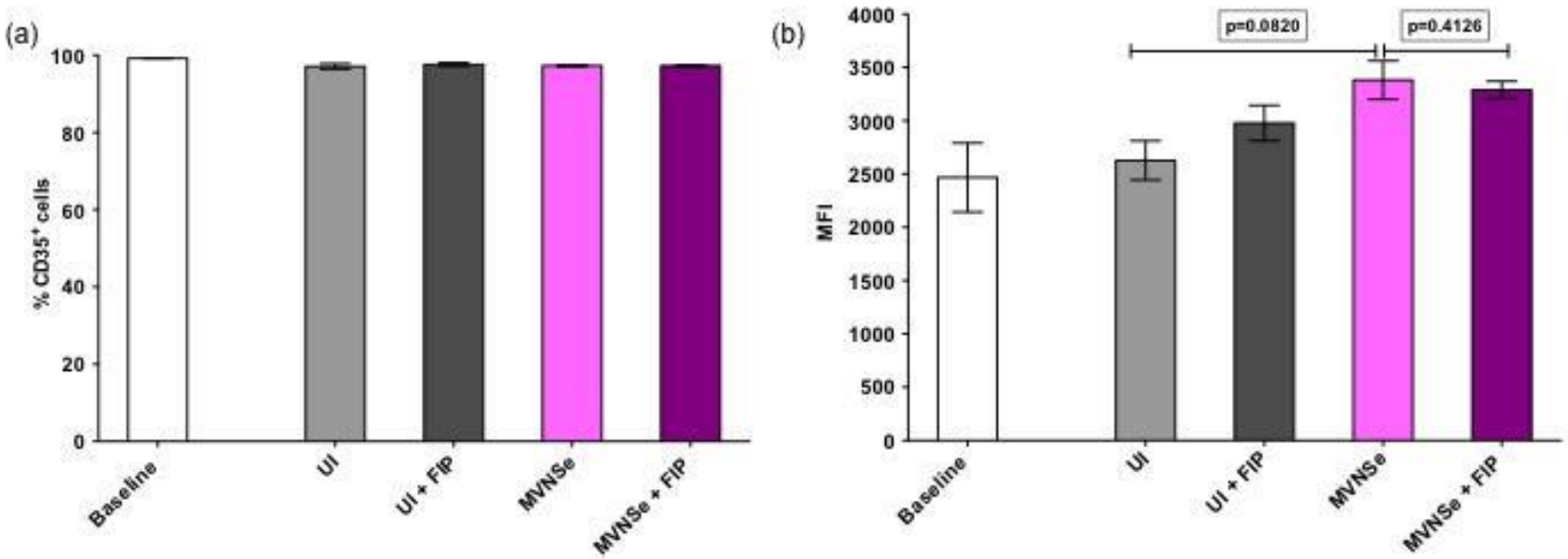

Figure 5-4: Secretory vesicle marker expression on neutrophils in co-culture: The percentage of cells expressing (% positive cells) (a) and MFI (b) of CD35 on neutrophils at baseline (white) (n=3), after MVNSe infection (n=3) in the presence (dark pink) or absence (light pink) of FIP and uninfected control (n=3) in the presence (dark grey) or absence (light grey) of FIP. MFI of the degranulation marker was normalised against the respective isotype controls. 'Baseline' represents the expression on freshly isolated neutrophils. The bars show the mean±SEM. Paired t test was performed to obtain the P-values.

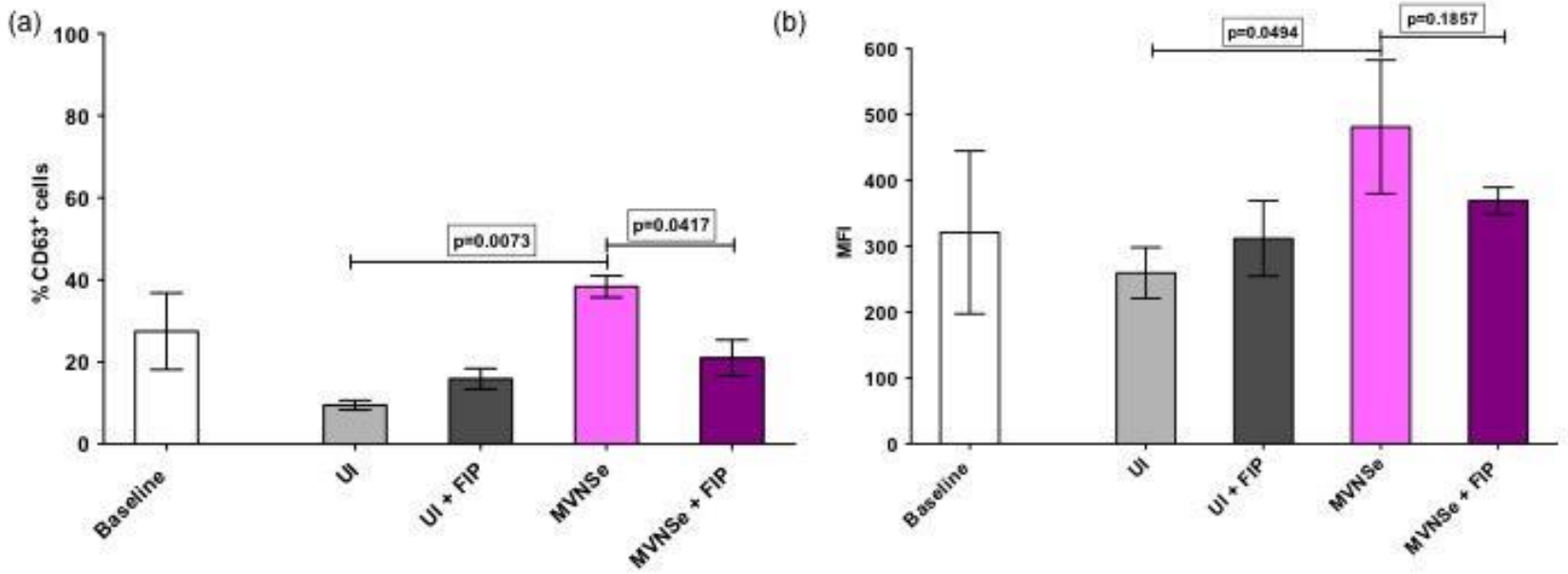

Figure 5-5: Azurophilic granules marker expression on neutrophils in co-culture: The percentage of cells expressing (% positive cells) (a) and MFI (b) of CD63 on neutrophils at baseline (white) (n=3), after MVNSe infection (n=3) in the presence (dark pink) or absence (light pink) of FIP and uninfected control (n=3) in the presence (dark grey) or absence (light grey) of FIP. MFI of the degranulation marker was normalised against the respective isotype controls. 'Baseline' represents the expression on freshly isolated neutrophils. The bars show the mean±SEM. Paired t test was performed to obtain the P-values.

5.3.2 ROS generation by neutrophils when co-cultured with MV-infected Jurkat cells in the presence and absence of FIP:

ROS generation precedes neutrophil degranulation[465]. In order to investigate if MV infection of targets cells had any effect on ROS generation by neutrophils, Jurkat cells were infected with MV, and 24hpi, neutrophils from healthy donors (N=3) were added at 8:1 E:T ratio. Experiments were carried out in the presence or absence of FIP to test the role of cell-cell fusion. Freshly extracted neutrophils were used to determine the baseline ROS levels. The gating strategy is shown in Fig 5-6 on representative FACS plots. Within the neutrophil and target cell (infected/uninfected) co-culture, the percentage of cells expressing ROS was calculated on the neutrophil population alone (Fig 5-6a). The gates were set on the ROS production by neutrophils in co-culture with uninfected Jurkat cells (Fig 5-6b) in the presence or absence of FIP, based on which, the ROS percentage and MFI in FIP (Fig5-6c) and no FIP (Fig 5-6d) infected conditions were determined.

Figure 5-7a and b show the percentage cells expressing ROS and the MFI of ROS expressing cells, respectively. Neutrophils co-cultured with MV-infected Jurkat cells showed a higher MFI *and* percentage of cells stained positive for ROS compared to neutrophils co-cultured with uninfected Jurkat cells. The increase in ROS production was abrogated upon blocking of cell-cell fusion with FIP. However, the observations were not statistically significant possibly due to the low power of the experiment.

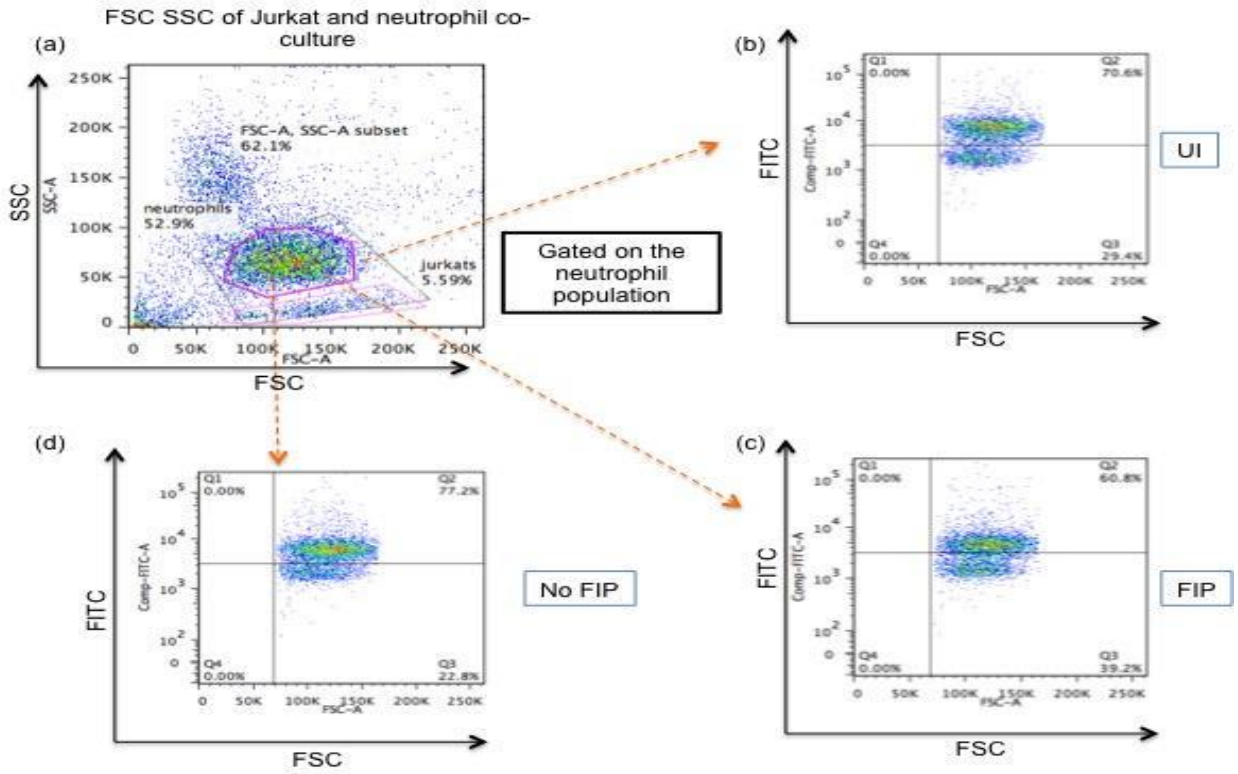

Figure 5-6: Gating strategy to assess ROS production by neutrophils in co-culture: Representative FACS plots showing the gating strategy used to assess ROS production. Based on the FSC/SSC in Jurkats and neutrophil co-culture, neutrophil subset was gated (pink gate) (a). The ROS percentage was determined on the neutrophil population alone by CellROX® green reagent in the FITC channel. The quadrant gates for uninfected co-culture control was set to determine the baseline ROS production (b), based on which the percentage ROS production by neutrophils in FIP (c) and no FIP (d) conditions were determined.

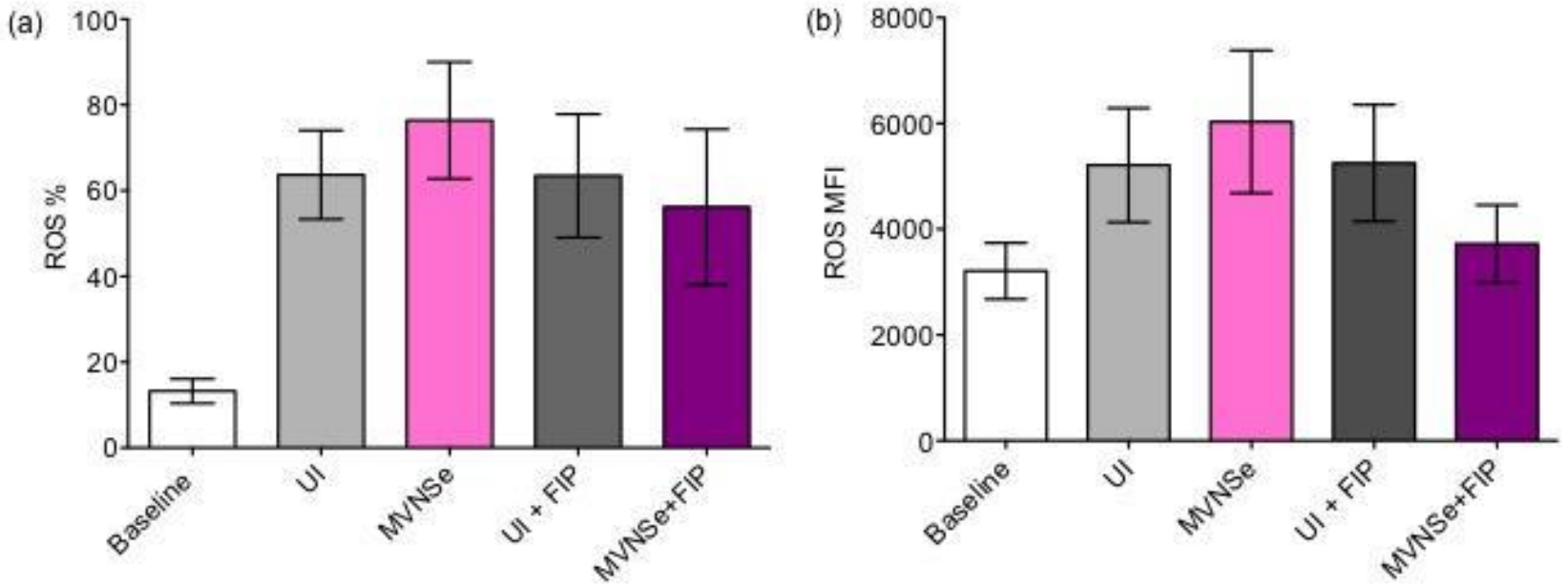

Figure 5-7: ROS on neutrophils in co-culture: The percentage of cells expressing (% positive cells) (a) and MFI (b) of ROS on neutrophils at baseline (white) (n=3), after MVNSe infection (n=3) in the presence (dark pink) or absence (light pink) of FIP and uninfected control (n=3) in the presence (dark grey) or absence (light grey) of FIP. 'Baseline' represents the ROS expression on freshly isolated neutrophils. The bars show the mean±SEM.

5.3.3 Neutrophils produce significant amounts of IFNα and IFNβ when co-cultured with MV-infected Jurkat cells, which disappears in the presence of FIP:

To test whether fusion between the MV-infected Jurkat target cells and neutrophils can lead to type I IFN production, infected Jurkat target cells were co-cultured with neutrophils for 24 hours in the presence or absence of FIP and the supernatant from the cultures was collected and quantified for IFNα/β production by ELISA. A number of important control conditions were included to ensure that any IFN produced was from the neutrophils and not the target cells and that it was definitely a response to MV infection; target cells alone, MV-infected target cells alone, neutrophils alone, MV-infected neutrophils alone and target cells with neutrophils but no MV were all included as experimental conditions and each was repeated with the addition of FIP (N=3). Figure 5-8a shows the results for IFNα production. Neutrophils produced 161-5594 pg/ml of IFNα but only when co-cultured with MV-infected Jurkat cells (light pink bars). None of the other experimental control conditions generated any IFNα, confirming that the virus, target cells and neutrophils were all necessary for the interferon response. There was a very substantial reduction in IFNα production upon addition of FIP (0-315pg/ml). The experiment failed to reach significance due to very low IFNα produced by one donor (161pg/ml). Therefore, the absolute quantities of IFNα produced in the infected Jurkat cell/neutrophil co-culture in the presence or absence of FIP were analysed separately and are shown in Fig 5-8b. Figure 5-8c shows the data for IFNβ. Neutrophils co-cultured with MV-infected Jurkat cells secreted IFNβ in the range of 54-92pg/ml (light pink bar), which

was significantly (p=0.0111) abrogated upon addition of FIP (0-2.9pg/ml). Again, there was little or no IFNβ production without the presence of both MV-infected target cells plus neutrophils. The absolute quantities of IFNβ produced in the infected Jurkat cell/neutrophil co-culture in the presence or absence of FIP were analysed separately and are shown in Fig 5-8d.

These data indicated that neutrophils are the source of IFNs after contact with MV-infected target cells and that IFN is produced specifically when the neutrophils are in contact with the MV-infected Jurkat target cells. The substantial reduction in the IFN production in the presence of FIP suggested that fusion between neutrophils and MV-infected Jurkat cells might be involved in the generation of an IFN response.

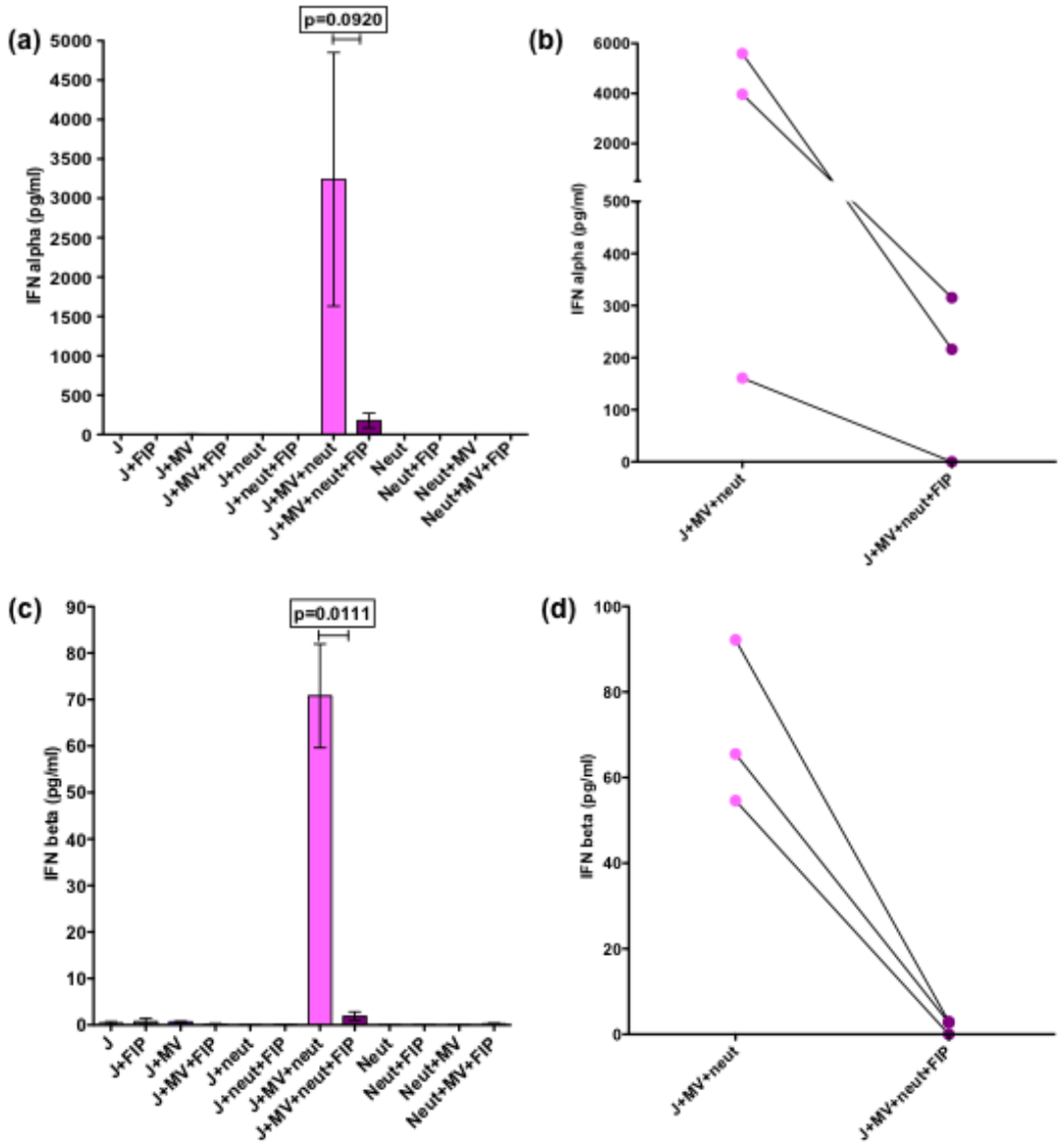

Figure 5-8: Effect of FIP on type I IFN production in Jurkat/neutrophil co-culture: IFNα (a) and IFNβ (c) production in infected and uninfected Jurkats, neutrophils and Jurkat/neutrophil co-culture in the presence or absence of FIP in all conditions by ELISA. IFNα (b) and IFNβ (d) production only in MV-infected Jurkat/neutrophil co-culture conditions in the presence (dark pink dots) or absence (light pink dots) of FIP. The bars in (a) and (c) show the mean±SEM. Paired t test was performed to obtain the P-values.

5.3.4 The (RIG-I like receptor) RLR signalling pathway is upregulated when MV-infected Jurkat cells are co-cultured with neutrophils compared to neutrophils and Jurkat cells alone.

To determine the upstream events of the type I IFN production, the induction of genes in the RLR signalling pathway was quantified by RQPCR. Similarly to the previous experiments, this was carried out in the presence and absence of FIP in order to evaluate the contribution of fusion. Jurkat cells and/or neutrophils were infected and either co-cultured or incubated on their own for 24 hours and the RIG-I/MDA5 and MAVS gene expression determined. The level of expression was normalised to the uninfected controls of each condition. The data are shown in Fig 5-9. Both RIG-I and MDA5 were very modestly upregulated in neutrophils but not Jurkats after direct infection with MV. However, after co-culture of neutrophils with infected Jurkat cells, expression of both RIG-I and MDA5 were increased 20-40 fold with some reduction upon FIP addition. There was no significant upregulation of MAVS in any of the conditions. These data show that the presence of both MV-infected target cells and neutrophils together is important for activation of the RLR signalling pathway. Since minimal upregulation was observed in Jurkat cells infected with MV compared to neutrophils infected with MV, it can be speculated that when in co-culture, MV-infected Jurkat cells stimulate the RLR signalling pathway particularly in the neutrophils. The relative lack of change upon FIP addition suggests that this upstream step is not fusion-related.

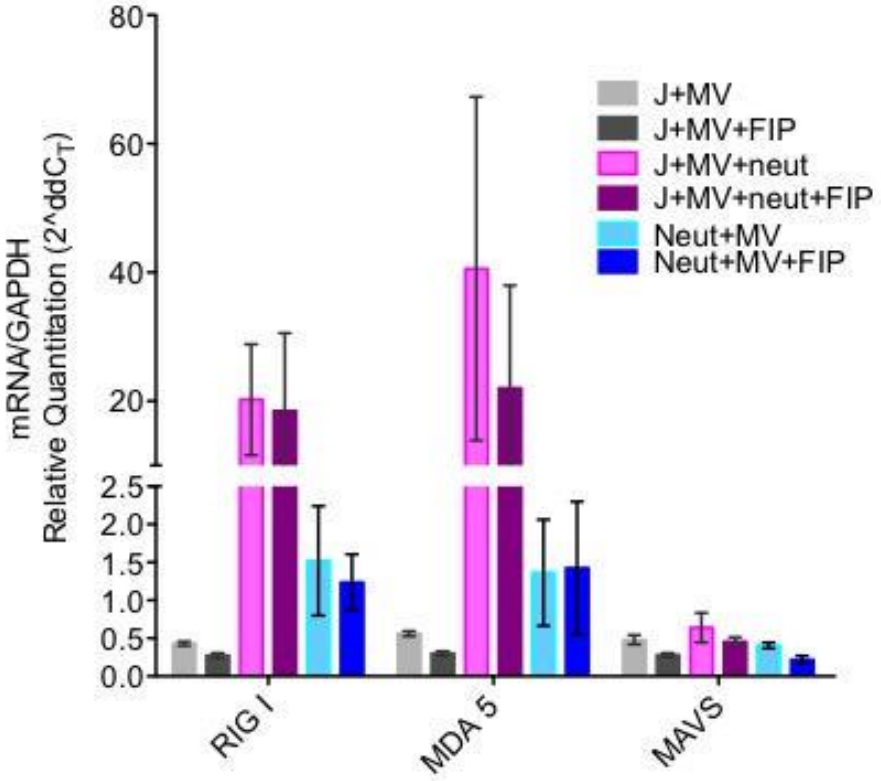

Figure 5-9: Quantification of genes of the RLR signalling pathway in Jurkat/neutrophil co-cultures: RIG-I, MDA5 and MAVS genes quantified by RQPCR in MV-infected Jurkat cells on their own (grey bars), neutrophils on their own (blue bars) and Jurkat/neutrophil co-culture (pink bars) in the presence (dark shades) or absence (light shades) of FIP. The data is normalised to uninfected controls and represented as relative quantities to GAPDH house keeping gene by ΔΔCt method. N=3. The data is represented as mean±SEM.

5.3.5 IFN does not have any direct cytotoxic effect on MV-infected or uninfected Jurkat cells

In order to test whether type I IFN generation by neutrophils could be, in part, responsible for the target cell cytotoxicity observed, exogenous IFN was added in increasing concentrations to Jurkat cells which had been infected with MV or mock-infected. Both cell numbers (Figs 5-10a and b) and percentage cell viability (Fig 5-11a and b) in uninfected controls were significantly higher than the MVNSe infected cells but did not change with increasing concentrations of IFNα or IFNβ. Taken together the data suggest that the production of IFN by neutrophils does not directly result in the Jurkat target cell cytotoxicity we observed.

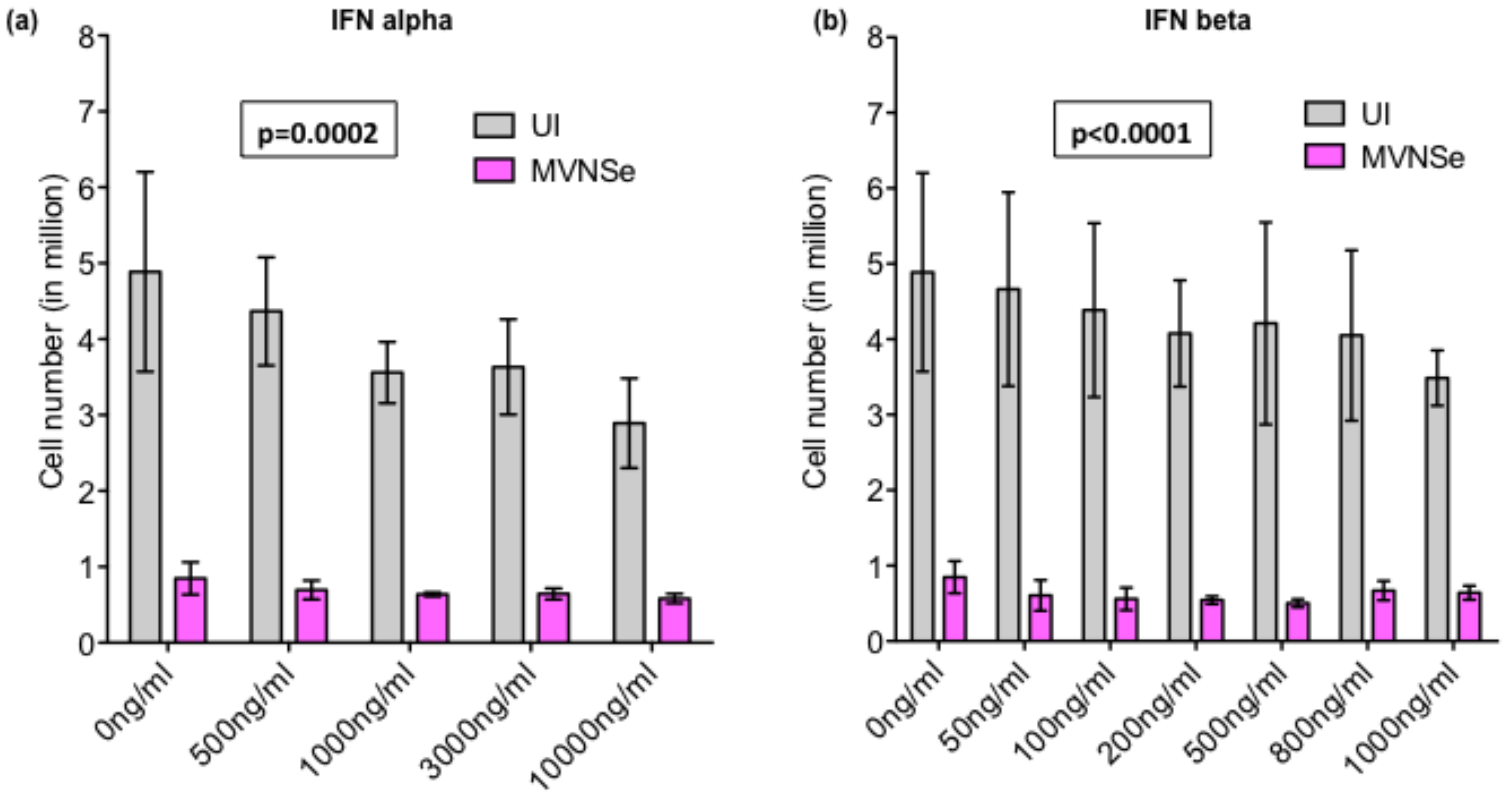

Figure 5-10: Effect of exogenous type I IFN on Jurkat cell number: Jurkat cell numbers counted by trypan blue in uninfected (grey) and MVNSe infected (pink) conditions, 24hpi in variable concentrations of IFNα (a) and IFNβ (b). Paired t test was performed to obtain the P-values.

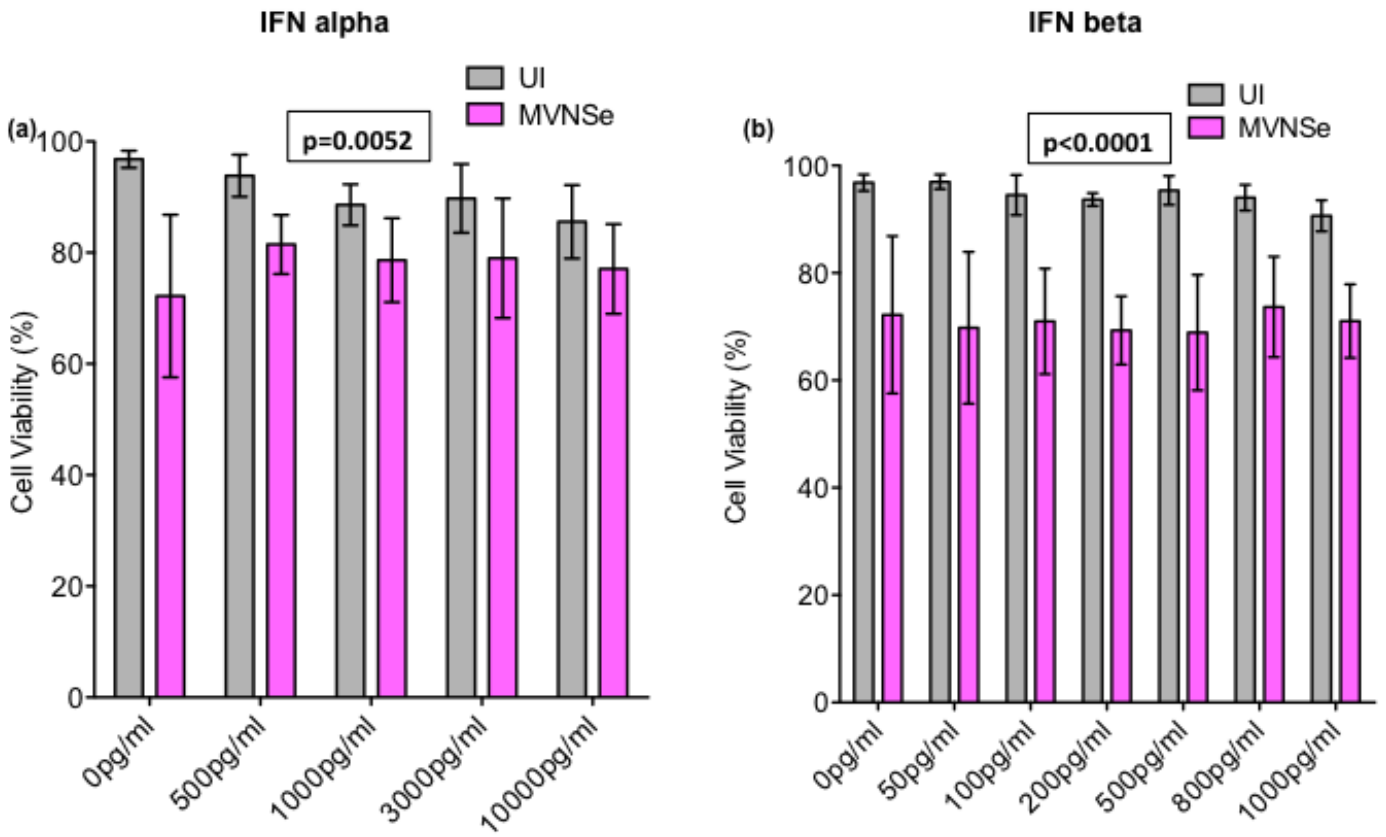

Figure 5-11**: Effect of exogenous type I IFN on Jurkat cell viability:** Percentage Jurkat cell viability determined by trypan blue in uninfected (grey) and MVNSe infected (pink) conditions, 24hpi in variable concentrations of IFNα (a) and IFNβ (b). Paired t test was performed to obtain the P-values.

5.3.6 Neutrophils produce a significant quantity of soluble TRAIL when cultured with MV-infected Jurkat cells, which is abrogated in the presence of FIP:

Tumour necrosis factor (TNF) – related apoptosis-inducing ligand (TRAIL) is a member of the TNF superfamily, which is selectively cytotoxic in cancer cells and its production by neutrophils is known to be consequent on IFNα stimulation[466]. In our previous publication, MV infection of neutrophils was shown to induce TRAIL secretion in the absence of *de novo* synthesis, by triggering release of pre-fabricated TRAIL, via direct effect upon degranulation[357]. To test whether the observed upregulation of type I IFNs can lead to soluble TRAIL production, infected Jurkat target cells were co-cultured with neutrophils for 24 hours in the presence or absence of FIP and the supernatant from the cultures was collected and quantified for soluble TRAIL production by ELISA (Fig 5-12). Important control conditions similar to IFN secretion ELISA experiment were included – target cells alone, MV-infected target cells alone, neutrophils alone, MV-infected neutrophils alone and target cells with neutrophils but no MV. Neutrophils co-cultured with MV-infected Jurkat cells produced significantly high levels of soluble TRAIL (1000 – 1200pg/ml) compared to neutrophils in the presence of uninfected Jurkat cells (200pg/ml) ($p=0.0290$). In the presence of FIP, TRAIL production was significantly reduced ($p=0.0119$) to that seen in uninfected conditions (250-500pg/ml), suggesting again that fusion between Jurkat target cells and neutrophils may be a key component of the cytotoxic response of neutrophils.

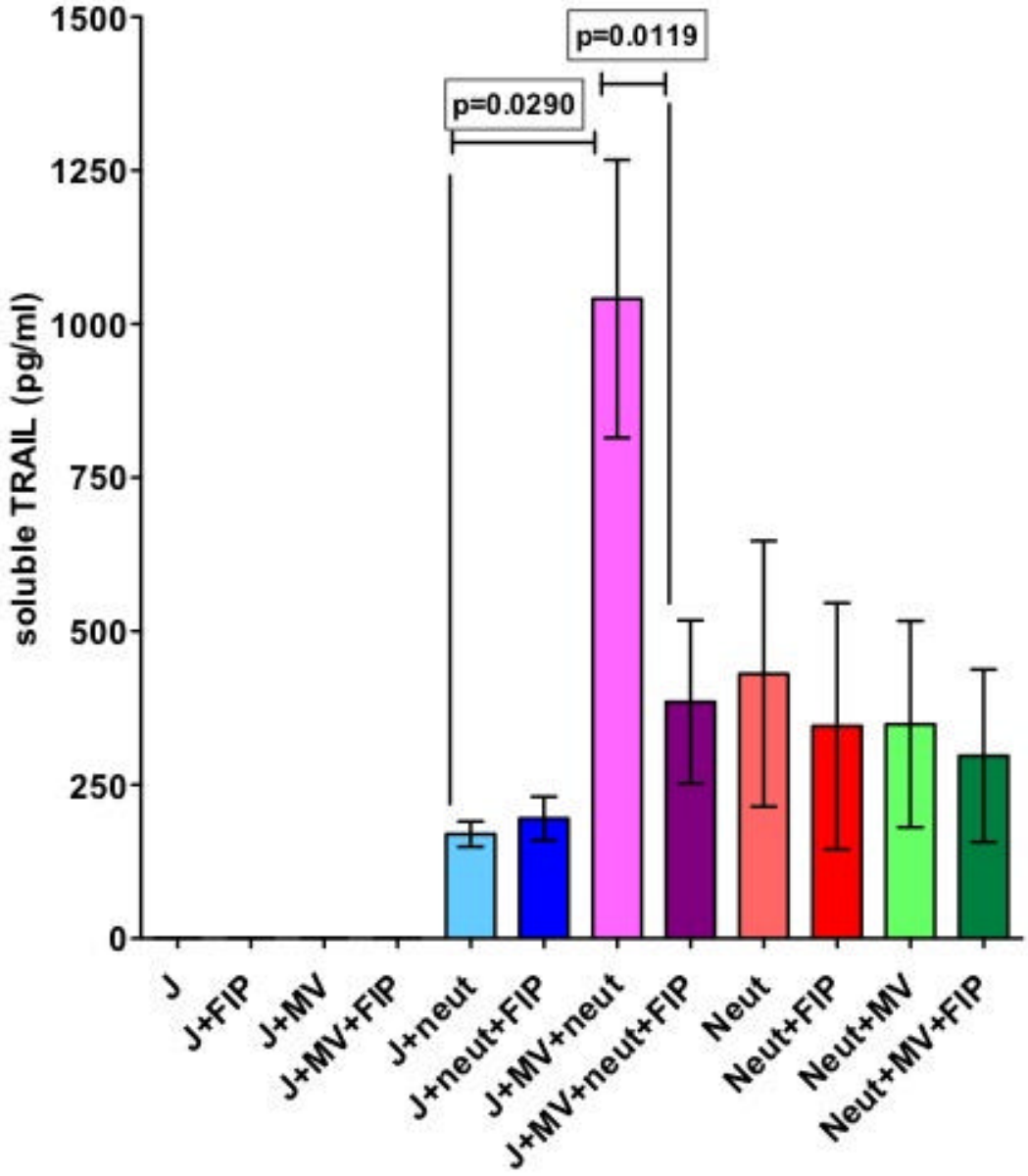

Figure 5-12: Effect of FIP on soluble TRAIL production in Jurkat/neutrophil co-culture: Soluble TRAIL production determined in infected and uninfected Jurkats, neutrophils and Jurkat/neutrophil co-culture in the presence or absence of FIP in all conditions by ELISA. The bars in (a) and (c) show the mean±SEM. Paired t test was performed to obtain the P-values.

To determine whether this quantity of TRAIL may be responsible for the neutrophil-mediated cytotoxicity, a dose response experiment to evaluate the direct effect of recombinant human TRAIL (rhTRAIL) on Jurkat cells was

performed. (This experiment was carried out by my colleague Dr. Zhang, and I have permission to include the data here). Data in Fig 5-13 shows that soluble TRAIL below 5000pg/ml did not induce significant cell death in Jurkat cells when compared to the untreated negative control (0pg/ml) *in-vitro*. This implies that, even though contact with MV-infected Jurkat cells clearly induces neutrophils to release soluble TRAIL, release into the supernatant in these experiments (or the cell milieu, *in-vivo*) might not be the mechanism by which a significant biological effect is exerted. The abrogation in TRAIL secretion in the presence of FIP further suggests that possible fusion between MV-infected Jurkat cells and neutrophils may be at least in part responsible for the neutrophil-mediated cytotoxicity that was observed.

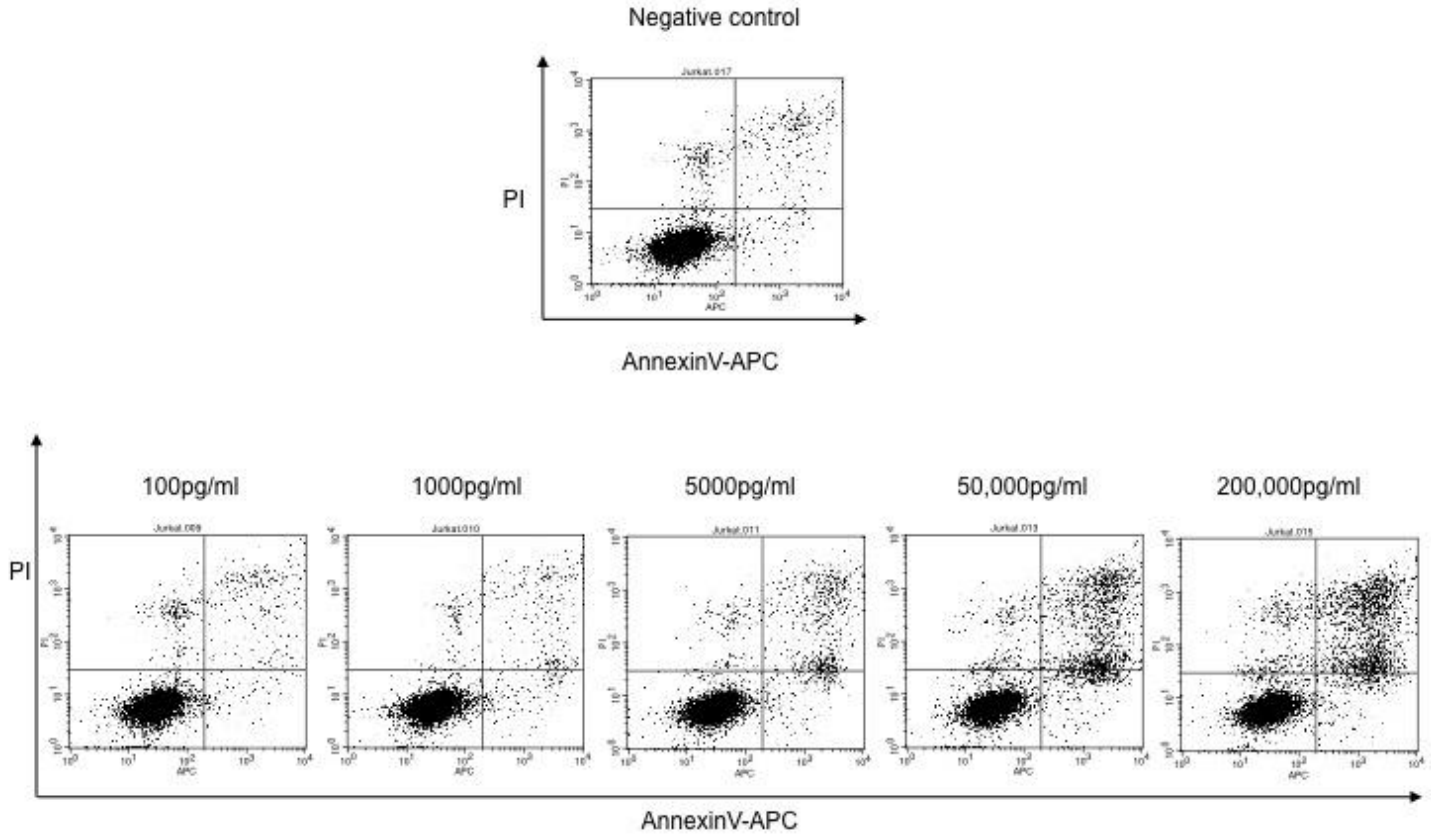

Figure 5-13: A dose response experiment of Jurkat cells to recombinant human TRAIL: Jurkat cells treated with increasing concentrations of soluble TRAIL *in-vitro* and flow cytometry analysis done to determine percentage of AnnexinV-PI positive cells.

5.3.7 Live cell imaging show possible fusion between neutrophils and MV-induced syncytium:

All the data so far with FIP suggested, but did not prove that fusion between neutrophils and MV-infected target cells is an important element of the effects found. Therefore to be certain, live cell imaging was used to determine whether fusion between the infected Jurkat cells and neutrophils could be visualised.

5.3.7.1 Optimisation:

5.3.7.1.1 Basic conditions for observation of cell-cell fusion using target cells alone:

To optimise the basic conditions for observation of cell-cell fusion and to understand the timing of the events, Jurkat cells were infected with MVNSeGFP and immobilised onto fibronectin-coated plates. Uninfected Jurkat cells, stained with 3μM CMTPX red, were added to the immobilised cells. Cells were imaged every 5 mins for 1.5 hours from start of co-culture at 40X to create a time-lapse video (for full video see Appendix – SV5-1). Snapshots from the SV5-1 show a fusion event between the MV-GFP infected green Jurkat syncytium and a red uninfected single Jurkat cell at the 20^{th} min post start of co-culture (shown by the white arrows in Fig 5-14 and a purple arrow in SV5-1). The observed fusion between target cells was rapid and occurred within 15-20 mins of start of the co-culture. Based on this experiment, the infected vs. uninfected cell ratio of 1:1 was set to be the optimal ratio.

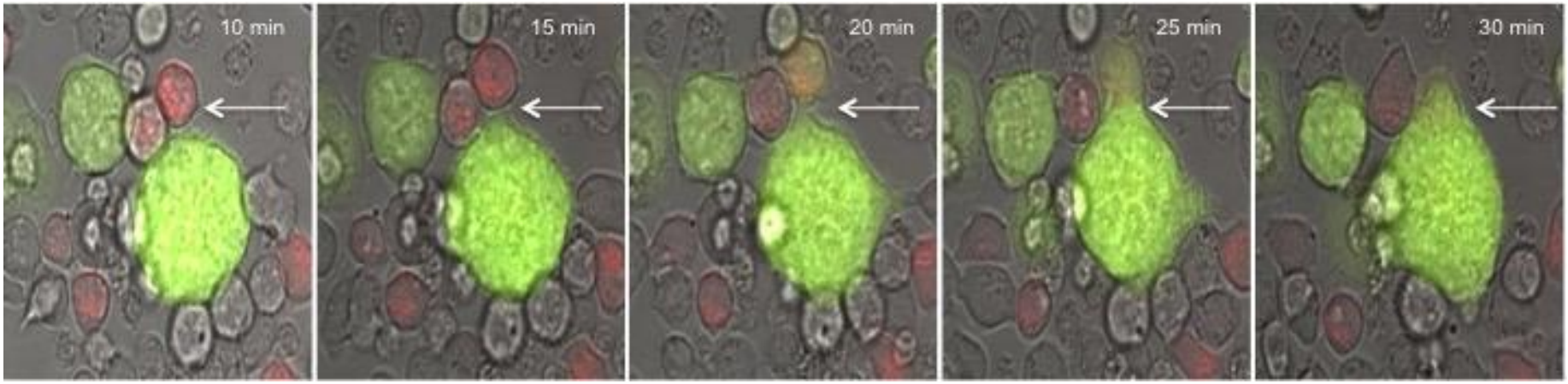

Figure 5-14: Images from MVNSeGFP infected and uninfected Jurkat cell co-culture: Uninfected Jurkat cells stained with CMTPX red dye (red cells) were added at 1:1 ratio to 24-well fibronectin coated tissue culture plates containing MVNSeGFP infected Jurkat cells (green), 24hpi. Images were taken at 40X zoom using an ELWD lens. Images from SV5-1 (Appendix) showing a fusion event (white arrows) are shown over a time period of 30 mins.

5.3.7.1.2 Basic conditions for observation of Jurkat-neutrophil fusion:

Next, MVNSeGFP infected Jurkat cells were immobilised onto fibronectin coated plates and then CMTPX-stained neutrophils extracted freshly from a donor were added at 1:1 ratio. Imaging was carried out every 5mins for 2.5 hours at 40X. Fig 5-15 shows snapshots from SV5-2 between 5^{th} and 130^{th} min. Unlike the previous experiment with target cells alone, neutrophils were not observed to fuse with MVNSeGFP infected Jurkat syncytia. Instead, neutrophils were seen interacting and clustering beneath the green Jurkat syncytia at later time-points, suggesting ongoing interaction between the MV-induced target syncytia and uninfected neutrophils. However, even 2.5 hours later, no hetero-fusion events were detected. The whole series of events are shown in SV5-2 (white arrows) (for full video see Appendix).

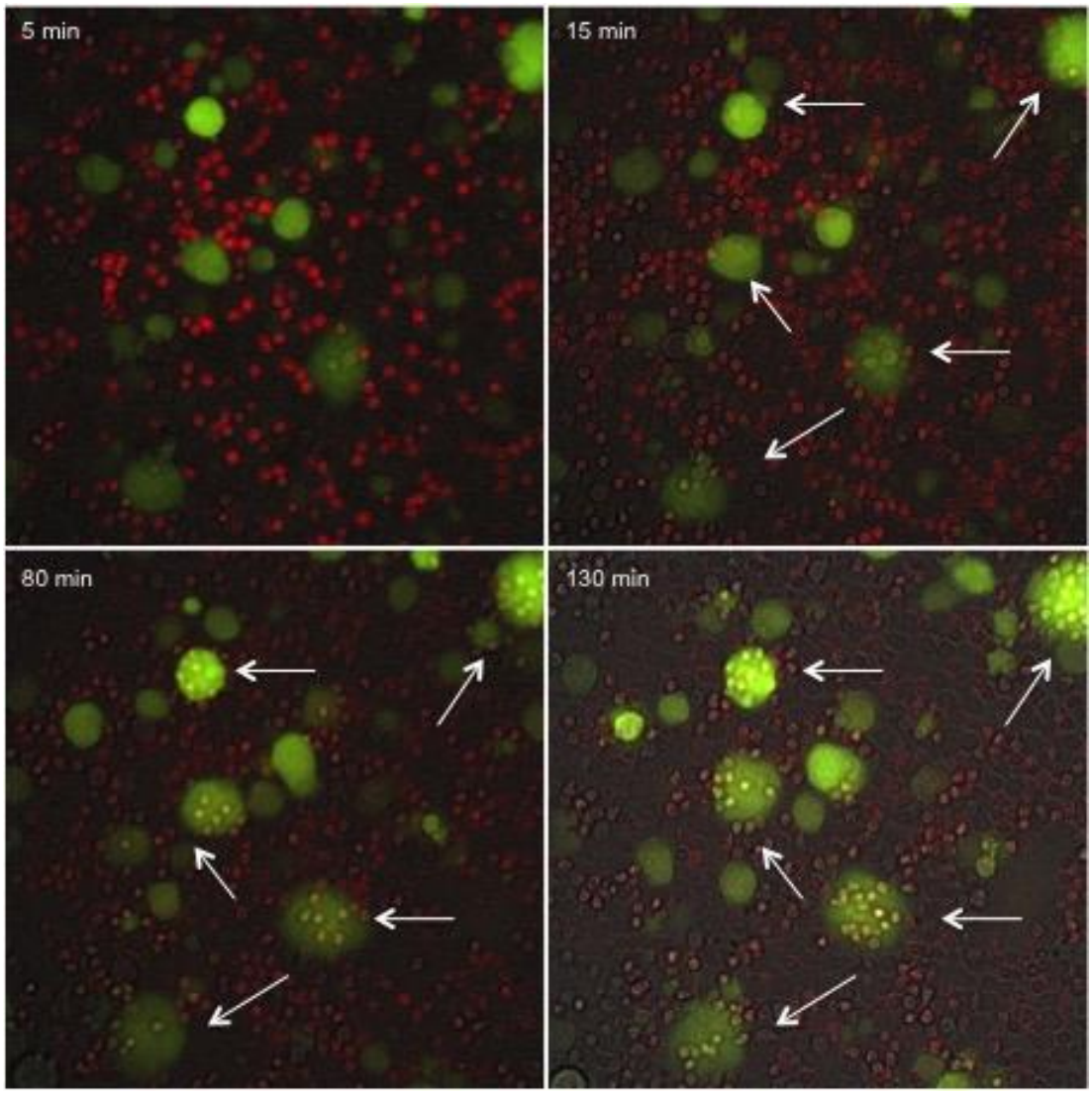

Figure 5-15: Images from MVNSeGFP infected Jurkat cells and uninfected neutrophils in co-culture: Uninfected neutrophils stained with CMTPX red dye (red cells) were added to MVNSeGFP infected Jurkat cells (green) attached to fibronectin coated 24-well tissue culture plates, 24hpi. Images were taken at 40X zoom using an ELWD lens. Images from SV5-2 (Appendix) showing neutrophils clustering under green GFP positive MV-infected Jurkat cell syncytia (white arrows) are shown over a time period of 130 mins.

5.3.7.1.3 Fusion between neutrophils and MV-infected adherent Vero cell line:

Jurkat cells and neutrophils are both non-adherent cells, making their visualisation on the same focal plane somewhat challenging. Therefore, as a proof of principle, the next experiment was designed to determine whether neutrophils could fuse with MV-induced syncytia. To achieve that, adherent Vero cells that can form a monolayer were plated onto a 12-well tissue culture plate and infected with MVNSeGFP at an MOI of 1.0. Red CMTPX stained neutrophils were added to the infected Vero cells at 1:1 ratio and then imaged every 5 mins for 3 hours at 40X zoom. SV5-3a and SV5-3b (for full video see Appendix) suggested that the neutrophils (red) might be adhering to the syncytia, which may be indicative of an interaction of the neutrophil cell membrane with the membrane of the target syncytia. The interacting neutrophils then collapsed and flattened on the surface of the syncytia (shown by the white arrow), appearing to be fusing with the syncytia. Finally, the dying green Vero syncytium in the same experiment shrunk and completely collapsed at the end of 5 hours of co-culture (for full video see Appendix - SV5-4), along with the interacting neutrophils, indicating attachment and interaction of neutrophils with the syncytia. This experiment suggested that neutrophils can actively interact with the MV-induced syncytia and possibly fuse with them, but this fusion is delayed when compared to target-target cell fusion. Whether the constantly changing morphology of the neutrophils that was observed is related to a fusion event is yet to be established. This is however a preliminary observation that needs to be

confirmed by more quantitative methods. An important consideration in this experiment is whether this fusion event between neutrophil and Vero syncytia is real and occurring at the same focal plane. Since Vero syncytia form a monolayer, it can therefore be presumed that the neutrophils are in the same plane as the syncytia. This can be further elucidated with Z-stack confocal imaging at different focal planes, to visualise the entirety of the sample.

Preliminary imaging data indicated that visualisation of two target cells fusing after MV infection is possible. Additionally, neutrophils were clearly shown to interact closely with infected target cells (Jurkat and Vero) with possible fusion.

5.4 DISCUSSION:

In this chapter, viral infection induced fusion between infected target cell and effector cell was investigated as a possible novel mechanism of MV-mediated oncolysis. Addition of FIP, which was used to block fusion, abrogated neutrophil mediated killing of MV-infected Jurkat cells. It was a significant and very consistent observation across all the 10 neutrophils from different healthy donors that were tested, suggesting fusion as a possible mechanism of target cell killing.

Degranulation and ROS generation are two crucial mechanisms that activated neutrophils use to combat infection[467]. In a previous publication, MVMor infection of neutrophils was shown to lead to neutrophil degranulation

and neutrophil activation[357]. Another *paramyxovirus* – respiratory syncytial virus (RSV) that is also known to cause cell-cell fusion, has also been shown to stimulate neutrophil degranulation, which was determined by myeloperoxidase release, though the effect of fusion blocking was not investigated[468]. It was later reported that the fusion protein of RSV causes NADPH oxidase derived ROS production and ERK and p38 MAPK phosphorylation[469]. The effect of target-neutrophil cell fusion on neutrophil degranulation and ROS generation was assessed in this chapter. Typically, azurophilic granules undergo very limited and controlled exocytosis, due to their highly toxic and pathogenic content[320]. When MVNSe infected Jurkat cells were co-cultured with neutrophils, the most significant degranulation was of azurophilic granules, which was abrogated in the presence of FIP. The other granules exhibited some upregulation upon infection, which was also associated with fusion. However, differences in their expression levels were not statistically significant requiring further investigation. Furthermore, neutrophils, in the presence of Jurkat cells, produced higher levels of ROS compared to untreated neutrophils at baseline. This was further increased when Jurkat cells were themselves infected. The blocking of fusion led to reduced ROS generation by neutrophils. These experiments suggested that fusion between MV-infected Jurkats and neutrophils might be able to enhance the cytotoxic phenotype of the neutrophils, thereby making it a potent killer of cancer cells.

Other players of the neutrophil cytotoxic effector response, such as Neutrophil Extracellular Traps (NETs), incorporated by neutrophils, might

also play a role in neutrophil-specific MV oncolysis[470]. Traditionally thought to be involved in bacterial infections, NETs have now emerged as important contenders in viral infections. NETs are comprised of sticky, complex mesh of de-condensed strands of nuclear DNA formed by the release of granular and nuclear contents of neutrophils in the extracellular space in response to bacterial or viral stimuli[470]. The fusion protein of respiratory syncytial virus (RSV) has been shown to promote TLR4 dependent NET formation by human neutrophils[469]. Whether NET formation is induced by measles virus infection of Jurkat cells is of interest and might have an effect that needs to be elucidated.

The components of the IFN response pathway were investigated in the target cells infected with MV in the presence of neutrophils in this chapter. An early response to viral infection is the generation of IFNα/β, but the role of IFN in MV infection is not very clear[237]. RNA viruses induce IFNβ production in the cytoplasm through RIG-I, MDA5 or LGP2 or through the TLR3 in the endosome[471]. The RIG-I of the RLR pathway can recognise the 5'-triphosphate-ended RNA of MV small RNA leader transcript. This leads to activation of the pathway downstream via activation of the IRF genes (IRF 1,3,7) leading to IFN production[449]. Both RIG-I and MDA5 gene expression were significantly increased in the co-culture conditions compared to the individually infected cells, but addition of FIP did not have any significant effect. Whether other pathways involving proteins like STING, a recently identified adaptor molecule found on the mitochondrial membrane and

believed to act in conjunction with RIG-I and MAVS, have any role to play still needs to be elucidated[472].

In a different study, MV infection of mature DCs (mDCs) induced multinucleated syncytia that led to enhanced production of IFNα/β, which was inhibited by addition of FIP. This clearly showed the contribution of MV-induced syncytia in an anti-viral immune response[449]. In this chapter, the high expression of the RIG-I and MDA5 genes, irrespective of low MAVS expression, in the co-culture experiments correlated with very high amounts of type I IFNs, and FIP completely abrogated the IFN production in these co-cultures. Although production of type I IFN has been long believed to be a hindrance in anti-cancer virotherapy, there is growing body of evidence showing that they contribute to the induction of tumour associated antigen (TAA) specific tumour responses[473]. Newcastle disease virus treatment combined with CTLA4 blockade was reported to eradicate B16 melanomas through immune responses that require IFNAR1[474]. Also Semliki Forest virus was shown to elicit an anti-tumour CTL response only if the host expresses IFNAR1[475]. Type I IFN has been reported to have anti-cancer function and contribute in immune-surveillance and the success of conventional chemotherapy[473]. Moreover, targeted anti-cancer agents, radiotherapy and immunotherapy rely on type I IFN signalling, which may mainly function by stimulating anti-cancer immune responses[473]. In this chapter, infected neutrophils or Jurkat cells on their own, uninfected neutrophils and Jurkat cells in co-culture, did not produce any detectable levels of IFN, suggesting

neutrophils are only able to elicit an IFN response when in co-culture with infected Jurkat cells.

Type I IFNs are known to directly inhibit the proliferation of tumour and virus infected cells and increase class I MHC expression, enhancing antigen recognition and is approved for systemic therapy in a variety of diseases including solid and haematological malignancies, multiple sclerosis and chronic viral hepatitis[476]. Nevertheless, high levels of IFN in the co-culture experiments were not found to be directly toxic to the infected Jurkat cells as treatment with increasing amounts of exogenous IFN did not have any effect on the target cell number and percentage of target cell viability, suggesting that IFN did not have a direct cytotoxic effect on the Jurkat cells in these experiments.

Immune cells, such as monocytes and neutrophils, can be stimulated by IFNα to release biologically active soluble TRAIL. This, in turn, can exert selective apoptotic activities towards tumour cells and virus-infected cells[477]. MV infection of neutrophils has been shown to induce neutrophils to produce pre-formed soluble TRAIL from their granules[357]. Besides, MV-infected human DCs were also shown to produce functional TRAIL[478]. In the co-culture experiments in this chapter, significant levels of soluble TRAIL was detected in the conditions where high IFNα/β levels were produced, which decreased in the presence of FIP. However, from previous un-published data from the lab, we know that soluble TRAIL below 5ng/ml is not sufficient to induce significant death in Jurkat cells *in-vitro*. Therefore, the level of soluble

TRAIL produced (1-1.25ng/ml) in these experiments, might not have been responsible for a direct cytotoxic effect on the target cells.

All the experiments where addition of FIP abrogated the neutrophil-specific lysis of MV-infected target cells suggested that fusion between target and effector cells was possibly playing a crucial role in target cell killing. However, the downstream event of fusion that might have a direct role in killing of target cells was not clear. Neutrophils have been shown to bind and fuse with Epstein Barr Virus (EBV) followed by penetration and subsequent localisation to the nucleus of the neutrophils. Visualising the fusion of the viral envelope with the neutrophil cell membrane by electron microscopy showed the presence of EBV particles inside the vacuoles, suggesting phagocytosis of the virus particles by the neutrophils, which was followed by apoptosis[479]. It was therefore postulated that the visualisation of neutrophils co-cultured with infected Jurkat cells might provide some insight into the actual mechanism of neutrophil mediated MV cytotoxicity of Jurkat cells. To investigate that, imaging experiments were designed. As both Jurkat cells and neutrophils are suspension cells, the main technical challenge was to make one adhere to the plates to form a monolayer, which needs further optimisation. Some of the preliminary experiments with an adherent cell line, Vero (which forms large syncytia upon infection with MV) and neutrophils, showed possible fusion events across all the area of the syncytium. This was a proof of principle experiment showing that neutrophils are capable of fusing with MV-induced syncytia. However, it was evident that MV-infected Jurkat cells can clearly fuse with uninfected Jurkat cells in a very short span of time.

Nonetheless, multiple experiments trying to show fusion between the infected Jurkat cells and neutrophils were not very successful due to technical reasons and needs further optimisation and experimentation. At the same time, these experiments need to be repeated in the presence of FIP, to attribute any of the observation to be fusion related.

Overall, data in this chapter suggest that MV infection of Jurkat target cells stimulate neutrophils to develop a cytotoxic effector phenotype. All aspects of which are blocked by fusion inhibition and hence, may be and is potentially mediated by fusion between infected Jurkat cells and neutrophils.

Chapter 6: General Discussion

Measles virus (MV) has been established as a candidate for oncolytic virotherapy of haematological malignancies[480]. Data from this thesis has contributed to adding acute lymphoblastic leukaemia (ALL) to the list of applicable therapeutic uses and indeed has shown that ALL is particularly sensitive to MV oncolysis[386]. Data from phase I/II clinical trials indicated use of oncolytic MV as a safe and well tolerated oncolytic agent[173,277,292,390]. While there is much advancement in this field, the mechanisms of oncolysis remain unclear. Understanding the mechanism by which MV kills cancer cells holds a crucial key to its continuing success. This thesis has tried to address some of the mechanisms that might be playing a role in MV-mediated oncolysis. My data show, it is extremely likely, that more than one single credible mechanism is in play and 'one size fits all' model of "MV therapy for cancer" probably does not exist.

Once the virus is delivered to the specific location of tumour, direct oncolysis of the cancer cells alone is very unlikely to deplete all malignant cells satisfactorily due to the heterogeneity of the cancer microenvironment. The involvement of the immune system will be indispensable to generate a more potent response[70]. In previous work from my host laboratory the distribution of the virus within the tumour environment, even after IT injection was very patchy. However, the tumours regressed completely, suggesting a role of an anti-tumour immune response induced by the MV infection[175]. The tumours were infiltrated with neutrophils but not NK cells or macrophages.

This led us to the initial investigation of the role of neutrophils in MV-mediated oncolysis in detail.

6.1 GCSF AS A POTENTIAL ENHANCER OF MV ONCOLYSIS *IN-VIVO*:

MV modified to express hGCSF was used in chapter 3 to enhance the oncolytic activity of MV by stimulating one of the important members of the innate immune system – neutrophils. Unexpectedly, the role of neutrophils was remarkably different, even in two different models of B-cell malignancy. While it was already established by previous work from our lab[280] that Raji model is sensitive to neutrophil-specific lysis enhanced by MV *in-vivo*, this was reiterated by extended findings in chapter 3. Firstly, in the neutrophil depletion experiments the efficacy of MV therapy was abrogated in the depleted conditions only in Raji model, showing their importance in MV-mediated killing. Secondly, MV expressing GCSF in the Raji disseminated model enhanced the neutrophil infiltration in the peripheral blood of mice and correlated with improved survival when compared to the unmodified MV. By contrast, the results in the Nalm-6 disseminated model were unexpected; no enhanced effect of addition of the hGCSF gene was observed in MVhGCSF treated mice when compared to MVNSe. Besides, unpredictably, the Nalm-6 ALL progressed rapidly in the disseminated groups treated with hGCSF (expressed by MV or on its own).

GCSF is widely used in the clinical treatment of patients with aggressive B-cell malignancies and has been shown to improve outcome[393]. A clinical trial NCT01331590 is being conducted, evaluating the role of GCSF

in priming the bone marrow of ALL patients for subsequent chemotherapy targeting[396]. Additionally, in an AML trial, GCSF has been used as a growth factor primer as it has been indicated to sensitise the leukaemia cells to chemotherapy. In this clinical trial the four-year cancer free survival was improved in patients treated with GCSF at induction, compared to the non-treated group (42% to 33%). In the Raji model, MVhGCSF might carry an advantage, especially in combination with non-myelosuppressive chemotherapies. However, based on our data that showed an unexpectedly aggressive progression of Nalm-6 leukaemia *in-vivo* by MV expressing hGCSF, future studies would need to proceed very cautiously as any benefit from hGCSF as expressed by oncolytic viruses could be difficult to predict and may even vary from patient to patient.

6.2 MECHANISMS OF MV ONCOLYSIS *IN-VITRO*:

6.2.1 ADCC as a mechanism of MV oncolysis:

The difference in neutrophil mediated response to MV infection *in-vivo*, led to investigation of the mechanisms in detail in chapter 4 and chapter 5. However, an *in-vitro* model was used to probe into the mechanisms using human neutrophils. In chapter 4, ADCC was explored as a mechanism based on previous data from the lab. ADCC, a mechanism by which antibody coated cells can induce cytotoxicity via a network of immune effector cells is also implicated in virus eradication after natural infection. More than 18 different mAbs are approved for clinical use for treating cancer[481] and can kill cancer cells by ADCC[482,483]. Monoclonal antibody bound to the effector cells

and in case of viral infection, the antibodies directed against the viral-infected cells can be recognised by effector cells and lead to cell killing by ADCC[484-487]. Furthermore, systemic administration of virus hidden in immune-cells in combination with mAb like rituximab and cetuximab therapies can facilitate NK cell mediated ADCC[488]. The presence of anti-MV antibody in the serum[239-241] can be a potential facilitator of ADCC during measles oncolytic virotherapy[427] and previous data from the lab using Jurkat cells had indicated ADCC to be a likely mechanism of MV oncolysis. Nevertheless, after elaborate study in different other cell lines in chapter 4, ADCC could not be proven as a mechanism of MV oncolysis *in-vitro* in the cell lines examined except in Jurkats.

6.2.2 Fusion between neutrophils and MV-infected target cells as a potential mechanism of oncolysis:

Chapter 5 focussed on fusion as a mechanism of MV-mediated oncolysis. The hypothesis was derived from findings in chapter 4 in which the neutrophil-specific lysis of MV-infected Jurkat cells was higher after target cells were infected with a fusogenic MVNSe strain, than after infection with the less fusogenic MVMor strain. The complete abrogation of neutrophil-specific lysis of MV-infected Jurkat cells in the presence of FIP was also prominent. Therefore, it was proposed that the neutrophils might possibly fuse with the MV-infected tumour cells thereby generating a cytotoxic neutrophil phenotype that can ultimately kill the tumour cells.

In chapter 5, addition of FIP in neutrophil and MV-infected Jurkat cell co-culture was shown to abrogate the neutrophil cytotoxic phenotype and showed reduced cytotoxicity towards MV-infected Jurkat cells. This was suggestive of neutrophil fusing with MV-infected target cells leading to target cell killing. Cytotoxic phenotype included neutrophil degranulation, ROS production and activation of type I IFN signalling pathway and there was a trend observed, where addition of FIP reduced induction of neutrophil cytotoxic phenotype. Certain components of the RLR signalling pathway tested were shown to be involved (RIG-I, MDA5), whereas others were not (MAVS) and hypothetically several others that might be playing important role still require testing.

Sendai virus, a ssRNA virus which can also induce syncytia formation, has been shown to induce a pro-apoptotic phenotype in cancer cells via the RIG-I/MDA5 pathway activation, by regulated balance between pro and anti-apoptotic members of the BCL-2 protein family[489]. Furthermore, ssRNA of MV is known to activate the RIG-I/MDA5 signalling [490], which can potentially lead to IRF gene expression – this remains to be elucidated. It can be hypothesised that this may either directly upregulate pro-apoptotic genes like Noxa and TRAIL[489], leading to cell death, or could lead to activation of the anti-viral and anti-tumoural immunity via production of type I IFN and CXCL10. Additionally, as I have shown in chapter 5, a type I IFN response consequent on encountering MV-infected target cells can directly induce neutrophils to produce soluble TRAIL. Fusion blocking significantly reduced both type I IFN and TRAIL production by neutrophils.

In the *in-vivo* system of cancer therapy, where other members of the innate immune family will be present, the type I IFN could further activate NK cells to produce IFN gamma, which in turn can attract and activate a CTL mediated adaptive immune response against the tumour cells[489].

6.2.2.1 Technical challenges and considerations:

Attempts to visualise a fusion event between neutrophils and MV-infected target cells was not successful. However, live cell imaging did indicate clear interaction between the MV-induced syncytia in target cells and the neutrophils which needs further experimentation.

To determine fusion formation, various different methods have been used, including reporter assays[491], spectrofluorometric measurement of fluorescent probe redistribution, such as fluorescence dequenching, photosensitised labelling, and fluorescence resonance energy transfer (FRET)[492,493]. These methods provide an overall estimation of fusion. Although, methods and assays, which can help understand the detailed mechanism of fusion by monitoring the detailed kinetic changes in the lipid and cytosolic compartments have been used[494], they don't allow understanding of the functional and biological features of fusion and what effect this has on the surrounding environment, which should also be the subject of further work. Flow cytometric methods have also been used to determine cell-cell fusion[495]. However, determining the fusion and syncytia formation by flow cytometry needs expertise in analysing and being able to distinguish between cell aggregates and doublet due to actual syncytium

formation. The syncytium, on a flow cytometer show up with an FSC/SSC profile very similar to doublets, i.e. they are large (high FSC-A) and have unusual shapes (high FSC-W) and granularity (high SSC) that most people would typically gate out of their analysis[439]. All these will need to be taken into account before further experiments are designed to be certain that fusion between effector cells and MV-infected target cells is a possible mechanism of oncolysis.

6.2.3 Final Conclusions:

The concept of fusing immune cells with cancer cells has been used previously to make cancer vaccines, where hepatoma cells were fused with activated B-cells. The hybrid cells produced, lost their tumourigenicity and became immunogenic[496]. If the neutrophils are fusing with MV-infected cancer cells, they have the potential to generate a potent immunogenic effect, in turn alerting the immune system of the presence of tumour cells. Although conventionally, neutrophils are not seen as antigen presenting cells (APCs), there are reports that after virus infection they can prime naïve $CD8^+$ T-cells and cross-present antigens from the virus infected cells[497]. They can also acquire an APC phenotype in the presence of GMCSF by upregulating MHC class II and CD80/CD86 co-stimulatory molecules[498]. Therefore, upon fusion of neutrophils with MV-infected cancer cells, in addition to direct, neutrophil-mediated cytotoxicity, I would hypothesise, will generate a more specific immune response by presenting the tumour antigens of the virally infected cells. This will be a potential benefit, especially in a tumour

microenvironment known for their immunosuppressive properties[499]. This should be the subject of further work.

An additional potential value to MV-mediated target-immune cell fusion is the induction of cellular senescence, which has recently been shown to occur after MV-infection[448]. This is a robust mechanism that causes permanent cell cycle arrest of potentially harmful cells[500,501]. Chemotherapeutic drugs can induce tumour cell senescence[502-504], which leads to the phenomena called therapy induced senescence (TIS). TIS have been suggested to halt cancer cell progression by different dysfunctional apoptosis signalling mechanisms such as overexpression of anti-apoptotic BCl-2 proteins and caspase inhibition[504-507]. Senescent cells, which exhibit profoundly altered phenotype, support enhanced MV replication when compared to non-senescent cells[508]. Fusion mediated by MV might be able to generate a senescent phenotype in tumour cells enabling enhanced replication and more efficient direct killing of the tumour cells.

Overall the findings in this thesis suggest that neutrophils play an important role in MV-mediated killing of B-cell malignancies demonstrating specific toxicity against MV-infected target cells. This role can be enhanced by GCSF in very specific circumstances. However, I demonstrated that MVhGCSF would not be a safe and reliable tool for cancer therapy as the high levels of GCSF expressed by this virus can adversely affect tumour progression. My data indicates likely fusion induced by MV infection between cancer cells and neutrophils, which can potentially contribute to the

cytotoxicity. Further work is needed to confirm this fusion by direct visualisation. An investigation into the broader immunogenic effect of fusion of target cells and neutrophils and into MV-induced senescence would be an appropriate direction for further work.

References

1 Chabner, B. A. & Roberts, T. G., Jr. Timeline: Chemotherapy and the war on cancer. *Nature reviews. Cancer* **5**, 65-72, doi:10.1038/nrc1529 (2005).

2 Baskar, R., Lee, K. A., Yeo, R. & Yeoh, K. W. Cancer and Radiation Therapy: Current Advances and Future Directions. *International Journal of Medical Sciences* **9**, 193-199, doi:10.7150/ijms.3635 (2012).

3 Sawyers, C. Targeted cancer therapy. *Nature* **432**, 294-297, doi:10.1038/nature03095 (2004).

4 Baselga, J. Targeting tyrosine kinases in cancer: the second wave. *Science* **312**, 1175-1178, doi:10.1126/science.1125951 (2006).

5 Iqbal, N. & Iqbal, N. Imatinib: A Breakthrough of Targeted Therapy in Cancer. *Chemotherapy Research and Practice* **2014**, doi:10.1155/2014/357027 (2014).

6 Ottmann, O. G. & Pfeifer, H. Management of Philadelphia chromosome-positive acute lymphoblastic leukemia (Ph+ ALL). *Hematology / the Education Program of the American Society of Hematology. American Society of Hematology. Education Program*, 371-381, doi:10.1182/asheducation-2009.1.371 (2009).

7 Yarden, Y. The EGFR family and its ligands in human cancer. signalling mechanisms and therapeutic opportunities. *European journal of cancer (Oxford, England : 1990)* **37 Suppl 4**, S3-8 (2001).

8 Olayioye, M. A., Neve, R. M., Lane, H. A. & Hynes, N. E. The ErbB signaling network: receptor heterodimerization in development and cancer. *Embo j* **19**, 3159-3167, doi:10.1093/emboj/19.13.3159 (2000).

9 Dotan, E., Aggarwal, C. & Smith, M. R. Impact of Rituximab (Rituxan) on the Treatment of B-Cell Non-Hodgkin's Lymphoma. *Pharmacy and Therapeutics* **35**, 148-157 (2010).

10 Carter, P. *et al.* Humanization of an anti-p185HER2 antibody for human cancer therapy. *Proceedings of the National Academy of Sciences of the United States of America* **89**, 4285-4289 (1992).

11 Garnock-Jones, K. P., Keating, G. M. & Scott, L. J. Trastuzumab: A review of its use as adjuvant treatment in human epidermal growth

factor receptor 2 (HER2)-positive early breast cancer. *Drugs* **70**, 215-239, doi:10.2165/11203700-000000000-00000 (2010).

12 Welniak, L. A., Blazar, B. R. & Murphy, W. J. Immunobiology of allogeneic hematopoietic stem cell transplantation. *Annual review of immunology* **25**, 139-170, doi:10.1146/annurev.immunol.25.022106.141606 (2007).

13 Ghosh, A., Holland, A. M. & van den Brink, M. R. Genetically engineered donor T cells to optimize graft-versus-tumor effects across MHC barriers. *Immunological reviews* **257**, 226-236, doi:10.1111/imr.12142 (2014).

14 Kalos, M. *et al.* T cells with chimeric antigen receptors have potent antitumor effects and can establish memory in patients with advanced leukemia. *Science translational medicine* **3**, 95ra73, doi:10.1126/scitranslmed.3002842 (2011).

15 Kochenderfer, J. N. *et al.* Eradication of B-lineage cells and regression of lymphoma in a patient treated with autologous T cells genetically engineered to recognize CD19. *Blood* **116**, 4099-4102, doi:10.1182/blood-2010-04-281931 (2010).

16 Brentjens, R. J. *et al.* CD19-targeted T cells rapidly induce molecular remissions in adults with chemotherapy-refractory acute lymphoblastic leukemia. *Science translational medicine* **5**, 177ra138, doi:10.1126/scitranslmed.3005930 (2013).

17 Grupp, S. A. *et al.* Chimeric antigen receptor-modified T cells for acute lymphoid leukemia. *The New England journal of medicine* **368**, 1509-1518, doi:10.1056/NEJMoa1215134 (2013).

18 Sharpe, M. & Mount, N. Genetically modified T cells in cancer therapy: opportunities and challenges. *Disease Models & Mechanisms* **8**, 337-350, doi:10.1242/dmm.018036 (2015).

19 Stanislawski, T. *et al.* Circumventing tolerance to a human MDM2-derived tumor antigen by TCR gene transfer. *Nature immunology* **2**, 962-970, doi:10.1038/ni1001-962 (2001).

20 Schmid, D. A. *et al.* Evidence for a TCR affinity threshold delimiting maximal CD8 T cell function. *J Immunol* **184**, 4936-4946, doi:10.4049/jimmunol.1000173 (2010).

21 Lagisetty, K. H. & Morgan, R. A. Cancer therapy with genetically-modified T cells for the treatment of melanoma. *The journal of gene medicine* **14**, 400-404, doi:10.1002/jgm.2636 (2012).

22 Robbins, P. F. *et al.* Tumor regression in patients with metastatic synovial cell sarcoma and melanoma using genetically engineered lymphocytes reactive with NY-ESO-1. *J Clin Oncol* **29**, 917-924, doi:10.1200/jco.2010.32.2537 (2011).

23 Morgan, R. A. *et al.* Cancer regression and neurological toxicity following anti-MAGE-A3 TCR gene therapy. *Journal of immunotherapy (Hagerstown, Md. : 1997)* **36**, 133-151, doi:10.1097/CJI.0b013e3182829903 (2013).

24 Morrison, C. Developers seek to finetune toxicity of T-cell therapies. *Nat Biotechnol* **32**, 1171-1172, doi:10.1038/nbt1214-1171 (2014).

25 Kantoff, P. W. *et al.* Sipuleucel-T immunotherapy for castration-resistant prostate cancer. *The New England journal of medicine* **363**, 411-422, doi:10.1056/NEJMoa1001294 (2010).

26 Korman, A. J., Peggs, K. S. & Allison, J. P. Checkpoint blockade in cancer immunotherapy. *Advances in immunology* **90**, 297-339, doi:10.1016/s0065-2776(06)90008-x (2006).

27 Mahoney, K. M., Rennert, P. D. & Freeman, G. J. Combination cancer immunotherapy and new immunomodulatory targets. *Nat Rev Drug Discov* **14**, 561-584, doi:10.1038/nrd4591 (2015).

28 Pardoll, D. M. The blockade of immune checkpoints in cancer immunotherapy. *Nature reviews. Cancer* **12**, 252-264, doi:10.1038/nrc3239 (2012).

29 Vanneman, M. & Dranoff, G. Combining immunotherapy and targeted therapies in cancer treatment. *Nature reviews. Cancer* **12**, 237-251 (2012).

30 Hodi, F. S. *et al.* Immunologic and clinical effects of antibody blockade of cytotoxic T lymphocyte-associated antigen 4 in previously vaccinated cancer patients. *Proceedings of the National Academy of Sciences of the United States of America* **105**, 3005-3010, doi:10.1073/pnas.0712237105 (2008).

31 Russell, S. J., Peng, K. W. & Bell, J. C. Oncolytic virotherapy. *Nat Biotechnol* **30**, 658-670, doi:10.1038/nbt.2287 (2012).

32 Fielding, A. K. Measles as a potential oncolytic virus. *Reviews in medical virology* **15**, 135-142, doi:10.1002/rmv.455 (2005).

33 G., D. The influence of complicating diseases upon leukemia. **127,**, 563–592 ((1904).).

34 Pelner, L., Fowler, G. A. & Nauts, H. C. Effects of concurrent infections and their toxins on the course of leukemia. *Acta medica Scandinavica. Supplementum* **338**, 1-47 (1958).

35 Bierman, H. R. *et al.* Remissions in leukemia of childhood following acute infectious disease: staphylococcus and streptococcus, varicella, and feline panleukopenia. *Cancer* **6**, 591-605 (1953).

36 Sinkovics, J. & Horvath, J. New developments in the virus therapy of cancer: a historical review. *Intervirology* **36**, 193-214 (1993).

37 Kelly, E. & Russell, S. J. History of oncolytic viruses: genesis to genetic engineering. *Molecular therapy : the journal of the American Society of Gene Therapy* **15**, 651-659, doi:10.1038/sj.mt.6300108 (2007).

38 Southam, C. M. Present status of oncolytic virus studies. *Transactions of the New York Academy of Sciences* **22**, 657-673 (1960).

39 Asada, T. Treatment of human cancer with mumps virus. *Cancer* **34**, 1907-1928, doi:10.1002/1097-0142(197412)34:6<1907::AID-CNCR2820340609>3.0.CO;2-4 (1974).

40 Martuza, R. L., Malick, A., Markert, J. M., Ruffner, K. L. & Coen, D. M. Experimental therapy of human glioma by means of a genetically engineered virus mutant. *Science* **252**, 854-856 (1991).

41 Ganjavi, H., Gee, M., Narendran, A., Freedman, M. H. & Malkin, D. Adenovirus-mediated p53 gene therapy in pediatric soft-tissue sarcoma cell lines: sensitization to cisplatin and doxorubicin. *Cancer Gene Ther* **12**, 397-406, doi:10.1038/sj.cgt.7700798 (2005).

42 Ganly, I. *et al.* A phase I study of Onyx-015, an E1B attenuated adenovirus, administered intratumorally to patients with recurrent head and neck cancer. *Clin Cancer Res* **6**, 798-806 (2000).

43 Ramesh, N. *et al.* CG0070, a conditionally replicating granulocyte macrophage colony-stimulating factor--armed oncolytic adenovirus for

the treatment of bladder cancer. *Clin Cancer Res* **12**, 305-313, doi:10.1158/1078-0432.ccr-05-1059 (2006).

44 Errington, F. *et al.* Inflammatory tumour cell killing by oncolytic reovirus for the treatment of melanoma. *Gene therapy* **15**, 1257-1270, doi:10.1038/gt.2008.58 (2008).

45 Etoh, T. *et al.* Oncolytic viral therapy for human pancreatic cancer cells by reovirus. *Clin Cancer Res* **9**, 1218-1223 (2003).

46 Sei, S. *et al.* Synergistic antitumor activity of oncolytic reovirus and chemotherapeutic agents in non-small cell lung cancer cells. *Molecular cancer* **8**, 47, doi:10.1186/1476-4598-8-47 (2009).

47 Hirasawa, K. *et al.* Oncolytic reovirus against ovarian and colon cancer. *Cancer research* **62**, 1696-1701 (2002).

48 Maitra, R. *et al.* Oncolytic reovirus preferentially induces apoptosis in KRAS mutant colorectal cancer cells, and synergizes with irinotecan. *Oncotarget* **5**, 2807-2819, doi:10.18632/oncotarget.1921 (2014).

49 Twigger, K. *et al.* Reovirus exerts potent oncolytic effects in head and neck cancer cell lines that are independent of signalling in the EGFR pathway. *BMC cancer* **12**, 368, doi:10.1186/1471-2407-12-368 (2012).

50 Myers, R. *et al.* Oncolytic activities of approved mumps and measles vaccines for therapy of ovarian cancer. *Cancer Gene Ther* **12**, 593-599, doi:10.1038/sj.cgt.7700823 (2005).

51 Phuong, L. K. *et al.* Use of a vaccine strain of measles virus genetically engineered to produce carcinoembryonic antigen as a novel therapeutic agent against glioblastoma multiforme. *Cancer research* **63**, 2462-2469 (2003).

52 Peng, K. W. *et al.* Systemic therapy of myeloma xenografts by an attenuated measles virus. *Blood* **98**, 2002-2007 (2001).

53 Fernandez, M., Porosnicu, M., Markovic, D. & Barber, G. N. Genetically engineered vesicular stomatitis virus in gene therapy: application for treatment of malignant disease. *Journal of virology* **76**, 895-904 (2002).

54 Stewart, J. H. t., Ahmed, M., Northrup, S. A., Willingham, M. & Lyles, D. S. Vesicular stomatitis virus as a treatment for colorectal cancer. *Cancer Gene Ther* **18**, 837-849, doi:10.1038/cgt.2011.49 (2011).

55 Ebert, O. *et al.* Syncytia induction enhances the oncolytic potential of vesicular stomatitis virus in virotherapy for cancer. *Cancer research* **64**, 3265-3270 (2004).

56 Schneider, T., Gerhards, R., Kirches, E. & Firsching, R. Preliminary results of active specific immunization with modified tumor cell vaccine in glioblastoma multiforme. *Journal of neuro-oncology* **53**, 39-46 (2001).

57 Phuangsab, A., Lorence, R. M., Reichard, K. W., Peeples, M. E. & Walter, R. J. Newcastle disease virus therapy of human tumor xenografts: antitumor effects of local or systemic administration. *Cancer letters* **172**, 27-36 (2001).

58 MacKie, R. M., Stewart, B. & Brown, S. M. Intralesional injection of herpes simplex virus 1716 in metastatic melanoma. *Lancet* **357**, 525-526, doi:10.1016/s0140-6736(00)04048-4 (2001).

59 Chahlavi, A., Todo, T., Martuza, R. L. & Rabkin, S. D. Replication-competent herpes simplex virus vector G207 and cisplatin combination therapy for head and neck squamous cell carcinoma. *Neoplasia (New York, N.Y.)* **1**, 162-169 (1999).

60 Au, G. G., Lincz, L. F., Enno, A. & Shafren, D. R. Oncolytic Coxsackievirus A21 as a novel therapy for multiple myeloma. *British journal of haematology* **137**, 133-141, doi:10.1111/j.1365-2141.2007.06550.x (2007).

61 Au, G. G., Lindberg, A. M., Barry, R. D. & Shafren, D. R. Oncolysis of vascular malignant human melanoma tumors by Coxsackievirus A21. *International journal of oncology* **26**, 1471-1476 (2005).

62 Gentschev, I. *et al.* Preclinical Evaluation of Oncolytic Vaccinia Virus for Therapy of Canine Soft Tissue Sarcoma. *PloS one* **7**, e37239, doi:10.1371/journal.pone.0037239 (2012).

63 Kelly, K. J. *et al.* Novel oncolytic agent GLV-1h68 is effective against malignant pleural mesothelioma. *Human gene therapy* **19**, 774-782, doi:10.1089/hum.2008.036 (2008).

64 Kelly, K. J. *et al.* Real-time intraoperative detection of melanoma lymph node metastases using recombinant vaccinia virus GLV-1h68 in an immunocompetent animal model. *International journal of cancer. Journal international du cancer* **124**, 911-918, doi:10.1002/ijc.24037 (2009).

65 Chalikonda, S. *et al.* Oncolytic virotherapy for ovarian carcinomatosis using a replication-selective vaccinia virus armed with a yeast cytosine deaminase gene. *Cancer Gene Ther* **15**, 115-125, doi:10.1038/sj.cgt.7701110 (2008).

66 Zhang, Q. *et al.* Eradication of solid human breast tumors in nude mice with an intravenously injected light-emitting oncolytic vaccinia virus. *Cancer research* **67**, 10038-10046, doi:10.1158/0008-5472.can-07-0146 (2007).

67 Toyoda, H., Yin, J., Mueller, S., Wimmer, E. & Cello, J. Oncolytic treatment and cure of neuroblastoma by a novel attenuated poliovirus in a novel poliovirus-susceptible animal model. *Cancer research* **67**, 2857-2864, doi:10.1158/0008-5472.can-06-3713 (2007).

68 Gromeier, M., Lachmann, S., Rosenfeld, M. R., Gutin, P. H. & Wimmer, E. Intergeneric poliovirus recombinants for the treatment of malignant glioma. *Proceedings of the National Academy of Sciences of the United States of America* **97**, 6803-6808 (2000).

69 Workenhe, S. T. & Mossman, K. L. Oncolytic Virotherapy and Immunogenic Cancer Cell Death: Sharpening the Sword for Improved Cancer Treatment Strategies. *Molecular therapy : the journal of the American Society of Gene Therapy* **22**, 251-256, doi:10.1038/mt.2013.220 (2014).

70 Prestwich, R. J. *et al.* The case of oncolytic viruses versus the immune system: waiting on the judgment of Solomon. *Human gene therapy* **20**, 1119-1132, doi:10.1089/hum.2009.135 (2009).

71 Folkman, J. Angiogenesis in cancer, vascular, rheumatoid and other disease. *Nat Med* **1**, 27-31 (1995).

72 Breitbach, C. J. *et al.* Oncolytic vaccinia virus disrupts tumor-associated vasculature in humans. *Cancer research* **73**, 1265-1275, doi:10.1158/0008-5472.can-12-2687 (2013).

73 Kaufman, H. L. *et al.* Local and distant immunity induced by intralesional vaccination with an oncolytic herpes virus encoding GM-CSF in patients with stage IIIc and IV melanoma. *Annals of surgical oncology* **17**, 718-730, doi:10.1245/s10434-009-0809-6 (2010).

74 Greiner, S. *et al.* The highly attenuated vaccinia virus strain modified virus Ankara induces apoptosis in melanoma cells and allows bystander dendritic cells to generate a potent anti-tumoral immunity.

Clinical and experimental immunology **146**, 344-353, doi:10.1111/j.1365-2249.2006.03177.x (2006).

75 Prestwich, R. J. *et al.* Tumor infection by oncolytic reovirus primes adaptive antitumor immunity. *Clin Cancer Res* **14**, 7358-7366, doi:10.1158/1078-0432.ccr-08-0831 (2008).

76 Hanahan, D. & Weinberg, Robert A. Hallmarks of Cancer: The Next Generation. *Cell* **144**, 646-674, doi:10.1016/j.cell.2011.02.013.

77 Chiocca, E. A. Oncolytic viruses. *Nature reviews. Cancer* **2**, 938-950, doi:10.1038/nrc948 (2002).

78 Angarita, F. A., Acuna, S. A., Ottolino-Perry, K., Zerhouni, S. & McCart, J. A. Mounting a strategic offense: fighting tumor vasculature with oncolytic viruses. *Trends in molecular medicine* **19**, 378-392, doi:10.1016/j.molmed.2013.02.008 (2013).

79 Tysome, J. R., Lemoine, N. R. & Wang, Y. Update on oncolytic viral therapy – targeting angiogenesis. *OncoTargets and therapy* **6**, 1031-1040, doi:10.2147/ott.s46974 (2013).

80 Liu, T. C., Galanis, E. & Kirn, D. Clinical trial results with oncolytic virotherapy: a century of promise, a decade of progress. *Nature clinical practice. Oncology* **4**, 101-117, doi:10.1038/ncponc0736 (2007).

81 Nemunaitis, J. *et al.* Selective replication and oncolysis in p53 mutant tumors with ONYX-015, an E1B-55kD gene-deleted adenovirus, in patients with advanced head and neck cancer: a phase II trial. *Cancer research* **60**, 6359-6366 (2000).

82 Rodriguez, R. *et al.* Prostate attenuated replication competent adenovirus (ARCA) CN706: a selective cytotoxic for prostate-specific antigen-positive prostate cancer cells. *Cancer research* **57**, 2559-2563 (1997).

83 Yu, D. C., Chen, Y., Seng, M., Dilley, J. & Henderson, D. R. The addition of adenovirus type 5 region E3 enables calydon virus 787 to eliminate distant prostate tumor xenografts. *Cancer research* **59**, 4200-4203 (1999).

84 Liu, B. L. *et al.* ICP34.5 deleted herpes simplex virus with enhanced oncolytic, immune stimulating, and anti-tumour properties. *Gene therapy* **10**, 292-303, doi:10.1038/sj.gt.3301885 (2003).

85 Mastrangelo, M. J. *et al.* Intratumoral recombinant GM-CSF-encoding virus as gene therapy in patients with cutaneous melanoma. *Cancer Gene Ther* **6**, 409-422, doi:10.1038/sj.cgt.7700066 (1999).

86 Huebner, R. J., Rowe, W. P., Schatten, W. E., Smith, R. R. & Thomas, L. B. Studies on the use of viruses in the treatment of carcinoma of the cervix. *Cancer* **9**, 1211-1218 (1956).

87 Southam, C. M. & Moore, A. E. West Nile, Ilheus, and Bunyamwera virus infections in man. *The American journal of tropical medicine and hygiene* **31**, 724-741 (1951).

88 Southam, C. M. & Moore, A. E. Induced virus infections in man by the Egypt isolates of West Nile virus. *The American journal of tropical medicine and hygiene* **3**, 19-50 (1954).

89 Shimizu, Y., Hasumi, K., Okudaira, Y., Yamanishi, K. & Takahashi, M. Immunotherapy of advanced gynecologic cancer patients utilizing mumps virus. *Cancer detection and prevention* **12**, 487-495 (1988).

90 Okuno, Y. *et al.* Studies on the use of mumps virus for treatment of human cancer. *Biken journal* **21**, 37-49 (1978).

91 Toolan, H. W., Saunders, E. L., Southam, C. M., Moore, A. E. & Levin, A. G. H-1 VIRUS VIREMIA IN THE HUMAN. *Proceedings of the Society for Experimental Biology and Medicine. Society for Experimental Biology and Medicine (New York, N.Y.)* **119**, 711-715 (1965).

92 Hunter-Craig, I., Newton, K. A., Westbury, G. & Lacey, B. W. Use of vaccinia virus in the treatment of metastatic malignant melanoma. *British medical journal* **2**, 512-515 (1970).

93 Roenigk, H. H., Jr, Deodhar, S., Jacques, R. & Burdick, K. IMmunotherapy of malignant melanoma with vaccinia virus. *Archives of Dermatology* **109**, 668-673, doi:10.1001/archderm.1974.01630050014003 (1974).

94 Mastrangelo MJ, e. a. A pilot study demonstrating the feasibility of using intratumoral vaccinia injections as a vector for gene transfer. . *Vaccine Res.* **4**, 55–69 (1995).

95 Wheelock, E. F. & Dingle, J. H. OBSERVATIONS ON THE REPEATED ADMINISTRATION OF VIRUSES TO A PATIENT WITH ACUTE LEUKEMIA. A PRELIMINARY REPORT. *The New England*

journal of medicine **271**, 645-651, doi:10.1056/nejm196409242711302 (1964).

96 Cassel, W. A. & Garrett, R. E. NEWCASTLE DISEASE VIRUS AS AN ANTINEOPLASTIC AGENT. *Cancer* **18**, 863-868 (1965).

97 Csatary, L. K. *et al.* Attenuated veterinary virus vaccine for the treatment of cancer. *Cancer detection and prevention* **17**, 619-627 (1993).

98 Csatary, L. K. & Bakacs, T. Use of Newcastle disease virus vaccine (MTH-68/H) in a patient with high-grade glioblastoma. *JAMA : the journal of the American Medical Association* **281**, 1588-1589 (1999).

99 Csatary, L. K. *et al.* MTH-68/H oncolytic viral treatment in human high-grade gliomas. *Journal of neuro-oncology* **67**, 83-93 (2004).

100 Senzer, N. N. *et al.* Phase II clinical trial of a granulocyte-macrophage colony-stimulating factor-encoding, second-generation oncolytic herpesvirus in patients with unresectable metastatic melanoma. *J Clin Oncol* **27**, 5763-5771, doi:10.1200/jco.2009.24.3675 (2009).

101 Park, B. H. *et al.* Use of a targeted oncolytic poxvirus, JX-594, in patients with refractory primary or metastatic liver cancer: a phase I trial. *Lancet Oncol* **9**, 533-542, doi:10.1016/S1470-2045(08)70107-4 (2008).

102 Khuri, F. R. *et al.* a controlled trial of intratumoral ONYX-015, a selectively-replicating adenovirus, in combination with cisplatin and 5-fluorouracil in patients with recurrent head and neck cancer. *Nat Med* **6**, 879-885, doi:10.1038/78638 (2000).

103 Andtbacka, R. H. *et al.* Talimogene Laherparepvec Improves Durable Response Rate in Patients With Advanced Melanoma. *J Clin Oncol* **33**, 2780-2788, doi:10.1200/jco.2014.58.3377 (2015).

104 Black, A. J. & Morris, D. G. Clinical trials involving the oncolytic virus, reovirus: ready for prime time? *Expert review of clinical pharmacology* **5**, 517-520, doi:10.1586/ecp.12.53 (2012).

105 Freeman, A. I. *et al.* Phase I/II Trial of Intravenous NDV-HUJ Oncolytic Virus in Recurrent Glioblastoma Multiforme. *Molecular therapy : the journal of the American Society of Gene Therapy* **13**, 221-228, doi:http://www.nature.com/mt/journal/v13/n1/suppinfo/mt200627s1.html (2006).

106 Nuesch, J. P., Lacroix, J., Marchini, A. & Rommelaere, J. Molecular pathways: rodent parvoviruses--mechanisms of oncolysis and prospects for clinical cancer treatment. *Clin Cancer Res* **18**, 3516-3523, doi:10.1158/1078-0432.ccr-11-2325 (2012).

107 Fields, B. N., Knipe, D. M. & Howley, P. M. *Fields virology*. 5th edn, (Wolters Kluwer Health/Lippincott Williams & Wilkins, 2007).

108 Cathomen, T. *et al.* A matrix-less measles virus is infectious and elicits extensive cell fusion: consequences for propagation in the brain. *EMBO J* **17**, 3899-3908, doi:10.1093/emboj/17.14.3899 (1998).

109 Sedlmeier, R. & Neubert, W. J. The replicative complex of paramyxoviruses: structure and function. *Adv Virus Res* **50**, 101-139 (1998).

110 Escoffier, C. & Gerlier, D. Infection of chicken embryonic fibroblasts by measles virus: adaptation at the virus entry level. *Journal of virology* **73**, 5220-5224 (1999).

111 Baron, M. D. & Barrett, T. Rinderpest viruses lacking the C and V proteins show specific defects in growth and transcription of viral RNAs. *Journal of virology* **74**, 2603-2611 (2000).

112 Patterson, J. B., Thomas, D., Lewicki, H., Billeter, M. A. & Oldstone, M. B. V and C proteins of measles virus function as virulence factors in vivo. *Virology* **267**, 80-89, doi:10.1006/viro.1999.0118 (2000).

113 Boxer, E. L., Nanda, S. K. & Baron, M. D. The rinderpest virus non-structural C protein blocks the induction of type 1 interferon. *Virology* **385**, 134-142, doi:10.1016/j.virol.2008.11.022 (2009).

114 Sweetman, D. A., Miskin, J. & Baron, M. D. Rinderpest virus C and V proteins interact with the major (L) component of the viral polymerase. *Virology* **281**, 193-204, doi:10.1006/viro.2000.0805 (2001).

115 Griffin, D. E. & Oldstone, M. M. Measles. Pathogenesis and control. Introduction. *Current topics in microbiology and immunology* **330**, 1 (2009).

116 Dhiman, N., Jacobson, R. M. & Poland, G. A. Measles virus receptors: SLAM and CD46. *Reviews in medical virology* **14**, 217-229, doi:10.1002/rmv.430 (2004).

117 Manchester, M. *et al.* Measles virus recognizes its receptor, CD46, via two distinct binding domains within SCR1-2. *Virology* **233**, 174-184, doi:10.1006/viro.1997.8581 (1997).

118 Marie, J. C. *et al.* Linking innate and acquired immunity: divergent role of CD46 cytoplasmic domains in T cell induced inflammation. *Nature immunology* **3**, 659-666, doi:10.1038/ni810 (2002).

119 Naniche, D. *et al.* Human membrane cofactor protein (CD46) acts as a cellular receptor for measles virus. *Journal of virology* **67**, 6025-6032 (1993).

120 Cattaneo, R. Four Viruses, Two Bacteria, and One Receptor: Membrane Cofactor Protein (CD46) as Pathogens' Magnet. *Journal of virology* **78**, 4385-4388, doi:10.1128/jvi.78.9.4385-4388.2004 (2004).

121 Kemper, C. *et al.* Activation of human CD4+ cells with CD3 and CD46 induces a T-regulatory cell 1 phenotype. *Nature* **421**, 388-392, doi:10.1038/nature01315 (2003).

122 Schnorr, J. J. *et al.* Induction of maturation of human blood dendritic cell precursors by measles virus is associated with immunosuppression. *Proceedings of the National Academy of Sciences of the United States of America* **94**, 5326-5331 (1997).

123 Tatsuo, H., Ono, N., Tanaka, K. & Yanagi, Y. SLAM (CDw150) is a cellular receptor for measles virus. *Nature* **406**, 893-897, doi:10.1038/35022579 (2000).

124 Tatsuo, H. *et al.* Virus entry is a major determinant of cell tropism of Edmonston and wild-type strains of measles virus as revealed by vesicular stomatitis virus pseudotypes bearing their envelope proteins. *Journal of virology* **74**, 4139-4145 (2000).

125 Ono, N., Tatsuo, H., Tanaka, K., Minagawa, H. & Yanagi, Y. V domain of human SLAM (CDw150) is essential for its function as a measles virus receptor. *Journal of virology* **75**, 1594-1600, doi:10.1128/JVI.75.4.1594-1600.2001 (2001).

126 Navaratnarajah, C. K. *et al.* The heads of the measles virus attachment protein move to transmit the fusion-triggering signal. *Nature structural & molecular biology* **18**, 128-134, doi:10.1038/nsmb.1967 (2011).

127 Niwa, H., Yamamura, K. & Miyazaki, J. Efficient selection for high-expression transfectants with a novel eukaryotic vector. *Gene* **108**, 193-199 (1991).

128 Cocks, B. G. *et al.* A novel receptor involved in T-cell activation. *Nature* **376**, 260-263, doi:10.1038/376260a0 (1995).

129 Sidorenko, S. P. & Clark, E. A. Characterization of a cell surface glycoprotein IPO-3, expressed on activated human B and T lymphocytes. *J Immunol* **151**, 4614-4624 (1993).

130 Kruse, M. *et al.* Signaling lymphocytic activation molecule is expressed on mature CD83+ dendritic cells and is up-regulated by IL-1 beta. *J Immunol* **167**, 1989-1995 (2001).

131 Ohgimoto, S. *et al.* The haemagglutinin protein is an important determinant of measles virus tropism for dendritic cells in vitro. *The Journal of general virology* **82**, 1835-1844 (2001).

132 Minagawa, H., Tanaka, K., Ono, N., Tatsuo, H. & Yanagi, Y. Induction of the measles virus receptor SLAM (CD150) on monocytes. *The Journal of general virology* **82**, 2913-2917 (2001).

133 Tanaka, K., Minagawa, H., Xie, M. F. & Yanagi, Y. The measles virus hemagglutinin downregulates the cellular receptor SLAM (CD150). *Archives of virology* **147**, 195-203 (2002).

134 Noyce, R. S. *et al.* Tumor cell marker PVRL4 (nectin 4) is an epithelial cell receptor for measles virus. *PLoS pathogens* **7**, e1002240, doi:10.1371/journal.ppat.1002240 (2011).

135 Muhlebach, M. D. *et al.* Adherens junction protein nectin-4 is the epithelial receptor for measles virus. *Nature* **480**, 530-533, doi:10.1038/nature10639 (2011).

136 Hashimoto, K. *et al.* SLAM (CD150)-independent measles virus entry as revealed by recombinant virus expressing green fluorescent protein. *Journal of virology* **76**, 6743-6749 (2002).

137 Takeuchi, K., Miyajima, N., Nagata, N., Takeda, M. & Tashiro, M. Wild-type measles virus induces large syncytium formation in primary human small airway epithelial cells by a SLAM(CD150)-independent mechanism. *Virus research* **94**, 11-16 (2003).

138 Sakaguchi, M. *et al.* Growth of Measles Virus in Epithelial and Lymphoid Tissues of Cynomolgus Monkeys. *Microbiology and Immunology* **30**, 1067-1073, doi:10.1111/j.1348-0421.1986.tb03036.x (1986).

139 McChesney, M. B. *et al.* Experimental measles. I. Pathogenesis in the normal and the immunized host. *Virology* **233**, 74-84, doi:10.1006/viro.1997.8576 (1997).

140 Noyce, R. S. & Richardson, C. D. Nectin 4 is the epithelial cell receptor for measles virus. *Trends in Microbiology* **20**, 429-439, doi:10.1016/j.tim.2012.05.006 (2012).

141 Enders, G. in *Medical Microbiology* (ed S. Baron) (1996).

142 Enders, J. F. & Peebles, T. C. Propagation in tissue cultures of cytopathogenic agents from patients with measles. *Proceedings of the Society for Experimental Biology and Medicine. Society for Experimental Biology and Medicine (New York, N.Y.)* **86**, 277-286 (1954).

143 Vaccination Against Measles. *British medical journal* **2**, 1274-1275 (1961).

144 Katz, S. L., Morley, D. C. & Krugman, S. ATtenuated measles vaccine in nigerian children. *American Journal of Diseases of Children* **103**, 402-405, doi:10.1001/archpedi.1962.02080020414047 (1962).

145 Moss, W. J. & Strebel, P. Biological feasibility of measles eradication. *The Journal of infectious diseases* **204 Suppl 1**, S47-53, doi:10.1093/infdis/jir065 (2011).

146 Bankamp, B., Takeda, M., Zhang, Y., Xu, W. & Rota, P. A. Genetic characterization of measles vaccine strains. *The Journal of infectious diseases* **204 Suppl 1**, S533-548, doi:10.1093/infdis/jir097 (2011).

147 Hilleman, M. R. *et al.* Development and evaluation of the Moraten measles virus vaccine. *JAMA : the journal of the American Medical Association* **206**, 587-590 (1968).

148 Atkinson, W. *et al. Epidemiology and prevention of vaccine-preventable diseases*. (Public Health Foundation, 2011).

149 Makino, S. Development and characteristics of live AIK-C measles virus vaccine: a brief report. *Reviews of infectious diseases* **5**, 504-505 (1983).

150 Jayaraman, K. S. Biotech boom. *Nature* **436**, 480-483, doi:10.1038/436480a (2005).

151 Strebel, P. M., Papania, M. J., Halsey, N., Plotkin, S. & Orenstein, W. Measles vaccine. *Vaccines* **6**, 352-387 (2004).

152 Moss, W. J. & Griffin, D. E. Measles. *Lancet* **379**, 153-164, doi:10.1016/s0140-6736(10)62352-5 (2012).

153 Moss, W. J. & Griffin, D. E. Global measles elimination. *Nature reviews. Microbiology* **4**, 900-908, doi:10.1038/nrmicro1550 (2006).

154 Zhang, Y. *et al.* New Measles Virus Genotype Associated with Outbreak, China. *Emerging infectious diseases* **16**, 943-947, doi:10.3201/eid1606.100089 (2010).

155 Riddell, M. A., Rota, J. S. & Rota, P. A. Review of the temporal and geographical distribution of measles virus genotypes in the prevaccine and postvaccine eras. *Virology journal* **2**, 87, doi:10.1186/1743-422x-2-87 (2005).

156 Finsterbusch, T. *et al.* Measles viruses of genotype H1 evade recognition by vaccine-induced neutralizing antibodies targeting the linear haemagglutinin noose epitope. *The Journal of general virology* **90**, 2739-2745, doi:10.1099/vir.0.013524-0 (2009).

157 Klingele, M. *et al.* Resistance of recent measles virus wild-type isolates to antibody-mediated neutralization by vaccinees with antibody. *Journal of medical virology* **62**, 91-98 (2000).

158 Agocs, M. M., Markowitz, L. E., Straub, I. & Domok, I. The 1988-1989 measles epidemic in Hungary: assessment of vaccine failure. *International journal of epidemiology* **21**, 1007-1013 (1992).

159 Cutts, F. T. & Markowitz, L. E. Successes and failures in measles control. *The Journal of infectious diseases* **170 Suppl 1**, S32-41 (1994).

160 Hayden, G. F. Clinical Review : Measles Vaccine Failure: A Survey of Causes and Means of Prevention. *Clinical Pediatrics* **18**, 155-156, doi:10.1177/000992287901800308 (1979).

161 Rota, J. S. *et al.* Genetic analysis of measles viruses isolated in the United States, 1995-1996. *The Journal of infectious diseases* **177**, 204-208 (1998).

162 Jones-Engel, L. & Engel, G. A. Disease risk analysis: A paradigm for using health-based data to inform primate conservation and public health. *American journal of primatology* **68**, 851-854, doi:10.1002/ajp.20292 (2006).

163 Nakamura, T. & Russell, S. J. Oncolytic measles viruses for cancer therapy. *Expert opinion on biological therapy* **4**, 1685-1692, doi:10.1517/14712598.4.10.1685 (2004).

164 Kaplan, L. J., Daum, R. S., Smaron, M. & McCarthy, C. A. Severe measles in immunocompromised patients. *JAMA : the journal of the American Medical Association* **267**, 1237-1241 (1992).

165 Moss, W. J., Cutts, F. & Griffin, D. E. Implications of the human immunodeficiency virus epidemic for control and eradication of measles. *Clinical infectious diseases : an official publication of the Infectious Diseases Society of America* **29**, 106-112, doi:10.1086/520136 (1999).

166 Permar, S. R., Griffin, D. E. & Letvin, N. L. Immune containment and consequences of measles virus infection in healthy and immunocompromised individuals. *Clinical and vaccine immunology : CVI* **13**, 437-443, doi:10.1128/CVI.13.4.437-443.2006 (2006).

167 Jurgens, E. M. *et al.* Measles Fusion Machinery Is Dysregulated in Neuropathogenic Variants. *mBio* **6**, doi:10.1128/mBio.02528-14 (2015).

168 Bellini, W. J. *et al.* Subacute sclerosing panencephalitis: more cases of this fatal disease are prevented by measles immunization than was previously recognized. *The Journal of infectious diseases* **192**, 1686-1693, doi:10.1086/497169 (2005).

169 Schneider-Schaulies, J., Meulen, V. & Schneider-Schaulies, S. Measles infection of the central nervous system. *Journal of neurovirology* **9**, 247-252, doi:10.1080/13550280390193993 (2003).

170 Rima, B. K. & Duprex, W. P. Molecular mechanisms of measles virus persistence. *Virus research* **111**, 132-147, doi:10.1016/j.virusres.2005.04.005 (2005).

171 Rota, J. S., Wang, Z. D., Rota, P. A. & Bellini, W. J. Comparison of sequences of the H, F, and N coding genes of measles virus vaccine strains. *Virus research* **31**, 317-330 (1994).

172 Griffin, D. E., Pan, C. H. & Moss, W. J. Measles vaccines. *Frontiers in bioscience : a journal and virtual library* **13**, 1352-1370 (2008).

173 Heinzerling, L. *et al.* Oncolytic measles virus in cutaneous T-cell lymphomas mounts antitumor immune responses in vivo and targets interferon-resistant tumor cells. *Blood* **106**, 2287-2294, doi:10.1182/blood-2004-11-4558 (2005).

174 Russell, S. J. & Peng, K. W. Measles virus for cancer therapy. *Current topics in microbiology and immunology* **330**, 213-241 (2009).

175 Grote, D. *et al.* Live attenuated measles virus induces regression of human lymphoma xenografts in immunodeficient mice. *Blood* **97**, 3746-3754 (2001).

176 Peng, K. W. *et al.* Intraperitoneal therapy of ovarian cancer using an engineered measles virus. *Cancer research* **62**, 4656-4662 (2002).

177 Blechacz, B. *et al.* Engineered measles virus as a novel oncolytic viral therapy system for hepatocellular carcinoma. *Hepatology (Baltimore, Md.)* **44**, 1465-1477, doi:10.1002/hep.21437 (2006).

178 McDonald, C. J. *et al.* A measles virus vaccine strain derivative as a novel oncolytic agent against breast cancer. *Breast cancer research and treatment* **99**, 177-184, doi:10.1007/s10549-006-9200-5 (2006).

179 Hoffmann, D., Bangen, J. M., Bayer, W. & Wildner, O. Synergy between expression of fusogenic membrane proteins, chemotherapy and facultative virotherapy in colorectal cancer. *Gene therapy* **13**, 1534-1544, doi:10.1038/sj.gt.3302806 (2006).

180 Singh, M., Cattaneo, R. & Billeter, M. A. A Recombinant Measles Virus Expressing Hepatitis B Virus Surface Antigen Induces Humoral Immune Responses in Genetically Modified Mice. *Journal of virology* **73**, 4823-4828 (1999).

181 Frank Radecke, P. S., Henriette Schneider, Karin Kaelin, Marion Huber, Christina Dotsch, Gudrun Christiansen and Martin A.Billeter'. Rescue of measles viruses from cloned DNA. *The EMBO Journal* **14**, 5773-5784 (1995).

182 Graham, F. L., Smiley, J., Russell, W. C. & Nairn, R. Characteristics of a human cell line transformed by DNA from human adenovirus type 5. *The Journal of general virology* **36**, 59-74, doi:10.1099/0022-1317-36-1-59 (1977).

183 Auwaerter, P. G. *et al.* Measles virus infection in rhesus macaques: altered immune responses and comparison of the virulence of six different virus strains. *The Journal of infectious diseases* **180**, 950-958, doi:10.1086/314993 (1999).

184 El Mubarak, H. S. *et al.* Infection of cynomolgus macaques (Macaca fascicularis) and rhesus macaques (Macaca mulatta) with different wild-type measles viruses. *The Journal of general virology* **88**, 2028-2034, doi:10.1099/vir.0.82804-0 (2007).

185 Van Binnendijk, R. S., Van der Heijden, R. W., Van Amerongen, G., UytdeHaag, F. G. & Osterhaus, A. D. Viral replication and development of specific immunity in macaques after infection with different measles virus strains. *The Journal of infectious diseases* **170**, 443-448 (1994).

186 Zhu, Y. D. *et al.* Experimental measles. II. Infection and immunity in the rhesus macaque. *Virology* **233**, 85-92, doi:10.1006/viro.1997.8575 (1997).

187 Kato, S., Nagata, K. & Takeuchi, K. Cell Tropism and Pathogenesis of Measles Virus in Monkeys. *Frontiers in Microbiology* **3**, doi:10.3389/fmicb.2012.00014 (2012).

188 Kobune, F. *et al.* Nonhuman primate models of measles. *Laboratory animal science* **46**, 315-320 (1996).

189 Russell, S. J. & Peng, K. W. Viruses as anticancer drugs. *Trends in pharmacological sciences* **28**, 326-333, doi:10.1016/j.tips.2007.05.005 (2007).

190 Levy, B. M. & Mirkovic, R. R. An epizootic of measles in a marmoset colony. *Laboratory animal science* **21**, 33-39 (1971).

191 Albrecht, P., Lorenz, D., Klutch, M. J., Vickers, J. H. & Ennis, F. A. Fatal measles infection in marmosets pathogenesis and prophylaxis. *Infection and immunity* **27**, 969-978 (1980).

192 Hsu, E. C. *et al.* Artificial mutations and natural variations in the CD46 molecules from human and monkey cells define regions important for measles virus binding. *Journal of virology* **71**, 6144-6154 (1997).

193 Manchester, M. & Rall, G. F. Model Systems: transgenic mouse models for measles pathogenesis. *Trends Microbiol* **9**, 19-23 (2001).

194 Mrkic, B. *et al.* Measles virus spread and pathogenesis in genetically modified mice. *Journal of virology* **72**, 7420-7427 (1998).

195 Mrkic, B. *et al.* Lymphatic dissemination and comparative pathology of recombinant measles viruses in genetically modified mice. *Journal of virology* **74**, 1364-1372 (2000).

196 Roscic-Mrkic, B. *et al.* Roles of macrophages in measles virus infection of genetically modified mice. *Journal of virology* **75**, 3343-3351, doi:10.1128/jvi.75.7.3343-3351.2001 (2001).

197 Hahm, B. *et al.* Measles Virus Infects and Suppresses Proliferation of T Lymphocytes from Transgenic Mice Bearing Human Signaling Lymphocytic Activation Molecule. *Journal of virology* **77**, 3505-3515, doi:10.1128/jvi.77.6.3505-3515.2003 (2003).

198 Welstead, G. G. *et al.* Measles virus replication in lymphatic cells and organs of CD150 (SLAM) transgenic mice. *Proceedings of the National Academy of Sciences of the United States of America* **102**, 16415-16420, doi:10.1073/pnas.0505945102 (2005).

199 Ohno, S. *et al.* Measles virus infection of SLAM (CD150) knockin mice reproduces tropism and immunosuppression in human infection. *Journal of virology* **81**, 1650-1659, doi:10.1128/jvi.02134-06 (2007).

200 Sellin, C. I. *et al.* High pathogenicity of wild-type measles virus infection in CD150 (SLAM) transgenic mice. *Journal of virology* **80**, 6420-6429, doi:10.1128/JVI.00209-06 (2006).

201 Druelle, J., Sellin, C. I., Waku-Kouomou, D., Horvat, B. & Wild, F. T. Wild type measles virus attenuation independent of type I IFN. *Virology journal* **5**, 22, doi:10.1186/1743-422X-5-22 (2008).

202 Shingai, M. *et al.* Wild-type measles virus infection in human CD46/CD150-transgenic mice: CD11c-positive dendritic cells establish systemic viral infection. *J Immunol* **175**, 3252-3261 (2005).

203 Wyde, P. R., Stittelaar, K. J., Osterhaus, A. D., Guzman, E. & Gilbert, B. E. Use of cotton rats for preclinical evaluation of measles vaccines. *Vaccine* **19**, 42-53 (2000).

204 Wyde, P. R., Moore-Poveda, D. K., Daley, N. J. & Oshitani, H. Replication of clinical measles virus strains in hispid cotton rats. *Proceedings of the Society for Experimental Biology and Medicine. Society for Experimental Biology and Medicine (New York, N.Y.)* **221**, 53-62 (1999).

205 Thormar, H., Mehta, P. D., Barshatzky, M. R. & Brown, H. R. Measles virus encephalitis in ferrets as a model for subacute sclerosing panencephalitis. *Laboratory animal science* **35**, 229-232 (1985).

206 Von Messling, V., Springfeld, C., Devaux, P. & Cattaneo, R. A Ferret Model of Canine Distemper Virus Virulence and Immunosuppression. *Journal of virology* **77**, 12579-12591, doi:10.1128/jvi.77.23.12579-12591.2003 (2003).

207 Singh, S. K. *Human Respiratory Viral Infections*. (Taylor & Francis, 2014).

208 De Swart, R. L. Measles studies in the macaque model. *Current topics in microbiology and immunology* **330**, 55-72 (2009).

209 Ferreira, C. S. *et al.* Measles virus infection of alveolar macrophages and dendritic cells precedes spread to lymphatic organs in transgenic mice expressing human signaling lymphocytic activation molecule (SLAM, CD150). *Journal of virology* **84**, 3033-3042, doi:10.1128/JVI.01559-09 (2010).

210 Kirby, A. C., Coles, M. C. & Kaye, P. M. Alveolar macrophages transport pathogens to lung draining lymph nodes. *J Immunol* **183**, 1983-1989, doi:10.4049/jimmunol.0901089 (2009).

211 Moench, T. R., Griffin, D. E., Obriecht, C. R., Vaisberg, A. J. & Johnson, R. T. Acute measles in patients with and without neurological involvement: distribution of measles virus antigen and RNA. *The Journal of infectious diseases* **158**, 433-442 (1988).

212 Esolen, L. M., Park, S. W., Hardwick, J. M. & Griffin, D. E. Apoptosis as a cause of death in measles virus-infected cells. *Journal of virology* **69**, 3955-3958 (1995).

213 Ebihara, T. *et al.* Induction of NKG2D ligands on human dendritic cells by TLR ligand stimulation and RNA virus infection. *International immunology* **19**, 1145-1155, doi:10.1093/intimm/dxm073 (2007).

214 Takeda, K. & Akira, S. TLR signaling pathways. *Seminars in immunology* **16**, 3-9 (2004).

215 Thompson, A. J. & Locarnini, S. A. Toll-like receptors, RIG-I-like RNA helicases and the antiviral innate immune response. *Immunology and cell biology* **85**, 435-445, doi:10.1038/sj.icb.7100100 (2007).

216 Jensen, S. & Thomsen, A. R. Sensing of RNA viruses: a review of innate immune receptors involved in recognizing RNA virus invasion. *Journal of virology* **86**, 2900-2910, doi:10.1128/JVI.05738-11 (2012).

217 Takeuchi, O. & Akira, S. Recognition of viruses by innate immunity. *Immunological reviews* **220**, 214-224, doi:10.1111/j.1600-065X.2007.00562.x (2007).

218 Aaronson, D. S. & Horvath, C. M. A road map for those who don't know JAK-STAT. *Science* **296**, 1653-1655, doi:10.1126/science.1071545 (2002).

219 Darnell, J. E., Jr., Kerr, I. M. & Stark, G. R. Jak-STAT pathways and transcriptional activation in response to IFNs and other extracellular signaling proteins. *Science* **264**, 1415-1421 (1994).

220 Grandvaux, N. *et al.* Transcriptional profiling of interferon regulatory factor 3 target genes: direct involvement in the regulation of interferon-stimulated genes. *Journal of virology* **76**, 5532-5539 (2002).

221 Bieback, K. *et al.* Hemagglutinin Protein of Wild-Type Measles Virus Activates Toll-Like Receptor 2 Signaling. *Journal of virology* **76**, 8729-8736, doi:10.1128/jvi.76.17.8729-8736.2002 (2002).

222 Diebold, S. S., Kaisho, T., Hemmi, H., Akira, S. & Reis e Sousa, C. Innate antiviral responses by means of TLR7-mediated recognition of single-stranded RNA. *Science* **303**, 1529-1531, doi:10.1126/science.1093616 (2004).

223 Heil, F. *et al.* Species-specific recognition of single-stranded RNA via toll-like receptor 7 and 8. *Science* **303**, 1526-1529, doi:10.1126/science.1093620 (2004).

224 Hornung, V. *et al.* Replication-dependent potent IFN-alpha induction in human plasmacytoid dendritic cells by a single-stranded RNA virus. *J Immunol* **173**, 5935-5943 (2004).

225 Schlender, J. *et al.* Inhibition of toll-like receptor 7- and 9-mediated alpha/beta interferon production in human plasmacytoid dendritic cells by respiratory syncytial virus and measles virus. *Journal of virology* **79**, 5507-5515, doi:10.1128/JVI.79.9.5507-5515.2005 (2005).

226 Ramos, H. J. & Gale, M. RIG-I Like Receptors and Their Signaling Crosstalk in the Regulation of Antiviral Immunity. *Current opinion in virology* **1**, 167-176, doi:10.1016/j.coviro.2011.04.004 (2011).

227 Ikegame, S. *et al.* Both RIG-I and MDA5 RNA helicases contribute to the induction of alpha/beta interferon in measles virus-infected human cells. *Journal of virology* **84**, 372-379, doi:10.1128/jvi.01690-09 (2010).

228 Runge, S. *et al.* In vivo ligands of MDA5 and RIG-I in measles virus-infected cells. *PLoS pathogens* **10**, e1004081, doi:10.1371/journal.ppat.1004081 (2014).

229 Naniche, D. & Oldstone, M. B. Generalized immunosuppression: how viruses undermine the immune response. *Cellular and molecular life sciences : CMLS* **57**, 1399-1407 (2000).

230 Nakatsu, Y., Takeda, M., Ohno, S., Koga, R. & Yanagi, Y. Translational inhibition and increased interferon induction in cells infected with C protein-deficient measles virus. *Journal of virology* **80**, 11861-11867, doi:10.1128/jvi.00751-06 (2006).

231 Caignard, G. *et al.* Measles virus V protein blocks Jak1-mediated phosphorylation of STAT1 to escape IFN-alpha/beta signaling. *Virology* **368**, 351-362, doi:10.1016/j.virol.2007.06.037 (2007).

232 Devaux, P., von Messling, V., Songsungthong, W., Springfeld, C. & Cattaneo, R. Tyrosine 110 in the measles virus phosphoprotein is required to block STAT1 phosphorylation. *Virology* **360**, 72-83, doi:10.1016/j.virol.2006.09.049 (2007).

233 Palosaari, H., Parisien, J. P., Rodriguez, J. J., Ulane, C. M. & Horvath, C. M. STAT protein interference and suppression of cytokine signal transduction by measles virus V protein. *Journal of virology* **77**, 7635-7644 (2003).

234 McAllister, C. S. *et al.* Mechanisms of protein kinase PKR-mediated amplification of beta interferon induction by C protein-deficient measles virus. *Journal of virology* **84**, 380-386, doi:10.1128/jvi.02630-08 (2010).

235 Devaux, P., Hodge, G., McChesney, M. B. & Cattaneo, R. Attenuation of V- or C-defective measles viruses: infection control by the inflammatory and interferon responses of rhesus monkeys. *Journal of virology* **82**, 5359-5367, doi:10.1128/JVI.00169-08 (2008).

236 Permar, S. R. *et al.* Increased thymic output during acute measles virus infection. *Journal of virology* **77**, 7872-7879 (2003).

237 Griffin, D. E. Measles virus-induced suppression of immune responses. *Immunological reviews* **236**, 176-189, doi:10.1111/j.1600-065X.2010.00925.x (2010).

238 Stokes, J., Jr., Reilly, C. M., Buynak, E. B. & Hilleman, M. R. Immunologic studies of measles. *American journal of hygiene* **74**, 293-303 (1961).

239 Norrby, E., Orvell, C., Vandvik, B. & Cherry, J. D. Antibodies against measles virus polypeptides in different disease conditions. *Infection and immunity* **34**, 718-724 (1981).

240 Black, F. L. Measles active and passive immunity in a worldwide perspective. *Progress in medical virology. Fortschritte der medizinischen Virusforschung. Progres en virologie medicale* **36**, 1-33 (1989).

241 Malvoisin, E. & Wild, F. Contribution of measles virus fusion protein in protective immunity: anti-F monoclonal antibodies neutralize virus infectivity and protect mice against challenge. *Journal of virology* **64**, 5160-5162 (1990).

242 Chen, R. T. *et al.* Measles antibody: reevaluation of protective titers. *The Journal of infectious diseases* **162**, 1036-1042 (1990).

243 Organization, W. H. Immunological basis for immunization. . *Module 7: measles [WHO/EPI/GEN/98.17]. Vol. 2003. Geneva: World Health Organization; 1993.*

244 Forthal, D. N. *et al.* Measles virus-specific functional antibody responses and viremia during acute measles. *The Journal of infectious diseases* **169**, 1377-1380 (1994).

245 Fujinami, R. S. & Oldstone, M. B. Antiviral antibody reacting on the plasma membrane alters measles virus expression inside the cell. *Nature* **279**, 529-530 (1979).

246 Fujinami, R. S. & Oldstone, M. B. Alterations in expression of measles virus polypeptides by antibody: molecular events in antibody-induced antigenic modulation. *J Immunol* **125**, 78-85 (1980).

247 Beckford, A. P., Kaschula, R. O. & Stephen, C. Factors associated with fatal cases of measles. A retrospective autopsy study. *South African medical journal = Suid-Afrikaanse tydskrif vir geneeskunde* **68**, 858-863 (1985).

248 Ryon, J. J., Moss, W. J., Monze, M. & Griffin, D. E. Functional and phenotypic changes in circulating lymphocytes from hospitalized zambian children with measles. *Clinical and diagnostic laboratory immunology* **9**, 994-1003 (2002).

249 Sidorenko, S. P. & Clark, E. A. The dual-function CD150 receptor subfamily: the viral attraction. *Nature immunology* **4**, 19-24, doi:10.1038/ni0103-19 (2003).

250 Engel, P., Eck, M. J. & Terhorst, C. The SAP and SLAM families in immune responses and X-linked lymphoproliferative disease. *Nature reviews. Immunology* **3**, 813-821, doi:10.1038/nri1202 (2003).

251 Fugier-Vivier, I. *et al.* Measles virus suppresses cell-mediated immunity by interfering with the survival and functions of dendritic and T cells. *The Journal of experimental medicine* **186**, 813-823 (1997).

252 Laine, D. *et al.* Measles virus nucleoprotein induces cell-proliferation arrest and apoptosis through NTAIL-NR and NCORE-FcgammaRIIB1 interactions, respectively. *The Journal of general virology* **86**, 1771-1784, doi:10.1099/vir.0.80791-0 (2005).

253 McChesney, M. B., Kehrl, J. H., Valsamakis, A., Fauci, A. S. & Oldstone, M. B. Measles virus infection of B lymphocytes permits cellular activation but blocks progression through the cell cycle. *Journal of virology* **61**, 3441-3447 (1987).

254 Naniche, D., Reed, S. I. & Oldstone, M. B. Cell cycle arrest during measles virus infection: a G0-like block leads to suppression of retinoblastoma protein expression. *Journal of virology* **73**, 1894-1901 (1999).

255 Bluming, A. Z. & Ziegler, J. L. Regression of Burkitt's lymphoma in association with measles infection. *Lancet* **2**, 105-106 (1971).

256 Dingli, D. *et al.* Image-guided radiovirotherapy for multiple myeloma using a recombinant measles virus expressing the thyroidal sodium iodide symporter. *Blood* **103**, 1641-1646, doi:10.1182/blood-2003-07-2233 (2004).

257 Studebaker, A. W. *et al.* Oncolytic measles virus prolongs survival in a murine model of cerebral spinal fluid-disseminated medulloblastoma. *Neuro-oncology* **14**, 459-470, doi:10.1093/neuonc/nor231 (2012).

258 Li, H., Peng, K. W., Dingli, D., Kratzke, R. A. & Russell, S. J. Oncolytic measles viruses encoding interferon beta and the thyroidal sodium iodide symporter gene for mesothelioma virotherapy. *Cancer Gene Ther* **17**, 550-558, doi:10.1038/cgt.2010.10 (2010).

259 Iankov, I. D. *et al.* Demonstration of anti-tumor activity of oncolytic measles virus strains in a malignant pleural effusion breast cancer model. *Breast cancer research and treatment* **122**, 745-754, doi:10.1007/s10549-009-0602-z (2010).

260 Msaouel, P. *et al.* Engineered measles virus as a novel oncolytic therapy against prostate cancer. *The Prostate* **69**, 82-91, doi:10.1002/pros.20857 (2009).

261 Allen, C. *et al.* Interleukin-13 Displaying Retargeted Oncolytic Measles Virus Strains Have Significant Activity Against Gliomas With Improved Specificity. *Molecular therapy : the journal of the American Society of Gene Therapy* **16**, 1556-1564 (2008).

262 Galanis E, H. L., Cliby W, Peethambaram PP, Long HJ, Kaur JS, Haluska P, Jr, Sloan JA, Peng K, Russell SJ. Phase I trial of intraperitoneal (IP) administration of a measles virus (MV) derivative expressing the human carcinoembryonic antigen (CEA) in recurrent ovarian cancer (OvCa). *J Clin Oncol.* **26(15S) Abs 5538** (2008).

263 Ungerechts, G. *et al.* An immunocompetent murine model for oncolysis with an armed and targeted measles virus. *Molecular therapy : the journal of the American Society of Gene Therapy* **15**, 1991-1997, doi:10.1038/sj.mt.6300291 (2007b).

264 Horvat, B. *et al.* Transgenic mice expressing human measles virus (MV) receptor CD46 provide cells exhibiting different permissivities to MV infections. *Journal of virology* **70**, 6673-6681 (1996).

265 Rall, G. F. *et al.* A transgenic mouse model for measles virus infection of the brain. *Proceedings of the National Academy of Sciences of the United States of America* **94**, 4659-4663 (1997).

266 Oldstone, M. B. *et al.* Measles virus infection in a transgenic model: virus-induced immunosuppression and central nervous system disease. *Cell* **98**, 629-640 (1999).

267 Myers, R. M. *et al.* Preclinical pharmacology and toxicology of intravenous MV-NIS, an oncolytic measles virus administered with or without cyclophosphamide. *Clinical pharmacology and therapeutics* **82**, 700-710, doi:10.1038/sj.clpt.6100409 (2007).

268 Schneider, U., Bullough, F., Vongpunsawad, S., Russell, S. J. & Cattaneo, R. Recombinant measles viruses efficiently entering cells through targeted receptors. *Journal of virology* **74**, 9928-9936 (2000).

269 Bucheit, A. D. *et al.* An oncolytic measles virus engineered to enter cells through the CD20 antigen. *Molecular therapy : the journal of the American Society of Gene Therapy* **7**, 62-72 (2003).

270 Hammond, A. L. *et al.* Single-chain antibody displayed on a recombinant measles virus confers entry through the tumor-associated carcinoembryonic antigen. *Journal of virology* **75**, 2087-2096, doi:10.1128/JVI.75.5.2087-2096.2001 (2001).

271 Peng, K. W. *et al.* Oncolytic measles viruses displaying a single-chain antibody against CD38, a myeloma cell marker. *Blood* **101**, 2557-2562, doi:10.1182/blood-2002-07-2195 (2003).

272 Vongpunsawad, S., Oezgun, N., Braun, W. & Cattaneo, R. Selectively receptor-blind measles viruses: Identification of residues necessary for SLAM- or CD46-induced fusion and their localization on a new hemagglutinin structural model. *Journal of virology* **78**, 302-313 (2004).

273 Nakamura, T. *et al.* Rescue and propagation of fully retargeted oncolytic measles viruses. *Nat Biotechnol* **23**, 209-214, doi:10.1038/nbt1060 (2005).

274 Paraskevakou, G. *et al.* Epidermal growth factor receptor (EGFR)-retargeted measles virus strains effectively target EGFR- or EGFRvIII expressing gliomas. *Molecular therapy : the journal of the American Society of Gene Therapy* **15**, 677-686, doi:10.1038/sj.mt.6300105 (2007).

275 Muhlebach, M. D. *et al.* Liver cancer protease activity profiles support therapeutic options with matrix metalloproteinase-activatable oncolytic measles virus. *Cancer research* **70**, 7620-7629, doi:10.1158/0008-5472.can-09-4650 (2010).

276 Springfeld, C. *et al.* Oncolytic efficacy and enhanced safety of measles virus activated by tumor-secreted matrix metalloproteinases. *Cancer research* **66**, 7694-7700, doi:10.1158/0008-5472.can-06-0538 (2006).

277 Galanis, E. *et al.* Phase I trial of intraperitoneal administration of an oncolytic measles virus strain engineered to express carcinoembryonic antigen for recurrent ovarian cancer. *Cancer research* **70**, 875-882, doi:10.1158/0008-5472.CAN-09-2762 (2010).

278 Mandell, R. B., Mandell, L. Z. & Link, C. J., Jr. Radioisotope concentrator gene therapy using the sodium/iodide symporter gene. *Cancer research* **59**, 661-668 (1999).

279 Hutzen, B. *et al.* Treatment of medulloblastoma using an oncolytic measles virus encoding the thyroidal sodium iodide symporter shows enhanced efficacy with radioiodine. *BMC cancer* **12**, 508, doi:10.1186/1471-2407-12-508 (2012).

280 Grote, D., Cattaneo, R. & Fielding, A. K. Neutrophils contribute to the measles virus-induced antitumor effect: enhancement by granulocyte macrophage colony-stimulating factor expression. *Cancer research* **63**, 6463-6468 (2003).

281 Iankov, I. D. *et al.* Expression of immunomodulatory neutrophil-activating protein of Helicobacter pylori enhances the antitumor activity of oncolytic measles virus. *Molecular therapy : the journal of the American Society of Gene Therapy* **20**, 1139-1147, doi:10.1038/mt.2012.4 (2012).

282 Ungerechts, G. *et al.* Lymphoma chemovirotherapy: CD20-targeted and convertase-armed measles virus can synergize with fludarabine. *Cancer research* **67**, 10939-10947, doi:10.1158/0008-5472.can-07-1252 (2007a).

283 Parker, W. B. *et al.* Metabolism and metabolic actions of 6-methylpurine and 2-fluoroadenine in human cells. *Biochemical pharmacology* **55**, 1673-1681 (1998).

284 Ungerechts, G. *et al.* Mantle cell lymphoma salvage regimen: synergy between a reprogrammed oncolytic virus and two chemotherapeutics. *Gene therapy* **17**, 1506-1516, doi:10.1038/gt.2010.103 (2010).

285 Bossow, S. *et al.* Armed and targeted measles virus for chemovirotherapy of pancreatic cancer. *Cancer Gene Ther* **18**, 598-608, doi:10.1038/cgt.2011.30 (2011).

286 Sioka, C. & Kyritsis, A. P. Central and peripheral nervous system toxicity of common chemotherapeutic agents. *Cancer chemotherapy and pharmacology* **63**, 761-767, doi:10.1007/s00280-008-0876-6 (2009).

287 Lange, S. *et al.* A novel armed oncolytic measles vaccine virus for the treatment of cholangiocarcinoma. *Human gene therapy* **24**, 554-564, doi:10.1089/hum.2012.136 (2013).

288 Zaoui, K. *et al.* Chemovirotherapy for head and neck squamous cell carcinoma with EGFR-targeted and CD/UPRT-armed oncolytic measles virus. *Cancer Gene Ther* **19**, 181-191, doi:10.1038/cgt.2011.75 (2012).

289 Guillerme, J. B. *et al.* Measles virus vaccine-infected tumor cells induce tumor antigen cross-presentation by human plasmacytoid dendritic cells. *Clin Cancer Res* **19**, 1147-1158, doi:10.1158/1078-0432.CCR-12-2733 (2013).

290 NCT00408590. Oncolytic virus therapy in treating patients with progressive, recurrent, or refractory ovarian epithelial cancer or primary peritoneal cancer. *NIH, Bethesda, MD; USA* (2008).

291 Therasse, P. *et al.* New guidelines to evaluate the response to treatment in solid tumors. European Organization for Research and Treatment of Cancer, National Cancer Institute of the United States, National Cancer Institute of Canada. *Journal of the National Cancer Institute* **92**, 205-216 (2000).

292 Russell, S. J. *et al.* Remission of disseminated cancer after systemic oncolytic virotherapy. *Mayo Clinic proceedings* **89**, 926-933, doi:10.1016/j.mayocp.2014.04.003 (2014).

293 Dorig, R. E., Marcil, A., Chopra, A. & Richardson, C. D. The human CD46 molecule is a receptor for measles virus (Edmonston strain). *Cell* **75**, 295-305 (1993).

294 Anderson, B. D., Nakamura, T., Russell, S. J. & Peng, K. W. High CD46 receptor density determines preferential killing of tumor cells by oncolytic measles virus. *Cancer research* **64**, 4919-4926, doi:10.1158/0008-5472.CAN-04-0884 (2004).

295 Takano, A. *et al.* Identification of nectin-4 oncoprotein as a diagnostic and therapeutic target for lung cancer. *Cancer research* **69**, 6694-6703, doi:10.1158/0008-5472.can-09-0016 (2009).

296 DeRycke, M. S. *et al.* Nectin 4 Overexpression in Ovarian Cancer Tissues and Serum: Potential Role as a Serum Biomarker. *American journal of clinical pathology* **134**, 835-845, doi:10.1309/ajcpgxk0fr4mhihb (2010).

297 Fabre-Lafay, S. *et al.* Nectin-4 is a new histological and serological tumor associated marker for breast cancer. *BMC cancer* **7**, 73, doi:10.1186/1471-2407-7-73 (2007).

298 Egeblad, M. & Werb, Z. New functions for the matrix metalloproteinases in cancer progression. *Nature reviews. Cancer* **2**, 161-174, doi:10.1038/nrc745 (2002).

299 Nagini, S. RECKing MMP: relevance of reversion-inducing cysteine-rich protein with kazal motifs as a prognostic marker and therapeutic target for cancer (a review). *Anti-cancer agents in medicinal chemistry* **12**, 718-725 (2012).

300 Hadler-Olsen, E., Winberg, J. O. & Uhlin-Hansen, L. Matrix metalloproteinases in cancer: their value as diagnostic and prognostic markers and therapeutic targets. *Tumour biology : the journal of the International Society for Oncodevelopmental Biology and Medicine* **34**, 2041-2051, doi:10.1007/s13277-013-0842-8 (2013).

301 Miest, T. S., Frenzke, M. & Cattaneo, R. Measles virus entry through the signaling lymphocyte activation molecule governs efficacy of mantle cell lymphoma radiovirotherapy. *Molecular therapy : the journal of the American Society of Gene Therapy* **21**, 2019-2031, doi:10.1038/mt.2013.171 (2013).

302 Zygiert, Z. Hodgkin's disease: remissions after measles. *Lancet* **1**, 593 (1971).

303 Liu, C. *et al.* Combination of measles virus virotherapy and radiation therapy has synergistic activity in the treatment of glioblastoma multiforme. *Clin Cancer Res* **13**, 7155-7165, doi:10.1158/1078-0432.CCR-07-1306 (2007).

304 Gauvrit, A. *et al.* Measles virus induces oncolysis of mesothelioma cells and allows dendritic cells to cross-prime tumor-specific CD8 response. *Cancer research* **68**, 4882-4892, doi:10.1158/0008-5472.CAN-07-6265 (2008).

305 Donnelly, O. G. *et al.* Measles virus causes immunogenic cell death in human melanoma. *Gene therapy* **20**, 7-15, doi:10.1038/gt.2011.205 (2013).

306 Le Goffic, R. *et al.* Transcriptomic analysis of host immune and cell death responses associated with the influenza A virus PB1-F2 protein. *PLoS pathogens* **7**, e1002202, doi:10.1371/journal.ppat.1002202 (2011).

307 Lillard, J. W., Jr., Boyaka, P. N., Chertov, O., Oppenheim, J. J. & McGhee, J. R. Mechanisms for induction of acquired host immunity by neutrophil peptide defensins. *Proceedings of the National Academy of Sciences of the United States of America* **96**, 651-656 (1999).

308 Lieschke, G. J. *et al.* Mice lacking granulocyte colony-stimulating factor have chronic neutropenia, granulocyte and macrophage progenitor cell deficiency, and impaired neutrophil mobilization. *Blood* **84**, 1737-1746 (1994).

309 Kolaczkowska, E. & Kubes, P. Neutrophil recruitment and function in health and inflammation. *Nature reviews. Immunology* **13**, 159-175, doi:10.1038/nri3399 (2013).

310 Mogensen, T. H. Pathogen Recognition and Inflammatory Signaling in Innate Immune Defenses. *Clinical Microbiology Reviews* **22**, 240-273, doi:10.1128/CMR.00046-08 (2009).

311 Yoneyama, M. *et al.* The RNA helicase RIG-I has an essential function in double-stranded RNA-induced innate antiviral responses. *Nature immunology* **5**, 730-737, doi:10.1038/ni1087 (2004).

312 Kanneganti, T. D., Lamkanfi, M. & Nunez, G. Intracellular NOD-like receptors in host defense and disease. *Immunity* **27**, 549-559, doi:10.1016/j.immuni.2007.10.002 (2007).

313 Drescher, B. & Bai, F. Neutrophil in Viral Infections, Friend or Foe? *Virus research* **171**, 1-7, doi:10.1016/j.virusres.2012.11.002 (2013).

314 Saitoh, T. *et al.* Neutrophil extracellular traps mediate a host defense response to human immunodeficiency virus-1. *Cell host & microbe* **12**, 109-116, doi:10.1016/j.chom.2012.05.015 (2012).

315 Hufford, M. M. *et al.* Influenza-infected neutrophils within the infected lungs act as antigen presenting cells for anti-viral CD8(+) T cells. *PloS one* **7**, e46581, doi:10.1371/journal.pone.0046581 (2012).

316 Denkers, E. Y., Del Rio, L. & Bennouna, S. Neutrophil production of IL-12 and other cytokines during microbial infection. *Chemical immunology and allergy* **83**, 95-114 (2003).

317 Sheshachalam, A., Srivastava, N., Mitchell, T., Lacy, P. & Eitzen, G. Granule Protein Processing and Regulated Secretion in Neutrophils. *Frontiers in immunology* **5**, doi:10.3389/fimmu.2014.00448 (2014).

318 Lacy, P. Mechanisms of degranulation in neutrophils. *Allergy, asthma, and clinical immunology : official journal of the Canadian Society of Allergy and Clinical Immunology* **2**, 98-108, doi:10.1186/1710-1492-2-3-98 (2006).

319 Manara, F. S., Chin, J. & Schneider, D. L. Role of degranulation in activation of the respiratory burst in human neutrophils. *Journal of leukocyte biology* **49**, 489-498 (1991).

320 Perskvist, N., Roberg, K., Kulyte, A. & Stendahl, O. Rab5a GTPase regulates fusion between pathogen-containing phagosomes and cytoplasmic organelles in human neutrophils. *Journal of cell science* **115**, 1321-1330 (2002).

321 Ricevuti, G. *et al.* Assay of phagocytic cell functions. *Allergie et immunologie* **25**, 55-66 (1993).

322 Chen, Y. & Junger, W. G. Measurement of oxidative burst in neutrophils. *Methods in molecular biology* **844**, 115-124, doi:10.1007/978-1-61779-527-5_8 (2012).

323 Karlsson, A. & Dahlgren, C. Assembly and activation of the neutrophil NADPH oxidase in granule membranes. *Antioxidants & redox signaling* **4**, 49-60, doi:10.1089/152308602753625852 (2002).

324 Dahlgren, C. & Karlsson, A. Respiratory burst in human neutrophils. *J Immunol Methods* **232**, 3-14 (1999).

325 Underhill, D. M. & Ozinsky, A. Phagocytosis of microbes: complexity in action. *Annual review of immunology* **20**, 825-852, doi:10.1146/annurev.immunol.20.103001.114744 (2002).

326 Aderem, A. & Underhill, D. M. Mechanisms of phagocytosis in macrophages. *Annual review of immunology* **17**, 593-623, doi:10.1146/annurev.immunol.17.1.593 (1999).

327 Ren, Y. & Savill, J. Apoptosis: the importance of being eaten. *Cell death and differentiation* **5**, 563-568, doi:10.1038/sj.cdd.4400407 (1998).

328 Barber, G. N. Host defense, viruses and apoptosis. *Cell death and differentiation* **8**, 113-126, doi:10.1038/sj.cdd.4400823 (2001).

329 Hashimoto, Y., Moki, T., Takizawa, T., Shiratsuchi, A. & Nakanishi, Y. Evidence for phagocytosis of influenza virus-infected, apoptotic cells

by neutrophils and macrophages in mice. *J Immunol* **178**, 2448-2457 (2007).

330 Lerat, H. *et al.* In vivo tropism of hepatitis C virus genomic sequences in hematopoietic cells: influence of viral load, viral genotype, and cell phenotype. *Blood* **91**, 3841-3849 (1998).

331 Hoar, D. I., Bowen, T., Matheson, D. & Poon, M. C. Hepatitis B virus DNA is enriched in polymorphonuclear leukocytes. *Blood* **66**, 1251-1253 (1985).

332 Catterall, A. P., Murray-Lyon, I. M., Zuckerman, A. J. & Harrison, T. J. Southern hybridisation analysis of HBV DNA in peripheral blood leucocytes and of different cell types: Changes during the natural history and with interferon-α therapy in patients with hepatitis B virus infection. *Journal of medical virology* **43**, 269-275, doi:10.1002/jmv.1890430314 (1994).

333 Orenstein, J. M. In vivo cytolysis and fusion of human immunodeficiency virus type 1-infected lymphocytes in lymphoid tissue. *The Journal of infectious diseases* **182**, 338-342, doi:10.1086/315640 (2000).

334 Gerna, G., Baldanti, F. & Revello, M. G. Pathogenesis of human cytomegalovirus infection and cellular targets. *Human immunology* **65**, 381-386, doi:10.1016/j.humimm.2004.02.009 (2004).

335 Zhao, Y. *et al.* Neutrophils may be a vehicle for viral replication and dissemination in human H5N1 avian influenza. *Clinical infectious diseases : an official publication of the Infectious Diseases Society of America* **47**, 1575-1578, doi:10.1086/593196 (2008).

336 Noffz, G., Qin, Z., Kopf, M. & Blankenstein, T. Neutrophils but not eosinophils are involved in growth suppression of IL-4-secreting tumors. *J Immunol* **160**, 345-350 (1998).

337 Sharar, S. R., Winn, R. K. & Harlan, J. M. The adhesion cascade and anti-adhesion therapy: an overview. *Springer seminars in immunopathology* **16**, 359-378 (1995).

338 Di Carlo, E. The intriguing role of polymorphonuclear neutrophils in antitumor reactions. *Blood* **97**, 339-345, doi:10.1182/blood.V97.2.339 (2001).

339 Alvarez, M. J. *et al.* Secreted protein acidic and rich in cysteine produced by human melanoma cells modulates polymorphonuclear

leukocyte recruitment and antitumor cytotoxic capacity. *Cancer research* **65**, 5123-5132, doi:10.1158/0008-5472.CAN-04-1102 (2005).

340 Chen, Y. L., Chen, S. H., Wang, J. Y. & Yang, B. C. Fas ligand on tumor cells mediates inactivation of neutrophils. *J Immunol* **171**, 1183-1191 (2003).

341 Suttmann, H. *et al.* Neutrophil granulocytes are required for effective Bacillus Calmette-Guerin immunotherapy of bladder cancer and orchestrate local immune responses. *Cancer research* **66**, 8250-8257, doi:10.1158/0008-5472.can-06-1416 (2006).

342 Kemp, T. J. *et al.* Neutrophil stimulation with Mycobacterium bovis bacillus Calmette-Guerin (BCG) results in the release of functional soluble TRAIL/Apo-2L. *Blood* **106**, 3474-3482, doi:10.1182/blood-2005-03-1327 (2005).

343 Ludwig, A. T. *et al.* Tumor necrosis factor-related apoptosis-inducing ligand: a novel mechanism for Bacillus Calmette-Guerin-induced antitumor activity. *Cancer research* **64**, 3386-3390, doi:10.1158/0008-5472.can-04-0374 (2004).

344 Breitbach, C. J. *et al.* Targeted inflammation during oncolytic virus therapy severely compromises tumor blood flow. *Molecular therapy : the journal of the American Society of Gene Therapy* **15**, 1686-1693, doi:10.1038/sj.mt.6300215 (2007).

345 Breitbach, C. J. *et al.* Targeting tumor vasculature with an oncolytic virus. *Molecular therapy : the journal of the American Society of Gene Therapy* **19**, 886-894, doi:10.1038/mt.2011.26 (2011).

346 Nozawa, H., Chiu, C. & Hanahan, D. Infiltrating neutrophils mediate the initial angiogenic switch in a mouse model of multistage carcinogenesis. *Proceedings of the National Academy of Sciences of the United States of America* **103**, 12493-12498, doi:10.1073/pnas.0601807103 (2006).

347 De Larco, J. E., Wuertz, B. R. K. & Furcht, L. T. The Potential Role of Neutrophils in Promoting the Metastatic Phenotype of Tumors Releasing Interleukin-8. *American Association for Cancer Research* **10**, 4895-4900, doi:10.1158/1078-0432.ccr-03-0760 (2004).

348 Granot, Z. *et al.* Tumor entrained neutrophils inhibit seeding in the premetastatic lung. *Cancer Cell* **20**, 300-314, doi:10.1016/j.ccr.2011.08.012 (2011).

349 Lopez-Lago, M. A. *et al.* Neutrophil chemokines secreted by tumor cells mount a lung antimetastatic response during renal cell carcinoma progression. *Oncogene* **32**, 1752-1760, doi:10.1038/onc.2012.201 (2013).

350 Colombo, M. P., Modesti, A., Parmiani, G. & Forni, G. Local cytokine availability elicits tumor rejection and systemic immunity through granulocyte-T-lymphocyte cross-talk. *Cancer research* **52**, 4853-4857 (1992).

351 Hicks, A. M. *et al.* Transferable anticancer innate immunity in spontaneous regression/complete resistance mice. *Proceedings of the National Academy of Sciences of the United States of America* **103**, 7753-7758, doi:10.1073/pnas.0602382103 (2006).

352 Granot, Z. & Fridlender, Z. G. Plasticity beyond cancer cells and the "immunosuppressive switch". *Cancer research* **75**, 4441-4445, doi:10.1158/0008-5472.can-15-1502 (2015).

353 Fridlender, Z. G. *et al.* Polarization of tumor-associated neutrophil phenotype by TGF-beta: "N1" versus "N2" TAN. *Cancer Cell* **16**, 183-194, doi:10.1016/j.ccr.2009.06.017 (2009).

354 Mishalian, I., Granot, Z. & Fridlender, Z. G. The diversity of circulating neutrophils in cancer. *Immunobiology*, doi:10.1016/j.imbio.2016.02.001 (2016).

355 Sagiv, J. Y. *et al.* Phenotypic diversity and plasticity in circulating neutrophil subpopulations in cancer. *Cell reports* **10**, 562-573, doi:10.1016/j.celrep.2014.12.039 (2015).

356 Mabuchi, S. *et al.* Pretreatment leukocytosis is an indicator of poor prognosis in patients with cervical cancer. *Gynecologic oncology* **122**, 25-32, doi:10.1016/j.ygyno.2011.03.037 (2011).

357 Zhang, Y. *et al.* Attenuated, oncolytic, but not wild-type measles virus infection has pleiotropic effects on human neutrophil function. *J Immunol* **188**, 1002-1010, doi:10.4049/jimmunol.1102262 (2012).

358 Nicola, N. A., Metcalf, D., Matsumoto, M. & Johnson, G. R. Purification of a factor inducing differentiation in murine myelomonocytic leukemia cells. Identification as granulocyte colony-stimulating factor. *The Journal of biological chemistry* **258**, 9017-9023 (1983).

359 Welte, K. *et al.* Purification and biochemical characterization of human pluripotent hematopoietic colony-stimulating factor. *Proceedings of the*

National Academy of Sciences of the United States of America **82**, 1526-1530 (1985).

360 Tamura, M. *et al.* Induction of neutrophilic granulocytosis in mice by administration of purified human native granulocyte colony-stimulating factor (G-CSF). *Biochemical and biophysical research communications* **142**, 454-460 (1987).

361 DeLuca, E., Sheridan, W. P., Watson, D., Szer, J. & Begley, C. G. Prior chemotherapy does not prevent effective mobilisation by G-CSF of peripheral blood progenitor cells. *British journal of cancer* **66**, 893-899 (1992).

362 Sheridan, W. P. *et al.* Effect of peripheral-blood progenitor cells mobilised by filgrastim (G-CSF) on platelet recovery after high-dose chemotherapy. *Lancet* **339**, 640-644 (1992).

363 Grigg, A. P. *et al.* Optimizing dose and scheduling of filgrastim (granulocyte colony-stimulating factor) for mobilization and collection of peripheral blood progenitor cells in normal volunteers. *Blood* **86**, 4437-4445 (1995).

364 Ravandi, F. & Estrov, Z. Eradication of leukemia stem cells as a new goal of therapy in leukemia. *Clin Cancer Res* **12**, 340-344, doi:10.1158/1078-0432.ccr-05-1879 (2006).

365 Avalos, B. R. Molecular analysis of the granulocyte colony-stimulating factor receptor. *Blood* **88**, 761-777 (1996).

366 Duhrsen, U. *et al.* Effects of recombinant human granulocyte colony-stimulating factor on hematopoietic progenitor cells in cancer patients. *Blood* **72**, 2074-2081 (1988).

367 Roberts, A. W. G-CSF: a key regulator of neutrophil production, but that's not all! *Growth factors (Chur, Switzerland)* **23**, 33-41, doi:10.1080/08977190500055836 (2005).

368 Franzke, A. *et al.* G-CSF as immune regulator in T cells expressing the G-CSF receptor: implications for transplantation and autoimmune diseases. *Blood* **102**, 734-739, doi:10.1182/blood-2002-04-1200 (2003).

369 Pan, L., Delmonte, J., Jr., Jalonen, C. K. & Ferrara, J. L. Pretreatment of donor mice with granulocyte colony-stimulating factor polarizes donor T lymphocytes toward type-2 cytokine production and reduces

severity of experimental graft-versus-host disease. *Blood* **86**, 4422-4429 (1995).

370 Mielcarek, M., Martin, P. J. & Torok-Storb, B. Suppression of alloantigen-induced T-cell proliferation by CD14+ cells derived from granulocyte colony-stimulating factor-mobilized peripheral blood mononuclear cells. *Blood* **89**, 1629-1634 (1997).

371 Arpinati, M., Green, C. L., Heimfeld, S., Heuser, J. E. & Anasetti, C. Granulocyte-colony stimulating factor mobilizes T helper 2-inducing dendritic cells. *Blood* **95**, 2484-2490 (2000).

372 Rutella, S. *et al.* Granulocyte colony-stimulating factor promotes the generation of regulatory DC through induction of IL-10 and IFN-alpha. *European journal of immunology* **34**, 1291-1302, doi:10.1002/eji.200324651 (2004).

373 G., K. Beitrag zur Kollektiven Behandlung Pharmakologischer Reihenversuche. . *Arch Exp Path Pharma.* **162**, 480–487, doi:10.1007/BF01863914. (1931).

374 Pfaffle, M. W. A new mathematical model for relative quantification in real-time RT-PCR. *Nucleic acids research* **29** (2001).

375 Fielding, A. K. The treatment of adults with acute lymphoblastic leukemia. *Hematology / the Education Program of the American Society of Hematology. American Society of Hematology. Education Program*, 381-389, doi:10.1182/asheducation-2008.1.381 (2008).

376 Castleton, A. *et al.* Human mesenchymal stromal cells deliver systemic oncolytic measles virus to treat acute lymphoblastic leukemia in the presence of humoral immunity. *Blood* **123**, 1327-1335, doi:10.1182/blood-2013-09-528851 (2014).

377 Avalos, B. R. *et al.* Dissociation of the Jak kinase pathway from G-CSF receptor signaling in neutrophils. *Experimental hematology* **25**, 160-168 (1997).

378 Dong, F. *et al.* Identification of a nonsense mutation in the granulocyte-colony-stimulating factor receptor in severe congenital neutropenia. *Proceedings of the National Academy of Sciences of the United States of America* **91**, 4480-4484 (1994).

379 Nicholson, S. E. *et al.* Tyrosine kinase JAK1 is associated with the granulocyte-colony-stimulating factor receptor and both become tyrosine-phosphorylated after receptor activation. *Proceedings of the*

National Academy of Sciences of the United States of America **91**, 2985-2988 (1994).

380 Nicholson, S. E., Novak, U., Ziegler, S. F. & Layton, J. E. Distinct regions of the granulocyte colony-stimulating factor receptor are required for tyrosine phosphorylation of the signaling molecules JAK2, Stat3, and p42, p44MAPK. *Blood* **86**, 3698-3704 (1995).

381 Bashey, A., Healy, L. & Marshall, C. J. Proliferative but not nonproliferative responses to granulocyte colony-stimulating factor are associated with rapid activation of the p21ras/MAP kinase signalling pathway. *Blood* **83**, 949-957 (1994).

382 Tanaka, H., Okada, Y., Kawagishi, M. & Tokiwa, T. Pharmacokinetics and pharmacodynamics of recombinant human granulocyte-colony stimulating factor after intravenous and subcutaneous administration in the rat. *The Journal of pharmacology and experimental therapeutics* **251**, 1199-1203 (1989).

383 Frank, T. *et al.* Pegylated granulocyte colony-stimulating factor conveys long-term neuroprotection and improves functional outcome in a model of Parkinson's disease. *Brain : a journal of neurology* **135**, 1914-1925, doi:10.1093/brain/aws054 (2012).

384 Ohdo, S. *et al.* Influence of dosing time on pharmacological action of G-CSF in mice. *Life sciences* **62**, PL163-168 (1998).

385 Kotto-Kome, A. C. *et al.* Evidence that the granulocyte colony-stimulating factor (G-CSF) receptor plays a role in the pharmacokinetics of G-CSF and PegG-CSF using a G-CSF-R KO model. *Pharmacological research : the official journal of the Italian Pharmacological Society* **50**, 55-58, doi:10.1016/j.phrs.2003.12.011 (2004).

386 Patel, B. *et al.* Differential cytopathology and kinetics of measles oncolysis in two primary B-cell malignancies provides mechanistic insights. *Molecular therapy : the journal of the American Society of Gene Therapy* **19**, 1034-1040, doi:10.1038/mt.2011.44 (2011).

387 Han, Y. & Cutler, J. E. Assessment of a mouse model of neutropenia and the effect of an anti-candidiasis monoclonal antibody in these animals. *The Journal of infectious diseases* **175**, 1169-1175 (1997).

388 Brown, C. R., Blaho, V. A. & Loiacono, C. M. Treatment of mice with the neutrophil-depleting antibody RB6-8C5 results in early development of experimental lyme arthritis via the recruitment of Gr-1-

polymorphonuclear leukocyte-like cells. *Infection and immunity* **72**, 4956-4965, doi:10.1128/iai.72.9.4956-4965.2004 (2004).

389 Hernandez-Ilizaliturri, F. J. *et al.* Neutrophils contribute to the biological antitumor activity of rituximab in a non-Hodgkin's lymphoma severe combined immunodeficiency mouse model. *Clin Cancer Res* **9**, 5866-5873 (2003).

390 Galanis, E. *et al.* Oncolytic measles virus expressing the sodium iodide symporter to treat drug-resistant ovarian cancer. *Cancer research* **75**, 22-30, doi:10.1158/0008-5472.CAN-14-2533 (2015).

391 Shirafuji, N. *et al.* Granulocyte colony-stimulating factor stimulates human mature neutrophilic granulocytes to produce interferon-alpha. *Blood* **75**, 17-19 (1990).

392 Nicola, N. A. Why do hemopoietic growth factor receptors interact with each other? *Immunology today* **8**, 134-140, doi:10.1016/0167-5699(87)90140-X (1987).

393 Bendall, L. J. & Bradstock, K. F. G-CSF: From granulopoietic stimulant to bone marrow stem cell mobilizing agent. *Cytokine Growth Factor Rev* **25**, 355-367, doi:10.1016/j.cytogfr.2014.07.011 (2014).

394 Parameswaran, R., Yu, M., Lim, M., Groffen, J. & Heisterkamp, N. Combination of drug therapy in acute lymphoblastic leukemia with a CXCR4 antagonist. *Leukemia : official journal of the Leukemia Society of America, Leukemia Research Fund, U.K* **25**, 1314-1323, doi:10.1038/leu.2011.76 (2011).

395 Welschinger, R. *et al.* Plerixafor (AMD3100) induces prolonged mobilization of acute lymphoblastic leukemia cells and increases the proportion of cycling cells in the blood in mice. *Experimental hematology* **41**, 293-302 e291, doi:10.1016/j.exphem.2012.11.004 (2013).

396 G. Uy, W. S., Y.-M. Hsu, J.E. Churpek, P. Westervelt, J. DiPersio, et al. in *55th ASH annual meeting and exposition, American Society of Hematology,* (New Orleans, 2013).

397 Basnett, J., Cisterne, A., Bradstock, K., Bendall.L. in *54th ASH annual meeting and exposition, American Society of Hematology* (Atlanta, GA 2012).

398 Saito, Y. *et al.* Induction of cell cycle entry eliminates human leukemia stem cells in a mouse model of AML. *Nat Biotechnol* **28**, 275-280, doi:10.1038/nbt.1607 (2010).

399 Shimazaki, C. *et al.* Serum levels of endogenous and exogenous granulocyte colony-stimulating factor after autologous blood stem cell transplantation. *Experimental hematology* **23**, 1497-1502 (1995).

400 Lehrer, R. I. & Ganz, T. Antimicrobial polypeptides of human neutrophils. *Blood* **76**, 2169-2181 (1990).

401 Harmsen, M. C. *et al.* Antiviral effects of plasma and milk proteins: lactoferrin shows potent activity against both human immunodeficiency virus and human cytomegalovirus replication in vitro. *The Journal of infectious diseases* **172**, 380-388 (1995).

402 Levy, O. Antibiotic proteins of polymorphonuclear leukocytes. *European journal of haematology* **56**, 263-277 (1996).

403 Heijnen, I. A. *et al.* Generation of HER-2/neu-specific cytotoxic neutrophils in vivo: efficient arming of neutrophils by combined administration of granulocyte colony-stimulating factor and Fcgamma receptor I bispecific antibodies. *J Immunol* **159**, 5629-5639 (1997).

404 Stockmeyer, B. *et al.* Triggering Fc alpha-receptor I (CD89) recruits neutrophils as effector cells for CD20-directed antibody therapy. *J Immunol* **165**, 5954-5961 (2000).

405 Teillaud, J.-L. in *eLS* (John Wiley & Sons, Ltd, 2001).

406 Perussia, B. *et al.* Immune interferon and leukocyte-conditioned medium induce normal and leukemic myeloid cells to differentiate along the monocytic pathway. *The Journal of experimental medicine* **158**, 2058-2080 (1983).

407 Repp, R. *et al.* Neutrophils express the high affinity receptor for IgG (Fc gamma RI, CD64) after in vivo application of recombinant human granulocyte colony-stimulating factor. *Blood* **78**, 885-889 (1991).

408 Challacombe, J. M. *et al.* Neutrophils are a key component of the antitumor efficacy of topical chemotherapy with ingenol-3-angelate. *J Immunol* **177**, 8123-8132 (2006).

409 Parrish, C. *et al.* Oncolytic reovirus enhances rituximab-mediated antibody-dependent cellular cytotoxicity against chronic lymphocytic

leukaemia. *Leukemia : official journal of the Leukemia Society of America, Leukemia Research Fund, U.K* **29**, 1799-1810, doi:10.1038/leu.2015.88 (2015).

410 Kayagaki, N. *et al.* Type I interferons (IFNs) regulate tumor necrosis factor-related apoptosis-inducing ligand (TRAIL) expression on human T cells: A novel mechanism for the antitumor effects of type I IFNs. *The Journal of experimental medicine* **189**, 1451-1460 (1999).

411 Van der Kolk, L. E., De Haas, M., Grillo-Lopez, A. J., Baars, J. W. & Van Oers, M. H. Analysis of CD20-dependent cellular cytotoxicity by G-CSF-stimulated neutrophils. *Leukemia : official journal of the Leukemia Society of America, Leukemia Research Fund, U.K* **16**, 693-699, doi:10.1038/sj.leu.2402424 (2002).

412 Polack, F. P. *et al.* Successful DNA immunization against measles: neutralizing antibody against either the hemagglutinin or fusion glycoprotein protects rhesus macaques without evidence of atypical measles. *Nat Med* **6**, 776-781, doi:10.1038/77506 (2000).

413 Parks, C. L. *et al.* Analysis of the Noncoding Regions of Measles Virus Strains in the Edmonston Vaccine Lineage. *Journal of virology* **75**, 921-933, doi:10.1128/jvi.75.2.921-933.2001 (2001a).

414 Parks, C. L. *et al.* Comparison of predicted amino acid sequences of measles virus strains in the Edmonston vaccine lineage. *Journal of virology* **75**, 910-920, doi:10.1128/JVI.75.2.910-920.2001 (2001b).

415 Bankamp, B., Fontana, J. M., Bellini, W. J. & Rota, P. A. Adaptation to cell culture induces functional differences in measles virus proteins. *Virology journal* **5**, 129, doi:10.1186/1743-422X-5-129 (2008).

416 Siebens, H., Tevethia, S. S. & Babior, B. M. Neutrophil-mediated antibody-dependent killing of herpes-simplex-virus-infected cells. *Blood* **54**, 88-94 (1979).

417 Oleske, J. M. *et al.* Human polymorphonuclear leucocytes as mediators of antibody-dependent cellular cytotoxicity to herpes simplex virus-infected cells. *Clinical and experimental immunology* **27**, 446-453 (1977).

418 TOSHIAKI IHARA, S. E. S., ALLAN M. ARBETER, and STANLEY A. PLOTKIN. . Effects of Interferon on Natural Killing and Antibody-Dependent Cellular Cytotoxicity Against Varicella-Zoster Virus-Infected and Uninfected Target Cells. *Journal of Interferon Research.* **3(3):** , 263-269. , doi:doi:10.1089/jir.1983.3.263. (2009).

419 Forthal, D. N. & Landucci, G. In vitro reduction of virus infectivity by antibody-dependent cell-mediated immunity. *J Immunol Methods* **220**, 129-138 (1998).

420 Forthal, D. N., Landucci, G., Katz, J. & Tilles, J. G. Comparison of measles virus-specific antibodies with antibody-dependent cellular cytotoxicity and neutralizing functions. *The Journal of infectious diseases* **168**, 1020-1023 (1993).

421 Iankov, I. D. *et al.* Immunoglobulin g antibody-mediated enhancement of measles virus infection can bypass the protective antiviral immune response. *Journal of virology* **80**, 8530-8540, doi:10.1128/JVI.00593-06 (2006).

422 Carroll, A. M., Hardy, R. R., Petrini, J. & Bosma, M. J. T cell leakiness in scid mice. *Current topics in microbiology and immunology* **152**, 117-123 (1989).

423 Bergman, I., Basse, P. H., Barmada, M. A., Griffin, J. A. & Cheung, N. K. Comparison of in vitro antibody-targeted cytotoxicity using mouse, rat and human effectors. *Cancer immunology, immunotherapy : CII* **49**, 259-266 (2000).

424 Mestas, J. & Hughes, C. C. Of mice and not men: differences between mouse and human immunology. *J Immunol* **172**, 2731-2738 (2004).

425 Doeing, D. C., Borowicz, J. L. & Crockett, E. T. Gender dimorphism in differential peripheral blood leukocyte counts in mice using cardiac, tail, foot, and saphenous vein puncture methods. *BMC clinical pathology* **3**, 3, doi:10.1186/1472-6890-3-3 (2003).

426 Gessner, J. E., Heiken, H., Tamm, A. & Schmidt, R. E. The IgG Fc receptor family. *Annals of hematology* **76**, 231-248 (1998).

427 Marie, J. C. *et al.* Cell surface delivery of the measles virus nucleoprotein: a viral strategy to induce immunosuppression. *Journal of virology* **78**, 11952-11961, doi:10.1128/JVI.78.21.11952-11961.2004 (2004).

428 Michał Zarzycki, L. T. Cell Lines as a Model for Immune Cells in Research and Didactics. *Biology International* **Vol. 54** (2009).

429 Weiss, A., Wiskocil, R. L. & Stobo, J. D. The role of T3 surface molecules in the activation of human T cells: a two-stimulus requirement for IL 2 production reflects events occurring at a pre-translational level. *J Immunol* **133**, 123-128 (1984).

430 Gillis, S., Scheid, M. & Watson, J. Biochemical and biologic characterization of lymphocyte regulatory molecules. III. The isolation and phenotypic characterization of Interleukin-2 producing T cell lymphomas. *J Immunol* **125**, 2570-2578 (1980).

431 Stellrecht, K. A., Sperber, K. & Pogo, B. G. Stimulation of lymphokines in Jurkat cells persistently infected with vaccinia virus. *Journal of virology* **66**, 2046-2050 (1992).

432 Girard, D., Gosselin, J., Heitz, D., Paquin, R. & Beaulieu, A. D. Effects of interleukin-2 on gene expression in human neutrophils. *Blood* **86**, 1170-1176 (1995).

433 Li, J., Gyorffy, S., Lee, S. & Kwok, C. S. Effect of recombinant human interleukin 2 on neutrophil adherence to endothelial cells in vitro. *Inflammation* **20**, 361-372 (1996).

434 McLain, L. & Dimmock, N. J. A human CD4+ T-cell line expresses functional CD64 (Fc gamma RI), CD32 (Fc gamma RII), and CD16 (Fc gamma RIII) receptors but these do not enhance the infectivity of HIV-1-IgG complexes. *Immunology* **90**, 109-114 (1997).

435 Wirthmueller, U., Kurosaki, T., Murakami, M. S. & Ravetch, J. V. Signal transduction by Fc gamma RIII (CD16) is mediated through the gamma chain. *The Journal of experimental medicine* **175**, 1381-1390 (1992).

436 Yokoyama, W. M. & Plougastel, B. F. M. Immune functions encoded by the natural killer gene complex. *Nature reviews. Immunology* **3**, 304-316 (2003).

437 Bankamp, B., Kearney, S. P., Liu, X., Bellini, W. J. & Rota, P. A. Activity of polymerase proteins of vaccine and wild-type measles virus strains in a minigenome replication assay. *Journal of virology* **76**, 7073-7081 (2002).

438 Ciechonska, M., Key, T. & Duncan, R. Efficient Reovirus- and Measles Virus-Mediated Pore Expansion during Syncytium Formation Is Dependent on Annexin A1 and Intracellular Calcium. *Journal of virology* **88**, 6137-6147, doi:10.1128/jvi.00121-14 (2014).

439 Gabrijel, M. *et al.* Quantification of cell hybridoma yields with confocal microscopy and flow cytometry. *Biochemical and biophysical research communications* **314**, 717-723 (2004).

440 Horn, G. P. *et al.* Enhanced Cytotoxicity without Internuclear Spread of Adenovirus upon Cell Fusion by Measles Virus Glycoproteins. *Journal of virology* **79**, 1911-1917, doi:10.1128/jvi.79.3.1911-1917.2005 (2005).

441 Lamb, R. A. & Jardetzky, T. S. Structural basis of viral invasion: lessons from paramyxovirus F. *Current opinion in structural biology* **17**, 427-436, doi:10.1016/j.sbi.2007.08.016 (2007).

442 Boutilier, J. & Duncan, R. The reovirus fusion-associated small transmembrane (FAST) proteins: virus-encoded cellular fusogens. *Current topics in membranes* **68**, 107-140, doi:10.1016/b978-0-12-385891-7.00005-2 (2011).

443 Duncan, R. Extensive sequence divergence and phylogenetic relationships between the fusogenic and nonfusogenic orthoreoviruses: a species proposal. *Virology* **260**, 316-328, doi:10.1006/viro.1999.9832 (1999).

444 Shmulevitz, M. & Duncan, R. A new class of fusion-associated small transmembrane (FAST) proteins encoded by the non-enveloped fusogenic reoviruses. *Embo j* **19**, 902-912, doi:10.1093/emboj/19.5.902 (2000).

445 Clancy, E. K. & Duncan, R. Reovirus FAST Protein Transmembrane Domains Function in a Modular, Primary Sequence-Independent Manner To Mediate Cell-Cell Membrane Fusion. *Journal of virology* **83**, 2941-2950, doi:10.1128/jvi.01869-08 (2009).

446 Scheller, C. & Jassoy, C. Syncytium formation amplifies apoptotic signals: a new view on apoptosis in HIV infection in vitro. *Virology* **282**, 48-55, doi:10.1006/viro.2000.0811 (2001).

447 Villenave, R. *et al.* Cytopathogenesis of Sendai virus in well-differentiated primary pediatric bronchial epithelial cells. *Journal of virology* **84**, 11718-11728, doi:10.1128/jvi.00798-10 (2010).

448 Chuprin, A. *et al.* Cell fusion induced by ERVWE1 or measles virus causes cellular senescence. *Genes & development* **27**, 2356-2366, doi:10.1101/gad.227512.113 (2013).

449 Herschke, F. *et al.* Cell-cell fusion induced by measles virus amplifies the type I interferon response. *Journal of virology* **81**, 12859-12871, doi:10.1128/JVI.00078-07 (2007).

450 Allen, C. *et al.* Oncolytic measles virus strains in the treatment of gliomas. *Expert opinion on biological therapy* **8**, 213-220, doi:10.1517/14712598.8.2.213 (2008).

451 Burns, J. C., Friedmann, T., Driever, W., Burrascano, M. & Yee, J. K. Vesicular stomatitis virus G glycoprotein pseudotyped retroviral vectors: concentration to very high titer and efficient gene transfer into mammalian and nonmammalian cells. *Proceedings of the National Academy of Sciences of the United States of America* **90**, 8033-8037 (1993).

452 Fielding, A. K. *et al.* A hyperfusogenic gibbon ape leukemia envelope glycoprotein: targeting of a cytotoxic gene by ligand display. *Human gene therapy* **11**, 817-826, doi:10.1089/10430340050015437 (2000).

453 Errington, F. *et al.* Fusogenic membrane glycoprotein-mediated tumour cell fusion activates human dendritic cells for enhanced IL-12 production and T-cell priming. *Gene therapy* **13**, 138-149, doi:10.1038/sj.gt.3302609 (2006).

454 Bateman, A. *et al.* Fusogenic membrane glycoproteins as a novel class of genes for the local and immune-mediated control of tumor growth. *Cancer research* **60**, 1492-1497 (2000).

455 Bateman, A. R. *et al.* Viral fusogenic membrane glycoproteins kill solid tumor cells by nonapoptotic mechanisms that promote cross presentation of tumor antigens by dendritic cells. *Cancer research* **62**, 6566-6578 (2002).

456 Higuchi, H. *et al.* Viral fusogenic membrane glycoprotein expression causes syncytia formation with bioenergetic cell death: implications for gene therapy. *Cancer research* **60**, 6396-6402 (2000).

457 Linardakis, E. *et al.* Enhancing the efficacy of a weak allogeneic melanoma vaccine by viral fusogenic membrane glycoprotein-mediated tumor cell-tumor cell fusion. *Cancer research* **62**, 5495-5504 (2002).

458 Yosuke Morodomi, M. I., Mamoru Hasegawa, Tatsuro Okamoto, Yoshihiko Maehara and Yoshikazu Yonemitsu. Prof. Ming Wei (Ed.), InTech, . Sendai Virus-Based Oncolytic Gene Therapy, Novel Gene Therapy Approaches, . *Available from:* http://www.intechopen.com/books/novel-gene-therapy-approaches/sendai-virus-based-oncolytic-gene-therapy, doi:DOI: 10.5772/55328. (2013).

459 Gainey, M. D., Manuse, M. J. & Parks, G. D. A Hyperfusogenic F Protein Enhances the Oncolytic Potency of a Paramyxovirus Simian Virus 5 P/V Mutant without Compromising Sensitivity to Type I Interferon. *Journal of virology* **82**, 9369-9380, doi:10.1128/jvi.01054-08 (2008).

460 Guedan, S. *et al.* GALV expression enhances the therapeutic efficacy of an oncolytic adenovirus by inducing cell fusion and enhancing virus distribution. *Gene therapy* **19**, 1048-1057, doi:10.1038/gt.2011.184 (2012).

461 Richardson, C. D., Scheid, A. & Choppin, P. W. Specific inhibition of paramyxovirus and myxovirus replication by oligopeptides with amino acid sequences similar to those at the N-termini of the F1 or HA2 viral polypeptides. *Virology* **105**, 205-222 (1980).

462 Richardson, C. D. & Choppin, P. W. Oligopeptides that specifically inhibit membrane fusion by paramyxoviruses: studies on the site of action. *Virology* **131**, 518-532 (1983).

463 Ennis, M. K. *et al.* Mutations in the stalk region of the measles virus hemagglutinin inhibit syncytium formation but not virus entry. *Journal of virology* **84**, 10913-10917, doi:10.1128/jvi.00789-10 (2010).

464 Mathieu, C. *et al.* Prevention of measles virus infection by intranasal delivery of fusion inhibitor peptides. *Journal of virology* **89**, 1143-1155, doi:10.1128/jvi.02417-14 (2015).

465 Segal, A. W. How Neutrophils Kill Microbes. *Annual review of immunology* **23**, 197-223, doi:10.1146/annurev.immunol.23.021704.115653 (2005).

466 Tecchio, C. *et al.* IFNalpha-stimulated neutrophils and monocytes release a soluble form of TNF-related apoptosis-inducing ligand (TRAIL/Apo-2 ligand) displaying apoptotic activity on leukemic cells. *Blood* **103**, 3837-3844, doi:10.1182/blood-2003-08-2806 (2004).

467 Faurschou, M. & Borregaard, N. Neutrophil granules and secretory vesicles in inflammation. *Microbes and infection / Institut Pasteur* **5**, 1317-1327 (2003).

468 Jaovisidha, P., Peeples, M. E., Brees, A. A., Carpenter, L. R. & Moy, J. N. Respiratory syncytial virus stimulates neutrophil degranulation and chemokine release. *J Immunol* **163**, 2816-2820 (1999).

469 Funchal, G. A. *et al.* Respiratory syncytial virus fusion protein promotes TLR-4-dependent neutrophil extracellular trap formation by human neutrophils. *PloS one* **10**, e0124082, doi:10.1371/journal.pone.0124082 (2015).

470 Jenne, C. N. & Kubes, P. Virus-Induced NETs – Critical Component of Host Defense or Pathogenic Mediator? *PLoS pathogens* **11**, doi:10.1371/journal.ppat.1004546 (2015).

471 Meylan, E. & Tschopp, J. Toll-like receptors and RNA helicases: two parallel ways to trigger antiviral responses. *Molecular cell* **22**, 561-569, doi:10.1016/j.molcel.2006.05.012 (2006).

472 Arnoult, D., Carneiro, L., Tattoli, I. & Girardin, S. E. The role of mitochondria in cellular defense against microbial infection. *Seminars in immunology* **21**, 223-232, doi:10.1016/j.smim.2009.05.009 (2009).

473 Zitvogel, L., Galluzzi, L., Kepp, O., Smyth, M. J. & Kroemer, G. Type I interferons in anticancer immunity. *Nature reviews. Immunology* **15**, 405-414, doi:10.1038/nri3845 (2015).

474 Zamarin, D. *et al.* Localized oncolytic virotherapy overcomes systemic tumor resistance to immune checkpoint blockade immunotherapy. *Science translational medicine* **6**, 226ra232, doi:10.1126/scitranslmed.3008095 (2014).

475 Melero, I. *et al.* Strict requirement for vector-induced type I interferon in efficacious antitumor responses to virally encoded IL12. *Cancer research* **75**, 497-507, doi:10.1158/0008-5472.can-13-3356 (2015).

476 Hervas-Stubbs, S. *et al.* Direct Effects of Type I Interferons on Cells of the Immune System. *American Association for Cancer Research* **17**, 2619-2627 (2011).

477 Cassatella, M. A. On the production of TNF-related apoptosis-inducing ligand (TRAIL/Apo-2L) by human neutrophils. *Journal of leukocyte biology* **79**, 1140-1149, doi:10.1189/jlb.1005558 (2006).

478 Vidalain, P. O. *et al.* Measles Virus Induces Functional TRAIL Production by Human Dendritic Cells. *Journal of virology* **74**, 556-559 (2000).

479 Larochelle, B., Flamand, L., Gourde, P., Beauchamp, D. & Gosselin, J. Epstein-Barr virus infects and induces apoptosis in human neutrophils. *Blood* **92**, 291-299 (1998).

480 Bais, S., Bartee, E., Rahman, M. M., McFadden, G. & Cogle, C. R. Oncolytic virotherapy for hematological malignancies. *Advances in virology* **2012**, 186512, doi:10.1155/2012/186512 (2012).

481 Jarboe, J., Gupta, A. & Saif, W. in *Human Monoclonal Antibodies: Methods and Protocols* (ed Michael Steinitz) 61-77 (Humana Press, 2014).

482 Cartron, G. *et al.* Therapeutic activity of humanized anti-CD20 monoclonal antibody and polymorphism in IgG Fc receptor FcgammaRIIIa gene. *Blood* **99**, 754-758 (2002).

483 Weng, W. K. & Levy, R. Two immunoglobulin G fragment C receptor polymorphisms independently predict response to rituximab in patients with follicular lymphoma. *J Clin Oncol* **21**, 3940-3947, doi:10.1200/jco.2003.05.013 (2003).

484 Clynes, R. A., Towers, T. L., Presta, L. G. & Ravetch, J. V. Inhibitory Fc receptors modulate in vivo cytotoxicity against tumor targets. *Nat Med* **6**, 443-446, doi:10.1038/74704 (2000).

485 Manches, O. *et al.* In vitro mechanisms of action of rituximab on primary non-Hodgkin lymphomas. *Blood* **101**, 949-954, doi:10.1182/blood-2002-02-0469 (2003).

486 Arnould, L. *et al.* Trastuzumab-based treatment of HER2-positive breast cancer: an antibody-dependent cellular cytotoxicity mechanism? *British journal of cancer* **94**, 259-267, doi:10.1038/sj.bjc.6602930 (2006).

487 Jegaskanda, S., Weinfurter, J. T., Friedrich, T. C. & Kent, S. J. Antibody-dependent cellular cytotoxicity is associated with control of pandemic H1N1 influenza virus infection of macaques. *Journal of virology* **87**, 5512-5522, doi:10.1128/jvi.03030-12 (2013).

488 Adair, R. A. *et al.* Cytotoxic and immune-mediated killing of human colorectal cancer by reovirus-loaded blood and liver mononuclear cells. *International journal of cancer. Journal international du cancer* **132**, 2327-2338, doi:10.1002/ijc.27918 (2013).

489 Kaneda, Y. The RIG-I/MAVS signaling pathway in cancer cell-selective apoptosis. *Oncoimmunology* **2**, doi:10.4161/onci.23566 (2013).

490 Schlee, M. Master sensors of pathogenic RNA - RIG-I like receptors. *Immunobiology* **218**, 1322-1335, doi:10.1016/j.imbio.2013.06.007 (2013).

491 Rucker, J. *et al.* Cell-cell fusion assay to study role of chemokine receptors in human immunodeficiency virus type 1 entry. *Methods in enzymology* **288**, 118-133 (1997).

492 Blumenthal, R., Gallo, S. A., Viard, M., Raviv, Y. & Puri, A. Fluorescent lipid probes in the study of viral membrane fusion. *Chemistry and physics of lipids* **116**, 39-55 (2002).

493 Struck, D. K., Hoekstra, D. & Pagano, R. E. Use of resonance energy transfer to monitor membrane fusion. *Biochemistry* **20**, 4093-4099 (1981).

494 Melikyan, G. B., Barnard, R. J., Abrahamyan, L. G., Mothes, W. & Young, J. A. Imaging individual retroviral fusion events: from hemifusion to pore formation and growth. *Proceedings of the National Academy of Sciences of the United States of America* **102**, 8728-8733, doi:10.1073/pnas.0501864102 (2005).

495 Huerta, L., Lopez-Balderas, N., Larralde, C. & Lamoyi, E. Discriminating in vitro cell fusion from cell aggregation by flow cytometry combined with fluorescence resonance energy transfer. *Journal of virological methods* **138**, 17-23, doi:10.1016/j.jviromet.2006.07.012 (2006).

496 Guo, Y. *et al.* Effective tumor vaccine generated by fusion of hepatoma cells with activated B cells. *Science* **263**, 518-520 (1994).

497 Di Pilato, M. *et al.* NFkappaB activation by modified vaccinia virus as a novel strategy to enhance neutrophil migration and HIV-specific T-cell responses. *Proceedings of the National Academy of Sciences of the United States of America* **112**, E1333-1342, doi:10.1073/pnas.1424341112 (2015).

498 Matsushima, H. *et al.* Neutrophil differentiation into a unique hybrid population exhibiting dual phenotype and functionality of neutrophils and dendritic cells. *Blood* **121**, 1677-1689, doi:10.1182/blood-2012-07-445189 (2013).

499 Rabinovich, G. A., Gabrilovich, D. & Sotomayor, E. M. Immunosuppressive strategies that are mediated by tumor cells. *Annual review of immunology* **25**, 267-296, doi:10.1146/annurev.immunol.25.022106.141609 (2007).

500 Kuilman, T., Michaloglou, C., Mooi, W. J. & Peeper, D. S. The essence of senescence. *Genes & development* **24**, 2463-2479, doi:10.1101/gad.1971610 (2010).

501 Campisi, J. Cellular senescence: putting the paradoxes in perspective. *Current opinion in genetics & development* **21**, 107-112, doi:10.1016/j.gde.2010.10.005 (2011).

502 Rodier, F. & Campisi, J. Four faces of cellular senescence. *The Journal of cell biology* **192**, 547-556, doi:10.1083/jcb.201009094 (2011).

503 Collado, M. & Serrano, M. Senescence in tumours: evidence from mice and humans. *Nature reviews. Cancer* **10**, 51-57 (2010).

504 Mooi , W. J. & Peeper , D. S. Oncogene-Induced Cell Senescence — Halting on the Road to Cancer. *New England Journal of Medicine* **355**, 1037-1046, doi:doi:10.1056/NEJMra062285 (2006).

505 CRESCENZI, E., PALUMBO, G. & BRADY, H. J. M. Bcl-2 activates a programme of premature senescence in human carcinoma cells. *Biochemical Journal* **375**, 263-274, doi:10.1042/bj20030868 (2003).

506 Rebbaa, A., Zheng, X., Chou, P. M. & Mirkin, B. L. Caspase inhibition switches doxorubicin-induced apoptosis to senescence. *Oncogene* **22**, 2805-2811 (2003).

507 Schmitt, C. A. *et al.* A Senescence Program Controlled by p53 and p16INK4a Contributes to the Outcome of Cancer Therapy. *Cell* **109**, 335-346, doi:http://dx.doi.org/10.1016/S0092-8674(02)00734-1 (2002).

508 Weiland, T. *et al.* Enhanced killing of therapy-induced senescent tumor cells by oncolytic measles vaccine viruses. *International journal of cancer. Journal international du cancer* **134**, 235-243, doi:10.1002/ijc.28350 (2014).

Appendix: Live cell imaging (CD-ROM)

Supplementary Video 1 (SV5-1): Time-lapse video with uninfected and MVNSeGFP infected Jurkat cells: Jurkat cells stained with CMTPX red dye were added at a ratio of 1:1 to MVNSeGFP infected Jurkat cells that are attached to fibronectin coated 24-well tissue culture plates. The plates were then imaged at 40X using ELWD lens every 5 mins for 1.5 hours. The purple arrow shows a fusion event.

Supplementary Video 2 (SV5-2): Time-lapse video with uninfected neutrophils and MVNSeGFP infected Jurkat cells: Uninfected neutrophils stained with CMTPX red dye (red cells) were added to MVNSeGFP infected Jurkat cells (green) attached to fibronectin coated 24-well tissue culture plates, 24hpi. Images were then taken at 40X zoom using an ELWD lens. Neutrophils clustering under green GFP positive MV-infected Jurkat cell syncytia (white arrows) are shown over a time period of 2.5 hours.

Supplementary Video 3 (SV5-3a and 3b): Time-lapse video with uninfected neutrophils and MVNSeGFP infected Vero cells: Vero cells cultured in 12-well tissue culture plates were infected with MVNSeGFP. Twenty-four hours post infection, neutrophils stained with CMTPX red dye were added to the infected Vero cells at 1:1 ratio. The videos 3a (green, red and bright field image overlay) and 3b (red and bright field overlay) were taken over a period of 3 hours and show neutrophils (red) interacting with the

Vero syncytium (green), alongside constant changing morphology before collapsing completely (white arrows).

Supplementary Video 4 (SV5-4): Time-lapse video with uninfected neutrophils and MVNSeGFP infected Vero cells: Vero cells cultured in 12-well tissue culture plates were infected with MVNSeGFP. Twenty-four hours post infection, neutrophils stained with CMTPX red dye were added at 1:1 ratio. The video was taken between 3 and 5 hours of co-culture and show neutrophils (red) with flattened morphology on the surface of the green syncytium (shown by blue arrows). The green syncytium collapses at the end of 5-hour co-culture dragging along the red neutrophils.